UNIVERSITY OF SOUTHAMPTON

FACULTY OF YOUR NATURAL AND ENVIRONMENTAL SCIENCES

Ocean and Earth Sciences

Biogeography of spring phytoplankton communities from the Labrador Sea: drivers, trends, ecological traits and biogeochemical implications

by

Glaucia Moreira Fragoso

Thesis for the degree of Doctor of Philosophy

November 2016

UNIVERSITY OF SOUTHAMPTON

ABSTRACT

FACULTY OF YOUR NATURAL AND ENVIRONMENTAL SCIENCES

Ocean and Earth Sciences

Thesis for the degree of Doctor of Philosophy

BIOGEOGRAPHY OF SPRING PHYTOPLANKTON COMMUNITIES FROM THE LABRADOR SEA: DRIVERS, TRENDS, ECOLOGICAL TRAITS AND BIOGEOCHEMICAL IMPLICATIONS

Glaucia Moreira Fragoso

The Labrador Sea is a high latitude sea of the sub-Arctic region known to be an important oceanic sink for atmospheric CO_2 due to intensive convective mixing during winter and the development of extensive phytoplankton blooms that occur during spring and summer. Therefore, a broad-scale investigation of the response of phytoplankton community composition to environmental forcing is essential for understanding planktonic food-web organization and biogeochemical functioning in the Labrador Sea. The aim of the research included in this thesis is to investigate the biogeographical and biochemical aspects of phytoplankton communities resulting from the contrasting hydrographical zones that divide the Labrador Sea into distinct ecological provinces. In Chapter 2, the phytoplankton community structure from near surface waters during spring and early summer (2011 to 2014) was investigated in detail, including species composition and environmental controls. This initial results demonstrated that the Labrador Sea spring and early summer blooms were composed of contrasting phytoplankton communities, for which taxonomic segregation appeared to be controlled by the physical and chemical characteristics of the dominant water masses. In Chapter 3, further work included an investigation of spring phytoplankton communities from surface waters of the Labrador Sea using pigment-based data and CHEMTAX analysis over ten-years (2005-2014). The photophysiological parameters (derived from photosynthesis-irradiance curves) and biochemical (particulate organic carbon to nitrogen ratio (POC:PON)) values differed among distinct phytoplankton communities. These results have provided a baseline of current distributions and an evaluation of the biogeochemical role of spring phytoplankton communities in the Labrador Sea, which will improve our understanding of potential long-term responses of phytoplankton communities in high-latitude oceans to a changing climate. In Chapter 4, potential indicator phytoplankton species of Atlantic and Arctic waters were investigated during spring in the Labrador Sea to identify possible functional traits driving biogeography. Future implications in trait biogeography and species distributions under a global warming scenario are discussed. In Chapter 5, a synthesis of the main findings of each result Chapter is included, in addition to schematic representation of the environmental controls on phytoplankton communities and species/classes succession from May to June in the Labrador Sea. Work that would increment our knowledge of phytoplankton from the Labrador Sea is suggested together with a final conclusion.

Table of Contents

List of Tables

List of Figures

DECLARATION OF AUTHORSHIP

I, Glaucia Moreira Fragoso,

declare that this thesis entitled

"Biogeography of spring phytoplankton communities from the Labrador Sea: drivers, trends, ecological traits and biogeochemical implications"

and the work presented in it are my own and has been generated by me as the result of my own original research.

I confirm that:

1. This work was done wholly or mainly while in candidature for a research degree at this University;
2. Where any part of this thesis has previously been submitted for a degree or any other qualification at this University or any other institution, this has been clearly stated;
3. Where I have consulted the published work of others, this is always clearly attributed;
4. Where I have quoted from the work of others, the source is always given. With the exception of such quotations, this thesis is entirely my own work;
5. I have acknowledged all main sources of help;
6. Where the thesis is based on work done by myself jointly with others, I have made clear exactly what was done by others and what I have contributed myself;
7. Parts of this work have been published as: (Fragoso et al., 2016a, 2016b):

Signed: .....

Date: .....

DEDICATION

I dedicate this work to my parents, Cláudio Fragoso and Vera Lúcia Fragoso for their encouragement, support and unconditional love.

Acknowledgements

Firstly and foremost, I would like to show my gratitude to my supervisors, Professor Duncan Purdie and Dr. Alex Poulton (National Oceanography Center, NOC), for their expertise, guidance and support throughout my thesis. Thanks to Duncan Purdie for being a mentor that believed in my potentials, encouraged me at this important stage of my academic career and always gave pragmatic solutions during times of insecurity in my research. Thanks to Alex for his enthusiasm, ideas and for giving me the opportunity to go to sea and to collaborate with other scientists. My work would also not be possible without many collaborators, including scientists and staff from Bedford Institute of Oceanography (BIO) in Canada. I owe a debt of gratitude to Dr. Igor Yashayaev (BIO) and Dr. Erica Head (BIO) for their assistance, thoughtful advice and collaborative work. I also cannot forget to thank Stephanie Henson (NOC) for suggesting the opportunity to go on a cruise on board of *CCGS Hudson*, which culminated in the current PhD research topic. Additional thanks go to the Brazilian funding agency, *Ciência sem Fronteiras* (*Science without Borders*), that sponsored my PhD stipend and fees (CNPq, 201449/2012-9) and to the National Environment Research Council grant (NE/H017097/1) through an added value award that partially funded my research.

I am grateful for the many officers, crew, technicians and scientists from on board of *CCGS Hudson* (HUD-2013-008) and *RSS James Clark Ross* (JR274). I'm indebted to all those people that helped me with various technical aspects of my PhD, including Sinhue Torres-Valdes who was a great support and a fun cruise mate and Mark Stinchcombe for collecting the samples from the JR302 cruise. Special thanks to Elaine Mitchell (The Scottish Association for Marine Science) for her expertise and guidance on Arctic phytoplankton taxonomy and Richard Pearce (NOC) for assisting me with the Scanning Electron Microscope. I am grateful to Shir Akbari, Dr. Katsia Pabortsava, Dr. Chris Daniels and my lab-mates for their technical support.

Special thanks go to my office mates Amonsak Sawusdee, Bew Charoenvattanaporn and Chris Bird for their companionship during these years of PhD research. It is also a pleasure to thanks my close NOC friends: Anna Rumyantseva, Despo Polyviou, Giang Tran, Nina Rosset and Renata Khouri for the laughter and support that you provided when I was dealing with frustrations during my research. My gratitude goes to my Brazilian friends living in Southampton that helped me to deal with homesickness while sharing good

Brazilian music and food. Thanks to my many friends from home that were always present in my life even whilst being thousands of miles away. My deepest gratitude goes to my parents, Vera Lucia Moreira Fragoso and Claudio de Lima Fragoso, who have always believed and supported me. Finally, I would like to thank my partner David Aldridge for his love and companionship throughout these years. My thesis would not have been possible without the love and support of Dave, family and friends; I will always cherish them for their encouragement and for making this dream possible.

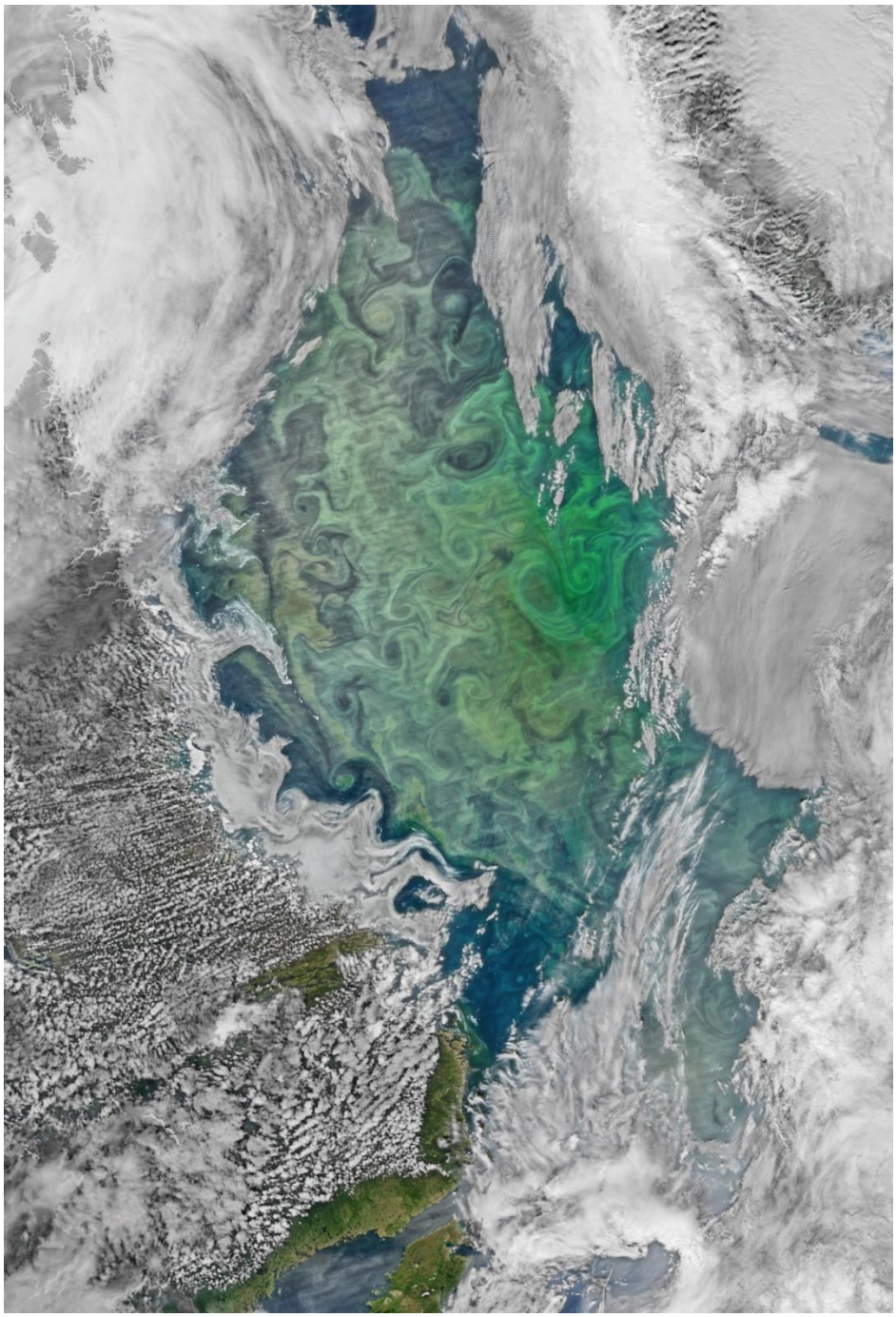

“Chaos is order yet undeciphered” – José Saramago (Portuguese writer)

Definitions and Abbreviations

α^B - Photosynthetic efficiency

β - Photo-inhibition parameter

E_k - Light intensity approximating the onset of saturation

E_s - Saturation irradiance

λ_1 - Marginal effects

λa - Conditional effects

μ_∞ - Maximum growth rate

σ_θ - Isopycnals

ACAROT - α-carotene

AMOC - Atlantic Meridional Overturning Circulation

ANCOVA – ANalysis of CO-VAriance

ANOSIM - ANalysis Of SIMilarity

ALLOX - Alloxanthin

AP - Accessory Pigments

AR7W - Atlantic Repeat Hydrography Line 7 West section

AZOMP - Atlantic Zone Off-Shelf Monitoring Program

BCAROT - β-carotene

BIO – Bedford Institute of Oceanography

BUT19 - 19'-butanoyloxyfucoxanthin

CB - Central Basin

CCA - Canonical Correspondence Analysis

CLIVAR – Climate and Ocean: Variability, Predictability and Change

CHEMTAX – CHEMical TAXonomy

Chl in setae - presence of chlorophyll a in setae

Chl*a* - Chlorophyll *a*

CHLA - Chlorophyll *a*

CHLB - Chlorophyll *b*

CHLC12 - Chlorophyll $c_1 + c_2$

CHLC3 - Chlorophyll c_3

CHLIDEA - Chlorophyllide *a*

CHRYSO – Chrysophytes

Cloud-S - Cloud-shaped colony

CPR - Continuous Plankton Recorder

C:N:P – Carbon to Nitrogen to Phosphorus ratio

CO_2 – Carbon Dioxide

COCCO - Coccolithophore

DCCA - Detrending Canonical Correspondence Analysis

DIADINOX – Diadinoxanthin

DIAT - Diatom

DIATOX - Diatoxanthin

DMS – Dimethylsulfide

DMSP – Dimethylsulfoniopropionate

DOC – Dissolved Organic Carbon

DON – Dissolved Organic Nitrogen

EGC – East Greenland Current

ESD - Estimated Spherical Diameter

FOV - Fields Of View

FUCOX – Fucoxanthin

GBIF - Global Biodiversity Information Facility

GSh - Greenland Shelf

GSl - Greenland Slope

HEX19 - 19'-hexanoyloxyfucoxanthin

HOL - Holococcolithophore

HPLC - High-Performance Liquid Chromatography

LC – Labrador Current

LM - Light Microscope

LSh - Labrador Shelf

LSl - Labrador Slope

LSW – Labrador Sea Water

MDL - Maximum Dimension Length

MLD – Mixed Layer Depth

N_2O – Nitrous Oxide

NAO – North Atlantic Oscillation

NH_4^+ - Ammonium

nMDS- Non-metric multi-dimensional scaling

Needle-S - Needle-shaped cell or colony

NO_3^- - Nitrate

PAR - Photosynthetically Active Radiation

PERID - Peridinin

P_m^B - Maximum photosynthetic rate normalized to chlorophyll biomass

PP - Phytoplankton Production

PPC - PhotoProtective Carotenoid

PRASINO – Prasinoxanthin

PO_4^{3-} - Phosphate

POC – Particulate Organic Carbon

POC_{phyto} – Phytoplankton-derived Organic Carbon

PON - Particulate Organic Nitrogen

PPP - Photosynthetic Pigment

PRYM - Prymnesiophytes

PSC - PhotoSynthetic Carotenoid

Q_{min} - Minimum quota

RDA – Redundancy Analysis

Ribbon-S = Ribbon-shaped colony

SEM - Scanning Electron Microscope

SI – Stratification Index

Si* - Silicate minus nitrate concentration

SILICO - Silicoflagellates

SIMPER - SIMilarity PERcentages analysis

$Si(OH)_4$ – Silicate

Sphere-S = Sphere-shaped cell

SST – Sea Surface Temperature

Star-S = Star- or zigzag-shaped colony

S/V - Surface area to Volume ratio

TC - Total Carotenoids

TChl*a* - Total Chlorophyll *a*

T-S - Potential Temperature and Salinity plot

Tube-S = Tube/cylinder-shaped form

VIOLAX - Violaxanthin

WGC – West Greenland Current

WOCE – World Ocean Circulation Experiment

ZEA - Zeaxanthin

Chapter 1: Introduction

1.1 Phytoplankton

1.1.1 The importance of studying marine phytoplankton

Phytoplankton are organisms that play a key role in maintaining world oceans ecosystem functioning. In spite of their small biomass (comprising only 1 – 2 % of the total global plant carbon), phytoplankton are extremely efficient primary producers, being responsible for nearly half of global carbon fixation (Falkowski, 1994). Marine phytoplankton act in the flow of energy by providing food for higher trophic levels and sustaining complex aquatic food webs (Berglund et al., 1994; Kiørboe, 1993). Almost all marine organisms depend, either directly or indirectly, on phytoplankton for their survival (Hoppenrath et al., 2009).

The photosynthetic abilities of phytoplankton regulate the Earth's climate over broad time scales (Falkowski, 2012, 1998; Sigman and Boyle, 2000). Marine phytoplankton impact the carbon cycle by incorporating CO_2 into organic matter during photosynthesis, which can be exported to the deep ocean through the biological pump (Arrigo, 2007) (Fig. 1.1). Similarly to terrestrial plants, marine phytoplankton impacts directly the CO_2 and O_2 fluxes between the atmosphere and the ocean through photosynthesis (Falkowski, 1998). They also regulate, indirectly, the albedo and cloud cover by producing dimethylsulfoniopropionate (DMSP), which breakdown products form dimethylsulfide (DMS) that contributes to cloud formation (Curson et al., 2011; Sunda et al., 2002).

Phytoplankton not only affect the climate but are also sensitive to climate change (Wu et al., 2016; Falkowski and Oliver, 2007) and because of their short turnover times (hours to days), marine phytoplankton communities respond quickly, in a matter of days to weeks, to any changes occurring in the physical habitat. Changes in phytoplankton composition are cascaded out to higher trophic levels, representing the first level of integration of hydroclimatic forcing in the pelagic foodweb (Beaugrand, 2005). Thus, the effects of

hydroclimatic variability, such as nutrients concentration, irradiance levels and temperature, affect phytoplankton on the organismal level, which ultimately impact on the whole ecosystem (Beaugrand, 2005). Phytoplankton are sensitive indicators of climate change because of their non-commercialisation and non-linear responses to environmental perturbation, which can result in an irreversible shift to a different ecosystem state (Burthe et al., 2015).

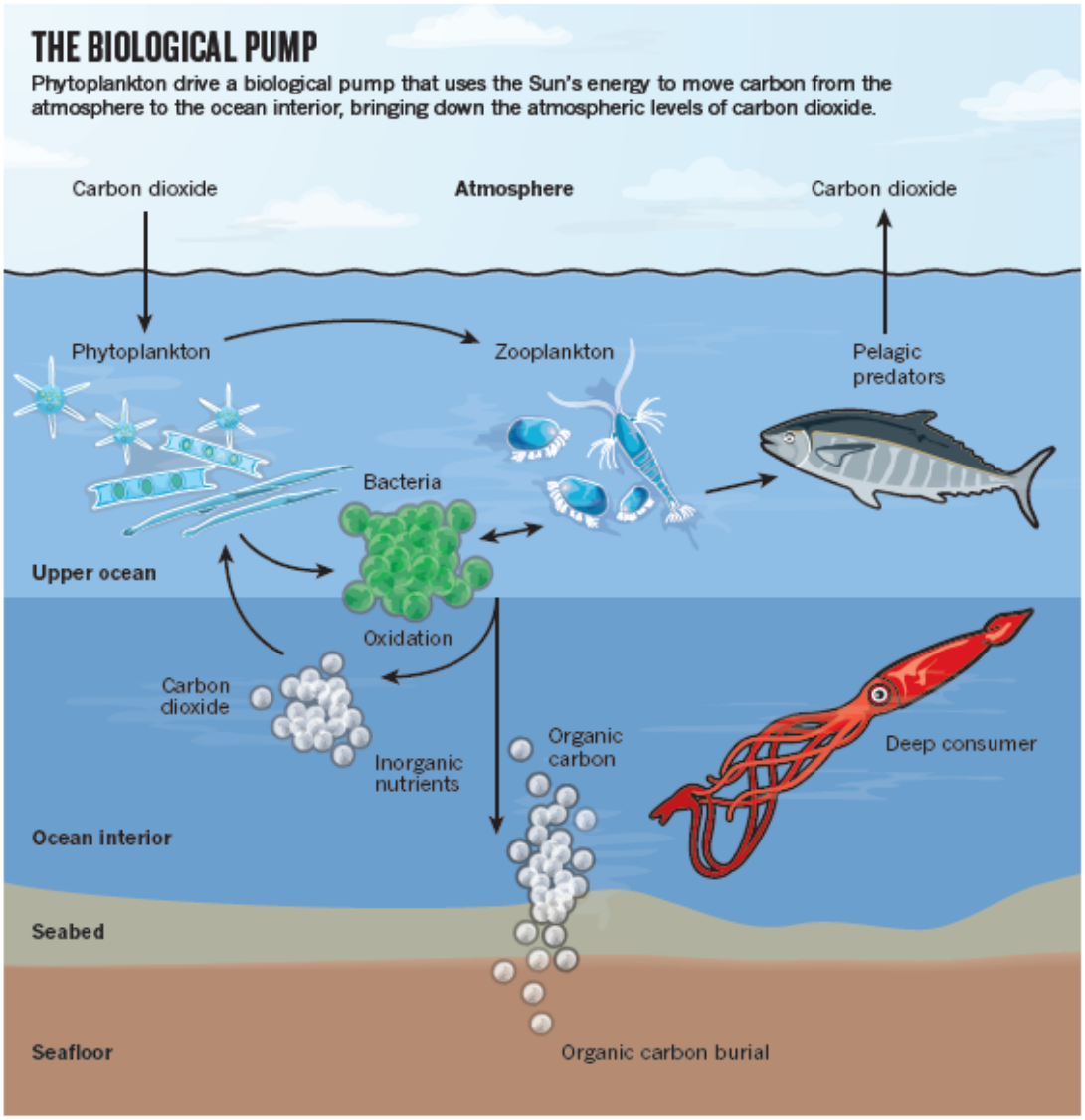

Figure 1.1 Scheme of the biological pump (Falkowski, 2012)

In addition to their overall biogeochemical significance, phytoplankton are ideal organisms to study in relation to climate-induced impact because they have relatively simple life history traits compared to other marine organisms (Litchman et al., 2007; Litchman and Klausmeier, 2008). Fortunately, phytoplankton can be studied in both natural environments and under laboratory conditions due to their short life cycle, providing a unique opportunity to quantify physiological responses of populations to environmental change (Edwards et al., 2013a, 2013b; Thomas et al., 2012). The advantage of using phytoplankton as model organisms to address questions related to climate change is that, in addition to the amount of information collected from field and laboratory experiments, phytoplankton population dynamics are also relatively easy to model, again, due to their short life span (Klausmeier et al., 2008). An underlying understanding of the drivers of phytoplankton growth is crucial to predict present and future changes in marine biogeochemical cycles as the climate continues to change.

1.1.2 Phytoplankton growth

The environmental factors that regulate phytoplankton growth are, mostly, irradiance levels, macro- and micronutrient concentrations and temperature ranges. Biological-related factors, such as predation, viral infection, competition and mutualism also regulate phytoplankton population growth. When conditions are suitable for phytoplankton growth and when population growth exceed loss processes, such as lysis, sinking and predation, phytoplankton form blooms with biomass increasing by up to 3 orders of magnitude over a time scale of days (Irigoien et al., 2004a).

Light is an essential resource for phytoplankton photosynthesis. In marine systems, attenuation of light caused by the medium, dissolved molecules and suspended particles (including phytoplankton themselves) can alter the overall intensity of light and vertical gradient spectral distribution (Kirk, 1994). Moreover, the amount of light that penetrates the surface waters and that is absorbed by phytoplankton is controlled by the degree of vertical mixing of the water column (Sverdrup, 1953). Strong winds deepen the mixed layer, which reduces the amount of light available for phytoplankton, whereas stratification resulting from increased solar heating (thermal stratification) or freshwater input (ice melt

or riverine input) provide enough light for phytoplankton to grow (Doney, 2006; Smith and Jones, 2015).

Macro- (mostly in the form of nitrate, phosphate and silicate, for diatoms and silicoflagellates) and micronutrients (iron, molybdenum, zinc, and others) are essential requirements for phytoplankton growth. Net phytoplankton growth rate is zero at the basal nutrient requirement, known as minimum quota (Q_{min}), where the minimal amount of resource is used for maintaining basal cellular functions (Klausmeier et al., 2008). Phytoplankton growth rates increase asymptotically as nutrient supply rises, approaching a theoretical maximum growth rate (μ_∞), where nutrient concentrations are non-limiting (Klausmeier et al., 2008). The nutrient quota above the minimum is the excedent amount of energy that the cells store for future growth and reproduction (Caperon, 1968; Droop, 1968). The external nutrient concentration also influences the uptake rate of nutrients in phytoplankton and, consequently, their growth (Litchman and Klausmeier, 2008). In marine systems, the amount of vertical mixing in the water also regulates the amount of nutrients that is reintroduced to the surface waters.

Temperature is considered the major environmental axis that governs the distribution of all organisms in the world, including phytoplankton (Litchman and Klausmeier, 2008). In phytoplankton, temperature controls enzymetic rates used in several physiological processes, such as photosynthesis, respiration, nutrient uptake and motility (Thomas et al., 2012). Phytoplankton growth is also strongly affected by ranges of temperature, given that each phytoplankton species has a temperature optimum where growth rate is at its maximum when resources (nutrients and light) are non-limiting (Eppley, 1972).

Biotic relationships, mainly as zooplankton grazing and virus infection can also regulate phytoplankton growth in marine systems. Zooplankton grazing is a top-down control of phytoplankton biomass and has been assumed to be a size-dependent mechanism, though similar grazing pressure has been found in phytoplankton groups with distinct size classes (Marañón, 2015). Microzooplankton have been attributed as the major phytoplankton grazers, accounting for consuming 60–75% of daily phytoplankton production (PP) across the world's oceans (Landry and Calbet, 2004), whereas mesozooplankton, and in particular copepods, consume in general 10–40% of the primary production (Calbet, 2001). Phytoplankton have been suggested to develop a combination of predation avoidance mechanisms to escape zooplankton grazing, such as larger cell size, colony formation, possession of spines or toxic coumpounds (Irigoien, 2005).

Virus infection is also a factor that induces phytoplankton losses in marine systems (Suttle, 2007; Suttle et al., 1990). As the most abundant lifeform in the oceans (roughly $10^6 – 10^9$ particles per ml), viruses are a major form of mortatility to all marine organisms, including all phytoplankton classes (from cyanobateria from diatoms), and have been shown to reduce primary production by as much as 78% (Suttle, 2007; Suttle et al., 1990).

1.1.3 Phytoplankton diversity and community structure

Phytoplankton are an extremely diverse and polyphyletic group (classes), largely spanning over several orders of magnitude in cell size (from approximately 0.1 μm^3 in a small cyanobacteria to > 10^8 μm^3 in the largest diatom, Marañón, 2015) (Fig. 1.2). Likewise, phytoplankton exihibit a large range in morphological and physiological aspects, nutrient and light requirements, trophic and predation-avoidance strategies (Falkowski, 2004). Their evolutionary trajectory, which has over billions of years, shaped modern species diversity and their ecological functionality (Katz et al., 2004). The overall fitness of individuals within species assemblages is a response to the spatial and temporal heterogeinity of pelagic ecosystems, in addition to biotic relationships (eg. competition, mutualism, predation) on a geological timescale (Litchman et al., 2010). Over large spatial scales, marine phytoplankton communities are biogeographically organised, exhibiting contrasting patterns of distribution across global marine systems (Bibby et al., 2009; Cermeño et al., 2010; Follows et al., 2007).

Phytoplankton communities are structured by multiple marine phytoplankton species from different taxonomic levels that successfully coexist at the same time. The ability of multiple species to coexist on limited resources, in spite of the tendency for competition that exclude other species, is known as the "paradox of plankton" and has intrigued many scientist over time (Hutchinson, 1961). One of the arguments that explain phytoplankton diveristy in a community is usage of distinct resources, where lack of silica, for example, limits the growth of diatoms, whislt it has no impact on prymnesiophytes, given that the latter do not require silica for growth (the equilibrium approach). The other argument (non-equilibrium dynamics) is that the cause of coexistence is based on several external factors, such as fluctuation in the environment, periodic forcing and spatial heterogeneity. High environmental variability impacts the reorganization of relative abundance and

phytoplankton species composition, as a result of interaction between physical, chemical and biological variables (Calijuri et al., 2002). Thus, changes in habitat conditions dramatically alter community structure, revealing the "winners" and "losers" of a new habitat.

1.1.4 Using traits to understand the biogeography of marine phytoplankton communities

One approach to understanding the mechanisms of species coexistence and diversity in a phytoplankton community is to identify the relevant traits and trade-offs of key species (Litchman et al., 2010). Evolutionists, for a long time, have referred to traits simply as a surrogate of organismal performance, however, as trait-based analysis becomes more common among ecological studies, a more specific definition has been applied to avoid misconceptions (Violle et al., 2007). Thus, functional traits are morpho-physio-phenological traits that impact fitness indirectly via the three components of individual performance: growth, reproduction and survival (Violle et al., 2007). A trait-based analysis, therefore, investigates the ecological roles of a species that captures key aspects of organismal functionality in the system and has the potential to give a realistic prediction of biological communities in response to changes in the environment (Glibert, 2016; Litchman et al., 2007; Litchman and Klausmeier, 2008; McGill et al., 2006).

Phytoplankton cell size is a master trait that shapes ecological niches, given that it is correlated with many other physiological, ecological and life history traits (Marañón, 2015) (Fig.1.2). In terms of nutrient utilization, cell size is allometrically scaled with maximum nutrient uptake rate, half-saturation constant for uptake, and uptake affinity (Edwards et al., 2012; Litchman et al., 2007). Smaller cells, for example, have greater efficiency in acquisition of limiting nutrients due to their larger surface to volume ratios and smaller diffusion boundary layer, which ultimately limits nutrient transport to the cell (Finkel et al., 2009; Litchman et al., 2007; Litchman and Klausmeier, 2008). Likewise, smaller phytoplankton cells have lower sinking rates, and higher growth rates (Litchman et al., 2007; Richardson and Jackson, 2007). The trade-off of those cells is that they are more easily grazed when compared to larger phytoplankton that ultimately control the population size (Marañón, 2015). Conversely, larger cells tend to sink faster, however,

they confer greater plasticity in morphology (setae present in larger diatoms, for example), allowing them to increase their surface area to volume ratios and their friction in the water column (Nguyen et al., 2011; Pahlow et al., 1997; Smetacek, 1985; Snoeijs et al., 2002).

Light absorption also changes with phytoplankton cell size, where larger cells absorb fewer photons per unit pigment than smaller cells of the same shape, due to increased self-shading of pigment with increasing cell volume (Fujiki and Satotu, 2002). High levels of self-shading caused by larger cell volumes can be advantageous in stratified water columns when photon flux densities and ultra-violet light doses are high (Key et al., 2010). Conversely, smaller cells have the advantage to grow under low light conditions, such as in deep mixed layers, because of their greater amount of intracellular pigment per cell volume as compared to larger cells (Barton et al., 2013b). In addition to cell size, cell shape and coloniality are also relevant traits in phytoplankton communities. These morphological traits can be plastic, however, suggesting that they may differ depending on many environmental variables, such as light levels, nutrient concentrations and grazing pressures (Litchman and Klausmeier, 2008).

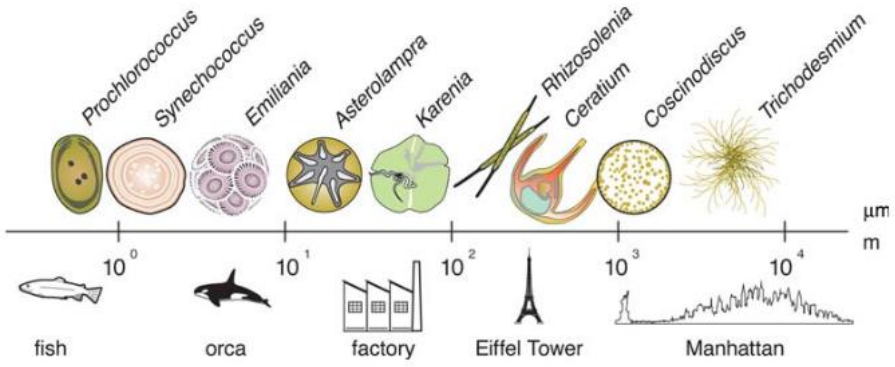

Figure 1.2 Examples showing the analogy between range of sizes observed in phytoplankton species and larger objects perceived from a human's perspective (Finkel et al., 2009)**.**

Resource utilization is another phytoplankton trait important for shaping phytoplankton communities. Some phytoplankton groups, for instance, may require distinct nutrients, while others do not, as mentioned above. Different phytoplankton groups also have specialized pigments that allow absorption of particular parts of the light spectrum as well as at different light intensities (Falkowski and Raven, 1997; Nair et al., 2008). To overcome nutrient limitation, some phytoplankton have acquired evolutionary strategies,

such as diazotrophic cyanobacteria that are able to fix nitrogen into bioavailable ammonia when nitrate concentrations are low (Snow et al., 2015). Flagellated phytoplakton are able to move within the water column, allowing effective nutrient foraging (Kruk et al., 2010). Mixotrophic phytoplankton, which presents both modes of feeding (autotrophic and heterotrophic), are a able to engulf pray when nutrient conditions are low and to photosynthetise under more eutrophic conditions (Troost et al., 2005). Other examples of phytoplankton traits explored in the literature are: ability to form resting stages, sexual or asexual reproduction, grazer resistance, temperature-related traits and many others (Litchman et al., 2010, 2007; Litchman and Klausmeier, 2008).

1.1.5 Phytoplankton species diversity: functional role

Phytoplankton communities and diversity impact differently on the functioning of aquatic ecosystems (Eggers et al., 2014), global climate (Falkowski, 1998) and cycles of nitrogen, silica, phosphorus and calcium, among other elements on a geological time scale (Falkowski, 1998; Field et al., 1998). The type of assemblage of phytoplankton has an intrinsically functional role in regulating biogeochemical pathways and fluxes, including the export of organic matter to the deep ocean. The coccolithophore, *Emiliania huxleyi*, for example, is thought to be a great contributor to the calcium carbonate pump because of their cosmopolitan and abundant distribution in the worlds ocean, and thus, has a crucial role in the global carbon cycle (Read et al., 2013; Rost and Riesebell, 2004). Diatoms, which are known to regulate silica biogeochemical cycles due to their silicate requirement for growth, are assumed to be the major contributor to the biological pump because of their heavy biogenic silica cell wall that allow them to sink faster to deeper waters (Smetacek et al., 2004). Some cyanobacteria are able to fix nitrogen, which can provide a significant amount of nitrogen to the oligotrophic regions of the ocean (Barton et al., 2013a; Tyrrell, 1999). *Phaeocystis*, a prymnesiophyte, is a major DMS producer that strongly contributes to cloud formation and is not as easily grazed as diatoms due to the exudation of mucilage (Haberman et al., 2003).

Phytoplankton community composition also impact the trends of elemental stoichiometry in surface and deep-waters. Around 60 years ago, Alfred C. Redfield concluded that phytoplankton growth in the surface ocean controls deep-ocean chemistry when he

observed similar trends of elemental ratios of carbon, nitrogen and phosphorus (C:N:P) in the plankton biomass and deep-water nutrients (Redfield, 1958). Although an average atomic C:N:P ratio of phytoplankton has claimed to be the canonical value of 106:16:1, known as the ‘‘Redfield ratio”, recent research has emphasized the variability of phytoplankton stoichiometry between different species (Karl et al., 2001; Michaels et al., 2001). Distinct phytoplankton assemblages, for example, have been reported to influence differently particulate (Martiny et al., 2013a, 2013b; Smith and Asper, 2001) and dissolved elemental stoichiometry (C:N:P) (Weber and Deutsch, 2010). Some explanations for canonical ratio deviations include intrinsically variation of phytoplankton groups (Ho et al., 2003; Quigg et al., 2003), phytoplankton physiology (Goldman et al., 1979; Quigg et al., 2003) and nutrient limitation affecting primary production (e.g., Falkowski and Raven, 1997; Moore et al., 2013). Unfortunately, detritus and dead plankton material also influence overall particulate C:N:P ratios in the ocean, which may complicate the interpretation of *in situ* observations of phytoplankton elemental stoichiometry (Martiny et al., 2013a).

Phytoplankton, therefore, are not only diverse in terms of their species, morphology and traits but phytoplankton assemblages also present distinct ecological functionality in the system, either in terms of the food web or their impact on biogeochemical cycles. Many studies focus simply on chlorophyll or fluorescence measurements and undermine the ecological and physiological aspects of phytoplankton assemblages. Because of their distinct functional roles in marine ecosystems, studying phytoplankton taxonomy, either in term of species, functional type or groups and their dynamics in aquatic ecosystems are crucial to efficiently understand the influence of phytoplankton communities in biogeochemical cycles and climate regulation.

1.2 High latitude phytoplankton

1.2.1 Marine phytoplankton from a changing Arctic/Sub-Arctic region

High latitude oceans, particularly the Arctic and the sub-Arctic, have been undergoing changes within the last few decades as a consequence of climate change. Rises in surface seawater temperature, weakening of thermohaline circulation, sea ice decline and increased sea surface freshening as a result of higher precipitation, river flow and sea ice and glacier meltwater inputs are the most noticeable changes occurring in the Arctic Ocean (Anisimov et al., 2007). Paleoclimatic analysis has indicated that the changes observed in the Arctic, including atmospheric CO_2 levels and sea surface temperature, were faster in the last century than previously recorded (Moritz et al., 2002). Rapid modification of environmental parameters (e.g. temperature, nutrients, salinity and CO_2) as a response to climate change provokes considerable shifts in the organization of marine ecosystems and biogeochemical cycles (Schofield et al., 2010).

The most obvious climate-driven trend in the Arctic Ocean within the last few decades is the accelerated decline of seasonal (< 1 year) and perennial (multi-year) sea ice (Comiso et al., 2008). The drastic loss of perennial sea ice occurs as a result of multi-year sea ice thinning (Kwok et al., 2009) and has been suggested as an irreversible trend to the Arctic sea ice cover (Serreze et al., 2009). Melting ice drives primary production because the influx of lower salinity water into the shelf induces water column stratification and provides a well-illuminated environment for phytoplankton growth. Primary production seems to have increased in surface waters with sea ice decline because it creates greater illuminated areas for phytoplankton growth (Arrigo et al., 2008; Pabi et al., 2008). Nonetheless, recent findings report the occurrence of extensive phytoplankton blooms (> 100 km) under thin ice (~1m) with biomass fourfold greater than in open waters (Arrigo et al., 2012). Under ice blooms have been suggested to be widespread in the Arctic Ocean due to its enormous ice-covered continental shelf (~50% of its area) and may refute current estimations of pan-Arctic primary production as ice-free areas increase (Arrigo et al., 2012).

Although greater light availability may stimulate phytoplankton growth in ice-free regions, Arctic phytoplankton seem not to be limited by light during the summer, alternatively, nutrients, usually nitrogen, appear to limit phytoplankton growth (Tremblay and Gagnon, 2009). Nitrogen limitation has been reported in Arctic phytoplankton blooms (Reigstad et al., 2002) (Tremblay et al., 2008) and is expected to be augmented in areas away from the shelf break, rivers and adjacent glaciers, such as the central Arctic Ocean (Tremblay and Gagnon, 2009). Enhanced water column stratification boosts nitrogen limitation in surface waters, given that the upward flux of nutrients from the deep is suppressed (Winder and Sommer, 2012), favouring phytoplankton species that are able to thrive under these conditions. A shift from larger phytoplankton cells (nanophytoplankton) to the smaller forms (picophytoplankton) was observed from 2004 to 2008, as the surface waters of the Canadian Arctic basin freshened (Li et al., 2009). These authors argue that under lower nitrogen conditions, small-sized phytoplankton benefit because of their high surface area to volume ratio, which enables rapid nutrient assimilation compared to larger cells. Higher stratification could also increase the abundance of small flagellates that are available to exploit nutrients in the lower euphotic zone.

The opposite force to thermal and, particularly, haline stratification in the Arctic Ocean is vertical mixing induced by extreme wind events, which have been reported to increase as the ice-free period becomes longer (Zhang et al., 2004). Therefore, although higher freshwater input, either from river runoff or glacial melt, is considered a major driving force causing water column stratification in the Arctic Ocean, stronger winds will likely inhibit stratification in ice-free waters and will provide nutrients to the upper layers. Higher river runoff or glacier melting may likewise be a potential source of nutrients that can sustain phytoplankton growth for a longer period. Greenland glacial runoff, for example, has been directly related to phytoplankton bloom intensity in the Labrador Sea within the last decade (Frajka-Williams and Rhines, 2010) and nutrient-rich meltwater from Iluliisat Glacier might have fuelled the phytoplankton bloom in West Greenland during summer 1993 (Jensen et al., 1999). Other forms of nitrogen derived from glacial meltwater, such as dissolved organic nitrogen (DON) have been suggested as an alternative source of nitrogen, when the nitrate pool is exhausted (Tremblay et al., 2008).

1.2.2 The Labrador Sea: geographical importance

The subpolar North Atlantic is one of the regions of the ocean most affected by the climate (Rhein et al., 2011), given that it is a site of deep water formation and is a driving force for the Atlantic Meridional Overturning Circulation (AMOC), an important component of global ocean circulation. The Labrador Sea is a subpolar high latitude marginal sea located to the northwestern Atlantic Ocean and the major source of the North Atlantic Deep Water (Dickson et al., 2002; Yashayaev, 2007; Yashayaev and Loder, 2009). The extreme winter heat losses combined with the subpolar gyre circulation mean that the Labrador Sea creates the deepest winter mixed layers (200 – 2000 m) in the North Atlantic, excluding the Nordic Seas and Baffin Bay (Yashayaev, 2007). Deep convection processes allow colder water to sink, forming the intermediate Labrador Sea Water (LSW) - a cold, relatively low salinity watermass (Yashayaev, 2007). The LSW contributes to the global ocean thermohaline circulation that redistributes heat from low latitudes to the poles and is a long-term indicator of climatic variability (Kieke and Yashayaev, 2015).

Because of intense deep convection processes, the Labrador Sea, in spite of its small size, has a large impact on global ocean physics, air-sea exchange and biogeochemical cycles (Martz et al., 2009; Strutton et al., 2011). This region is one of the few in the world's ocean where gases, such as oxygen and carbon dioxide (CO_2) are directly exchanged between the deep ocean and the atmosphere (Azetsu-Scott, 2003; DeGrandpre et al., 2006). The Labrador Sea has also been considered a major sink of anthropogenic CO_2, where surface carbon can directly and rapidly be transported to the deep ocean through the solubility pump by the formation of the high-density LSW (Tian et al., 2004). A large flux of oxygen as a consequence of convection also occurs, which oxygenates subsurface layers of the North Atlantic (Steinfeldt et al., 2009). Deep convection in the Labrador Sea may also influence the exchange of other biogenic/thermogenic trace gases, such as nitrous oxide (N_2O).

In addition to its influence in the ocean's circulation and gas exchange, the Labrador Sea plays a critical role in the marine carbon cycle and the biological pump. Intensive phytoplankton blooms during spring and summer forms a significant sink of atmospheric CO_2 from surface waters (DeGrandpre et al., 2006; Martz et al., 2009). Such blooms incorporate a large amount of CO_2 into organic matter (Martz et al., 2009), where, with the combination of deep water formation, can be rapidly flushed into deep waters (Strutton et

al., 2011). Phytoplankton bloom biomass in the Labrador Sea has been suggested to be rapidly exported (below 35 m within 15 days of the bloom) with little remineralization in the mixed layer, which support a large CO_2 sink to surface waters (Martz et al., 2009). Intense spring/summer blooms can also contribute to the dissolved organic matter pool either through bacterial lysis, the leakage or exudation of phytoplankton carbon (e.g., mucilaginous exopolymer from diatoms) or sloppy feeding by zooplankton in the Labrador Sea waters (van den Meersche et al., 2004). Active carbon export via respiration and mortality of migrating zooplankton contributes to 19% of the annual sinking flux, but only 6% of total carbon export. Dissolved organic carbon (DOC) export has been suggested to be the main form of export flux (greater than that of the sinking flux of particulate organic carbon (POC)) in the Labrador Sea and is mainly driven by deep, vertical convection (Tian et al., 2004).

1.2.3 The Labrador Sea: hydrographical setting

The Labrador Sea is a high latitudinal marginal sea of the subpolar North Atlantic located between Greenland and Canada. It is connected through the Arctic Ocean by two fresh and cold inflows that enter the Labrador Sea and form hydrographic fronts along the shelf break on both Labrador and Greenland shelves (Yashayaev, 2007)(Fig. 1.3). The Labrador Current (LC) covers the surface of the Labrador Shelf and is originated from the Arctic, as well as melting sea-ice waters coming from the Canadian Arctic Archipelago and Hudson Bay (Fig. 1.3). The West Greenland Current (WGC), which is located east of the Labrador Sea on the Greenland shelf, is a mixture of relatively warm and saline Atlantic water from the Irminger Current (IC) and cold, low salinity Arctic water from the East Greenland Current (EGC) (Yashayaev, 2007), in addition to sea ice and glacial melting waters (Fig. 1.3). The deep basin (4500m) located at the centre of the Labrador Sea forms a counterclockwise flow of relatively warm and salty waters originating from the Atlantic, particularly the Irminger Sea (Krawczyk et al., 2012) (Fig. 1.3). Further details of the Labrador Sea hydrography are described in Chapters 2 and 3.

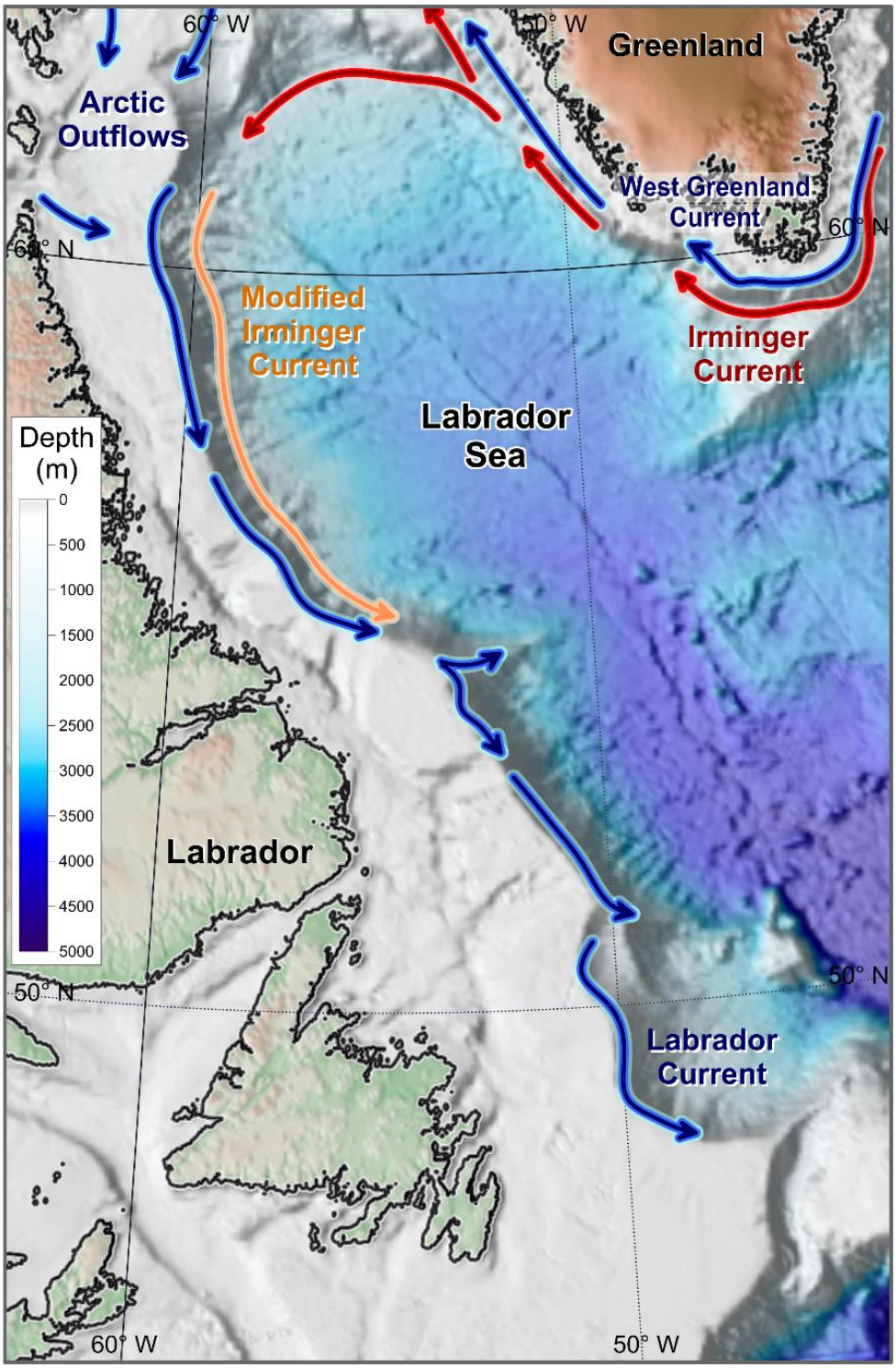

Figure 1.3 Map showing the location, bathymetry and main currents of the Labrador Sea. Image credit: Igor Yashayaev (Bedford Institute of Oceanography).

1.2.4 Spring phytoplankton from the Labrador Sea

The dynamics of the spring phytoplankton blooms observed from chlorophyll data in the Labrador Sea have been extensively reported in the literature (Frajka-Williams and Rhines, 2010; Frajka-Williams et al., 2009; Lacour et al., 2015; Wu et al., 2007; Wu et al., 2008a). Labrador Sea blooms differ from other regions of the North Atlantic because of regional differences in timing, starting first in the northern region as opposed to the south to north progression observed in other parts of the North Atlantic (Henson et al., 2009). In addition to their phenology (Frajka-Williams and Rhines, 2010; Lacour et al., 2015; Wu et al., 2007; Wu et al., 2008a), phytoplankton blooms in the Labrador Sea have been assumed to differ in cell size (Platt et al., 2005) and bio-optical properties (Cota, 2003; Lutz et al., 2003; Platt et al., 2005; Sathyendranath et al., 2004; Stuart et al., 2000).

In general, three distinct phytoplankton bloom regions have been reported to occur during spring in the Labrador Sea (Fig. 1.4). The first and the most intense bloom (up to 5.5 mg Chl*a* m^{-3}) occurs earlier in the season (usually starts in April) in the northeastern part of the Labrador Sea (near the Greenland coast) due to early seasonal onset of haline-driven stratification derived from the freshwater input from the West Greenland Current (Frajka-Williams and Rhines, 2010; Harrison et al., 2013; Stuart et al., 2000) (Fig. 1.4). The second bloom is located in the western Labrador Sea, near the Labrador shelf and varies interanually, since it is triggered following the rapid melting of sea ice that often covers the shelf well into the spring (Frajka-Williams and Rhines, 2010) (Fig. 1.4). The central Labrador bloom is weaker and occurs later in the season as result of thermal stratification (Frajka-Williams and Rhines, 2010) (Fig. 1.4). Light microscopic counts have shown that diatoms dominate the spring bloom on the Labrador Shelf, while the colony forming *Phaeocystis pouchetii* is the common phytoplankton dominating the areas of high chlorophyll near Greenland (West Greenland shelf) (Waniek et al., 2005), although diatoms also co-occur (Stuart et al., 2000). Dinoflagellates, coccolithophores and chrysophytes have been reported to be common after the spring bloom (Harrison et al., 2013).

Deep ventilation during winter brings high nutrient concentrations to the surface waters, which support intense blooms in spring once light becomes available (Tian et al., 2004). However, mesoscale processes, such as upwelling and transport by eddies, have been suggested to also sustain phytoplankton growth throughout the rest of the productive

season (Frajka-Williams and Rhines, 2010). Strong winds have been assumed to stimulate phytoplankton blooms during summer, when nutrients are replenished by vertical mixing and Ekman pumping (Wu et al., 2008b). Light availability, either through greater stratification, shallower mixed layers and daylight length has been suggested to play an important role in bloom initiation in the Labrador Sea (Frajka-Williams and Rhines, 2010; Frajka-Williams et al., 2009; Lacour et al., 2015; Wu et al., 2008a). Plankton community structure of the Labrador Sea has previously been assessed by bio-optical, pigment or microscopic observations (Harrison et al., 2013; Head et al., 2000; Strutton et al., 2011; Stuart et al., 2000). Nonetheless, a detailed quantitative taxonomic analysis of the environmental controls on phytoplankton communities and species composition of the Labrador Sea has not previously been carried out.

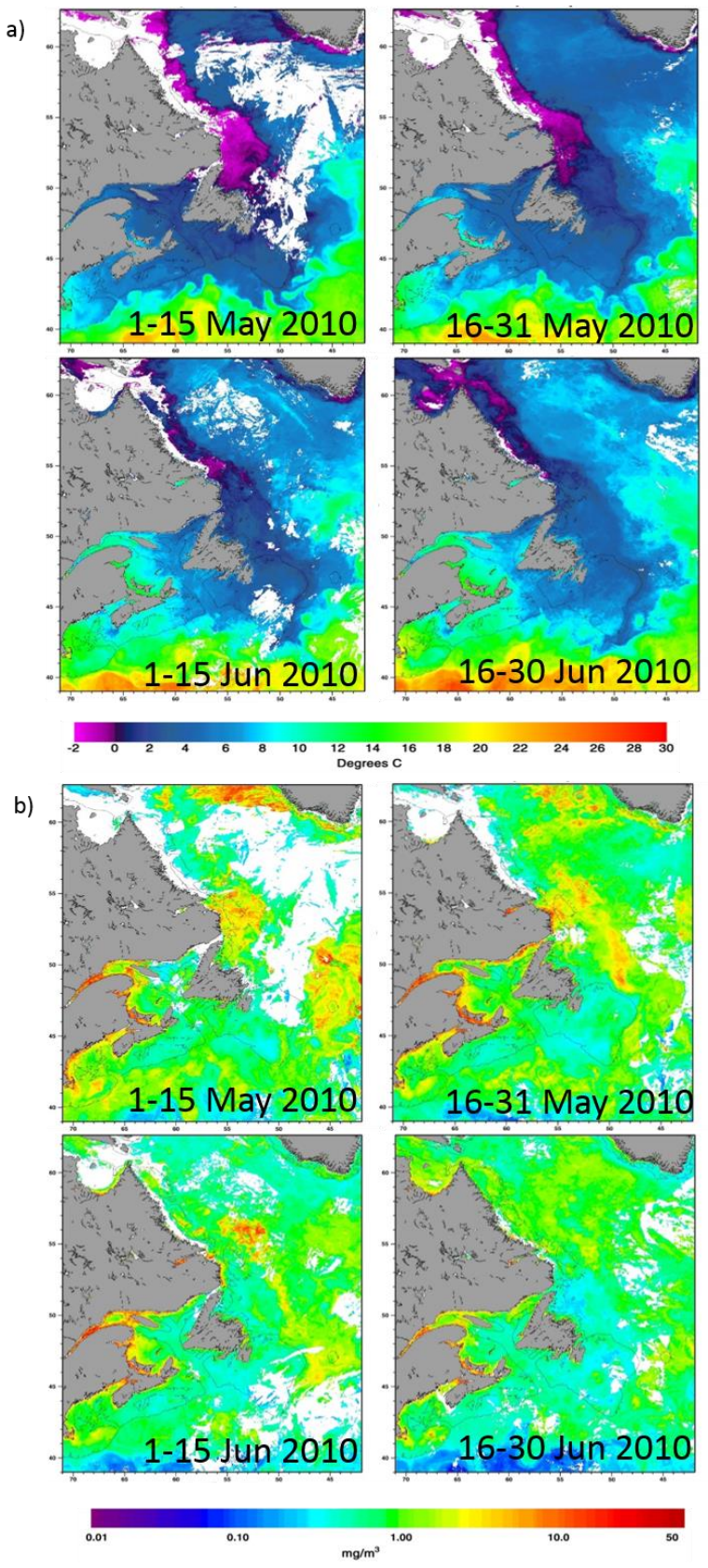

Figure 1.4 Semi-monthly composites of a) sea surface temperature (SST) and b) surface chlorophyll concentrations retrieved from NOAA (AVHRR) and MODIS-aqua satellites during May and June 2010. (Images retrieved from this site:http://www.bio.gc.ca/science/newtech-technouvelles/sensing-teledetection/composites-en.php)

1.2.5 Labrador Sea phytoplankton and climate change

The Labrador Sea is a key region for climate change studies because large scale atmospheric processes, such as the North Atlantic Oscillation (NAO) influence the level of mixing and stratification throughout the water column, the vertical mixing of nutrients and advective changes in water masses (Harrison et al., 2013). These environmental changes, in turn, influence the phenology and duration of phytoplankton blooms, in addition to species composition. Drinkwater et al. (2003) showed that positive NAO index resulted in stronger northwest winds over the Labrador Sea, causing deeper mixing and more sea ice in the region, which potentially delays the initiation of the spring bloom. In the central North Atlantic, south of Greenland and Iceland, later initiation of blooms in the mid-1980s and greater diatom to dinoflagellate ratios during summer blooms were related to a positive NAO index, whereas earlier blooms in the 1990s were associated with negative NAO and a higher abundance of dinoflagellates (Zhai et al., 2013).

Climate also influences sea ice conditions, which in turn has a major impact on primary productivity. The amount of ice-melt and freshwater input to the Labrador and Greenland shelves induces water column stratification and provides a well-illuminated environment for phytoplankton growth (Smith and Comiso, 2008; Smith and Nelson, 1990). Sea ice covers the entire Labrador Shelf until early April, when it melts rapidly along the southwest edge (Stuart et al., 2000). The Labrador Sea shelf shows great interannual variability in the timing and extent of seasonal sea-ice cover, thus it is expected that phytoplankton would respond to these interannual variations. Ice conditions have been shown to correlate negatively with primary production in the Greenland Sea and the Barents Sea, but not with Labrador shelf production (Harrison et al., 2013). As the accelerated decline of seasonal (< 1 year) and perennial (multi-year) sea ice continues (Comiso et al., 2008), the supply of freshwater into the Labrador Sea will likely increase, affecting the biological production in the shelf waters and the waters nearby. Greenland has lost an average of between 380 and 490 billion tonnes of ice each year – some 150 billion tonnes more than it gains in snow over the winter (Witze, 2008), and ice mass loss appears to be accelerating (Khan et al., 2010). Higher river runoff or glacier melting may likewise be a potential source of nutrients that can sustain phytoplankton growth for a longer period. Greenland glacial runoff has been directly related to bloom intensity in the Labrador Sea within the last decade (Frajka-Williams and Rhines, 2010) and nutrient-rich

meltwater from Iluliisat Glacier may have fuelled the phytoplankton bloom in West Greenland during summer 1993 (Jensen et al., 1999). Greenland meltwater has also been shown to provide a significant and potential bioavailable source of iron to phytoplankton (Bhatia et al., 2013). Forms of nitrogen derived from glacial meltwater, such as dissolved organic nitrogen (DON), have been suggested as an alternative source of nitrogen, when the nitrate pool is exhausted (Tremblay et al., 2008).

1.3 Motivation of study

1.3.1 Research questions

The dynamics of phytoplankton spring blooms in the Labrador Sea have been investigated within the past decade (Frajka-Williams and Rhines, 2010; Frajka-Williams et al., 2009; Lacour et al., 2015; Wu et al., 2007; Wu et al., 2008a). However, a detailed quantitative taxonomic analysis and an investigation of the environmental controls on the taxonomic segregation, in addition to multi-year comparison of phytoplankton community distributions and their biochemical signatures in the Labrador Sea has not previously been carried out. The following questions are addressed in this thesis:

- What are the main species of phytoplankton found in the Labrador Sea during spring?
- Are there bioindicator species of water masses and what are they?
- Do phytoplankton assemblages reocurr in the same water masses every year?
- What are the environmental factors that influence taxonomic segregation in the Labrador Sea?
- What is the contribution of phytoplankton communities to the Redfield ratio?
- Do phytoplankton communities present different Redfield ratios (carbon:nitrogen) and photophysiology?
- What are the main morpho-physiological traits influencing phytoplankton species biogeography in the Labrador Sea?

- What is the possible future scenario of spring phytoplankton communities if climate change in the Labrador Sea persists?

1.3.2 Thesis structure and objectives

The overall aim of this thesis is to investigate the drivers that shape the biogeographical patterns of spring phytoplankton communities in the Labrador Sea and the morpho-photo-physiological and biochemical traits associated with these communities. The organisation and structure of this thesis is indicated in Figure 1.5. A detailed examination of the spring phytoplankton community composition across the Labrador Sea and the main environmental factors associated with community distribution is discussed in Chapter 2. This initial analysis provided the foundation for the expanded analysis of phytoplankton community distribution and their photophysiological and biochemical signatures using ten-years of pigment data (Chapter 3) and the investigation of potential phytoplankton functional traits involved in species biogeography (Chapter 4). Chapter 5 summarised the main findings of this research, which ultimetly provided a comprehensive view of the ecological and biogeochemical significance of phytoplankton communities in the Labrador Sea.

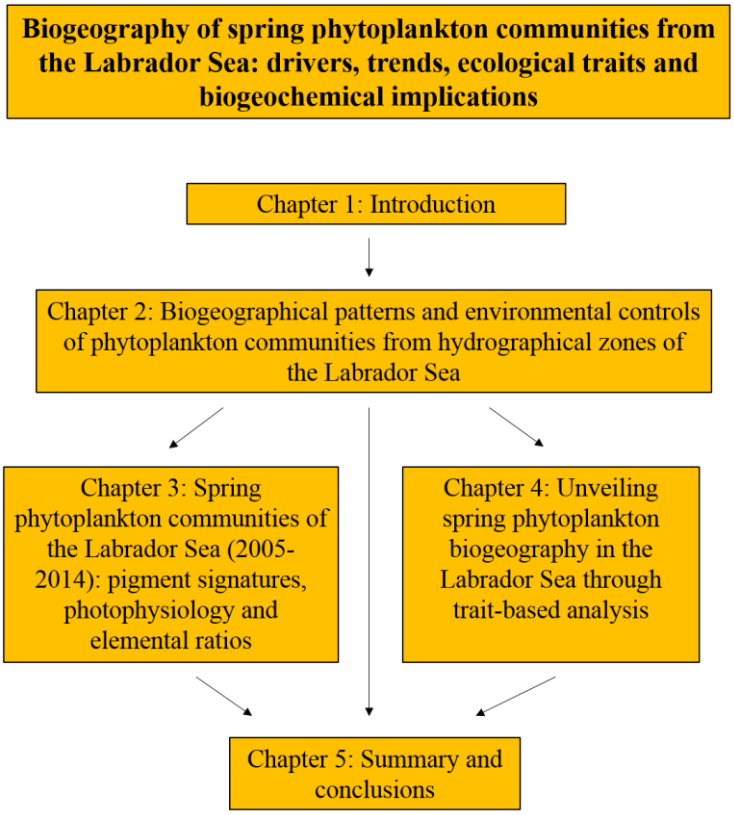

Figure 1.5 Thesis structure. Chapter 2 has been published in *Progress in Oceanography* and Chapter 3 is has been submitted as a discussion paper to *Biogeosciences Discussions* and is currently under public review. Chapter 4 is being prepared for publication for *Limnology and Oceanography*. All chapters maintained the same title in the publications.

1.3.2.1 Thesis objectives

Chapter 2: *Biogeographical patterns and environmental controls of phytoplankton communities from hydrographical zones of the Labrador Sea*

1) To provide a detailed taxonomic and biogeographical analyses of spring phytoplankton communities (2011-2014) across the Labrador Sea.
2) To assess the influence of vertical stability, either haline- or thermally-driven stratification on supporting phytoplankton blooms in the Labrador Sea.
3) To investigate the major hydrographic parameters that influence taxonomic segregation of phytoplankton blooms from the Labrador Sea.
4) To discuss the major environmental drivers for specific phytoplankton groups (e.g. *Phaeocystis pouchetii* and diatoms) in this high latitude sea.

Chapter 3: *Spring phytoplankton communities of the Labrador Sea (2005-2014): pigment signatures, photophysiology and elemental ratios*

1) To investigate the multi-year (2005-2014) distributions of late spring and early summer (May to June) phytoplankton communities using pigments.
2) To examine the overall biochemical traits, including particulate organic carbon (POC) to particulated organic nitrogen (PON) ratios associated with these phytoplankton communities.
3) To compare photophysiological parameters of each phytoplankton community.

Chapter 4: *Unveiling spring phytoplankton biogeography in the Labrador Sea through trait-based analysis*

1) To recognise the potential phytoplankton indicator species of North Atlantic and Arctic waters during spring in the Labrador Sea.
2) To identify possible traits that could be driving the biogeography of phytoplankton species in the Labrador Sea.
3) To examine the mechanisms involved in spring phytoplankton biogeography using trait-based approaches.
4) To discuss future implication in trait biogeography and species distribution under a global warming scenario.

Chapter 5: *Summary and Conclusions*

1) Synthesis of research
2) Future work
3) Concluding remarks

Chapter 2: Biogeographical patterns and environmental controls of phytoplankton communities from hydrographical zones of the Labrador Sea

Note: This Chapter has been published in *Progress in Oceanography* with the full reference: "Fragoso, G. M., Poulton, A. J., Yashayaev, I. M., Head, E. J., Stinchcombe, M. C., & Purdie, D. A. (2016). Biogeographical patterns and environmental controls of phytoplankton communities from contrasting hydrographical zones of the Labrador Sea. *Progress in Oceanography*, *141*, 212-226". G. M. F. was responsible for the phytoplankton counts and identification as well as the statistical analysis of the data. G. M. F. also prepared the first draft of the manuscript.

2.1 Abstract

The Labrador Sea is an important oceanic sink for atmospheric CO_2 because of intensive convective mixing during winter and extensive phytoplankton blooms that occur during spring and summer. Therefore, a broad-scale investigation of the responses of phytoplankton community composition to environmental forcing is essential for understanding planktonic food-web organisation and biogeochemical functioning in the Labrador Sea. Here, phytoplankton community structure (> 4μm) from near surface blooms (< 50 m) from spring and early summer (2011-2014) was investigated in detail, including species composition and environmental controls. Spring blooms (> 1.2 mg chl*a* m^{-3}) occurred on and near the shelves in May and in offshore waters of the central Labrador Sea in June due to haline- and thermal-stratification, respectively. Sea ice-related (*Fragilariopsis cylindrus* and *F. oceanica*) and Arctic diatoms (*Fossula arctica*, *Bacterosira bathyomphala* and *Thalassiosira hyalina*) dominated the relatively cold (< 0°C) and fresh (salinity < 33) waters over the Labrador shelf (e.g., on the southwestern side of the Labrador Sea), where sea-ice melt and Arctic outflow predominates. On the northeastern side of the Labrador Sea, intense blooms of the colonial prymnesiophyte *Phaeocystis pouchetii* and diatoms, such as *Thalassiosira nordenskioeldii*, *Pseudo-nitzschia granii* and *Chaetoceros socialis*, occurred in the lower nutrient waters (nitrate < 3.6 μM) of the West Greenland Current. The central Labrador Sea bloom occurred later in the season (June) and was dominated by Atlantic diatoms, such as *Ephemera planamembranacea* and *Fragilariopsis atlantica.* The data presented here demonstrate that the Labrador Sea spring and early summer blooms are composed of contrasting

phytoplankton communities, for which taxonomic segregation appears to be controlled by the physical and biogeochemical characteristics of the dominant water masses.

2.2 Introduction

Marine phytoplankton communities respond rapidly (days to weeks) to changes occurring in their physical environment due to their short generation times. Over the last few decades climate change has led to marked physical changes in the Arctic Ocean and adjacent sub-Arctic seas (Yashayaev et al., 2015) – changes which are likely to be reflected by responses in their phytoplankton communities (Anisimov et al., 2007). Climate-driven processes modify the major factors, such as light availability, nutrient input and grazing pressure that shape phytoplankton physiological traits and alter community structure (Montes-Hugo et al., 2009; Litchman et al., 2012). As the climate changes in these high latitude oceans, the parameters that define the phytoplankton phenology (seasonal and interannual variation), biomass, primary production and community structure, will all likely be modified. Alteration of the phytoplankton community propagates into marine food web dynamics and biogeochemical cycles (Finkel et al., 2009), due to traits regarding palatability, cell size, elemental stoichiometry and efficiency of carbon transport to deeper waters. A further advance in understanding the long-term responses of Arctic phytoplankton to climate change can be achieved from remote-sensing-derived observations (e.g., Arrigo et al., 2008; Pabi et al., 2008; Kahru et al., 2011; Ardyna et al., 2014) and *in situ* long-term monitoring (Head et al., 2003; Yashayaev, 2007; Yashayaev et al., 2015).

The Labrador Sea is a sub-Arctic region of the Northwest Atlantic located between Greenland and the eastern coast of Canada. In spite of its small size (< 1% of the Atlantic Ocean), the Labrador Sea plays a critical role in the marine carbon cycle because it is one of the most productive regions of the North Atlantic, which enhances the flux of atmospheric CO_2 into surface waters (DeGrandpre et al., 2006; Martz et al., 2009). Moreover, the Labrador Sea produces the densest of all water masses that are entirely formed in the subpolar North Atlantic (Yashayaev et al., 2015), where wintertime cooling and wind forcing cause convective sinking of dense surface water, transporting carbon rapidly to the deep ocean (Tian et al., 2004). The Labrador Sea is also a region susceptible

to climate change because it receives the discharge of Arctic ice-melt waters, which potentially increases the freshening of surface layers (Dickson et al., 2002; Yashayaev and Seidov, 2015). Due to its biogeochemical significance and potential vulnerability to climate change, a comprehensive understanding of the current phytoplankton communities in the Labrador Sea is crucial to detect climate change effects in the future.

The Labrador Sea is usually characterised by three distinct phytoplankton bloom regions during spring and early summer (Frajka-Williams et al., 2009, Frajka-Williams and Rhines, 2010). In contrast to the south to north progression observed in other regions of the North Atlantic (Henson et al., 2009), the northern bloom (north of 60ºN, in the eastern Labrador Sea) is more intense (satellite-derived chlorophyll (1998-2006) up to 5.5 mg chl*a* m^{-3}, Harrison et al., 2013) and starts early in the season (late April). This is due to the early onset of haline-driven stratification formed by freshwater input from the West Greenland Current (Stuart et al., 2000; Frajka-Williams and Rhines, 2010; Harrison et al., 2013; Lacour et al., 2015). The western bloom located on the Labrador Shelf varies inter-annually, since it is triggered by the rapid melting of sea ice that often covers the shelf well into spring (Wu et al., 2007). The Labrador Shelf bloom development starts as the ice retreats, which is usually in May, although it may occur later (June) in some years (Head et al., 2013). The central Labrador bloom is weaker (1998-2006 satellite-derived chlorophyll < 2 mg chl*a* m^{-3}, Harrison et al., 2013) and occurs later in the season (June) as a result of thermal stratification (Frajka-Williams and Rhines, 2010). Nutrient replenishment, occurring during deep winter mixing (200 – 2300 m) and dependent on cumulative surface heat loss, (Yashayaev and Loder, 2009), supports the phytoplankton spring bloom once light becomes available (Harrison et al., 2013). Storm events (Wu et al., 2008b) as well as upwelling events from cyclonic eddies (Yebra et al., 2009) and glacial meltwater (Bhatia et al., 2013) have all been suggested to sustain the blooms via nutrient replenishment after these are exhausted in surface waters.

The Labrador Sea acts as a receiving and blending basin for Atlantic and Arctic waters (Yashayaev et al., 2015) and, therefore, is an ideal region to study the influence of the environmental factors that shape the phytoplankton community structure due to the Atlantic and Arctic waters that divide the region into distinct hydrographic zones (Head et al., 2003, 2000). Hydrographic zones create ecological niches, where distinct phytoplankton communities occur (Acevedo-Trejos et al., 2013; Goes et al., 2014, Brun et al., 2015). Understanding the drivers of biogeographical patterns of phytoplankton communities in the Labrador Sea will provide insights about the habitat complexity of this

area, in addition to elucidating the phytoplankton responses to future changes. Plankton community structure from the Labrador Sea has previously been assessed by bio-optical, pigment or microscopic observations (Cota, 2003; Harrison et al., 2013; Head et al., 2000; Strutton et al., 2011; Stuart et al., 2000). Nonetheless, a detailed quantitative taxonomic analysis of the environmental controls on phytoplankton communities and species composition has not previously been carried out.

Based on *in situ* observations collected in the Labrador Sea during late spring and early summer (2011 – 2014), the specific goals of this study were to:

1) describe the biogeographical patterns of spring phytoplankton communities across the Labrador Sea,

2) investigate the major hydrographic parameters that influence taxonomic segregation of phytoplankton blooms from the upper 50 m in the Labrador Sea,

3) discuss the major environmental drivers for specific phytoplankton groups (e.g., *Phaeocystis pouchetii* and diatoms) in this high latitude sea.

2.3 Methods

2.3.1 Study area

The Labrador Sea and the entire subpolar North Atlantic receive buoyant fresh and cold Arctic outflow (Yashayaev et al., 2015) through two major pathways. One of these pathways connecting the Labrador Sea to the Arctic Ocean originates from the Baffin Island Current that crosses Davis Strait and subsequently merges with various southward inshore flows to become the Labrador Current (LC) (Fig. 2.1). The other pathway starts with the East Greenland Current (EGC) in the Greenland Sea (Yashayaev and Seidov, 2015), which turns around the southern tip of Greenland and flows northwards along the Greenland coast to become the West Greenland Current (WGC)(Yashayaev, 2007) (Fig. 2.1). The LC is composed of two main branches: an inshore branch, which occupies the Labrador Shelf, and an offshore branch, which is centred over the 1000 m contour. The

inshore branch receives waters of Arctic origin via Davis and Hudson Straits, whereas the offshore branch receives contributions from the outflow from Davis Strait and from the portion of the WGC that turns west and then south along the shelf-break (Head et al., 2013) (Fig. 2.1). The inflow from Hudson Strait contains a large riverine input from Hudson Bay, increasing the contribution of estuarine waters to this water mass (15% of total volume of the LC) (Straneo and Saucier, 2008). Local ice melting also influences the properties of the LC, given that the Labrador Shelf is a seasonal ice zone, where sea ice starts forming in mid-January, reaching its maximum extent at the end of March and starts to melt in May (Wu et al., 2007).

The shallow, fresh and cold WGC presents a mixture of low salinity Arctic water from the EGC and Greenland ice melt (collectively sourced from glaciers, icebergs and Greenland ice surface melt). The WGC is also influenced by the relatively warm and saline Atlantic water, which, in turn, originates from the Irminger Current (IC) (Yashayaev, 2007; Yashayaev and Seidov, 2015) (Fig. 2.1). Sea ice is prevented from forming on the Greenland Shelf, although icebergs are frequent (De Sève, 1999; Yankovsky and Yashayaev, 2014). The deep central basin (water depths from 3200 to 3700 m) of the Labrador Sea features a clockwise (anticyclonic) circulation, which in turn contributes to an anticlockwise (cyclonic) gyre nested along the outer rim of the deep basin (Yashayaev, 2007; Hall et al., 2013; Kieke and Yashayaev, 2015) (Fig. 2.1).

The Labrador Sea is a region with complex, yet, well-structured hydrography characterised by marked fronts maintained by the major currents such as the LC, IC and WGC. These oceanographic fronts separate characteristic zones composed of distinct water masses (Yashayaev, 2007). Boundary currents are concentrated at the Greenland and Labrador slopes, where anticyclonic/cyclonic mesoscale eddies are common, particularly Irminger Rings, located in the eastern part of the Labrador Sea (Frajka-Williams et al., 2009; Yebra et al., 2009).

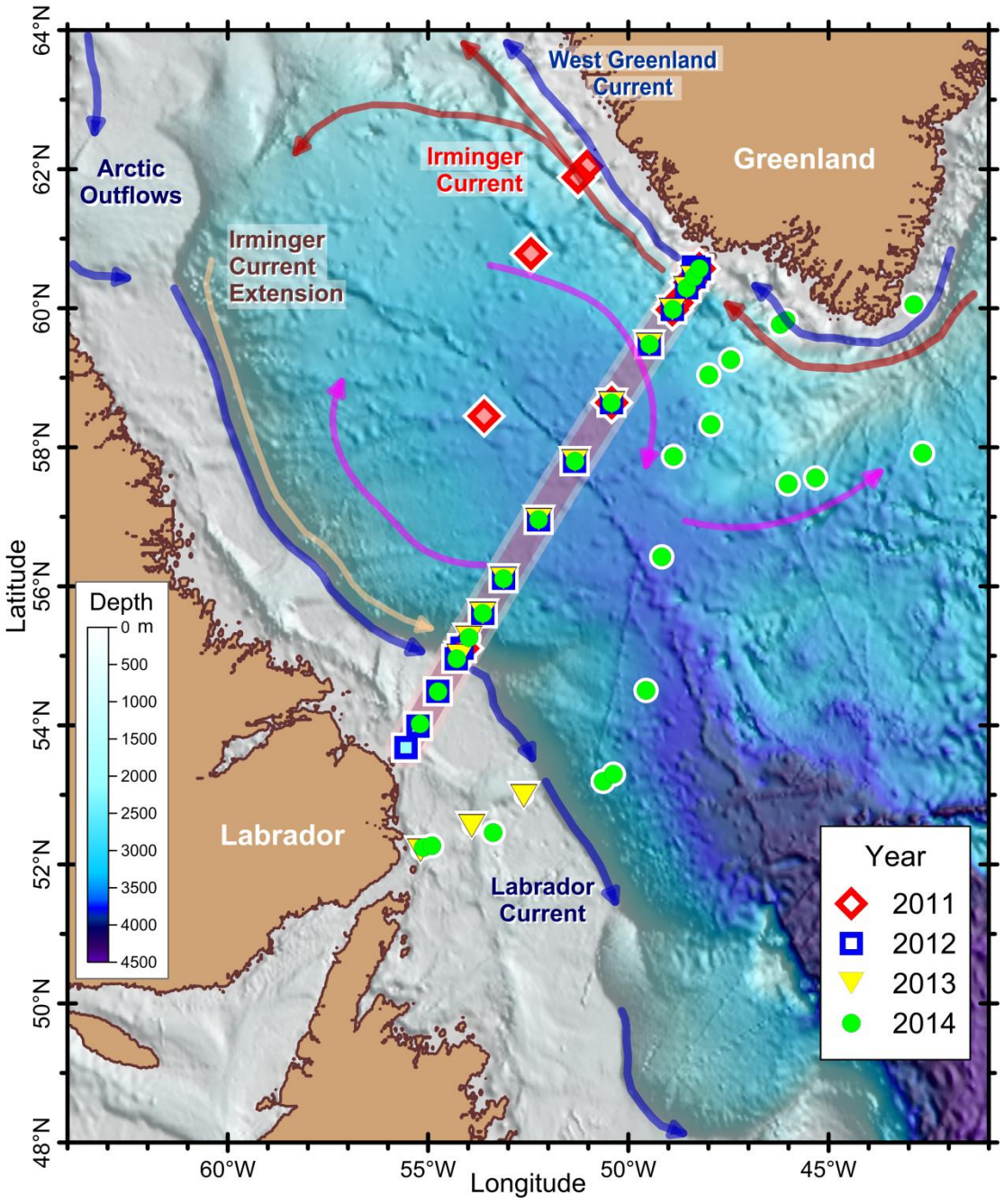

Figure 2.1 Map showing the stations and currents of the Labrador Sea. Stations were sampled along the AR7W transect (background line) during multiple years (2011 - 2014) or near the transect in 2011 (red diamonds), 2012 (blue squares), 2013 (inverted yellow triangles), and 2014 (green dots). Scale refers to bathymetry. Circulation elements - colder currents (Labrador Current, Arctic Outflows and West Greenland Current, blue solid arrows), warmer currents (Irminger Current and Extension, red and brown solid arrows, respectively) and the anticyclonic circulation gyre (pink solid arrows) of the Labrador Sea.

2.3.2 Sampling

Initiated as a part of the *World Ocean Circulation Experiment* (WOCE), and then included as a key component of the *Climate and Ocean: Variability, Predictability and Change* (CLIVAR) sampling plan, the oceanographic section *Atlantic Repeat Hydrography Line 7 West* (AR7W) (following WOCE terminology) running across the Labrador Sea has been occupied annually by the *Ocean and Ecosystem Science Division* of the *Bedford Institute of Oceanography* (BIO) since 1990. This sustained full-depth sampling and monitoring of one of the most critical ocean basins includes collection and analysis of a broad variety of physical, chemical, and biological observations across the Labrador Sea and has recently been established as the principal component of the *Atlantic Zone Off-Shelf Monitoring Program* (AZOMP) of the *Department of Fisheries and Oceans Canada*. This section line, still commonly referred to as AR7W, extends from Misery Point just inshore of the Hamilton Bank on the Labrador Shelf to Cape Desolation on the Greenland Shelf (Fig. 2.1). The transect has 28 fixed position hydrographic stations when ice conditions do not prevent sampling on either of the shelves, in addition to some extra stations that are sampled, which vary annually.

Data for this study were collected on five research cruises (HUD-2011-009, HUD-2012-001, HUD-2013-008, HUD-2014-007, and JR302) to the Labrador Sea. The dates of the respective expeditions carried out by the *CCGS Hudson* (HUD-Year-ID) were 11 – 17 May, 2011, 4 - 11 June, 2012, 9 - 21 May, 2013, and 7 - 14 May, 2014, and by the *RRS James Clark Ross* (JR302) – June 10 - 24, 2014. Stations were sampled on two transect crossings of the shelves and deep basin of the Labrador Sea (Fig. 2.1). The AR7W line was sampled annually on the *Hudson* with additional stations sampled south of the AR7W line in June 2014 on the JR302 cruise. In addition to these two transects, occasional other stations were also sampled in the Labrador Sea (Fig. 2.1).

Vertical profiles of temperature, salinity and chlorophyll fluorescence were measured with a CTD/rosette system. Water samples were collected on the upward CTD casts using 10-L Niskin bottles mounted on a rosette frame. Mixed layer depths (MLD) were calculated from the vertical density (σ_Θ) distribution and defined as the depth where σ_Θ changes by 0.03 kg m^{-3} from a stable surface value (~10 m) (Weller and Plueddemann, 1996). As this mixed layer depth criterion presents limitations in accurately identifying weakly versus strongly stratified water masses, an additional and more robust criterion was used to

measure stratification – a stratification index (SI). In this study, the SI was calculated as the difference in σ_Θ values between 60m and 10 m divided by the respective difference in depth (50 m).

For phytoplankton biomass determination from near surface waters of the Labrador Sea, mixed water samples from the upper 50 m (i.e., a mixture of 50 mL from each of 6 depths: 0, 10, 20, 30, 40, and 50m – (see Appendix A.1) and from the surface (<10 m) (in case of samples from early summer 2014 (JR302 cruise)) were collected and immediately preserved in acidic Lugol's solution to a final concentration of 2%. Samples were stored in dark glass bottles for later phytoplankton species identification and enumeration in the laboratory. Discrete water samples were collected for chlorophyll *a* (chl*a*) and nutrient analysis between the surface to a depth of 100 m at every 10 m or 25 m interval (for more details, see Appendix A.1). Samples for nutrient analysis were frozen at -20°C and measured using an autoanalyser (Alpkem RFA-300) or manually (ammonium, NH_4^+) using the hypochlorite method of Solórzano (1969) or the fluorometric method of Kerouel and Aminot (1997) (JR302 cruise). Chlorophyll *a* was extracted in 90% acetone for approximately 24 hours at -20°C and fluorometrically determined using a Turner Designs fluorometer (Holm-Hansen et al., 1965). Samples for particulate organic carbon (POC) were filtered (0.25 – 1L) onto 25 mm pre-combusted GF/F filters and rinsed with 0.01 N HCl filtered seawater to remove inorganic carbonates and oven-dried (60ºC) for 8-12 hours. Samples were kept dry and analysed in the laboratory using a Carbon-Hydrogen-Nitrogen (CHN) analyser (Collos, 2002).

2.3.3 Satellite observations

The seasonal progression of chlorophyll *a* concentrations from spring to summer from different regions of the Labrador Sea (Labrador Shelf, Central Basin and Greenland Shelf) was monitored through satellite observations. This analysis is important to investigate the stage of blooms from different regions to avoid biased interpretation of the spatial and temporal patterns of phytoplankton communities in the Labrador Sea during the period of study. For this analysis, remote sensing data of chlorophyll *a* concentrations (MODIS-Aqua, 4-km resolution, 8-day composites) were retrieved from GIOVANNI Online Data System (Ocean Color Project, NASA, http://giovanni.gsfc.nasa.gov/giovanni/). Selected

areas for chlorophyll *a* concentrations averages represent the Labrador Shelf and Slope (52°-55° N, 56°-52° W), the Central Basin (55°-59° N, 52°-47° W) and the Greenland Shelf and Slope (59°-60° N, 47°-43° W).

2.3.4 Phytoplankton enumeration

Lugols preserved samples were counted to determine phytoplankton (> 4 μm) abundance and taxonomic composition. According to cell abundance (previously observed under the light microscope), 10 or 25-mL of each sample was placed in a settling chamber for 24 h and examined using a Leiss inverted microscope under 100× or 200× magnification (Utermöhl, 1958). Large (> 50 μm) and numerically rare taxa were counted during full examination of the settling chamber at 100× magnification, whislt small (< 50 μm) and numerically dominant taxa were counted on 1 or 2 transects of the chamber at 200× magnification. At some stations where large taxa were dominant, such as the diatoms *Ephemera planamembranaceae* and *Thalassiosira* spp., at least 300 individuals were counted in 1 or 2 transects at 100× magnification. Counting units were considered as individuals cells, regardless of whether they were solitary or in a chain/colony, except for *Phaeocystis pouchetii* colonies, which were considered individuals categorised by colony size (small: <100 μm, medium: 100 - 199 μm, large: 200 - 300 μm and extra large > 300 μm). Cell abundance within each size category of colony was estimated as the average number of cells counted in at least 10 different colonies of that size category. *P. pouchetii* single cells, either -flagellated or derived from colonies, were counted and grouped together.

Diatoms and dinoflagellates were identified to genus or species whenever possible following Medlin and Priddle (1990), Tomas (1997) and Throndsen et al. (2007). Unidentified dinoflagellate taxa were grouped as small (4 - 29 μm) or large (>30 μm), and with reference to cell wall structure (naked or armored). Unidentified diatoms were grouped as centric or pennate according to a size category (i.e. 4 - 19 μm, 20 - 49 μm, 50 - 99 μm, 100 - 149 μm, 150 - 200 μm and >200 μm). *Thalassiosira* and *Fragilariopsis* species identification was only possible using a Scanning Electron Microscope (SEM), except for *Fragilariopsis atlantica*, and therefore *Fragilariopsis* genus were also categorised by size: small (4 - 19 μm), medium (20 - 50 μm) and large (>50 μm). The

genus *Chaetoceros* was also classified by size as large (subgenus *Phaeoceros*), medium (*C. decipiens*, *C. mitra*, *C. laciniosus*, *C. debilis*, *C. curvisetus*) or small (*C. compressum*, *C. socialis* and others which could not be identified to species level using the light microscope). It was not possible to identify most of the nanoflagellates, other than cryptophytes, *P. pouchetii* and small dinoflagellates, and therefore unidentified flagellates are not included in this study (median and standard error biomass = 12 ± 3% of total biomass).

2.3.5 Biovolume and biomass estimation

Cell biovolume was calculated based on geometrical shapes assigned for each taxa as suggested by Sun and Liu (2003). Cell dimensions of at least 10 specimens were measured and biovolume for each taxon was compared to the literature (Olenina et al., 2006). Cell carbon concentrations were estimated using carbon conversion factors for diatoms (Montagnes and Franklin, 2001) and other protists (Menden-Deuer and Lessard, 2000). For *P. pouchetii*, total carbon biomass consisted of cell biomass (either -flagellated, non-motile or colony-bound cells) and biomass contained in the mucus of *Phaeocystis* colonies. *P. pouchetii* cell carbon biomass was estimated based on geometrical shape as previously described, without any distinction between flagellate, non-motile or colony-bound cells. A mucus carbon conversion factor has previously been developed to convert from colony volume to total colony biomass for *P. antarctica* (213 ng C mm^{-3}, Mathot et al., 2000) and *P. globosa* (335 ng C mm^{-3}, Rousseau et al., 1990). Given the lack of data on carbon estimates of colonial mucus for *P. pouchetii*, the average colonial mucus reported from *P. antarctica* and *P. globosa* was applied for *P. pouchetii* colonies in this study (i.e., 274 ng C mm^{-3}). A regression analysis ($y = 1.01x + 240.92$; $r^2 = 0.47$; $n = 44$; $p < 0.0001$) of the carbon calculated from cell counts and carbon derived from POC analysis showed good agreement. The goodness-of-fit was confirmed by visually observing the normal distribution of the residuals.

2.3.6 Statistical analyses

Phytoplankton community structure in the Labrador Sea during late spring and early summer of 2011-2014 was investigated using PRIMER-E (v7) software (Clarke and Warwick, 2001). Biomass data from the 75 phytoplankton taxa (including species, genus and morphotypes) were normalised by performing a square root transformation, allowing each taxon to influence the similarity within and among samples. Bray-Curtis similarity was calculated between each pair of samples and a Cluster analysis of this matrix was generated to display the similarity relationship among samples. An arbitrary threshold (46% of similarity) was applied to link the samples that are more similar to each other (i.e., > 46% similar in terms of taxa composition) into Cluster groups.

A non-metric multi-dimensional scaling (nMDS) plot was used to visually display the similarity relationship between the respective pairs of samples derived from the Bray-Curtis similarity matrix. Thus, samples that reflected greater community resemblances were spatially closer than the ones that were less similar. The stress level of the nMDS plot is a measurement of how accurate the representation is, with lower stress values being associated with better visual representation of the similarity relationship in 2-D space. Bubble plots were constructed in the nMDS plots to identify the associations between blooms (in terms of carbon biomass and chl*a*) and physical parameters (MLD and SI). For this analysis, a threshold of median chlorophyll *a* biomass values greater than 1.2 mg chl*a* m^{-3} for each Cluster was applied to arbitrarily define bloom conditions in the upper 50 m.

The similarity percentage analysis (SIMPER) routine was used to explore the dissimilarities between Clusters and the similarities within Clusters of samples. Moreover, this output was used to identify the contributions from each taxon to the (average) overall similarity within Clusters at a cutoff of 90% cumulative contribution. A post-hoc analysis of similarity (one-way ANOSIM) was also applied to determine whether Clusters were statistically significantly different from each other in terms of their taxonomic composition.

To analyse the effects of gradients (environmental parameters) on the Labrador Sea phytoplankton biomass and community structure, a redundancy analysis (RDA) was performed using the CANOCO 4.5 software (CANOCO, Microcomputer Power, Ithaca, NY). This multivariate analysis determines the environmental variables (explanatory

variables) that best explain the distribution of the major selected taxa, by selecting the linear combination of environmental variables that yields the smallest total residual sum of squares in the taxonomic data (Peterson et al., 2007). Only taxa that contributed to more than 0.5% of total biomass (reduced from 75 to 11 taxa) were selected for RDA analysis. Detrending canonical correspondence analysis (DCCA) was used *a priori* to determine whether the data ordination method was linear (suitable for RDA analysis) or unimodal (suitable for Canonical Correspondence Analysis – CCA). A relatively small gradient length (< 2.5 standard deviation units according to DCCA analysis output) revealed that the ordination was linear-based and that RDA analysis was suitable (Lepš and Šmilauer, 2003). Forward-selection (*a posteriori* analysis) was used to identify a subset of environmental variables that significantly explained taxonomic distribution and community structure when analysed individually (λ_1, marginal effects) or included in the model where other forward-selected variables were analysed together (λa, conditional effects). Biomass data were log-transformed and a Monte Carlo permutation test (n = 999, reduced model) was applied to test the statistical significance ($p < 0.05$) of each of the forward-selected variables.

2.4 Results

2.4.1 Temporal variability of the study

The initiation and the progression of blooms in the Labrador Sea is expected to vary from year to year (Frajka-Williams and Rhines, 2010). In addition to the expected natural variability of chlorophyll *a* distributions, the sampling period in the Labrador Sea varied during this study (six weeks) (Fig. 2.2). During 2011, only the Central Basin and the Greenland Shelf were sampled. Sampling occurred early this year (mid-May), so chlorophyll concentrations were low (< 1 mg Chl*a* m^{-3}) in the Central Basin (pre-bloom condition), although it was high (> 4 mg Chl*a* m^{-3}) in the Greenland Shelf (bloom condition) (Fig. 2.2b-d). During 2012, sampling occurred later in the season (early June). At this time, the bloom at the Central Basin was in its peak (~ 1.5 mg Chl*a* m^{-3}), whereas the Labrador and the Greenland Shelf blooms were starting to decline, though

concentrations were still > 1 mg Chl*a* m^{-3} (Fig. 2.2b-d). During 2013, sampling occurred, again, early in the season (mid-May), being possible to sample the peak of Labrador and Greenland Shelf blooms (> 2 mg Chl*a* m^{-3}), while the Central Basin was found in a pre-bloom condition (< 1 mg Chl*a* m^{-3}) (Fig. 2.2b-d). In 2014, sampling occurred twice, early (early May) and late (mid-June) in the season. During the early sampling period of 2014, the Labrador Shelf and Central Basin were found in pre-bloom conditions (< 1 mg Chl*a* m^{-3}), whereas the Greenland Shelf bloom was found initiating (~ 1 mg Chl*a* m^{-3}) (Fig. 2.2b-d). During the late sampling period of 2014, the Labrador Shelf and the Central Basin blooms were starting to decline, although chlorophyll *a* concentrations were still high (> 1 mg Chl*a* m^{-3}), whereas the Greenland Shelf bloom had declined (post-bloom condition; < 0.5 mg Chl*a* m^{-3}) (Fig. 2.2b-d).

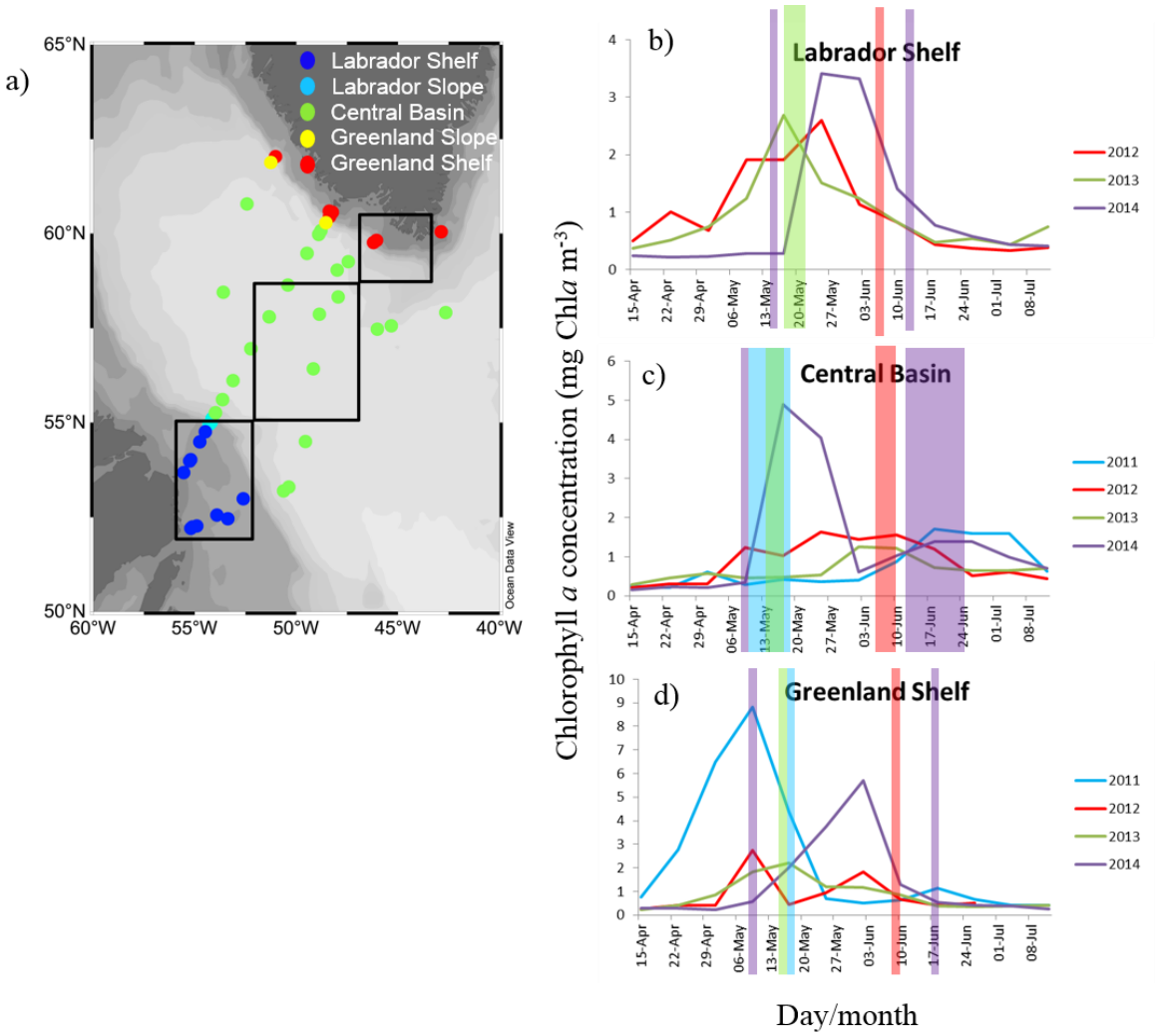

Figure 2.2 – Temporal progression of phytoplankton blooms from distinct regions of the Labrador Sea. Chlorophyll *a* averages were retrieved from areas that represent, approximately, the Labrador Shelf (lower box), Central Basin (middle box) and Greenland Shelf (upper box) (a). Temporal progression of chlorophyll *a* concentrations from mid-April to early-July (b-d) during 2011 (blue), 2012 (red), 2013 (green), 2014 (purple). The hatched area in the right panel represent the sampling period of correspondent colour-coded year.

2.4.2 Hydrography and nutrient distributions

The Labrador Sea was divided into five distinct zones based on its bathymetry – a wide and shallow shelf (< 250 m) and slope (250-1000 m) located close to Canada (Labrador Margin), a deep central Basin (> 3000 m) and a narrow and steep slope (2500-3000 m) and shelf (< 2500 m) on the Greenland Margin (Fig. 2.3a). Temperature and salinity from surface and sub-surface waters (upper 50 m) varied among these distinct zones across the

Labrador Sea (Fig. 2.3b). In general, colder (temperature < 2°C), fresher (salinity < 34) and less dense waters (σ_θ < 27 kg m^{-3}) were found on the shelves and slope regions (Fig. 2.3b), particularly on the Labrador Shelf and Slope and at the Greenland Shelf during late June (see the arrows in Fig. 2.3a,b), indicating the influence from the Arctic outflow. A warmer (temperature > 1°C), saltier (salinity > 33.5) and denser (σ_θ > 27 kg.m^{-3}) water mass with features of modified Atlantic waters (Irminger Current, IC) was found widely distributed in the central portion and Greenland slope of the Labrador Sea (Fig. 2.3). The temperature and salinity (T-S) properties from the surface and subsurface waters varied interanually (2011 - 2014) and seasonally (from early May until late June) during the period of study (Fig. 2.3b).

In spite of the interannual variability, the T-S properties of the surface/subsurface waters of most stations on the Labrador Shelf were generally colder and fresher (average T = -0.6°C and salinity = 32.6) than the waters on the Greenland Shelf (average T = 0.3°C and salinity = 33.1) during May, suggesting that the former was influenced by direct inputs of fresher and colder water from the Arctic, Hudson Bay, continental run-off and from local sea-ice melt (Fig. 2.3b). However, instances of extremely fresh and cold waters were also found in late June 2014 at some stations south of Greenland, suggesting the influence of additional glacial melt in this region (Fig. 2.3b, see arrows). The positions of fronts, usually recognised by a sharp gradient between Arctic and modified Atlantic (Subpolar Mode and IC) waters, varied from year to year, but were generally located near the continental slopes (data not shown).

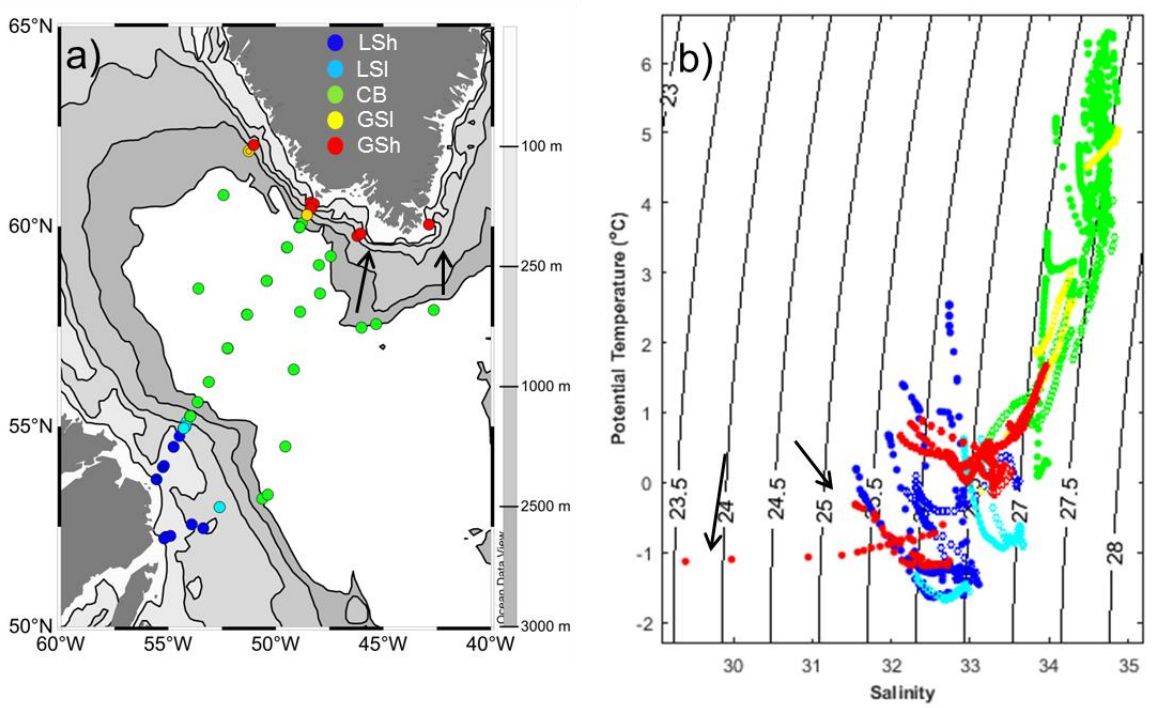

Figure 2.3 Biogeographical zones in the Labrador Sea classified by bathymetry: (a) Labrador Shelf (LSh), Labrador Slope (LSl), Central Basin (CB), Greenland Shelf (GSh) and Greenland Slope (GSl); and (b) potential temperature and salinity (T-S) with isopycnals (σθ) scatter plot of the upper 50 m waters from these five zones during May (open circles) and June (closed circles) of 2011 -2014. Arrows indicate the stations on the Greenland Shelf and the corresponding T-S signature during late June 2014. White background in (a) represents bathymetry deeper than 3000 m.

Nutrient concentrations from the surface and subsurface waters (upper 50 m) varied spatially and temporally across the Labrador Sea (Fig. 2.4). In general, the temporal variation in nutrient concentrations (nitrate, silicate, phosphate and Si* (silicate minus nitrate concentration)) had similar trends during May and June (Fig. 2.4a-f, 2.4i-l), except ammonium concentrations, which were clearly higher in the Central Basin and Greenland Shelf and Slope (median > 0.8 µM) during June (Fig. 2.4g,h). In general, nitrate, silicate and phosphate concentrations were lowest on the Greenland Shelf and Slope (Fig. 2.4a-f). Median nitrate concentrations were clearly higher in the Central Basin (> 8 µM in May and > 5 µM in June), (Fig. 2.4c,d). Median silicate concentrations were greater in the central western part of the Labrador Sea (Labrador Shelf and Slope, and Central Basin), where median concentrations were > 5 µM in May and > 4 µM in June (Fig. 2.4a,b). Phosphate concentrations were higher in the western part of the Labrador Sea, on the Labrador Shelf and Slope (median > 0.8 µM in May and > 0.5 µM in June) and decreased eastwards (Fig. 2.4e,f).

The central Basin had median Si* < 0 µM, which suggests that the phytoplankton from these regions experienced, in most cases, an excess of nitrate compared to silicate (median Si* = -4 µM during May and -1 µM during June, respectively), although there were some stations in the central Basin region where Si* values were > 0 µM (Si* up to 4 µM) (Fig. 2.4i,j). The Labrador Shelf had higher median Si*, particularly during June (Si* up to 1 µM) (Fig. 2.4j) and the Greenland Shelf had Si* values approaching zero (Fig. 2.4i,j). The Labrador Shelf also had higher Si* values at depth (Si* from -6 µM up to -1 µM approximately at 200 m or the deepest depth if bottom depth is < 200 m) compared to the other regions (Si* < -4 µM), although in general, these waters had an excess of nitrate compared to silicate (i.e. negative values, Fig. 2.4k,l). Higher Si* in shelf waters, particularly on the Labrador Shelf, may be associated with the input of riverine and glacial meltwaters enriched with silica.

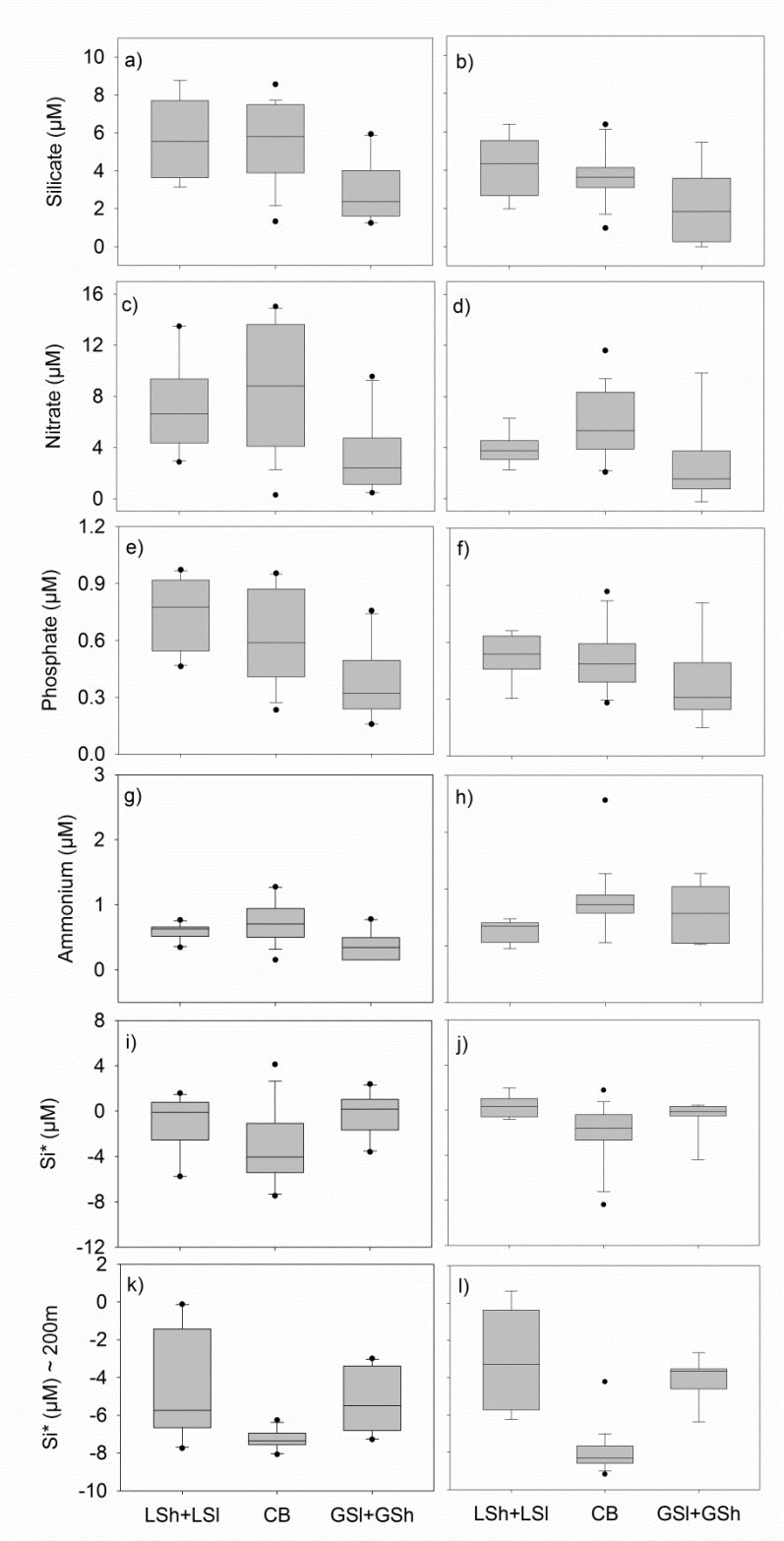

Figure 2.4 Boxplots (median, upper and lower quartile, minimum and maximum values and outliers) of (a,b) silicate, (c,d) nitrate, (e,f) phosphate and (g,h) ammonium concentrations, in addition to (i,j) Si* (silicate minus nitrate concentrations) from the upper 50 m and (k,l) from approximately 200 m water depth in May (left) and June (right) among each biogeographical zone of the Labrador Sea: Labrador Shelf (LSh) + Labrador Slope (LSl), Central Basin (CB) and Greenland Slope (GSl) + Greenland Shelf (GSh).

2.4.3 Chlorophyll a concentrations

Chlorophyll *a* biomass was concentrated within subsurface waters (upper 50 m) of the Labrador Sea (Appendices A.1 and A.2). Thus, average concentrations of chlorophyll (upper 50 m) were used to show the spatial variation of subsurface blooms across the Labrador Sea. The chlorophyll *a* distribution (average of the upper 50 m) varied spatially and interannually (Fig. 2.5). In general, the eastern Labrador Sea, near and within the Greenland Slope and Shelf waters, had the highest upper ocean (< 50 m) concentrations of chlorophyll *a*, particularly during May 2011 and 2013 (Fig. 2.5a,c; average >10 mg chl*a* m^{-3}). The Labrador Shelf and Slope also had relatively high upper ocean chlorophyll *a* values (>5 mg chl*a* m^{-3}) in all years, except during May 2014, possibly because sampling was before the formation of the bloom (Fig. 2.5d). The offshore waters of the central Basin generally had lower upper ocean chlorophyll *a* concentrations (<5 mg chl*a* m^{-3}) than the shelves in May, but later in the season (June 2012, 2014) average upper ocean chlorophyll *a* values were ~ 5 mg chl*a* m^{-3} (Fig. 2.5b,e).

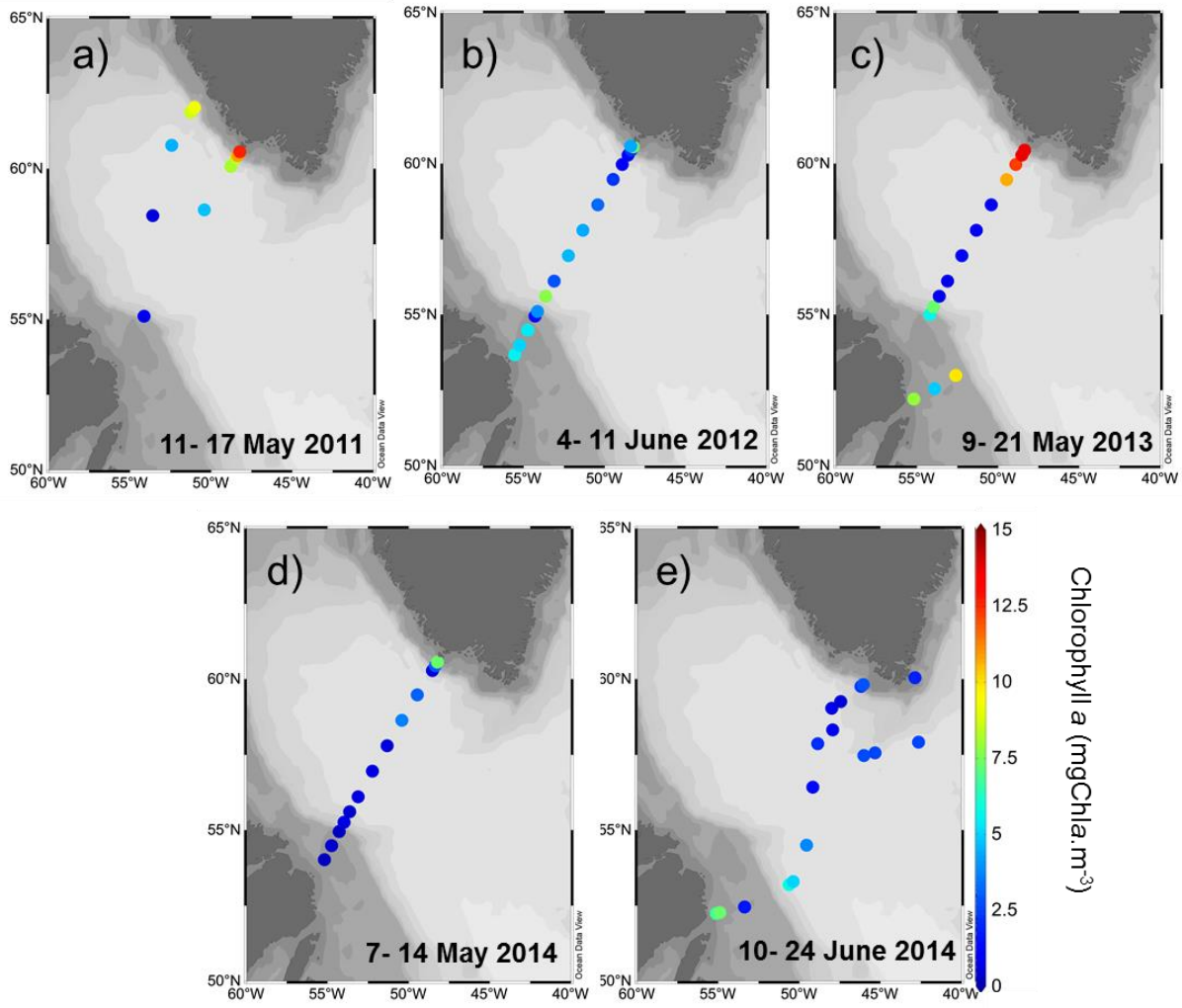

Figure 2.5 Chlorophyll *a* distribution (average of 0 – 50 m values) at each station of the Labrador Sea during late spring/early summer 2011 - 2014 (a-e). Cruise dates are given in each panel.

2.4.4 Phytoplankton community structure

Cluster analysis of phytoplankton biomass from the Labrador Sea during spring and summer of 2011 - 2014 distinguished seven major Clusters of samples with a similarity level of 46%. Non-metric multi-dimensional scaling (nMDS) analysis showed a two-dimensional spatial representation of the similarities within sampled stations based on the composition and biomass values (Fig. 2.6a). A stress level < 0.2 in the nMDS plot (Fig. 2.6a) corresponds to a 'suitable' two-dimensional representation of the similarity relationships of the samples within and between Clusters (as defined in Clarke, 1993). ANOSIM one-way analysis comparing each Cluster suggested that they were significantly

different in composition ($p = 0.001$, R statistic from pairwise analysis varied from 0.75 – 1), and that the Cluster groups are well separated, given that the R statistic values are approaching 1 (see Clarke and Warwick, 2001). Taxa whose cumulative contribution approximated 90% of the average similarity within each Cluster are shown in Table 2.1.

Cluster 1 (n = 12) included samples from the Labrador Shelf during June 2012 and 2014 and May of 2013 (Fig. 2.6c,d,f). This Cluster had the second highest average biomass (275 ± 131 mg C m^{-3}) compared to the other Clusters identified, with large contributions to the Group similarity from Arctic and sea-ice diatoms, such as *Thalassiosira* spp. (particularly *T. hyalina*), *Porosira glacialis*, *Fragilariopsis* spp. (particularly *F. cylindrus* and *F. oceanica*), *Fossula arctica*, *Bacterosira bathyomphala*, *Chaetoceros* spp. (e.g. *C. socialis* and *Phaeoceros*) and *Coscinodiscus centralis*, in addition to unidentified small dinoflagellates (< 30 μm), *Gyrodinium* spp., *Protoperidinium* spp. and cryptophytes (Table 2.1).

Cluster 2 (n = 10) contained samples with relatively high biomass (average of 169 ± 105 mg C m^{-3}) compared with Clusters 3, 6 and 7 but lower than Clusters 1, 4 and 5. These samples were from offshore waters of the centre of the Labrador Sea during June (early summer - 2012, 2014) (Fig. 2.6c,f). Sub-arctic North Atlantic diatoms, such as *Ephemera planamembranacea*, and *Fragilariopsis atlantica*, in addition to *Thalassiosira* spp. and dinoflagellates (unidentified small and large armored, *Gyrodinium* spp.) all contributed to the similarity of these samples (Table 2.1).

Dinoflagellates (unidentified small and *Gyrodinium* sp.), cryptophytes, silicoflagellates (*Dictyocha speculum*) and the diatom *Pseudo-nitzschia* spp. contributed to the similarity of samples in Cluster 3 (n = 12) (Table 2.1). These samples had the lowest average biomass overall (5 ± 4 mg C m^{-3}) and came from the western-central region of the Labrador Sea during May 2011, 2013, 2014 (late spring) (Table 2.1, Fig. 2.6b,d,e).

Cluster 4 (n = 8) included samples with the highest biomass overall (average = 304 ± 282 mg C m^{-3}) where the diatom *Rhizosolenia hebetata* f. *semispina* was the major contributor to the similarity between samples (64%) (Table 2.1). Other diatoms, including medium to large *Chaetoceros* spp. (e.g. *C. decipiens* and *Phaeoceros*) and *Pseudo-nitzschia granii*, dinoflagellates (unidentified naked), cryptophytes and the prymnesiophyte *Phaeocystis pouchetii* contributed up to almost 90% of the cumulative similarity (Table 2.1). Samples from this Cluster occurred only in the central region of the Labrador Sea and later in the season (mid-summer; late June) during 2014 (Fig. 2.6f).

The prymnesiophyte *Phaeocystis pouchetii* was the major contributor to samples in Cluster 5 (n = 28), with the third highest average biomass (248 ± 181 mg C m^{-3}) (Table 2.1). Diatoms such as *Thalassiosira* spp., *Rhizosolenia hebetata* f. *semispina*, *Pseudo-nitzschia granii*, *Porosira glacialis* and *Chaetoceros* (*Phaeoceros*, but mostly *C. socialis*), in addition to dinoflagellates (small unidentified and *Gyrodinium* spp.) also contributed cumulatively to almost 90% of similarity of these samples (Table 2.1). Samples from Cluster 5 also had the highest average chlorophyll *a* biomass (Table 2.2) and occurred in the central-eastern section of the Labrador Sea (along and/or on the nearby Greenland shelf) during all years (2011 - 2014) (Fig. 2.6b-f).

Cluster 6 (n = 2) comprised two samples from Greenland Shelf waters during summer 2014 (Fig. 2.6f), with relatively low biomass (87 ± 14 mg C m^{-3}) (Table 2.1). Small (e.g. *C. socialis*) and medium-sized diatoms, such as *Chaetoceros* spp. (e.g. *C. decipiens*), *Thalassiosira* spp. and *Rhizosolenia hebetata* f. *semispina*, in addition to the flagellate *P. pouchetii* contributed up to 77% of the similarity of these samples (Table 2.1).

Cluster 7 (n = 2) stations also had relatively low average biomass (33 ± 4 mg C m^{-3}) and was comprised of just two samples from the central Labrador Sea during May 2013 (Table 2.1, Fig. 2.6d). Samples from this Cluster represent a mixture of Clusters 3 and 5, where diatoms such as *Pseudo-nitzschia* spp., *Thalassiosira*, *Rhizosolenia hebetata* f. *semispina*, *Corethron criophilum*, in addition to *P. pouchetii* and dinoflagellates (small unidentified naked) contributed mostly to the similarity for these samples (Table 2.1).

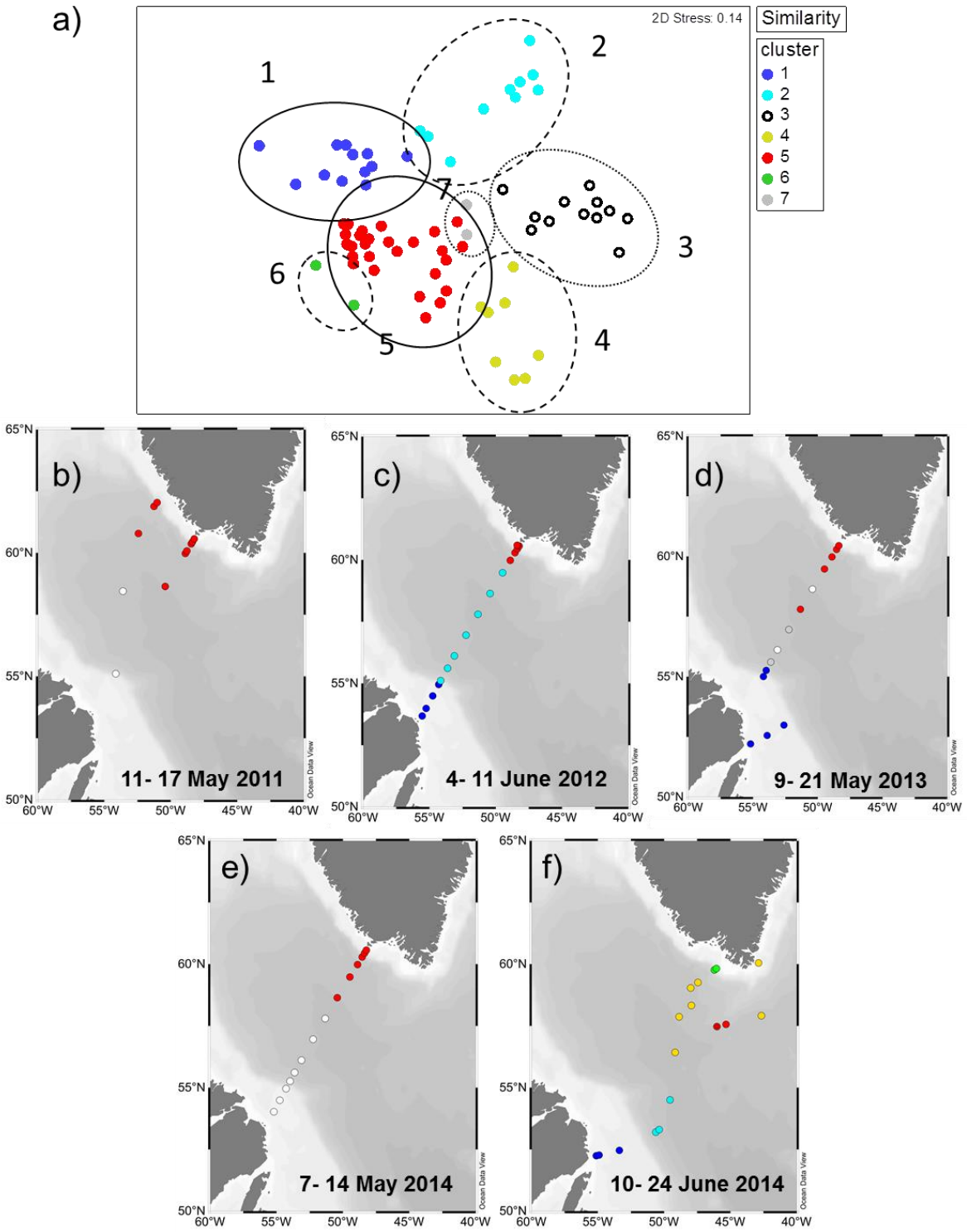

Figure 2.6 Cluster analysis of phytoplankton community composition across the Labrador Sea and in multiple years. (a) Non-metric Multi-dimensional scaling (nMDS) plot representing the similarity in phytoplankton community structure within sampled stations at 46% similarity level (outlines) based on carbon biomass values. Temporal aspects of the Clusters from communities observed during May and June (solid outline), May only (dotted outline) or June only (dashed outline) are revealed on the outlines that separates each Cluster. (b-f) Distribution maps of distinct Clusters represented in the nMDS plot at each station of the Labrador Sea during May and June of 2011 - 2014.

Table 2.1 Percentage contribution of each taxa to the similarity of sampled stations, cumulative contribution up to approximately 90% and average similarity and biomass within each cluster. Numbers in bold refer to taxa whose cumulative contribution were up to approximately 70%. See methods for size (small, medium, large) classification. NI.- non-identified genus/species.

Taxa	Cluster 1	Cluster 2	Cluster 3	Cluster 4	Cluster 5	Cluster 6	Cluster 7
Armored dinoflagellates NI	2.6	**5.8**	**13.1**				2.8
Bacterosira bathyomphala	2.4						
Chaetoceros spp. (medium)				1.9		**11.5**	
Chaetoceros spp. (small)	1.4				2.7	**30.6**	
Corethron criophilum							**7.4**
Coscinodiscus centralis	1.1						
Cryptophytes	1.5		**22.8**	2.9			**5.5**
Dictyocha speculum			1.9				
Ephemera planamembranacea		**49.5**					2.1
Eucampia groelandica							**3.8**
Fossula arctica	**3.7**						
Fragilariopsis atlantica		4.8					
Fragilariopsis spp. (large)	**3.6**						2.2
Fragilariopsis spp. (medium)	**6.1**					3.4	2.9
Fragilariopsis spp. (small)	3						1.6
Gyrodinium spp.	2.1	4.9	7		1.9	2.9	
Naked dinoflagellate NI (large)		3.6	4.5				2.3
Naked dinoflagellates NI	**5.2**	**12**	**32**	**8.7**	4.9		**10**
Nitzschia spp.							1.6
Phaeoceros spp.	1.9			6.8	2.2		2.3
Phaeocystis pouchetii				4.7	**42**	6.9	**6.5**
Porosira glacialis	**24.1**				3	2.8	
Protoperidinium spp.	1.7	**7.5**				5.4	
Pseudonitzschia granii				2.6	3.3		2.5
Pseudo-nitzschia spp			1.9				**14.3**
Rhisozolenia hebetata f. *semispina*				**64.2**	3.3	**9**	**10.1**
Thalassiosira spp.	**30.1**	5.2	**8.4**		**27.1**	**19.2**	**13.9**
Cumulative contribution (%)	90.3	93.4	91.5	91.7	90.3	91.7	91.6
Average similarity	59.7	60.1	56.2	62.8	57.1	74.4	79.7
Average biomass ($mgC.m^{-3}$)	275±13	169±10	5±4	304±28	248±18	87±14	33±4

2.4.5 Hydrographic influence on phytoplankton community structure

Hydrographic variables that explained the variance (explanatory variables) in the biomass of selected phytoplankton taxa (biomass greater than 0.5% of total) were investigated using redundancy analysis (RDA). The ordination diagram (Fig. 2.7) revealed associations between each taxon and the explanatory variables. Proximity of taxa to the environmental variables (arrows) in the same or opposite direction suggests positive or negative correlations, whereas no proximity indicates weak or a lack of correlation; the longer the

arrow, the stronger the correlation. The associations in the ordination diagram show that Arctic/polar diatoms (Cluster 1, such as *Fossula arctica*, *Coscinodiscus centralis*, *Fragilariopsis* spp., *Porosira glacialis* and *Thalassiosira* spp., in addition to *Chaetoceros* spp., particularly *C. socialis* - Cluster 6) occurred in colder (median temperature < 0°C), fresher (median salinity < 33.0) and more stratified waters (median SI > 14 x 10^{-3} kg m^{-4}) (Table 2.2).

Phaeocystis pouchetii (Cluster 5) dominated in waters where nutrient concentrations (mainly nitrate, but also phosphate and silicate) were low (median nitrate concentration < 3.7 μM) (Table 2.2). *Ephemera planamembranacea* (Cluster 2) and *Rhizosolenia hebetata* f. *semispina* (Cluster 4) were found in relatively warmer waters (median > 4.7°C) with higher salinities (median > 34.5). Dinoflagellates (unindentified small and *Protoperidinium*, Clusters 3 and 7) were common in less stratified waters (median SI = 0.1 x 10^{-3} kg m^{-4}) and higher nitrate (median > 9 μM), phosphate (median > 0.7 μM) and silicate (median > 4.5 μM) concentrations (i.e., pre-bloom conditions) (Fig. 2.7, Table 2.2).

The first axis (x- axis) of the analysis explained most of the variance (eigen-value = 23.9%, cumulative percentage variance between taxa and environmental factors = 58.0%), whereas all canonical axes explained 98.3% of the variance (axis 1, p = 0.001; all axes, p = 0.001) (Fig. 2.7, Table 2.3). This means that (1) the arrows displayed closer to the x-axis explained most of the variability in the data, and that (2) environmental variables explained almost 100% of the variation of the selected taxa, when all four axes were analysed together.

Forward selection showed that of all seven environmental factors (Table 2.3) included in the analysis, only four (temperature, nitrate, salinity and phosphate) best explained the variance in the phytoplankton taxa biomass when analysed together. When all the forward-selected variables were analysed together (conditional effects, referred to as λ_a in Table 2.3), temperature was the most significant explanatory variable (λ_a = 0.16, p = 0.001), followed by nitrate concentration and salinity (λ_a = 0.1, p = 0.001) (Table 2.3). Phosphate concentration was also a significant explanatory variable (λ_a = 0.03, p = 0.048) (Table 2.3). Although not significantly (p < 0.05) different (λ_a = 0.01, p = 0.094), silicate concentrations also had a slight influence as an explanatory variable (Table 2.3). Ammonium concentration and SI were not significant explanatory variables in this analysis.

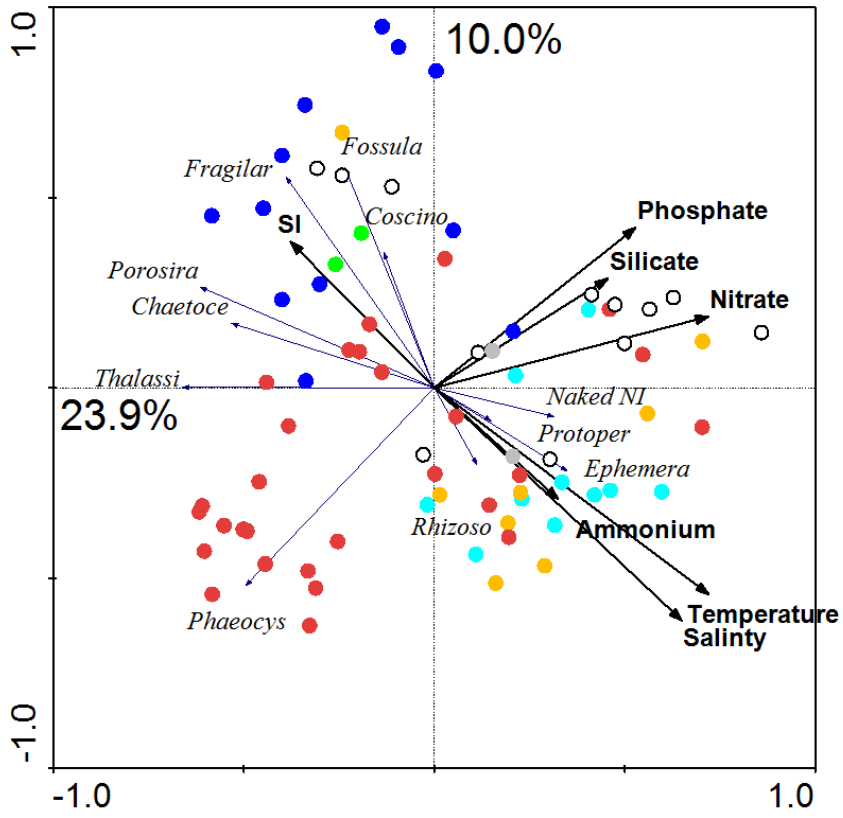

Figure 2.7 Ordination diagram generated from redundancy analysis (RDA). Triplot represents taxa carbon biomass (thin lines), the significant explanatory variables (thick lines) and samples/stations (closed circles; colours refers to cluster groups on Figure 2.5a). Chaetoce = small *Chaetoceros* (mostly *C. socialis*), Coscino= *Coscinodiscus centralis*, Ephemera = *Ephemera planamembranaceae*, Fossula = *Fossula arctica*, Fragilar = *Fragilariopsis* medium (mostly *F. cylindrus*), Naked NI = Small (< 30 µm) naked unidentified dinoflagellates, Phaeocys = *Phaeocystis pouchetii*, Porosira = *Porosira. glacialis*, Protoper = *Protoperidinium* spp., Rhizoso = *Rhizosolenia* spp., Thalassi = *Thalassiosira* spp. SI= Stratification Index.

Table 2.2 Median and standard error of hydrographic and biological parameters of each cluster. MLD= Mixed layer depth, SI= Stratification index.

Parameters	Cluster 1	Cluster 2	Cluster 3	Cluster 4	Cluster 5	Cluster 6	Cluster 7
σθ (kg.m^{-3})	26.2 ± 0.1	27.3 ± 0	27.6 ± 0.2	27.4± 0.2	27.1 ± 0.1	25.8 ± 0	27.5 ± 0.1
Salinity	32.6 ± 0.1	34.6 ± 0.1	34.8 ± 0.2	34.6 ± 0.4	33.9 ± 0.1	32.1 ± 0.1	34.6 ± 0.1
Temperature (°C)	-0.3 ± 0.2	4.8 ± 0.4	3.3 ± 0.6	4.9 ± 0.8	1.6 ± 0.3	-0.7 ± 0	3.3 ± 0
Silicate (μM)	4.3 ± 0.4	3.7 ± 0.3	7.6 ± 0.5	2.8 ± 0.6	3.5 ± 0.3	0.3 ± 0.1	4.7 ± 0.8
Phosphate (μM)	0.6 ± 0	0.5 ± 0.1	0.9 ± 0	0.4 ± 0.1	0.4 ± 0	0.2 ± 0	0.8 ± 0.1
Nitrate (μM)	3.8 ± 0.3	5.4 ± 0.7	13.4 ± 0.9	4.5 ± 1.2	3.6 ± 0.6	0.8 ± 0	9.9 ± 1.0
Si* (μM)	0.3 ± 0.1	-2.0 ± -0.6	-5.6 ± -1.6	-0.8 ± -0.3	-0.4 ± -0.1	-0.4 ± -0.3	-5.2 ± -3.7
Ammonia (μM)	0.4 ± 0.1	0.7 ± 0.1	0.5 ± 0.1	0.6 ± 0.3	0.6 ± 0.1	0	1.1 ± 0.1
MLD (m)	19.5 ± 1.4	20.0 ± 3.3	76.0 ± 89.5	24.0 ± 2.3	24.5 ± 4.9	15.0 ± 0	87.5 ± 3.5
C biomass (mgC.m^{-3})	262 ± 38	147 ± 33	4.0 ± 1.0	251 ± 100	228 ± 34	87 ± 10	33 ± 3
Chlorophyll (mgchl*a*.m^{-3})	5.6 ± 0.7	4.0 ± 0.5	0.5 ± 0.1	1.4 ± 0.2	5.9 ± 0.8	2.5 ± 0.3	1.0 ± 0.2
Stratification Index × 10^{-3} (kg m^{-4})	14.9 ± 4.8	6.6 ± 0.6	0.1 ± 0.4	7.4 ± 2.2	5.1 ± 1.2	16.0 ± 2.3	0.1 ± 0.01

Table 2.3 Variance explained by each explanatory variable (temperature (°C), nitrate, phosphate, silicate and ammonium (µM), salinity and SI × 10^{-3} (kg m^{-4})) when analysed alone (λ_1, marginal effects) or when included in the model where other forward-selected variables are analysed together (λa, conditional effects). Significant *p-values* (p< 0.05) and (*p<0.1) represents the variables that, together, significantly explain the variation in the analysis. SI= Stratification Index.**

Marginal Effects		Conditional Effects			
Variable	λ_1	Variable	λ_a	*P*	*F*
Temperature	0.16	Temperature	0.16	0.001**	13.37
Nitrate	0.15	Nitrate	0.1	0.001**	9.72
Salinity	0.14	Salinity	0.1	0.001**	10.77
Phosphate	0.11	Silicate	0.01	0.094*	1.88
Silicate	0.09	Phosphate	0.03	0.043**	2.44
SI	0.07	Ammonium	0.01	0.283	1.2
Ammonium	0.04	SI	0	0.665	0.62

Axes	1	2	3	4	Total variance
Eigen-values	0.239	0.100	0.056	0.010	1
Taxa-environment correlations	0.760	0.727	0.809	0.540	
Cumulative percentage variance					
of species data	23.9%	33.9%	39.5%	40.5%	
of species-environment relation	58.0%	82.3%	95.9%	98.3%	
Sum of all eigen-values					1
Sum of all canonical eigen-values					0.412

Test of significance of first canonical axis: eigen-value = 0.239; F-ratio = 20.702; P-value = 0.001 **
Test of significance of all canonical axis: Trace = 0.412; F-ratio = 6.606; P-value = 0.001**

2.4.6 Bloom development

To investigate the influence of hydrography on near surface (< 50 m) bloom development, MLD and SI were compared with Clusters that had a large biomass in terms of carbon and chlorophyll *a*. Five blooms (average chlorophyll *a* > 1.2 mg chl*a* m^{-3} per Cluster, see methods) belonged to Clusters 1, 2, 4, 5 and 6 and were composed of distinct phytoplankton communities observed in this study (Table 2.1). Shelf blooms, such as those located near or within Greenland Shelf waters (Clusters 5 and 6) and on the Labrador Shelf (Cluster 1) had the highest biomass values, particularly Clusters 5 and 1 (median chl*a* = 5.9 ± 0.8 mg chl*a* m^{-3} and 5.6 ± 0.7 mg chl*a* m^{-3}, respectively) (Table 2.2, Fig. 2.8a,b). Central Basin blooms (Clusters 2 and 4) were weaker than shelf blooms (average values of

chlorophyll *a* concentration were 4.0 ± 0.5 mg chl*a* m^{-3} and 1.4 ± 0.2 mg chl*a* m^{-3}, respectively) and occurred later in the season (June) (Table 2.2, Fig. 2.8a,b). Stations with shallow mixed layers (median < 25 m) and a higher stratification index (median SI > 5 x 10^{-3} kg m^{-4}) (Fig. 2.8c,d), also had relatively high average biomass in terms of carbon and chlorophyll *a* (Fig. 2.8a,b, Table 2.2). Low salinity waters (median < 33), found on the shelf (particularly Clusters 1 and 6) contributed to the shallow mixed layer depths (median < 20 m) and high stratification levels observed (i.e. haline stratification, median SI > 14 x 10^{-3} kg m^{-4}), whereas relatively high sea surface temperature in June (> 4°C) in the central region of the Labrador Sea induced stratification (median SI from 6.0 to 8.0 x 10^{-3} kg m^{-4}, Clusters 2 and 4) and shoaled the mixed layer (i.e. thermal stratification, median mixed layer depths < 25 m) (Table 2.2).

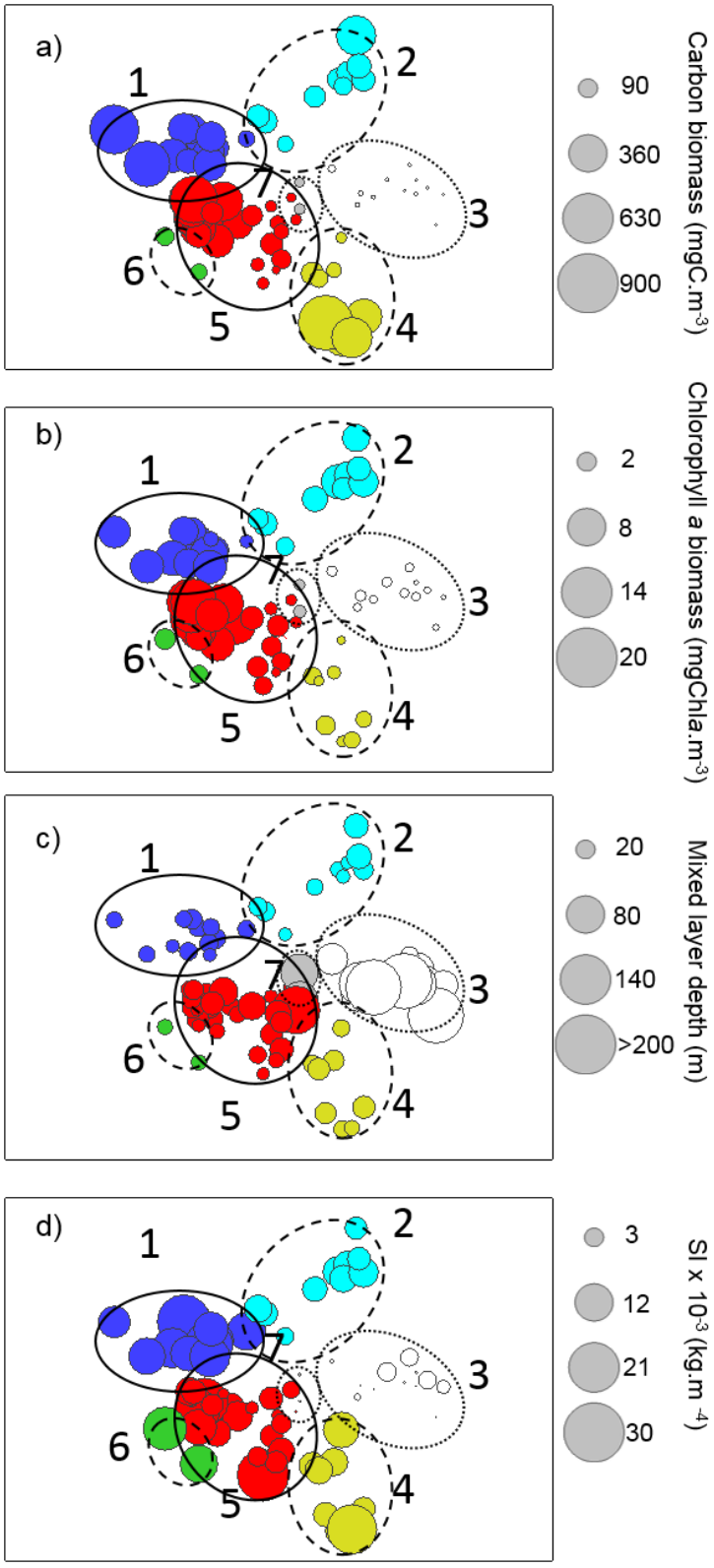

Figure 2.8 Bubble plots derived from nMDS (see Figure 2.5a) representing the average values (upper 50 m) of biomass in terms of (a) carbon, (b) chlorophyll *a*, (c) mixed layer depths (MLD), and (d) Stratification Index (SI) × 10^{-3} (kg m^{-4}) for the upper 60 m for each station. Filled colours refer to Cluster groups given in Figure 2.5a. Outlines around each Cluster represent the similarity in phytoplankton community structure within samples at 46% similarity level from samples collected during May and June (solid line), May only (dotted line) or June only (dashed line).

2.5 Discussion

2.5.1 Influence of Arctic and Atlantic waters on phytoplankton species composition

Phytoplankton community structure in the Labrador Sea during spring and early summer (2011 - 2014) varied according to the hydrographic characteristics (temperature, salinity and nutrient concentrations) of the distinct water masses of Atlantic (Irminger Current and Subpolar Mode Water derived from the North Atlantic Current) and Arctic (Labrador or West Greenland Current) origin, as well as their modifications at different stages of transformation. Overall, Arctic/polar phytoplankton species were present in the shelf waters, where the influence of Arctic waters was greater, whereas Atlantic phytoplankton species dominated in the central Labrador Sea, with a greater contribution of Atlantic water.

Blooms on the Labrador Shelf were comprised of Arctic and sea-ice diatoms that were able to grow in cold (< 0°C) and relatively fresh waters (< 33) (Table 2.2). In our study, polar/Arcto-boreal diatoms, such as *Thalassiosira* spp. (particularly *T. hyalina, T. antarctica var. borealis*, *T. nordenskioeldii*, *T. gravida* and *T. constricta*, data not shown) and *Bacterosira bathyomphala* were predominant in this region, which is consistent with the strong Arctic water influence via the Labrador Current on the Labrador Shelf (von Quillfeldt, 2001, 2000; Degerlund and Eilertsen, 2009; Sergeeva et al., 2010). Local sea ice melting also influenced the composition of diatoms in this region. The polar, cold water coastal diatom *Porosira glacialis* (Pike et al., 2009), and the sea-ice associated *Fossula arctica* and *Fragilariopsis* species (particularly *F. cylindrus* and *F. oceanica*; Caissie et al., 2010) were abundant in both shelf regions, particularly on the Labrador Shelf, where sea ice melts during spring.

Polar diatom species, including *Thalassiosira* spp. (particularly *T. gravida*, *T. nordenskioeldii*, *T. antarctica var. borealis* and *T. hyalina*), *P. glacialis* and *C. socialis*, in addition to Atlantic species (*Rhizosolenia hebetata* f. *semispina*), were also observed on and near the Greenland shelf, suggesting that these waters were a mixture of Arctic and Atlantic origin - a characteristic typical of waters off the West Greenland Current (De

Sève, 1999). Nonetheless, phytoplankton community structure differed from the Labrador Shelf, as the boreal prymnesiophyte *Phaeocystis pouchetii* was predominant in the eastern Labrador Sea (on and nearby the Greenland Shelf) during all study years, but was rarely observed on the Labrador Shelf. The reoccurring presence of *P. pouchetii* blooms in the central-eastern part of the Labrador Sea during spring is well-documented (Harrison et al., 2013; Head et al., 2000; Stuart et al., 2000, this study), suggesting that conditions in these waters are suitable for *P. pouchetii* growth every year (discussed below). *Pseudo-nitzschia granii*, a small needle-shaped diatom also observed in the eastern section of the Labrador Sea, had its distribution tightly linked to *P. pouchetii*, whose colonisation by the diatom species has been previously reported in Norwegian waters (Hasle and Heimdal, 1998; Sazhin et al., 2007). High abundances of *Chaetoceros socialis* (herein referred to as Cluster 6) could potentially have followed blooms of *P. pouchetii* and diatoms on the west Greenland Shelf. *Chaetoceros socialis* has frequently been found during the later stages of blooms in Arctic waters (e.g. Baffin Bay, von Quillfeldt, 2000), where they can grow at relatively low nutrient concentrations (particularly silicate) because of their small cell size (< 10 μm) and lightly silicified cell walls (Booth et al., 2002).

The diatom *Ephemera planamembranacea* was the most abundant species in offshore blooms observed in the central and central-western part of the Labrador Sea during June 2012 and 2014 (Fig. 2.6). This species, typically reported in high numbers in the North Atlantic (Semina, 1997; Barnard et al., 2004), has been previously associated with shallow mixed layers and relatively high nutrient concentrations (Yallop, 2001); similar to conditions found in this study (Fig. 2.7, Table 2.2). *Fragilariopsis atlantica* co-dominated with *E. planamembranacea* in the central Labrador Sea. Unlike *F. cylindrus* and *F. oceanica*, *F. atlantica* is not found in sea-ice, being restricted to the water column and is mainly found in the Northern Atlantic Ocean (Lundholm and Hasle, 2010). The centric diatom *Rhizosolenia hebetata* f. *semispina*, also a representative North Atlantic diatom, formed blooms in the central eastern portion of the Labrador Sea in the summer of 2014 (Fig. 2.6). High numbers of *Rhizosolenia hebetata* f. *semispina* were found in association with large (subgenus *Phaeoceros*, *Thalassiostrix longissima*) and medium-sized diatoms (e.g., *Chaetoceros decipiens*) in our study and have been previously observed in Norwegian waters (Hegseth and Sundfjord, 2008).

2.5.2 Environmental controls on *Phaeocystis* versus diatoms

In our study, all phytoplankton blooms were found in shallow mixed layers (median depth < 25 m) and stratified waters (median SI = 1 x 10^{-3} kg m^{-4}) (Table 2.2). However, during May 2014 a *P. pouchetii* bloom occurred in the eastern section of the Labrador Sea prior to the development of other phytoplankton blooms in the region. These *P. pouchetii* blooms were found in deeper mixed layers (~ 50 m) than in other years (data not shown). Whislt low irradiances are not required for *Phaeocystis* growth, given that it can also be found in shallow mixed layers (Fragoso, 2009; Fragoso and Smith, 2012), the ability to grow under low light levels may confer on this species an advantage compared to larger diatoms. *P. pouchetii* blooms have also been reported to occur earlier in the season (April) due to the earlier haline-driven stratification (Frajka-Williams et al., 2009; Frajka-Williams and Rhines, 2010; Head et al., 2000), when light levels are lower than in May or June and the mixed layer is still deep (< 100 m, Harrison et al., 2013).

Laboratory findings have also confirmed the ability of the southern ocean *Phaeocystis* species (*P. antarctica*) to grow faster and increase their photosynthetic efficiency under dynamic light intensities, typically found in deeper mixed layers (Arrigo et al., 2010a; Kropuenske et al., 2010, 2009; Mills et al., 2010). Because of their ability to grow under variable light, it is possible that *P. pouchetii* could grow and outcompete diatoms whislt the mixed layer depth shoals. As opposed to *P. pouchetii*, which is able to thrive under low light intensities, sea-ice diatoms (such as *F. cylindrus*) invest heavily in photoprotective mechanisms. This allows them to better adapt to higher light intensities, which are typically found in shallow mixed layers (Arrigo et al., 2010a; Kropuenske et al., 2010, 2009; Mills et al., 2010) as well as in late spring sea ice.

Nutrient resource competition has been suggested as one possible explanation for the spatial segregation of *Phaeocystis pouchetii* and diatom blooms in the Labrador Sea (Harrison and Li, 2008; Harrison et al., 2013) and elsewhere (Jiang et al., 2014). In our study, cylinder or ribbon-shaped chain diatoms (i.e. *Thalassiosira* spp., *Bacterosira bathyomphala* and *Fragilariopsis cylindrus*) dominated the Labrador Shelf waters. Such waters had only slightly higher Si* values compared to the Greenland Shelf (Cluster 1 compared to Cluster 5, see Table 2.2). Nonetheless, climatological studies show that the Labrador Shelf has a surplus of silicate (silicate minus nitrate, Si* > 0) in the upper 150 m that decreases eastward, which might explain the high number of diatoms in the west

(Harrison et al., 2013). In this study, a nitrate surplus of deep waters (~ 200 m) was evident across Labrador Sea shelves and basin (negative Si*); however, the Labrador Shelf and Slope had a higher surplus of silicate in deep waters compared to the central eastern section of the Labrador Sea (Fig. 2.4k,l). Hence, the availability of silicate in waters of the Labrador Shelf might influence the dominance of diatoms in this region as *P. pouchetii* does not require silicate, which could also be an explanation for the east-west taxonomic segregation. Silicate depletion, however, is not a necessary condition for *P. pouchetii* blooms, since it can co-dominate with diatoms when silicate is not limiting. Jiang et al. (2014) argued that, under conditions where *P. pouchetii* is dominant or co-dominant in a bloom, a sufficiently high pre-bloom concentration of nitrate (~ 8 μM for Massachusetts Bay) is needed (irrespective of the Si:N ratio). This would allow more time for this species to grow, given that *Phaeocystis* grows slower than diatoms (Jiang et al., 2014). Uptake rates of oxidised and reduced forms of nitrogen have also been considered as an explanation for contrasting *Phaeocystis* and diatom-dominated blooms in the North Sea, where *Phaeocystis* has been reported to have a greater advantage due to ammonium uptake compared with diatoms (Tungaraza et al., 2003). Ammonium concentration was greater in the central-eastern part of the Labrador Sea in this study (Fig. 2.4h), particularly in the Greenland Shelf and Slope during June, which could also have favoured the formation of *P. pouchetii* blooms in these waters.

Phaeocystis sp. colonies can control their buoyancy in the water column as a function of light levels (positive buoyancy under sufficient light conditions, Wang and Tang, 2010), which could also confer an advantage when accessing nutrients. In our study, *P. pouchetii* blooms on the Greenland Shelf were concentrated in the subsurface and sometimes below the mixed layer, being distributed within the upper 50 m, contrary to the diatom bloom on the Labrador Shelf which was restricted to the upper mixed layer (< 25 m) (Appendices A.1 and A.2). Similar to the results presented here, *Phaeocystis pouchetii* blooms have also been reported to be concentrated in subsurface waters around Greenland (Waniek et al., 2005; Frajka-Williams and Rhines, 2010) and are capable of reaching deeper waters in the Fram Strait (> 75 m in Vogt et al., 2012b).

Phaeocystis colonies may also be able to proliferate because of their ability to escape predation by size mismatch (Jakobsen and Tang, 2002; Tang, 2003), unpalatable and toxic substances production (Aanesen et al., 1998; Dutz et al., 2005) and poor nutritional value of their colony matrix (Tang et al., 2001). In the eastern region of the central Labrador Sea basin and in the Greenland slope and shelf regions, the copepod *Calanus finmarchicus* is

abundant in May-July (> 70,000 m^{-2}, 0-100 m, Head et al., 2003, 2013), where it dominates the biomass and is the most important grazer. Reports in the literature are somewhat contradictory as to whether *Phaeocystis* is a good food source for *Calanus* (see review by Nejstgaard et al., 2007), but most studies have been carried out with copepods and *Phaeocystis* from waters east of Greenland. In the northwest Atlantic, however, filtration rates for a mixed-species *Calanus* population from the Newfoundland Shelf were ~2.5 lower when they were feeding on natural seawater containing mainly *Phaeocystis* compared with when they were feeding on seawater that had a similar overall chlorophyll *a* concentration but contained a mixture of diatoms (Head and Harris, 1996).

2.5.3 Mixed layer depth, vertical stability and bloom development

Many studies of phytoplankton dynamics in the Labrador Sea have focused on how physical factors control the onset of the spring phytoplankton bloom (Wu et al., 2008a; Frajka-Williams et al., 2009; Frajka-Williams and Rhines, 2010; Lacour et al., 2015) . In our study, spring blooms in the Labrador Sea, irrespective of the hydrographic zone, occurred mostly in shallow mixed layers and areas of enhanced upper water column stratification, which suggests that vertical stability plays an important role in bloom development and maintenance. A similar observation was found by Wu et al. (2008a), who combined satellite-derived chlorophyll and historical data in modelling studies to confirm that mixed layer depth plays a critical role in initiating the spring bloom in the Labrador Sea. Whislt blooms occurring in and near the shelf regions were due to haline-driven stratification, thermal-stratification promoted blooms offshore, in the central Labrador Sea, as has been previously observed (Frajka-Williams et al., 2009; Head et al., 2013; Wu et al., 2008a).

Blooms have been reported to occur earlier along the eastern margin of the central basin, and/or on the Greenland shelf because of the relatively shallow winter mixed layer depth driven by haline stratification compared to the deep central basin (Frajka-Williams et al., 2009; Head et al., 2013). A more recent study using calculated mixed layer Photosynthetically Active Radiation (PAR) from Argo-floats and satellite observations showed that the mean PAR levels within the mixed layer (~ 2.5 mol photons m^{-2} d^{-1}) is the same during the initiation of the haline-driven bloom near the Greenland Shelf as it is in

the thermal driven bloom occurring in the central Labrador Sea, which starts one month later (Lacour et al., 2015). Although mean PAR values were not measured *in situ* but estimated from satellite and Argo-float observations, Lacour et al. (2015) concluded that increased light availability, driven by either thermal or haline stratification, seems to be strongly linked to bloom onset in the Labrador Sea. On the Labrador Shelf, shoaling of the mixed layer, resulting from melting ice, has previously been established as a major trigger of diatom blooms (Wu et al., 2007). However, in spite of a lack of sea ice on the Labrador shelf in May 2014, which could be an indication of sea ice melting, the mixed layer remained deep (~ 60 m), possibly due to strong winds.

2.6 Conclusions

In this study phytoplankton community structure from the Labrador Sea during spring and early summer of 2011 - 2014 varied according to the major hydrographic features (temperature, salinity and nutrient concentrations) of distinct water masses of Atlantic (Irminger Current), Arctic via Davis Strait (Labrador Current) or Arctic via Denmark Strait (West Greenland Current) origin. In spite of interannual variations, which in this study are difficult to assess because of the different sampling periods among years and short duration of analysed records, phytoplankton community structure in the Labrador Sea spring blooms had remarkably similar spatial and temporal patterns across the four years of sampling. Arctic/polar large (> 50 µm) diatoms dominated the blooms in the inshore branch of the LC, which were most influenced by Arctic and sea ice melt waters. *P. pouchetii* co-dominated with diatoms (*Pseudo-nitzschia granii*, *Thalassiosira* spp.) at the interface of the Arctic (WGC) and Atlantic (IC) waters. *Ephemera planamembranacea*, *Rhizosolenia hebetata* f. *semispina* and *Fragilariopsis atlantica* were the main species found in offshore waters of the central basin, which is strongly influenced by Atlantic waters. Lower salinities and temperatures were associated with the Arctic/polar species found in the shelf waters with higher influence of the Arctic outflow. Pre-bloom Si* (Si* from deeper waters), which were comparatively higher on the Labrador Shelf and Slopes, might have influenced the taxonomic segregation of polar diatoms dominating the west and *P. pouchetii* dominating the eastern blooms. Nonetheless, the reason why *P. pouchetii* forms large blooms in the central-eastern region of the Labrador Sea remains unclear.

In this study, shelf blooms occurred due to haline-driven stratification, whereas the central basin bloom occurred later (June), when higher surface temperatures promoted vertical stability. All blooms were found in shallow mixed layers (< 40 m) and more stratified waters, which confirms that vertical stability plays an important role in bloom development across the Labrador Sea. However, *Phaeocystis pouchetii* blooms were found in May 2014, when the mixed layer was deeper (median = 75 m). This confirms the ability of *P. pouchetii* to grow in deeper mixing layers, whereas Arctic/sea-ice diatom blooms were only found in shallower mixed layers (< 25 m).

Chapter 3: Spring phytoplankton communities of the Labrador Sea (2005-2014): pigment signatures, photophysiology and elemental ratios

Note: This Chapter has been submitted for publication in *Biogeosciences discussions* with the full reference: "Fragoso, G.M., Poulton, A.J., Yashayaev, I.M., Head, E.J.H., Purdie, D.A., 2016. Spring phytoplankton communities of the Labrador Sea (2005 - 2014): pigment signatures, photophysiology and elemental ratios. Biogeosciences Discuss. 1–43. doi:10.5194/bg-2016-295". G. M. F. was responsible for the pigment, particulate organic carbon and nitrogen analyses from the JR302 cruise (2014) as well as the statistical data analysis and CHEMTAX data processing. G. M. F. also prepared the first draft of the manuscript.

3.1 Abstract

The Labrador Sea is an ideal region to study the biogeographical, physiological and biogeochemical implications of shifts in phytoplankton communities due to sharp transitions of distinct water masses across its shelves and the central basin, intense nutrient delivery due to deep vertical mixing during winters and continual inflow of Arctic, Greenland melt and Atlantic waters. In this study, a decadal assessment (2005-2014) of late spring/early summer phytoplankton communities from surface waters of the Labrador Sea was provided based on pigment markers and CHEMTAX analysis, and their physiological and biogeochemical signatures. Diatoms were the most abundant group, blooming first in shallow mixed layers of haline-stratified Arctic shelf waters. Along with diatoms, chlorophytes co-dominated at the western end of the section (particularly in the polar waters of the Labrador Current (LC)), whilst *Phaeocystis* co-dominated in the east (modified polar waters of the West Greenland Current (WGC)). Pre-bloom conditions occurred in deeper mixed layers of the central Labrador Sea in May, where a mixed assemblage of flagellates (dinoflagellates, prasinophytes, prymnesiophytes, particularly coccolithophores, and chrysophytes/pelagophytes) occurred in low chlorophyll areas, succeeding to blooms of diatoms and dinoflagellates in thermally-stratified Atlantic waters in June. Light-saturated photosynthetic rates and saturation irradiance levels were higher at stations where diatoms were the dominant phytoplankton group (> 70 %), as opposed to stations where flagellates were more abundant (from 40 % up to 70 %). Phytoplankton communities from the WGC (*Phaeocystis* and diatoms) had lower light-limited photosynthetic rates, with little evidence of photo-inhibition, indicating greater tolerance to

a high light environment. By contrast, communities from the central Labrador Sea (dinoflagellates and diatoms), which bloomed later in the season (June), appeared to be more sensitive to high light levels. Ratios of accessory pigments (AP) to total chlorophyll *a* (TChl*a*) varied according to phytoplankton community composition, with polar phytoplankton (cold-water related) having lower AP to TChl*a* ratios. Phytoplankton communities associated with polar waters (LC and WGC) also had higher and more variable particulate organic carbon (POC) to particulate organic nitrogen (PON) ratios, suggesting the influence of detritus from freshwater input, derived from riverine, glacial and/or sea-ice meltwater. Long-term observational shifts in phytoplankton communities were not assessed in this study due to the short temporal frame (May to June) of the data. Nevertheless, these results have provided a baseline of current distributions and an evaluation of the biogeochemical role of spring phytoplankton communities in the Labrador Sea, which will improve our understanding of potential long-term responses of phytoplankton communities in high-latitude oceans to a changing climate.

3.2 Introduction

Marine phytoplankton form a taxonomically and functionally diverse group, with different requirements and modes of acquisition of light and nutrients, as well as strategies for resource competition and predation defence (Acevedo-Trejos et al., 2015; Bonachela et al., 2015; Falkowski, 2004). Thus, marine phytoplankton communities are structured by the overall fitness of individuals within species assemblages with respect to a variety of factors, including the physical setting, nutrient and light availability, dispersal, predation and competition for resources (Litchman and Klausmeier, 2008). Over large scales, environmental heterogeneity selects for phytoplankton assemblages, which creates biogeographical patterns of abundance, composition, traits and diversity distributions of phytoplankton communities in the global ocean (Barton et al., 2013a; Follows et al., 2007; Hays et al., 2005).

Phytoplankton communities also impact the structuring of marine ecosystems due to their functional community role in biogeochemical cycling, efficiency of carbon transport to deeper waters, palatability and transfer of energy to higher trophic levels. Diatoms, for example, are assumed to be the major contributor to the biological pump (Smetacek et al.,

2004), large *Phaeocystis* spp. (> 100 µm) colonies are apparently not grazed as efficiently as diatoms due to the exudation of mucilage (Haberman et al., 2003) and some cyanobacteria are able to fix nitrogen, which can provide a significant amount of nitrogen to the oligotrophic regions of the ocean (Barton et al., 2013a; Tyrrell, 1999). Distinct phytoplankton assemblages have been reported to influence differently particulate (Martiny et al., 2013a, 2013b; Smith and Asper, 2001) and dissolved elemental stoichiometry (C:N:P)(Weber and Deutsch, 2010), the drawdown of gases (Arrigo, 1999; Tortell et al., 2002) and the efficiency of carbon export (Guidi et al., 2009; Le Moigne et al., 2015). Patterns of phytoplankton stoichiometry appear to be consistent phylogenetically and within higher taxonomic levels (Ho et al., 2003; Quigg et al., 2003), although they may vary according to nutrient supply ratios (Bertilsson et al., 2003; Rhee, 1978), as well as phenotypically within species across the same population (Finkel et al., 2006). However, detritus and dead plankton material also influence overall particulate C:N:P ratios in the ocean, which complicates the interpretation of *in situ* observations of phytoplankton elemental stoichiometry (Martiny et al., 2013a).

The sub-Arctic North Atlantic is a complex system with contrasting hydrography that structures plankton communities within distinct biogeographical provinces (Fragoso et al., 2016b; Head et al., 2003; Li and Harrison, 2001; Platt et al., 2005; Sathyendranath et al., 2009, 1995). The Labrador Sea is a particularly interesting region to study the biogeographical and biogeochemical implications of phytoplankton communities due to the sharp transitions of distinct water masses across its shelves and basin (Yashayaev, 2007). Biogeographical regions of the Labrador Sea shape zooplankton (Head et al., 2000; Lutz et al., 2003) and phytoplankton community composition (Fragoso et al., 2016b), cell size (Platt et al., 2005) and bio-optical properties (Cota, 2003; Lutz et al., 2003; Platt et al., 2005; Sathyendranath et al., 2004; Stuart et al., 2000), as well as the seasonality of phytoplankton blooms (Frajka-Williams and Rhines, 2010; Lacour et al., 2015; Wu et al., 2007; Wu et al., 2008a). More recently, Fragoso et al. (2016) showed that the biogeography of phytoplankton communities in the Labrador Sea is shaped by specific species as indicators of Atlantic or Arctic waters, emphasising the potential importance of using phytoplankton composition as indicators of water masses.

Phytoplankton communities within a biogeographical region are subject to similar environmental conditions, such as temperature (Bouman et al., 2003), nutrient concentration (Browning et al., 2014) and irradiance (Arrigo et al., 2010a), and these, along with community composition (Bouman et al., 2005), affect their overall

photophysiological response. It has been suggested that irradiance (light levels and day length) and temperature are the primary factors that influence phytoplankton photophysiology in high-latitude Arctic/Atlantic waters, including the Labrador and Barents seas and Baffin Bay (Platt et al., 1982; Rey, 1991; Subba Rao and Platt, 1984), while the influence of phytoplankton composition on photophysiological patterns has not been investigated thoroughly.

Quantification of marine phytoplankton community composition, for large numbers of samples, is challenging if the time-consuming methods of microscopic identification and enumeration are employed. Moreover, small cells (< 5µm) are difficult to identify and count using light microscopy. To overcome these problems, quantification and analyses of phytoplankton pigments by high performance liquid chromatography (HPLC) has been widely used to monitor phytoplankton community distributions over large temporal and spatial scales (e.g., Aiken et al., 2009; Peloquin et al., 2013; Platt et al., 2005). Photosynthetic pigments (chlorophylls and carotenoids) are frequently used to identify taxonomic and functional groups. Pigment-based chemotaxonomy can be used to determine phytoplankton classes (Coupel et al., 2015, 2012; Gonçalves-Araujo et al., 2012), functional cell sizes (Aiken et al., 2009; Platt et al., 2005; Poulton et al., 2006) and assemblage dominance using accessory pigment ratios (Fragoso and Smith, 2012). The interpretation of the pigment data is not always straightforward, however, since some pigments are shared by several algal groups and can change according to local nutrient and light conditions (DiTullio et al., 2007; van Leeuwe and Stefels, 2007, 1998). The chemotaxonomic tool, CHEMTAX (CHEMical TAXonomy), provides a valuable approach to estimate phytoplankton class abundances when used in conjunction with microscopic information (Irigoien et al., 2004b; Mackey et al., 1996; Wright et al., 1996). CHEMTAX has the advantage of providing more information about phytoplankton classes than individual diagnostic pigments or ratios, and has been used widely to investigate phytoplankton biogeography on regional scales (Muylaert et al., 2006; Wright and Van den Enden, 2000) and globally (Swan et al., 2015).

In this study, the multi-year (2005-2014) distributions of late spring and early summer (May to June) phytoplankton communities in the various hydrographic settings across the shelves, slopes and deep basin of the Labrador Sea based on phytoplankton pigments was investigated. In addition, the overall photophysiological and biogeochemical traits associated with these phytoplankton communities was examined. Long-term analyses of phytoplankton communities and their potential biogeochemical and physiological

signatures are needed to comprehensively understand current conditions and to project possible responses of these communities to climate change. The results presented here will improve our understanding of potential long-term changes of phytoplankton communities in high-latitude oceans and provide a baseline description of the current distributions and biogeochemical traits of phytoplankton communities in the Labrador Sea with which future observations can be compared.

3.3 Methods

3.3.1 Study area

The Labrador Sea is a high latitude marginal sea located in the northwestern part of the Atlantic Ocean and is a transition zone of the Arctic and sub-Arctic ecosystems. It is bounded by Davis Strait to the north, Newfoundland to the south, the Labrador Coast of Canada to the west and Greenland to the east (Fig 3.1). The bathymetry of the Labrador Sea can be subdivided into the wide continental shelf and relatively gentle continental slope on its western side (the Labrador Shelf, > 500 km and < 250 m deep), narrow shelf and very steep continental slope on the eastern side (the Greenland Shelf, < 100 km and < 2500 m deep) and the deep basin (> 3000 m deep) confined by the continental slopes (Fragoso et al., 2016b).

The central deep basin (> 3000 m) of the Labrador Sea contains a counter-clockwise flow and is comprised of a mixture of, mostly, relatively warm and salty waters originating from the Atlantic, which is mainly identified as the Irminger Current (IC) and cold fresh water, originating from the Arctic *via* the surrounding shelves (Fig 3.1). The inshore branch of the Labrador Current (LC) overlies the Labrador Shelf and includes Arctic water originating from Baffin Bay and the Canadian Arctic Archipelago *via* Davis Strait and from Hudson Bay *via* Hudson Strait, together with inputs of melting sea ice, which originate locally or from farther north. The main branch of the Labrador Current flows along the Labrador slope from north to south and is centred at the 1000 m contour. It is composed of a mixture of Arctic water from Baffin Bay *via* Davis Strait and the branch of the West

Greenland Current that flows west across the mouth of Davis Strait. The West Greenland Current (WGC), which flows from south to north on the Greenland shelf and along the adjacent slope, is a mixture of cold, low salinity Arctic water exiting the Nordic Seas with the East Greenland Current (EGC) (Yashayaev, 2007), together with sea ice and glacial melt waters (Fig 3.1). More detailed descriptions of the hydrography of the Labrador Sea can be found elsewhere (Fragoso et al. 2016, Head et al.2013, Yashayaev and Seidov 2015, Yashayaev 2007).

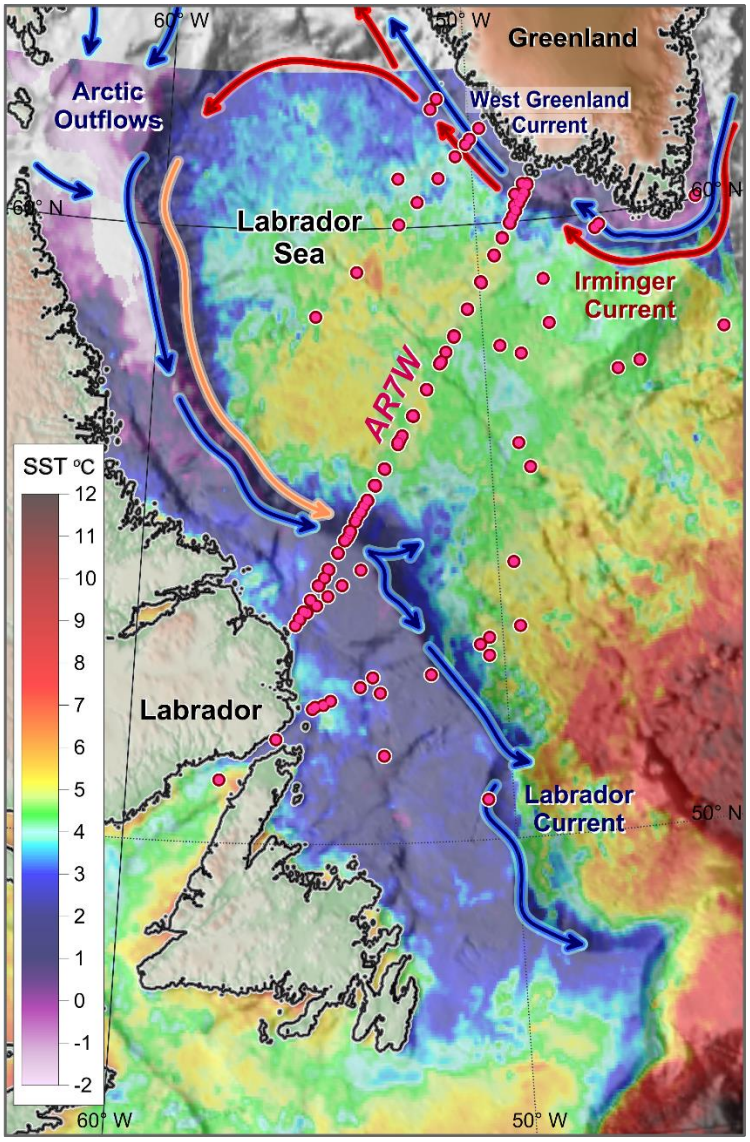

Figure 3.1 Map showing stations along the AR7W transect and additional stations sampled during late spring and early summer (2005–2014). The station positions are superimposed on a composite image of sea surface temperature for the last three weeks of May 2006 collected by the NOAA satellite (AVHRR). White patches represent ice (Labrador and Greenland coasts).

3.3.2 Sampling

Data for this study were obtained from stations along the AR7W Labrador Sea repeat hydrography line (World Ocean Circulation Experiment Atlantic Repeat 7-West section, for details see Fragoso et al., 2016), which runs between Misery Point on the Labrador coast (through Hamilton Bank on the Labrador Shelf) and Cape Desolation on the Greenland coast. Stations were sampled for over a decade (2005-2014) by scientists from the Canadian Department of Fisheries and Oceans during late spring and/or early summer (Table 3.1). Fixed stations were sampled on the AR7W section, across shelves and in the deep central basin, as well as some additional non-standard stations (Fig. 3.1).

Table 3.1 Research cruises, sampling dates and number of samples per cruise (n) where pigment data were collected in the Labrador Sea during early spring and late summer (2005-2014).

Cruise	Dates	Year	n
HUD-2005-16	29 May - 3 June	2005	25
HUD-2006-019	23 May - 31 May	2006	12
HUD-2007-011	11 May - 21 May	2007	32
HUD-2008-009	22 May - 29 May	2008	25
HUD-2009-015	18 May - 23 May	2009	26
HUD-2010-014	14 May - 24 May	2010	27
HUD-2011-009	11 May - 17 May	2011	33
HUD-2012-001	3 June - 11 June	2012	30
HUD-2013-008	9 May - 21 May	2013	27
JR302	10 June - 24 June	2014	16

Vertical profiles of temperature and salinity were measured with a Seabird CTD system. Water samples were collected using 10-L Niskin bottles mounted on the rosette frame. Mixed layer depths were calculated from the vertical density (σ_Θ) distribution and defined as the depth where σ_Θ changes by 0.03 kg m^{-3} from a stable surface value (~10 m) (Weller

and Plueddemann, 1996). A stratification index (SI) was calculated as the seawater density difference (between 10 m to 60 m) normalised to the equivalent difference in depth.

Water samples from the surface (near-surface) layer (< 10 m) were collected (0.5 L–1.5 L) for the determination of chlorophyll *a*, accessory pigments, nutrients, particulate organic carbon (POC) and nitrogen (PON) analysis, and for primary production measurements. Bulk chlorophyll *a* concentration was measured after extraction from filters in 90 % acetone at -20°C for approximately 24 hours and fluorescence was determined using a Turner Designs fluorometer (Holm-Hansen et al., 1965). Samples for detailed pigment analysis were filtered onto 25 mm glass fibre filters (GF/F Whatman Inc., Clifton, New Jersey) and immediately flash frozen in liquid nitrogen and kept frozen in a freezer (at -80° C) until analysis in the laboratory. Nutrient samples were analysed at sea (within 12 h of collection) on the SEAL AutoAnalyser III. Samples for POC and PON were filtered (0.25–1 L) onto 25 mm pre-combusted GF/F filters and frozen (-20^{o} C) and returned to the laboratory for later analysis. In the laboratory samples were oven-dried (60 ^{o}C) for 8-12 hours, stored in a dessicator, pelletelised in pre-combusted tin foil cups and analysed using a Perkin Elmer 2400 Series CHNS/O analyser as described in Pepin and Head (2009).

3.3.3 Pigment analysis

Pigments (chlorophyll *a* and accessory pigments) were quantified using reverse-phase (Beckman C18, 3 μm Ultrasphere column), High-Performance Liquid Chromatography (HPLC) according to the procedure described in Stuart and Head (2005), known as the "BIO method". Prior to analysis, pigments were extracted by homogenizing the frozen filters in 1.5 mL 95 % acetone, grinding the filters using a motorized grinder, centrifuging to remove the solids and taking an aliquot of the supernatant, which was buffered by dilution with 0.5 M aqueous ammonium acetate at a ratio of 2:1 before injection on to the column. The samples were run using a gradient elution method, with methanol, aqueous ammonium acetate and ethyl acetate as solvents (Stuart and Head 2005). Pigment peaks were identified and quantified by their retention times and absorbance or fluorescence signals, by comparison with those of pure pigments (Stuart and Head, 2005). A list of pigments identified and quantified for this study is included in Table 3.2.

Table 3.2 List of phytoplankton pigments and their distributions in algae classes, abbreviations and formulas.

Abbreviation	Name	Characteristic of the pigment	Present in/ Index of/Formula	Ref.
PSC	Photosynthetic carotenoid	Light harvesting	All algae	
PPC	Photoprotective carotenoid	Photoprotection	All algae	
PPP	Photosynthetic pigment	Light harvesting	All algae	
BUT19	19'-butanoyloxyfucoxanthin	PSC	Prymnesiophytes and crysophytes	1
HEX19	19'-hexanoyloxyfucoxanthin	PSC	Diatoms, prymnesiophytes and some dinoflagellates	2
ALLOX	Alloxanthin	PPC	Cryptophytes	1
ACAROT	α-carotene	PPC	Various	1
BCAROT	β-carotene	PPC	Various	1
CHLB	Chlorophyll *b*	PPP	Chlorophytes, prasinophytes, euglenophytes	1
CHLC12	Chlorophyll $c_1 + c_2$	PPP	Diatoms, prymnesiophytes, dinoflagellates, chrysophytes and raphidophytes	1
CHLC3	Chlorophyll c_3	PPP	Prymnesiophytes, chrysophytes	1
CHLIDEA	Chlorophyllide *a*	Degradation product of CHLA	Senescent phytoplankton	
DIADINOX	Diadinoxanthin	PPC	Diatoms, prymnesiophytes, dinoflagellates, chrysophytes and raphidophytes	1
DIATOX	Diatoxanthin	PPC	Diatoms, prymnesiophytes, dinoflagellates, chrysophytes and raphidophytes	1
FUCOX	Fucoxanthin	PSC	Diatoms, prymnesiophytes, raphidophytes and some dinoflagellates	1
CHLA	Chlorophyll *a*	PPP	All phytoplankton except *Prochlorococcus*	1
PERID	Peridinin	PSC	Some dinoflagellates	1
PRASINO	Prasinoxanthin	PPC	Some prasinophytes	1
VIOLAX	Violaxanthin	PPC	Chlorophytes, prasinophytes and eustigmatophytes	1
ZEA	Zeaxanthin	PPC	Cyanobacteria, *Prochlorococcus*, chlorophytes	1
TChl*a*	Total chlorophyll *a*		CHLA + CHLIDEA	
TC	Total carotenoids	Include all carotenoids	BUT19 + HEX19 + ALLOX + ACAROT + BCAROT + DIADINOX + DIATOX + FUCOX + PERID + PRASINO +	
AP	Accessory pigments	Include all pigments except CHLA	TC + CHLB + CHLC12 + CHLC3	
FUCOX/AP	Fucoxanthin to accessory pigments ratio		FUCOX/AP	

[1](Jeffrey et al., 1997), [2](Higgins et al., 2011).

3.3.4 Pigment interpretation

The CHEMTAX software (version 1.95, Mackey et al., 1996) was used to estimate ratios of abundance of distinct micro-algal classes to total chlorophyll *a* from *in situ* pigment measurements. The software utilises a factorization program that uses "best guess" ratios of accessory pigments to chlorophyll *a* that are derived for different classes from the literature and marker pigment concentrations of algal groups that are known to be present in the study area. This program uses the steepest descent algorithm to obtain the best fit to the data based on assumed pigment to chlorophyll *a* ratios. The initial matrices are optimized by generating 60 further pigment ratio tables using a random function (RAND in Microsoft Excel) as described in Coupel et al. (2015). The results of the six best output matrices (with the smallest residuals, equivalent to 10 % of all matrices) were used to calculate the averages of the abundance estimates and final pigment ratios. The following pigment chosen for CHEMTAX analysis were: 19-butanoyloxyfucoxanthin (BUT19), 19-hexanoyloxyfucoxanthin (HEX19), alloxanthin (ALLOX), chlorophyll *a* (CHLA), chlorophyll *b* (CHLB), chlorophyll *c*3 (CHLC3), fucoxanthin (FUCOX), peridinin (PERID), prasinoxanthin (PRASINO) and zeaxanthin (ZEA).

One of the main assumptions of the CHEMTAX method is that pigment ratios remain constant across the subset of samples that are being analysed (Swan et al., 2015). To satisfy this assumption, *a priori* analysis was performed, where pigment data were sub-divided into groups using cluster analysis (Bray-Curtis similarity) and each group was processed separately by the CHEMTAX program (Table 3.3). This approach was used because distinct phytoplankton communities have been observed in the Labrador Sea (Fragoso et al., 2016b) so that the ratio of accessory pigment to chlorophyll *a* probably varies within different water masses across the Labrador Sea (LC, IC and WGC). Pigment concentration data (BUT19, HEX19, ALLOX, CHLA, CHLB, CHLC3, FUCOX, PERID, PRASINO and ZEA) were standardized and fourth-root transformed before being analysed.

A first cluster analysis on transformed pigment data identified five major groups having 60 % similarity between samples. Clusters included stations partially located: 1) on the shelves, where FUCOX dominated at a few stations (I), 2) in the eastern part of the Labrador Sea, where most stations had high relative concentrations of FUCOX and CHLC3 (II), 3) in the central Labrador Sea, where a few stations had higher proportions of FUCOX, HEX19 and PERID (III), 4) on the western part of the section, where CHLB and

FUCOX were the main pigments at most stations (IV) and 5) in the central Labrador Sea, where most stations had a mixture of pigments (FUCOX, CHLC3, HEX19, CHLB, PERID and others) (V) (Fig 3.2). The other main requirement of the CHEMTAX method is that information about the phytoplankton taxonomy is used to assure that the pigment ratios are applied and interpreted correctly (Irigoien et al., 2004b). To satisfy this requirement, initial pigment ratios were carefully selected and applied to each cluster to adjust the pigments to the appropriate classes according to microscopic observations (Fragoso et al., 2016b) and literature information (see Table 3.3). Pigment ratio tables were based on the literature in waters having comparable characteristics to the Labrador Sea, such as Baffin Bay (Vidussi et al., 2004), the Beaufort Sea (Coupel et al., 2015) and the North Sea (Antajan et al., 2004; Muylaert et al., 2006) or from surface (high light) field data (Higgins et al., 2011) (Table 3.3).

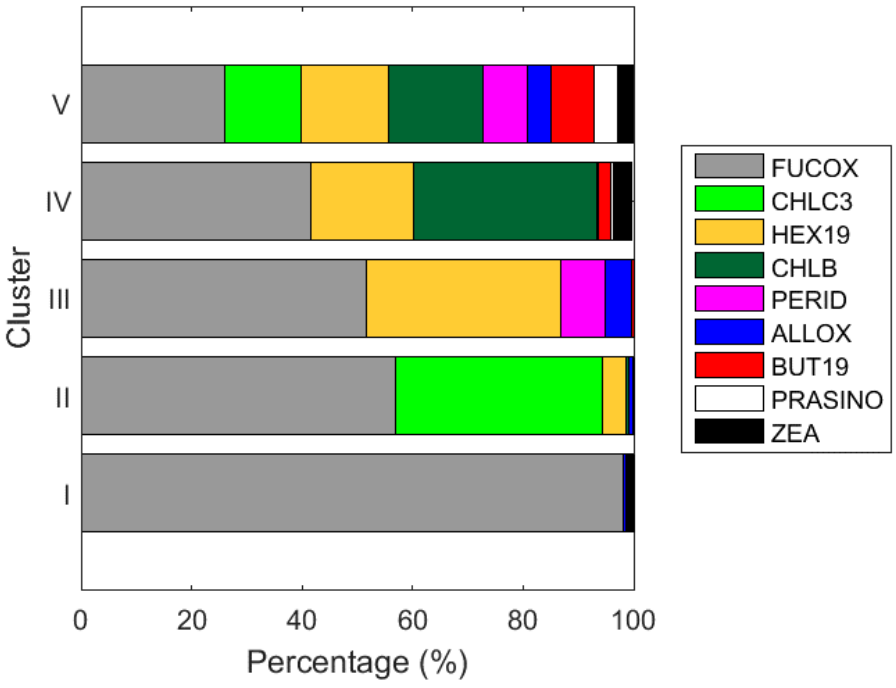

Figure 3.2 Percentage contribution of each pigment to the similarity of sampled stations in different clusters (I-V). Pigment abbreviations are described in Table 3.2.

Table 3.3 Final ratio matrix of accessory pigment to chlorophyll *a* for distinct algal classes for each cluster group.

Region	I & II (Eastern Labrador Sea)										
Class / Pigment	CHLB	CHLC3	FUCOX	PERID	ZEA	ALLOX	BUT19	HEX19	PRASINO	CHLA	Ref
Prasinophyte 1	0.459	0	0	0	0	0	0	0	0.075	1	2
Prasinophyte 2	0.650	0	0	0	0.008	0	0	0	0	1	2
Chlorophyte	0.168	0	0	0	0.040	0	0	0	0	1	2
Dinoflagellates	0	0	0	0.609	0	0	0	0	0	1	2,5
Cryptophycea	0	0	0	0	0	0.785	0	0	0	1	2
Phaeocystis	0	0.167	0.188	0	0	0	0	0	0	1	1
HAPTO-6	0	0.199	0.270	0	0	0	0.021	1.261	0	1	4
Chryso/Pelagophyte	0	0.120	0.454	0	0	0	0.589	0	0	1	2
Cyanobateria	0	0	0	0	0.262	0	0	0	0	1	3
Diatoms	0	0	0.328	0	0	0	0	0	0	1	2
Region	III & V (Central Labrador Sea)										
Class / Pigment	CHLB	CHLC3	FUCOX	PERID	ZEA	ALLOX	BUT19	HEX19	PRASINO	CHLA	Ref
Prasinophyte 1	0.316	0	0	0	0	0	0	0	0.129	1	2
Prasinophyte 2	0.716	0	0	0	0.008	0	0	0	0	1	2
Chlorophyte	0.171	0	0	0	0.025	0	0	0	0	1	2
Dinoflagellates	0	0	0	0.681	0	0	0	0	0	1	2,5
Dino-2	0	0.290	0.348	0	0	0	0.060	0.168	0	1	4
Cryptophycea	0	0	0	0	0	0.674	0	0	0	1	2
HAPTO-6	0	0.081	0.202	0	0	0	0.018	1.549	0	1	4
Chryso/Pelagophyte	0	0.049	0.184	0	0	0	0.264	0	0	1	2
Cyanobateria	0	0	0	0	0.142	0	0	0	0	1	3
Diatoms	0	0	0.512	0	0	0	0	0	0	1	2
Region	IV (Western Labrador Sea)										
Class / Pigment	CHLB	CHLC3	FUCOX	PERID	ZEA	ALLOX	BUT19	HEX19	PRASINO	CHLA	Ref
Prasinophyte 1	0.216	0	0	0	0	0	0	0	0.078	1	2
Prasinophyte 2	1.081	0	0	0	0.012	0	0	0	0	1	2
Chlorophyte	0.113	0	0	0	0.045	0	0	0	0	1	2
Dinoflagellates	0	0	0	0.785	0	0	0	0	0	1	2,5
Dino-2	0	0.028	0.049	0	0	0	0.018	0.040	0	1	4
Cryptophycea	0	0	0	0	0	0.703	0	0	0	1	2
HAPTO-7	0	0.030	0.389	0	0	0	0	1.218	0	1	4
Chryso/Pelagophyte	0	0.056	0.470	0	0	0	0.613	0	0	1	2
Diatoms	0	0	0.343	0	0	0	0	0	0	1	2

[1](Antajan et al., 2004)**, [2]**(Vidussi et al., 2004)**, [3]**(Muylaert et al., 2006)**, [4]**(Higgins et al., 2011)**, [5]**(Coupel et al., 2015)

Prasinophytes were separated into "prasinophyte type 1", which contains PRASINO and "prasinophyte type 2", such as *Pyramimonas* and *Micromonas*, with the latter previously found lacking PRASINO but containing ZEA in North Water Polynya (Canadian Arctic) (see Vidussi et al., 2004). Both genera were observed in light microscope counts in Labrador Sea samples (Fragoso et al., 2016b) and *M. pusilla* has been observed in the Beaufort Sea (Coupel et al., 2015), and was found to be one of the main pico-eukaryotes in the North Water Polynya (Canadian Arctic) from April to July of 1998 (Lovejoy et al., 2002). In addition to prasinophytes type 2, ZEA is also the major accessory pigment of cyanobacteria, such as *Synechococcus* spp., which has been previously observed in the Labrador Sea, particularly in Atlantic waters (Li et al., 2006), and which is also a minor pigment in chlorophytes (Vidussi et al., 2004). Because of its association with the warmer Atlantic waters, it was assumed that cyanobacteria were absent from very cold waters, such as the Labrador Current (Fragoso et al., 2016b). Prasinophytes contain CHLB, but so do chlorophytes (Vidussi et al., 2004), which were observed in large numbers with the microscope. Dinoflagellates were separated into those species that contain PERID, such as *Heterocapsa* sp. and *Amphidium* (Coupel et al., 2015; Higgins et al., 2011) and those that do not, such as *Gymnodinium* spp. (here defined as Dino-2 class as in Higgins et al. (2011)), but which may contain CHLC3, BUT19, HEX19 and FUCOX. Dinoflagellates were observed in lower concentrations in the eastern Labrador Sea, so that Dino-2 was assumed absent from this area (clusters I & II in Table 3.3). Cryptophytes (Cryptophycea in Table 3.3) are the only group to contain ALLOX.

Prymnesiophytes were divided into three groups: 1) *Phaeocystis pouchetii*, which was observed in high concentrations in the eastern Labrador Sea (Fragoso et al., 2016b) (clusters I & II, Table 3.3); 2) Prymnesiophyte HAPTO-7 (as in Higgins et al. (2011)), associated with *Chrysocromulina* spp. previously observed in the western Labrador Sea (in the Labrador Current, this study) (cluster IV, Table 3.3) and HAPTO-6 (as in Higgins et al. (2011)), which included the coccolithophores, particularly *E. huxleyi* associated with Atlantic waters (central-eastern region of the Labrador Sea) (clusters I, II, III and V, Table 3.3). *Phaeocystis pouchetii* occurred in waters having low HEX19 and BUT19 concentrations and high CHLC3 and FUCOX concentrations (cluster II, Fig. 3.2). Similar pigment compositions were found in *Phaeocystis globosa* blooms in Belgian Waters (Antajan et al., 2004; Muylaert et al., 2006) and high ratios of CHLC3 to CHLA were, previously, used to identify *Phaeocystis pouchetii* in the Labrador Sea (Stuart et al., 2000). Thus, CHLC3 and FUCOX were the only pigments that could be used to represent this

species. In addition to CHLC3 and FUCOX, HAPTO-7 included HEX19 and HAPTO-6 included HEX19 and BUT19 as in Higgins et al. (2011). Chrysophytes and pelagophytes, such as *Dictyocha speculum* have high ratios of BUT19 to CHLA (Coupel et al., 2015; Fragoso and Smith, 2012). Finally, diatoms were identified as containing high FUCOX:CHLA ratios (Vidussi et al., 2004) (Table 3.3).

3.3.5 Photosynthesis versus irradiance (P-E) incubations

Water samples were spiked with ^{14}C-bicarbonate and incubated in a light box under 30 different irradiance levels (from 1-600 W m^{-2}) at *in situ* temperature for 2 to 3 hours to measure parameters derived from photosynthesis versus irradiance (P-E) curves as described by Stuart et al. (2000). Measurements were fitted to the equation of (Platt and Gallegos, 1980, see Appendix B for more information) to determine the initial slope of the P-E curve, also known as the photosynthetic efficiency (α^B), the maximum photosynthetic rate normalized to chlorophyll biomass (P_m^B), the light intensity approximating the onset of saturation (E_k), the saturation irradiance (E_s) and the photo-inhibition parameter (β).

3.3.6 Statistical analysis

3.3.6.1 Phytoplankton-derived POC estimation

Fragoso et al. (2016) found a significant linear relationship between phytoplankton carbon calculated from phytoplankton cell counts and POC data using results from 2011-2014 surveys in the Labrador Sea ($POC = 1.01POC_{phyto} + 240.92$; $r^2 = 0.47$; $n = 44$; $p < 0.0001$). To estimate phytoplankton-derived carbon (POC_{phyto}) concentration (as opposed to total POC, which includes detritus and heterotrophic organisms), regression analysis was performed ($POC_{phyto} = 38.9Chl\textit{a}$; $r^2 = 0.9$; $n = 41$; $p < 0.0001$) using the carbon calculated from cell counts (derived from Fragoso et al., 2016) and measurements of total chlorophyll

a: this expression was then applied to estimate POC_{phyto} for stations where phytoplankton cell counts were not available (2005-2010).

3.3.6.2 Phytoplankton community structure

Phytoplankton community structure derived from pigment concentrations was investigated using PRIMER-E (v7) software (Clarke and Warwick, 2001). Chlorophyll *a* concentrations derived for each algal class resulting from CHEMTAX analysis were standardized (converted to percentage values) to obtain their relative proportions, which were fourth-root transformed to allow the least abundant groups to contribute to the analysis. Similarity matrices were generated from Bray-Curtis similarity for cluster analysis. A SIMPER (SIMilarity PERcentages) routine with a cut off of 90 % cumulative contribution to the similarity was used to reveal the contributions of each class to the overall similarity within clusters. One-way ANOSIM was also applied to determine whether taxonomic compositions of the clusters were significantly different.

A redundancy analysis (RDA) using the CANOCO 4.5 software (CANOCO, Microcomputer Power, Ithaca, NY) was performed to analyse the effects of environmental factors on the Labrador Sea phytoplankton community structure as described in Fragoso et al. (2016). Data were log-transformed and forward-selection (*a posteriori* analysis) identified the subset of environmental variables that significantly explained the taxonomic distribution and community structure when analysed individually (λ_1, marginal effects) or when included in a model where other forward-selected variables were analysed together (λa, conditional effects). A Monte Carlo permutation test (n=999, reduced model) was applied to test the statistical significance ($p < 0.05$) of each of the forward-selected variables.

3.4 Results

3.4.1 Environmental variables

Environmental parameters, as well as chlorophyll *a* (Chl*a*) concentrations varied noticeably along the southwest-northeast section of the Labrador Sea (Fig. 3.3). The shelf and slope regions (LSh, LSl, GSl, GSh) had colder and fresher waters (< 3 °C and < 33.5, respectively) compared to the central basin (CB), where surface waters were saltier (> 33.5) and warmer (> 3 °C), particularly in 2005, 2006, 2012 and 2014 (> 5 °C) (Fig. 3.3b, c). Shelf waters that were colder and fresher were the most highly stratified (SI > 5×10^{-3} kg m^{-4}), particularly on the Labrador Shelf (SI > 15×10^{-3} kg m^{-4}), whereas waters from the CB were less well stratified (SI < 5×10^{-3} kg m^{-4}), except at those stations where waters were slightly warmer than usual (> 5°C) during 2005, 2012 and 2014 (Fig. 3.3d). Chl*a* concentrations were higher (> 4 mg Chl*a* m^{-3}) at stations where waters were more highly stratified, particularly on the shelves (Fig. 3.3e). Nitrate, phosphate and silicate concentrations were inversely related to Chl*a* concentration, being lower (< 5, 0.5, 3 µmol L^{-1}, respectively) on the shelves and, during some years, in the CB (e.g. 2012), where blooms formed (Fig. 3.3e-h). POC:PON ratios were also higher (> 8) at most stations in shelf and slope waters and at a few stations in the CB during 2009 and 2011 (Fig. 3.3i). Shelf waters mostly had higher silicate:nitrate ($Si(OH)_4$:NO_3^-) ratios (> 1) than the CB, particularly the LSh (Fig. 3.3j). Labrador Sea surface waters usually had nitrate:phosphate (NO_3^-:PO_4^{3-}) < 16, although NO_3^-:PO_4^{3-} were higher in the CB than in shelf regions (> 10) (Fig. 3.3k).

3.4.2 CHEMTAX interpretation and group distributions

A cluster analysis of algal classes derived from CHEMTAX results revealed clusters of stations at various similarity levels (Fig. 3.4). ANOSIM one-way pairwise analysis between clusters suggested that they were significantly different in pigment algal composition ($p = 0.001$), although pairwise analysis of clusters C3a and C3b showed that these groups overlapped (more similar composition, R statistic = 0.33) than other clusters, which were clearly separated (R statistic values approached 1) (see Clarke and Warwick, 2001). The first division occurred at 61 %, separating three main clusters (A, B and C) (Fig. 3.4a). Cluster C was subdivided at 65 % resulting in clusters C1, C2 and C3 (Fig. 3.4a). A third division (similarity of 73 %) occurred at cluster C3 resulting in two other clusters C3a and C3b (Fig. 3.4a). Overall, six functional clusters (A, B, C1, C2, C3a and C3b) represented the distinct phytoplankton communities occurring in the Labrador Sea (Fig. 3.4a). These communities generally occupied different regions of the Labrador Sea, namely the Labrador Shelf/Slope (west, mainly Cluster C3a), Central Basin (middle, mainly Clusters C2 or C3b) and the Greenland Shelf/Slope (east, mainly Clusters C3a, A, B) (Fig. 3.4b,c).

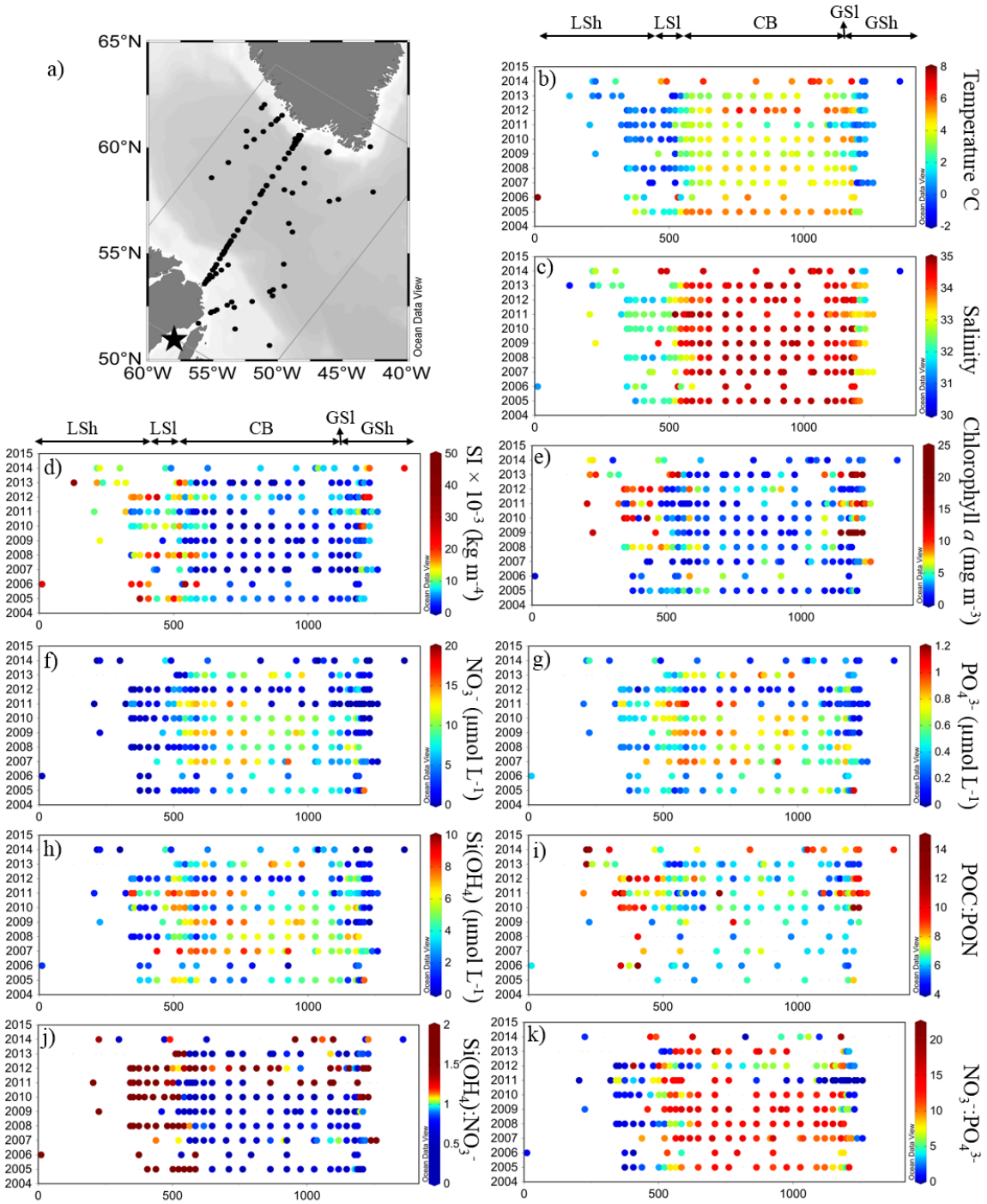

Figure 3.3 Values for environmental variables (temperature, salinity, stratification index (SI)), concentrations of nutrients (nitrate (NO_3^-), silicate ($Si(OH)_4$), phosphate (PO_4^{3-})), chlorophyll *a* and ratios between nutrients and for particulate organic carbon (POC) to particulate organic nitrogen (PON) at individual stations sampled between 2005 and 2014 (y-axis) and distances from a fixed reference position in the Northeast Gulf of St Lawrence shown by the star in Figure 3.3a (x-axis). LSh = Labrador Shelf, LSl = Labrador Slope, CB = Central Basin, GSl = Greenland Slope, GSh = Greenland Shelf.

Chl*a* concentrations were higher at stations where diatoms were especially dominant (Fig. 3.4b,c). Diatoms were the most abundant phytoplankton group in Labrador Sea waters, particularly at stations on the shelves, where communities were sometimes composed of almost 100 % diatoms (clusters A and C1) (Fig. 3.4b,c). Diatoms were also abundant at (or near to) the Greenland Shelf, where *Phaeocystis* was co-dominant (cluster B) and at (or near to) the Labrador Shelf in the west section, where chlorophytes were the second most abundant group (cluster C3a). Likewise, diatoms were dominant in the central Labrador Sea in some years (2008, 2012 and 2014, cluster C2), where dinoflagellates were also dominant (Fig. 3.4b,c). Most stations in the central basin had low Chl*a* concentrations and high diversity of algal groups (cluster C3b), with mixed assemblages of diatoms, dinoflagellates and other flagellates (Fig. 3.4b,c). The positions of fronts, usually characterised by sharp transitions in phytoplankton communities varied from year to year, but were generally located near the continental slopes (Fig. 3.4c).

3.4.3 Phytoplankton distributions and environmental controls

Distributions of surface phytoplankton communities in the Labrador Sea during spring and early summer (2005-2014) varied according to the water mass distributions across the shelves and central basin of the Labrador Sea. Potential temperatures and salinities also varied among these water masses (Fig. 3.5a). In general, chlorophytes and diatoms (cluster C3a) were associated with the inshore branch of the Labrador Current (LC), on the Labrador Shelf, where the surface waters were fresher (salinity < 33.5), colder (temperature < 2°C) and least dense (σ_Θ of most stations approximately < 26.5 kg m^{-3}) (Fig. 3.5a). Mixed assemblages (cluster C3b), as well as blooms (chlorophyll average = 4 mg Chl*a* m^{-3}) of dinoflagellates and diatoms (cluster C2) were associated with the warmer (temperature > 3°C), saltier (salinity > 34) and denser (σ_Θ of most stations < 27 kg m^{-3}) Atlantic water mass, and the Irminger Current (IC) (Fig. 3.5a). *Phaeocystis* (cluster B) dominated in waters of the West Greenland Current (WGC), which had intermediate temperatures (mostly 0-4°C) and salinities (33-34.5) when compared to those of the LC and IC (Fig. 3.5a).

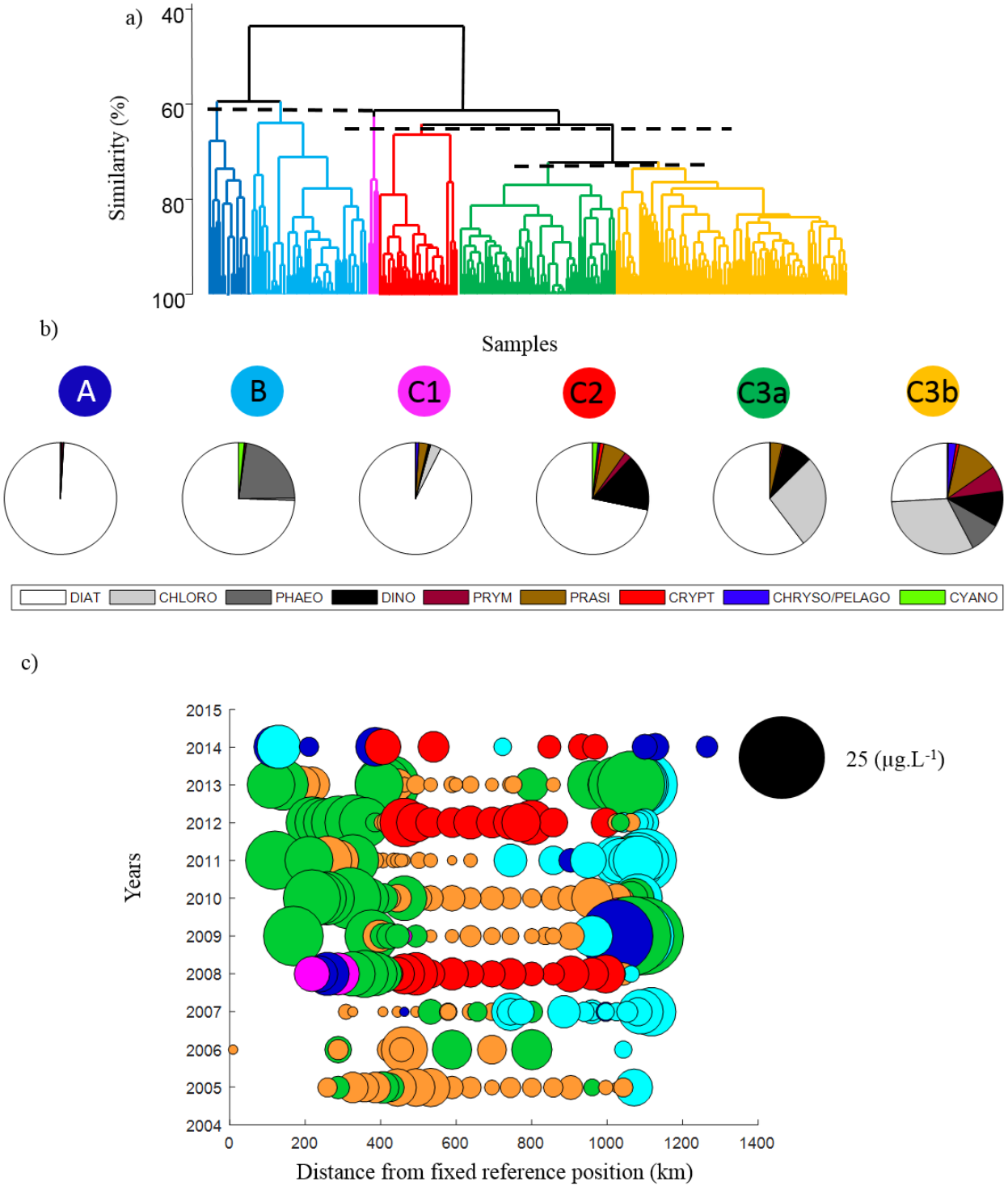

Figure 3.4 Dendrogram showing clustering of samples (a) and the proportion of chlorophyll *a* contributed by each phytoplankton class for each cluster (b). Spatial distribution of distinct phytoplankton communities (cluster groups) along the section, showing the distance from the star in Fig 3.3a) (c). Bubble size in (c) represents total chlorophyll *a* biomass (minimum = 0.3 mg Chl*a* m^{-3} and maximum = 25 mg Chl*a* m^{-3}).

Redundancy analysis (RDA) was used to investigate the hydrographic variables that explained the variance (explanatory variables) in the phytoplankton communities based on pigment analyses. The ordination diagram (Fig. 3.5b) revealed that most stations from distinct clusters were concentrated within one quadrant, where arrows representing environmental variables in the same or opposite directions of the clusters of stations suggest positive or negative correlations proportional to the length of the arrow. The first axis (x-axis) of the analysis, which explained most of the variance (eigen-value = 25.7 % of species data and 83.5 % of species-environment relation, Table 3.4), clearly shows that the phytoplankton communities respond strongly to spatial aspects of the data (Fig. 3.5b). Thus, stations in Arctic waters were to the left of the y-axis (low nutrient concentrations, temperature and salinity values), while stations located in Atlantic waters were to the right (opposite trend, Fig. 3.5b). Diatoms and chlorophytes (cluster C3a, upper left quadrant of Fig. 3.5b) were associated with lower salinities and temperatures and highly stratified waters. *Phaeocystis* and diatoms (cluster B, lower left quadrant of Fig. 3.5b) were associated with waters where nutrient concentrations (mainly nitrate, but also phosphate and silicate) were relatively low (average nitrate concentration from cluster B < 3 μM, Table 3.5). In Atlantic waters, temporal aspects of the data were also observed (upper and lower right quadrants (Fig. 3.5b)). Thus, mixed assemblages (cluster C3b) were associated with higher nutrient concentrations (pre-bloom conditions in Atlantic waters, upper right quadrant), whereas dinoflagellates and diatoms (cluster C2) were associated with warmer and saltier waters, resembling blooming conditions in Atlantic waters induced by thermal stratification (lower right quadrant of Figure 3.5b). Summed, the canonical axes explained 99.8 % of the variance (axis 1, p = 0.002; all axes, p = 0.002) (Table 3.4), which means that the environmental variables included in this analysis explained almost 100 % of the variability.

Forward selection showed that five of the six environmental factors (silicate, temperature, salinity, nitrate and phosphate) included in the analysis best explained the variance in the phytoplankton community distributions when analysed together (Table 3.4). When all variables were analysed together (conditional effects, referred to as λ_a in Table 3.4), silicate was the most significant explanatory variable (λ_a = 0.2, p = 0.001), followed by temperature (λ_a = 0.05, p = 0.001), salinity (λ_a = 0.02, p = 0.002), nitrate concentration (λ_a = 0.01, p = 0.016) and phosphate (λ_a = 0.02, p = 0.002) (Table 3.4). SI was the only explanatory variable that had no significance in explaining the distribution of phytoplankton communities (Table 3.4).

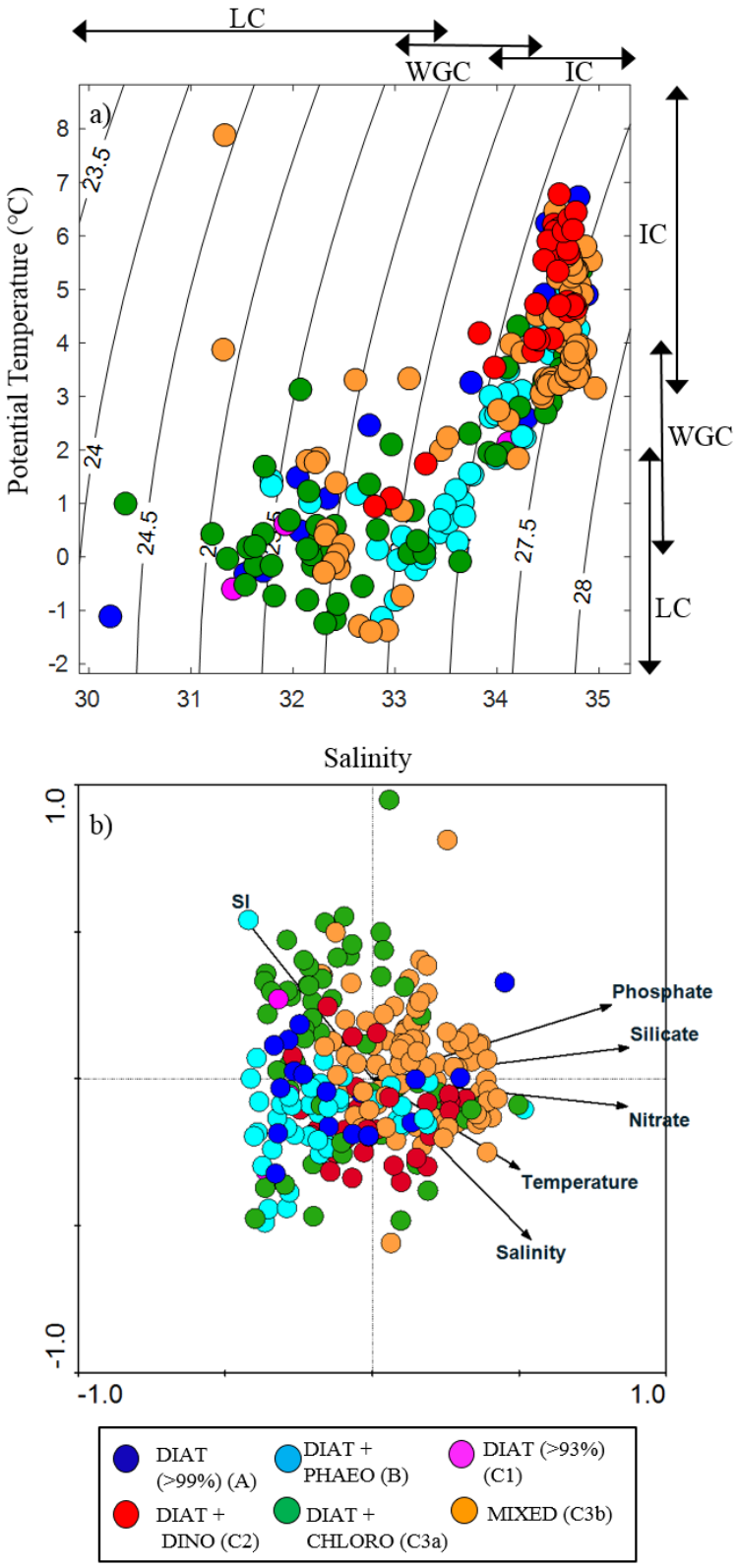

Figure 3.5 Positions of individual stations in relation to temperature (°C) and salinity (a) and redundancy analysis (RDA) ordination plot (b). The stations are colour-coded according to the cluster groups (see details in Figure 3.4). The TS plot (a) shows the approximate ranges of potential temperature (°C) and salinity of the Labrador Current (LC), the West Greenland Current (WGC) and the Irminger Current (IC). Arrows in (b) show the explanatory (environmental) variables used in the analysis.

Table 3.4 Results of the Redundancy Analyses (RDA) with the effects, eigenvalues and percentages of variance explained used in the analysis. Marginal (λ_1) and conditional effects (λ_a) refers to the absolute and additional effects, respectively, of the environmental variable (s) used in the RDA analysis after the automatic forward selection. Explanatory variables are temperature (°C), salinity, nitrate (NO_3^-), phosphate (PO_4^{3-}), silicate ($Si(OH)_4$) (µmol L^{-1}) and Stratification Index (SI) (kg m^{-4}). Significant p-values ($p < 0.05$) represents the variables that significantly explains the variation in the analyses.

Marginal Effects			Conditional Effects			
Variable	λ_1		Variable	λ_a	*P*	*F*
$Si(OH)_4$	0.2		$Si(OH)_4$	0.2	0.001	61.65
NO_3^-	0.19		Temperature	0.05	0.001	17.3
PO_4^{3-}	0.17		Salinity	0.02	0.002	6.94
Salinity	0.09		NO_3^-	0.01	0.016	4.31
Temperature	0.07		PO_4^{3-}	0.02	0.002	7.22
SI	0.06		SI	0.01	0.153	1.72
Axes	1	2	3	4		Total variance
Eigen-values	0.257	0.042	0.005	0.003		1
Taxa-environment correlations	0.676	0.404	0.321	0.245		
Cumulative percentage variance						
of species data	25.7	29.9	30.3	30.7		
of species-environment relation	83.5	97.2	98.8	99.8		
Sum of all eigenvalues						1
Sum of all canonical eigenvalues						0.307

Test of significance of first canonical axis: eigen-value = 0.257; F-ratio = 84.938; P-value = 0.002.

Test of significance of all canonical axis: trace = 0.307; F-ratio = 18.184; P-value = 0.002.

3.4.4 Phytoplankton distributions and elemental stoichiometry

Particulate organic carbon (POC) collected on filters can include organic carbon from a variety of sources, such as phytoplankton, bacteria, zooplankton, viruses and detritus (Sathyendranath et al., 2009). Assuming that phytoplankton associated organic carbon, as estimated from phytoplankton cell volumes (POC_{phyto}) is strongly correlated with Chl*a* values, the proportion of POC_{phyto} should increase in eutrophic waters, which usually occurs with high Chl*a* and POC concentrations, and that it should be lower in oligotrophic waters. Indeed, our results showed higher proportions of POC_{phyto} (> 60 %) in waters with higher POC concentrations (Fig. 3.6a). However, there were stations where POC levels were high and where the contribution of POC_{phyto} was low, suggesting that there may have been other sources of POC (e.g. detritus).

The relationships between POC_{phyto} and POC:PON also varied among the different phytoplankton community types (Fig. 3.6). In general, stations in shelf regions, which have higher inputs of Arctic and glacial melt waters (lower salinity values), where diatoms co-dominated with chlorophytes in the west and east (cluster C3a) or with *Phaeocystis* in the east (cluster B), had higher and more variable values for POC:PON ratios than did stations influenced by Atlantic water (Fig. 3.6b). Some shelf stations had relatively high proportions of POC_{phyto} to total POC, suggesting that phytoplankton community growth dominated by diatoms and chlorophytes (cluster C3a) contributed more to the total POC (most stations from cluster C3a had POC_{phyto} > 50 %) (Fig. 3.6b). On the other hand, some shelf stations, particularly the one dominated by diatoms and *Phaeocystis* (cluster B) had high POC:PON ratios (> 10), with low POC_{phyto} contributions, suggesting an increased contribution of detritus to the total POC (Fig. 3.6c). Stations influenced by Atlantic waters had generally lower contributions of POC_{phyto}, with most stations having POC:PON ratios < 6.6 (Fig. 3.6c).

3.4.5 Physiological patterns

Accessory pigments (AP) versus total chlorophyll *a* (TChl*a*) scatterplot from surface waters of the Labrador Sea showed a log-log linear relationship (Fig. 3.7). The slopes of these relationships varied within temperature (Fig. 3.7a) and among the distinct phytoplankton communities (Fig. 3.7b). Phytoplankton communities in cold waters (of Arctic origin), such as those co-dominated by diatoms and *Phaeocystis* in the east and diatoms and chlorophytes in the west, had a lower accessory pigments to TChl*a* ratio (logAP:logTChl*a*) (slope = 0.86 and 0.89, respectively) (Fig. 3.7b). Furthermore, communities from warmer waters (Irminger Current from Atlantic origin), particularly those co-dominated by diatoms and dinoflagellates had higher ratios of logAP:logChl*a* (slope = 1.03) (Fig. 3.7b). Slopes of the logAP to logTChl*a* relationships were not statistically different among the different communities (ANCOVA, $p > 0.05$), except for those communities co-dominated by diatoms and *Phaeocystis* (cluster B), which had a slope that was statistically different from the others (ANCOVA, $p= 0.016$).

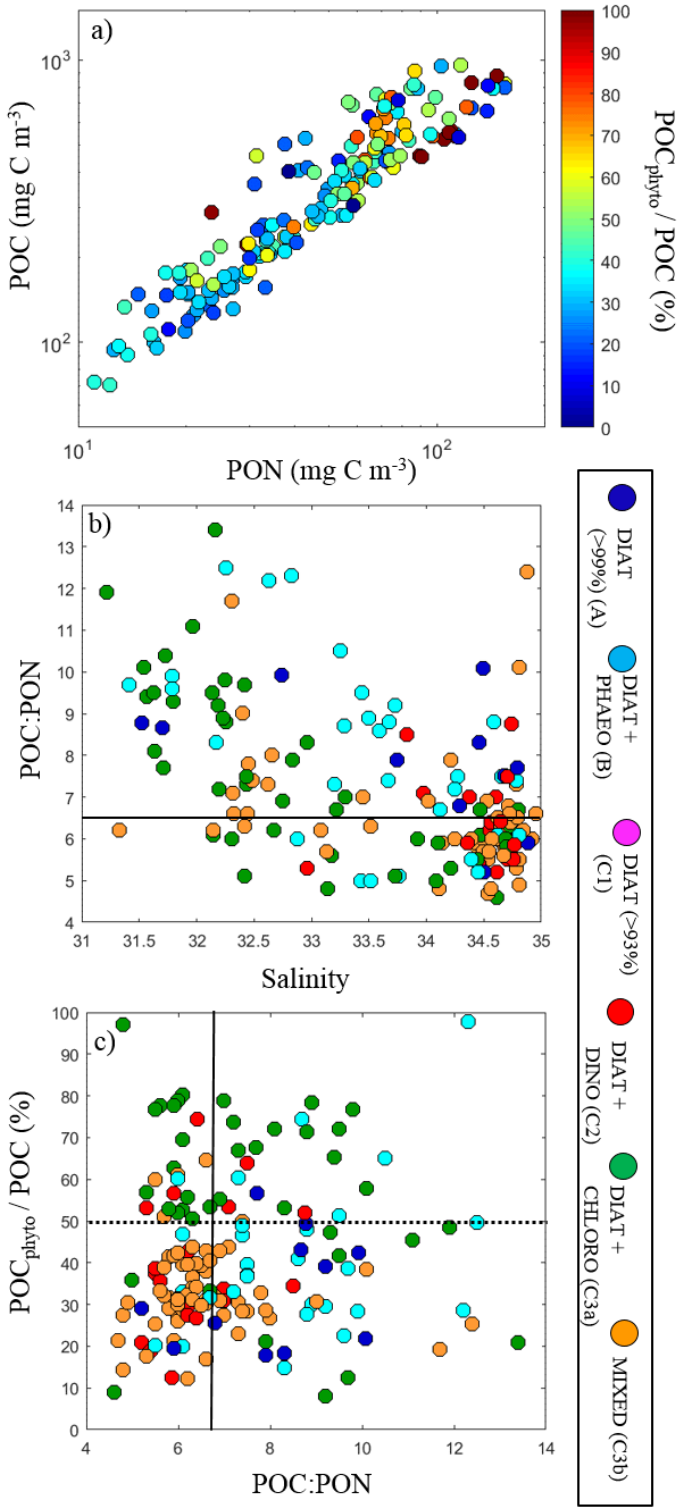

Figure 3.6 Relationship between particulate organic carbon (POC) and particulate organic nitrogen (PON) in a logarithmic scale, with the points (stations) as a function of phytoplankton-derived organic carbon content (POC_{phyto}/POC, %) (a), POC:PON *versus* salinity (b), phytoplankton-derived organic carbon content (POC_{phyto}/POC, %) *versus* the POC:PON ratio (c). The points (stations) in (b) and (c) are colour-coded according to the cluster groups (see details in Figure 3.4). Solid lines in (b) and (c) show the C:N Redfield ratio of 6.6 and the dashed line in (c) shows where POC_{phyto} contributes 50 % of the total POC.

Table 3.5 Average, standard deviations and number of observations (in parenthesis) of environmental and biological variables of each cluster group. MLD = mixed layer depth, SI= Stratification index, NO_3^- = nitrate, PO_4^{3-} = phosphate, $Si(OH)_4$ = silicate, DT= diatoxanthin, DD= diadinoxanthin, POC= particulate organic carbon, PON= particulate organic nitrogen, POC_{phyto} = phytoplankton-derived particulate organic carbon, α^B = initial slope of the photosynthesis-irradiance curve, P_m^B = maximum normalised photosynthesis, E_k = onset saturation irradiance, Es = saturation irradiance.

	Cluster A		Cluster B		Cluster C3a		Cluster C3b		Cluster C2		Cluster C1	
Temperature (°C)	2.8 ± 2.4	(17)	2.0 ± 1.8	(46)	1.6 ± 1.9	(62)	3.4 ± 1.9	(92)	4.8 ± 1.5	(32)	1.4 ± 1.7	(4)
Salinity	33.4 ± 1.5	(17)	33.7 ± 0.8	(46)	33.1 ± 1.2	(62)	34.1 ± 1.0	(92)	34.4 ± 0.5	(32)	33.0 ± 1.6	(4)
MLD (m)	32.2 ± 43.8	(17)	32.6 ± 23.4	(46)	31.2 ± 28.5	(62)	59 ± 71.1	(92)	29.8 ± 17.0	(32)	16.0 ± 4.2	(4)
SI x 10^{-3} (kg m^{-4})	9.1 ± 6.3	(17)	6.3 ± 5.7	(46)	10.7 ± 8.5	(62)	5.0 ± 6.8	(92)	6.1 ± 4.5	(31)	6.6 ± 8.5	(4)
NO_3^- (µmol L^{-1})	2.9 ± 4.7	(17)	2.7 ± 3.5	(46)	3.4 ± 4.3	(58)	8.4 ± 4.1	(83)	3.7 ± 3.9	(32)	3.8 ± 6.8	(4)
$Si(OH)_4$ (µmol L^{-1})	2.2 ± 2.7	(17)	2.8 ± 2.1	(46)	3.5 ± 2.4	(58)	5.4 ± 2.2	(83)	3.0 ± 2.2	(32)	2.3 ± 3.4	(4)
PO_4^{3-} (µmol L^{-1})	0.3 ± 0.3	(17)	0.3 ± 0.2	(45)	0.4 ± 0.2	(55)	0.7 ± 0.2	(79)	0.3 ± 0.2	(32)	0.4 ± 0.3	(4)
$Si(OH)_4$:NO_3^-	6.0 ± 11.8	(14)	3.6 ± 7.9	(37)	8.5 ± 18.2	(54)	1.1 ± 1.5	(82)	1.6 ± 1.8	(32)	3.9 ± 4.4	(4)
NO_3^-:PO_4^{3-}	8.2 ± 6.7	(11)	5.2 ± 5.0	(45)	5.9 ± 5.8	(55)	11.4 ± 4.1	(79)	8.7 ± 4.6	(32)	5.5 ± 7.1	(4)
Chlorophyll *a* (mgChl*a* m^{-3})	3.8 ± 4.7	(17)	5.5 ± 4.8	(45)	7.7 ± 5.6	(59)	2.0 ± 1.7	(91)	4.0 ± 1.8	(31)	8.8 ± 9.6	(4)
DT:(DT+DD)	0.01 ± 0.03	(16)	0.02 ± 0.05	(44)	0.04 ± 0.05	(62)	0.10 ± 0.10	(92)	0.08 ± 0.07	(32)	0.02 ± 0.04	(4)
(DD+DT):Chla	0.08 ± 0.07	(17)	0.03 ± 0.03	(46)	0.04 ± 0.02	(62)	0.07 ± 0.03	(92)	0.12 ± 0.03	(32)	0.07 ± 0.04	(4)
POC (mgC m^{-3})	245 ± 90	(4)	498 ± 198	(27)	533 ± 198	(45)	234 ± 145	(63)	512 ± 179	(15)	392 ± 418	(2)
PON (mgN m^{-3})	39 ± 16	(4)	65 ± 23	(27)	74 ± 30	(45)	37 ± 26	(64)	84 ± 33	(15)	42 ± 41	(2)
POC_{phyto} (%)	23.0 ± 5.2	(4)	49.2 ± 29.5	(26)	60.9 ± 25.6	(44)	33.3 ± 10.1	(64)	36.0 ± 11.4	(15)	37.8 ± 1.3	(2)
POC:PON	6.5 ± 1.2	(4)	7.8 ± 2.1	(27)	7.5 ± 2.1	(45)	6.6 ± 1.3	(64)	6.2 ± 0.9	(15)	8.6 ± 1.6	(2)
α^B (mgC [mg Chl*a*]$^{-1}$ h^{-1}[W m^{-2}] $^{-1}$) x10^{-2}	-		6.8 ± 6	(9)	9.2 ± 5	(10)	7.1 ± 4	(18)	7.1 ± 1.5	(4)	-	
P_m^B (mgC [mgChl*a*]$^{-1}$ h^{-1})	-		2.9 ± 1.1	(9)	2.3 ± 0.8	(10)	2.3 ± 0.6	(18)	3.2 ± 0.7	(4)	-	
E_k (Wm^{-2})	-		60 ± 33	(9)	29 ± 13	(10)	39 ± 14	(18)	46 ± 5	(4)	-	
Es (Wm^{-2})	-		62 ± 32	(9)	35 ± 18	(10)	43 ± 18	(18)	56 ± 8	(4)	-	
β (mgC [mgChl*a*]$^{-1}$ h^{-1}[W m^{-2}] $^{-1}$) x10^{-4}	-		4 ± 7	(9)	16 ± 23	(10)	10 ± 16	(18)	29 ± 24	(4)	-	

Photosynthetic parameters differed among the different phytoplankton communities. *Phaeocystis* and diatom communities near Greenland (cluster B) had the lowest photosynthetic efficiencies (average $\alpha^B = 6.8 \times 10^{-2}$ mg C [mg Chl*a*] h^{-1} [W m^{-2}] $^{-1}$) with relatively high onset saturation irradiances (average $E_k = 60 \pm 33$ W m^{-2}) and little photo-inhibition ($\beta = 4 \times 10^{-4}$ mg C [mg Chl*a*] h^{-1} [W m^{-2}] $^{-1}$) (Table 3.5). By contrast, phytoplankton communities dominated by diatoms and chlorophytes typically found in the Labrador Current (cluster C3a) were highly susceptible to photo-inhibition ($\beta = 16 \times 10^{-4}$ mg C [mg Chl*a*] h^{-1} [W m^{-2}] $^{-1}$), had lower onsetsaturation irradiances ($E_k = 29$ W m^{-2}) and higher photosynthetic efficiencies ($\alpha^B = 9.2 \times 10^{-2}$ mg C [mg Chl*a*] h^{-1} [W m^{-2}] $^{-1}$) (Table 3.5). Phytoplankton communities in Atlantic waters (clusters C3b and C2) had the highest levels of photoprotective pigments, such as those used in the xanthophyll cycle (diadinoxanthin (DD) + diatoxanthin (DT)):Chl*a* > 0.07), particularly those communities co-dominated by diatoms and dinoflagellates (cluster C2) from stratified Atlantic waters (Table 3.5). These communities were the most susceptible to photo-inhibition ($\beta = 29 \times 10^{-4}$ mg C [mg Chl*a*] h^{-1} [W m^{-2}] $^{-1}$), had the highest ratios of photoprotective pigments to Chl*a* ((DD+DT):Chl*a* = 0.12 ± 0.01), and the highest maximum photosynthetic rates ($P_m^B = 3.2 \pm 0.4$ mg C [mg Chl*a*] h^{-1} [W m^{-2}] $^{-1}$) (Table 3.5).

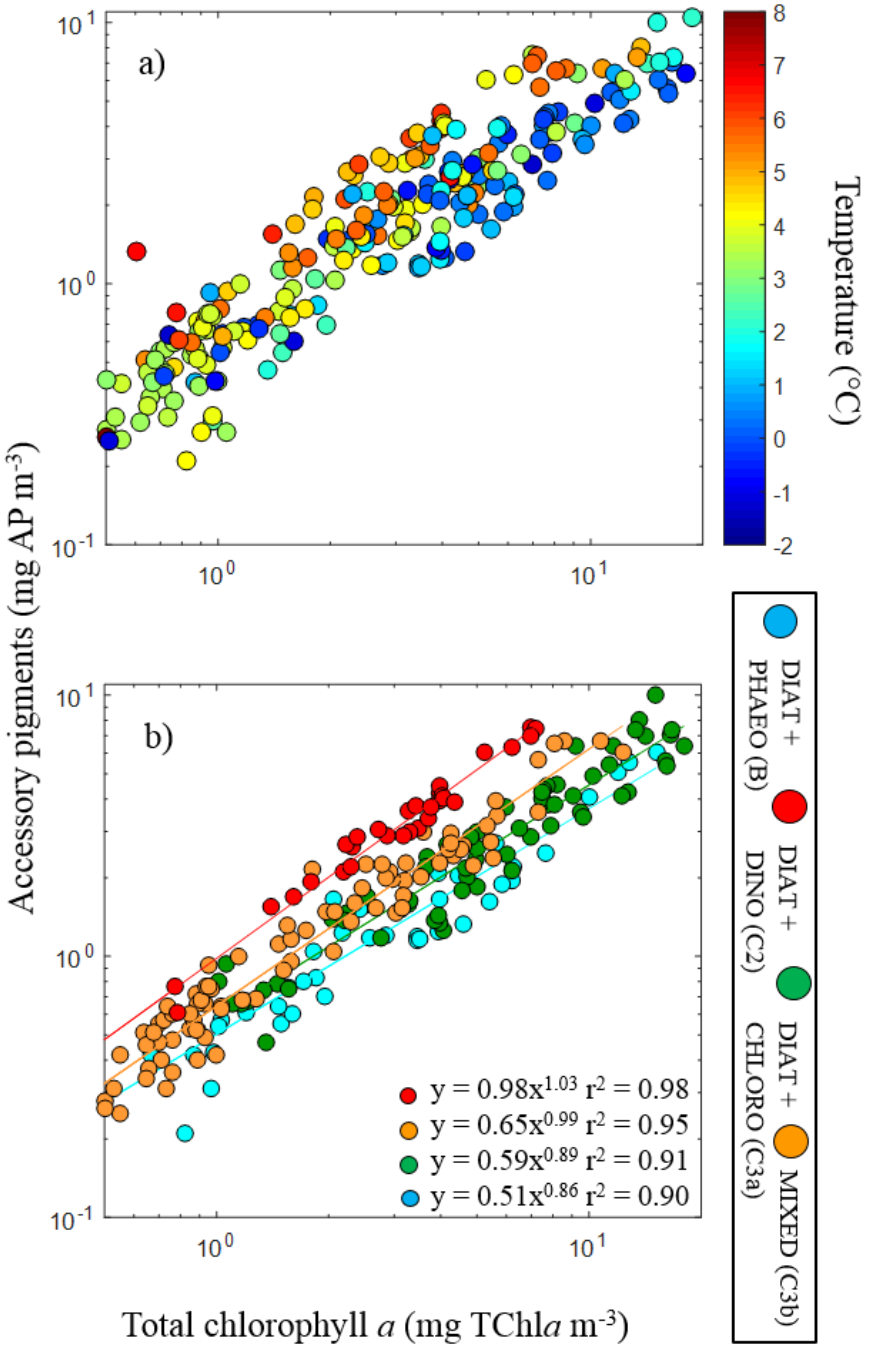

Figure 3.7 Relationship between total accessory pigments (mg AP m^{-3}) and total chlorophyll (mg TChl*a* m^{-3}) on a logarithmic scale, with the points (stations) according to temperature (a) and colour-coded according to phytoplankton community cluster group (see details in Figure 3.4) (b).

3.5 Discussion

3.5.1 Biogeography of phytoplankton communities in the Labrador Sea

In this study, our assessment of phytoplankton pigments from surface waters during spring/early summer of the Labrador Sea based on a decade of observations showed that the distribution of phytoplankton communities varied primarily with the distinct waters masses (Labrador, Irminger and Greenland Currents). There were three regions where major blooms (Chl*a* concentrations > 3 mg Chl*a* m^{-3}) occurred. For all three blooms, diatoms were predominant; however, they co-dominated with 1) chlorophytes in the west (mostly in the Labrador Current), 2) *Phaeocystis* in the east in the West Greenland Current and 3) dinoflagellates in the central basin of the Labrador Sea, once waters were thermally-stratified. While diatoms bloomed in shallower mixed layers (< 33 m, Table 3.5), a more diverse community was found in most years in deeper mixed layers (> 59 m) in the central basin, resembling pre-bloom conditions. These patterns are similar to those seen in other shelf and basin regions of Arctic/subarctic waters (Coupel et al., 2015; Fujiwara et al., 2014; Hill et al., 2005). It is well known that diatoms tend to dominate in high-nutrient regions of the ocean due to their high growth rates, while their low surface area to volume ratios mean that they do not do as well as nano- or picoplankton in low nutrient conditions (Gregg et al., 2003; Sarthou et al., 2005). In the Labrador Sea, deep winter mixing (200 – 2300 m) provides nutrients to the near surface layers, which supports phytoplankton spring blooms, particularly of diatoms once light becomes available (Fragoso et al., 2016b; Harrison et al., 2013; Yashayaev and Loder, 2009).

Chlorophytes were the second most abundant phytoplankton group, particularly in the central-western part of the Labrador Sea, but often occurring in the east as well. Chlorophytes are thought to contribute 1-13 % of total Chl*a* in the global ocean (Swan et al., 2015) and to inhabit transitional regions, where nutrient concentrations become limiting for diatoms, but are not persistently low enough to prevent growth due to nutrient limitation, as occurs in the oligotrophic gyres (Gregg et al., 2003; Gregg and Casey, 2007; Ondrusek et al., 1991). The Labrador Shelf is a dynamic region during springtime, where

melting sea ice in May provides a local freshwater input (Head et al., 2003). Melting sea ice provides intense stratification and shallow mixed layers for the phytoplankton and thus access to light, which promotes rapid growth of cold Arctic/ice-related phytoplankton near the sea ice shelf (Fragoso et al., 2016b), and which likely stimulates the succession from large diatoms to smaller phytoplankton forms, such as chlorophytes, as nutrients become exhausted. Chlorophytes, as well as Prasinophytes such as *Pyramimonas*, a genus found in high abundances in surface Labrador Shelf waters, might also be associated with melting sea ice, given that they have been found blooming (chlorophyll concentration ~ 30 mg Chl*a* m^{-3}) in low salinity melt waters (salinity = 9.1) under the Arctic pack-ice (Gradinger, 1996).

Dinoflagellates were associated with the Irminger Current, where they were occasionally found blooming with diatoms in the warmer, stratified Atlantic waters of the central basin. These blooms dominated by dinoflagellates and Atlantic diatom species, such as *Ephemera planamembranacea* and *Fragilariopsis atlantica*, start later in the season (end of May or June) as thermal stratification develops in the central Labrador Sea (Frajka-Williams and Rhines, 2010, Fragoso et al., 2016). Transition from diatoms to dinoflagellates has been well-documented in the North Atlantic between spring and summer, which occurs because dinoflagellates can use mixotrophic strategies to alleviate nutrient limitation as waters become warmer, highly stratified and nutrient-depleted (Barton et al., 2013a; Head and Pepin, 2010; Head et al., 2000; Henson et al., 2012; Leterme et al., 2005). The North Atlantic Oscillation index (NAO) and sea surface temperature (Zhai et al., 2013) appear to influence the relative proportions of diatoms and dinoflagellates as well as the variability in the start date of the North Atlantic bloom. A negative winter phase of NAO is associated with weaker northwest winds over the Labrador Sea and reductions in the depth of winter mixing and supply of nutrients to the upper layers (Drinkwater and Belgrano, 2003). Vertical stability, thermal stratification and the initiation of the spring bloom tend to occur earlier under negative NAO conditions and the proportion of dinoflagellates in the warmer, more nutrient-limited waters may be higher (Zhai et al., 2013). Unfortunately, it was not possible to investigate the influence of NAO on the relative contribution of dinoflagellates and diatoms in the Labrador Sea section of the North Atlantic in this study, given that the sampling period varied from early/mid-May to mid/late-June. On the other hand, abundances of dinoflagellates appeared to be higher in warmer waters (> 5°C), suggesting that the communities were shifting from diatoms to dinoflagellates as the water became stratified and nutrient concentrations decreased.

Phaeocystis and diatoms bloom together in the eastern central Labrador Sea (Fragoso et al., 2016b; Frajka-Williams and Rhines, 2010; Harrison et al., 2013; Head et al., 2000; Stuart et al., 2000; Wolfe et al., 2000). This is a region with high eddy kinetic energy during spring (Chanut et al., 2008; Frajka-Williams et al., 2009; Lacour et al., 2015), which causes the accumulation of low-salinity surface waters from the West Greenland Current and confines elevated levels of phytoplankton biomass, presumably of *Phaeocystis* and diatoms, in buoyant freshwater layers (Fragoso et al., 2016b). Mesoscale eddies may stimulate growth of *Phaeocystis* and diatoms by inducing partial stratification at irradiance levels that are optimal for their growth, but too low for their competitors (blooms in these eddies usually start in April). Lacour et al. (2015) showed that irradiance levels estimated from satellite-derived photosynthetically active irradiance (PAR) and mixed layer depth climatologies are similar for thermally and haline-stratified spring blooms in the Labrador Sea. Nonetheless, these authors recognise the need for *in situ* measurements to confirm whether Labrador Sea spring blooms, presumably composed of distinctive phytoplankton communities, respond in the same manner to light-mixing regimes. The ability of *Phaeocystis* to grow under dynamic light irradiances explains why they are often found in deeper mixed layers, such as those found in Antarctic polynyas (Arrigo, 1999; Goffart et al., 2000), although this genus can also occur in shallow mixed layers, such as those found close to ice edges (Fragoso and Smith, 2012; Le Moigne et al., 2015).

Mesoscale eddies are also often associated with elevated zooplankton abundances (Frajka-Williams et al., 2009; Yebra et al., 2009). In the Labrador Sea, lower grazing rates have been observed in blooms dominated/co-dominated by colonial *Phaeocystis*, which are often located in these eddies and which may, in turn, explain why this species is dominant (Head and Harris, 1996; Wolfe et al., 2000). Although the exact mechanism that facilitates *Phaeocystis* growth in the north-eastern region of the Labrador Sea is not clear, it is evident that blooms of this species are tightly linked to mesoscale eddies, and that this relationship needs further investigation to better explain their regular reoccurrence in these waters.

3.5.2 Phytoplankton composition and related biogeochemistry

Particulate organic carbon (POC) and nitrogen (PON) concentrations, as well as the molar ratio of POC:PON varied within distinct hydrographic zones, indicating the presence of different biogeochemical provinces in the Labrador Sea. A canonical Redfield ratio of 6.6 for POC:PON appears to represent the global average (Redfield, 1958), although regional variations on the order of 15 to 20 % have also been reported (Martiny et al., 2013a). The POC:PON appears to be closer to the Redfield ratio of 6.6 in productive sub-Arctic/Arctic waters, such as the northern Baffin Bay (Mei et al., 2005), the north-eastern Greenland shelf (Daly et al., 1999), and in Fram Strait and the Barents Sea (Tamelander et al., 2012). Crawford et al. (2015), however, recently reported very low POC:PON ratios in oligotrophic Arctic waters of the Beaufort Sea and Canada Basin, where depth-integrated values of the POC:PON ratio were ~ 2.65, much lower than those in more productive domains, such as the sub-Arctic central Labrador Sea (POC:PON ~ 4).

In this study, highly productive surface waters of Arctic origin (near or on the shelves) had higher phytoplankton-derived particulate organic carbon (POC_{phyto} > 43 % from total POC), as well as higher and more variable POC:PON ratios (average > 6.9) compared with stations influenced by Atlantic water (average POC:PON < 6.3, POC_{phyto} > 35 %). Diatoms have been suggested to contribute to larger phytoplankton-derived POC in Arctic/sub-Arctic waters (Crawford et al., 2015). The Labrador Shelf region, where blooms are generally dominated by large Arctic/ice-related diatoms (Fragoso et al., 2016b), had relatively high contributions of POC_{phyto} (> 50 %) to the total POC, even though smaller phytoplankton forms, such as chlorophytes, were also abundant. Low POC:PON ratios, as well as low POC_{phyto} concentrations were associated with Atlantic waters, which had greater contributions of flagellates (particularly before bloom initiation). Similar findings were reported by Crawford et al. (2015), where low POC_{phyto} was associated with larger contributions of flagellates (< 8 μm) in oligotrophic Arctic waters, such as the Beaufort Sea and Canada Basin. Crawford et al. (2015) also considered that POC:PON ratios might have been reduced by the presence of heterotrophic microbes (bacteria, flagellates and ciliates) since these microorganisms have POC:PON ratios lower than the canonical Redfield ratio of 6.6 (Lee and Fuhrman, 1987; Vrede et al., 2002). Bacteria and other heterotrophic organisms were not quantified in our study, although Li and Harrison (2001)

showed that bacterial biomass from surface waters was 62 % greater (average from 1989 to 1998 =13.8 mg C m^{-3}) in the central region than in shelf areas of the Labrador Sea.

Changes in POC:PON may be related to the physiological status of phytoplankton and/or community structure. In the North Water Polynya (Baffin Bay), POC:PON ratios during phytoplankton blooms increased between spring (5.8) and summer (8.9) as phytoplankton responded to nitrate starvation by producing N-poor photo-protective pigments (Mei et al., 2005). Daly et al. (1999) also found high POC:PON ratios (~8.9) in Arctic surface waters dominated by diatoms on the north-eastern Greenland shelf, which were attributed to nutrient limitation. Atlantic waters appear to have an excess of nitrate compared with Arctic waters (Harrison et al., 2013), which could explain why phytoplankton from Atlantic Waters had lower POC:PON ratios. Conversely, Arctic-influenced waters on or near the shelves had higher $Si(OH)_4$:NO_3^- and lower NO_3^-:PO_4^{3-} than those in the central basin in this study, which could also have contributed to the observed high POC:PON ratios.

A few stations in shelf waters of the Labrador Sea also had remarkably high POC:PON ratios (> 10), and low POC_{phyto} contributions, suggesting high contributions of detritus. These waters probably receive higher inputs of Arctic and glacial ice melt, which could introduce POC from external sources. Hood et al. (2015) showed that POC export from glaciers is large, particularly from the Greenland Ice Sheet and it occurs in suspended sediments derived from glacier meltwater. High POC:PON ratios (> 10), particularly in waters where *Phaeocystis* were abundant, may also be linked to the mucilaginous matrix of the *Phaeocystis* colonies (Palmisano et al., 1986). The mucopolysaccharide appears to contain excess carbon, particularly when nutrients start to become depleted and colonies become senescent (Alderkamp et al., 2007; Wassmann et al., 1990).

3.5.3 Physiological parameters of distinct phytoplankton communities

Accessories pigments (AP) are assumed to have a ubiquitous, global, log-log linear relationship with chlorophyll *a* in aquatic environments (Trees et al., 2000). This linear relationship is often used as an index of quality-control in pigment analysis, which are required due to uncertainties of the quantitative comparability of data among surveys,

related to differences in analytical procedures and sample storage methods used in different laboratories. In the current study, the slope of AP to total chlorophyll *a* (TChl*a*) on a logarithm scale (Fig. 3.7) passed the quality control criteria of slopes ranging from 0.7 to 1.4 and $r^2 > 0.90$ as applied in previous studies (e.g., Aiken et al., 2009; Peloquin et al., 2013; Thompson et al., 2011) and were within the range observed throughout worldwide aquatic systems (slope from 0.8 to 1.3 compared to 0.86 to 1.03 observed in our study) (Trees et al., 2000). An interesting trend was found where phytoplankton pigment ratios varied clearly within distinct communities in the Labrador Sea. According to our data, phytoplankton communities found in colder waters (of Arctic origin) had lower accessory pigments ratios to total chlorophyll *a* ratio (logAP:logTChl*a*) (slope = 0.86) when compared to communities from warmer waters (Irminger Current from Atlantic origin) (slope = 1.03). Changes in logAP:logTChl*a* as a function of phytoplankton community composition has been observed before, when Stramska et al. (2006) related a higher slope of logAP:logTChl*a* to dinoflagellates dominating during summer in northern polar Atlantic waters as opposed to lower ratios of flagellates occurring in spring. Trees et al. (2000) and Aiken et al. (2009) also reported lower logAP:logTChl*a* (slope < 1.00) in oligotrophic waters dominated by picoplankton as opposed to higher ratios in upwelling waters where microplankton, particularly diatoms, were dominant.

Environmental parameters, such as nutrients and light conditions, have also been suggested to influence logAP:logTChl*a* regardless of community composition (Trees et al., 2000). Nonetheless, in our study, these two parameters, analysed as nitrate and silicate concentrations and Stratification Index, did not vary with logAP:logTChl*a* (data not shown) as opposed to temperature. Phytoplankton community distributions varied clearly according to temperature with *Phaeocystis* occurring in colder, Arctic shelf waters and dinoflagellates in warmer, open ocean, Atlantic waters. Temperature, in this case, can be a proxy of ice melt input, where haline-stratified shelf waters can be considered less turbulent than thermally-stratified, open ocean, Atlantic waters, in spite of both being considered "stratified waters". It is possible that shelf, haline-stratified waters are more "steady", thus less turbulent, given that they are more stable and physically protected (close to the coast), whereas open waters are more exposed to winds, in spite of being thermally-stratified during summer. As a result of turbulence, phytoplankton cells potentially experience large variations in light intensity and spectra, which would favour species that invest in the light-havesting antenna, and thus increase accessory pigments concentrations (typically known as "sigma-type" response, Strzepek et al., 2012, 2011). In

more “steady” waters, phytoplankton could increase the number of reaction centers, which carries specialised chlorophyll *a* molecules (“n-type” response, Strzepek et al., 2012, 2011), without necessarily increasing the size of the light harvesting antennae.

The variation in photosynthetic parameters in the distinct phytoplankton biogeographical provinces demonstrated how each phytoplankton community responds to environmental conditions. Harrison and Platt (1986) found that the photophysiology of phytoplankton from the Labrador Sea is influenced by temperature and irradiance. Nonetheless, phytoplankton composition may also influence the values of the photosynthetic parameters. Light-saturated photosynthetic rates and saturation irradiances, for instance, were higher at stations where diatoms were dominant (> 70 %), as opposed to stations where flagellates were more abundant (from 40 % up to 70 %). Similar findings were reported by (Huot et al., 2013), who observed that light-saturated photosynthetic rates in the Beaufort Sea (Arctic Ocean) were higher for communities composed of large cells, presumably diatoms, compared to smaller flagellates.

Polar phytoplankton communities from shelf waters (east *versus* west) observed in this study had distinctive photo-physiological characteristics. Diatom/*Phaeocystis* dominated communities from waters located near Greenland (east) had low photosynthetic efficiency (average $\alpha^B = 6.8 \times 10^{-2}$ mg C [mg Chl*a*] h^{-1} [W m^{-2}] $^{-1}$) and high onset light-saturation irradiances (E_k = 60 W m^{-2}), while diatom/chlorophyte dominated communities on or near the Labrador Shelf (west) had the reverse (E_k = 29 W m^{-2}, $\alpha^B = 9.2 \times 10^{-2}$ mg C [mg Chl*a*] h^{-1} [W m^{-2}] $^{-1}$). Low photosynthetic efficiency and high light-saturation irradiance in diatom/*Phaeocystis* dominated communities mean that photosynthetic rates were relatively low at high light intensities, although photo-inhibition was low ($\beta = 4 \times 10^{-4}$ mg C [mg Chl*a*] h^{-1} [W m^{-2}] $^{-1}$). *Phaeocystis antarctica*, widespread in Antarctic waters, *relies* heavily on photo-damage recovery, such as D1 protein repair (Kropuenske et al., 2009), which could explain how these communities overcome photo-inhibition. These results were inconsistent with those reported by Stuart et al. (2000); however, who found a higher photosynthetic efficiency (α^B) for a population dominated by *Phaeocystis* near Greenland compared with that of a diatom dominated population near the Labrador coast. Stuart et al. (2000) attributed the higher α^B to the smaller cell size of *Phaeocystis*. In the current study, however, chlorophytes were present in high concentrations on the Labrador Shelf, which may explain the discrepancy between these results.

Phytoplankton communities from Atlantic waters (co-dominated by diatoms and dinoflagellates) were highly susceptible to photo-inhibition ($\beta = 29 \times 10^{-4}$ mg C [mg Chl*a*]

h^{-1} [W m^{-2}] $^{-1}$) compared with the other communities in the Labrador Sea. Days are longer and solar incidence is higher in June as compared to May at these latitudes (Harrison et al., 2013), which, in this study, was the time when dinoflagellates bloomed in the central Labrador Sea as a consequence of thermal stratification, which explains the sensitivity of this community to high-light levels. To cope with photo-damage, this phytoplankton community appeared to increase the levels of photoprotective pigments, such as those used in the xanthophyll cycle (diadinoxanthin (DD) + diatoxanthin (DT)). These communities also had high diatoxanthin levels compared with the polar phytoplankton communities, suggesting that the community was experiencing higher light intensities (Moisan et al., 1998).

3.5.4 Phytoplankton communities assessed by HPLC and CHEMTAX methods

Phytoplankton pigments and CHEMTAX methods provide information about phytoplankton community structure, and are especially powerful when used in conjunction with microscopic analysis (light and high resolution scanning electron microscopy) (Coupel et al., 2015, 2012; Eker-develi et al., 2012; Muylaert et al., 2006), cytometry (Devilla et al., 2005; Fujiki et al., 2009) and molecular techniques (Not et al., 2007; Piquet et al., 2014; Zhang et al., 2015). However, choosing the pigment markers in the CHEMTAX analysis and interpreting the results are not always straightforward and, therefore, conclusions need to be drawn with caution. Many environmental factors (primarily light and nutrients) (DiTullio et al., 2007; Henriksen et al., 2002; van Leeuwe and Stefels, 2007, 1998), in addition to natural variability among species from the same classes or even strains of the same species (Zapata et al., 2004) affect accessory pigment levels and ratios to chlorophyll *a*, which could introduce some uncertainties when applying CHEMTAX. Thus, phytoplankton abundances determined using CHEMTAX represent approximations based on pigment distributions. These limitations can, however, be lessened when this technique is combined with existing knowledge of main phytoplankton groups occurring in the samples through microscopic identification.

A number of studies have used CHEMTAX methods to determine phytoplankton community structure in Arctic/subarctic waters (Coupel et al., 2015, 2012; Lovejoy et al.,

2007; Piquet et al., 2014; Vidussi et al., 2004; Zhang et al., 2015). Spring phytoplankton communities from the Labrador Sea have already been investigated in detail (Fragoso et al., 2016b), although the analysis did not include most nano- and pico-flagellates (except cryptophytes and *Phaeocystis pouchetii*) and were done over only four years (2011-2014) at selected stations along the L3 (=AR7W) transect. Here, phytoplankton information from Fragoso et al. (2016) was combined with additional pigment analyses. Although cross comparison among these two techniques (carbon biomass estimated from microscopic counts *versu*s algal class chlorophyll *a* estimated from CHEMTAX) should not be expected to give exactly equivalent results, given that most flagellates observed in the pigment analysis were not counted under the microscope, some comparability should be possible, at least for the larger cells (e.g. diatoms).

Phaeocystis ($r^2 = 0.79$) and diatom ($r^2 = 0.74$) biomasses were well correlated when carbon biomasses estimated from microscopic counts were compared with CHEMTAX-derived algal chlorophyll *a* biomass (Appendix C). This confirms that using chlorophyll *c3* was appropriate for detecting and quantifying *Phaeocystis* biomass in the Labrador Sea. Similar associations have been observed in *Phaeocystis* from boreal waters (e.g. *P. pouchetii* but *P. globosa* as well; Antajan et al., 2004; Muylaert et al., 2006; Stuart et al., 2000; Wassmann et al., 1990), while other pigment markers have been used elsewhere, e.g. 19-hexanoyloxyfucoxanthin, which is characteristic of *Phaeocystis antarctica* in austral polar waters (Arrigo et al., 2014; Arrigo et al., 2010a; Fragoso and Smith, 2012; Fragoso, 2009). Dinoflagellates gave a poor correlation between biomass estimates made using the two methods ($r^2 = 0.12$, Appendix C) possibly because some heterotrophic dinoflagellates, which lack photosynthetic pigments, might have been included in the microscopic counts from Fragoso et al (2016). Cryptophyte biomass estimates were not related (Appendix C), likely because their biomass was underestimated in microscopic counts.

3.6 Conclusions

In this study, a geographical description of phytoplankton community structure in spring and early summer surface waters of the Labrador Sea based on pigment data from over a decade of sampling (2005-2014) was provided. Phytoplankton communities and their photophysiological and biogeochemical signatures were assessed using CHEMTAX, so

that a geographical baseline of the major phytoplankton groups has been provided for the central Labrador Sea and its adjacent continental shelves. In spite of interannual variability (due to differences in survey dates and natural variability), spring phytoplankton communities showed distinct spatial variations from east to west and there were clear temporal differences between May and June. The main conclusions of our study are that: 1) diatoms contributed most to the chlorophyll *a* in waters where phytoplankton blooms were observed (> 3 mg Chl*a* m^{-3}); while other groups (chlorophytes, dinoflagellates and *Phaeocystis*) were geographically segregated within distinct hydrographical zones; 2) a diverse mixed assemblage dominated by flagellates from several groups occurred in low chlorophyll, pre-bloom conditions in the central Labrador Sea; and 3) different phytoplankton communities had different ratios of accessory pigments to total chlorophyll *a*; and 4) POC:PON ratios were influenced by phytoplankton community composition, as well as freshwater input of allochthonous carbon in shelf waters which have nearby sources (e.g. melting glacial and sea- ice and river outflows).

Marine phytoplankton respond rapidly to changes in the ocean, and their responses directly impact local marine food webs and global biogeochemical cycles. Climate-driven processes modify the factors, including light availability, nutrient input and grazing pressure that shape phytoplankton physiological traits and alter community structure (Litchman et al., 2012; Montes-Hugo et al., 2009). High latitude seas, particularly the Labrador Sea, are regions that are extremely vulnerable to climate change and often show similar patterns of variability on interannual and decadal scales across the entire domain (Yashayaev and Seidov, 2015; Yashayaev et al., 2015) and they could, therefore, be subject to rapid shifts in phytoplankton biomass, size and species composition. Although climate-induced responses of phytoplankton communities in vulnerable regions are difficult to predict, the long-term observations of these communities reported here and the analysis of their biogeochemical and physiological signatures are important in order to create a baseline for evaluation of changes that will occur in the future, as greenhouse gas-driven warming continues in this and other regions of the global ocean.

Chapter 4: Unveiling spring phytoplankton biogeography in the Labrador Sea through a trait-based analyses

4.1 Abstract

The Labrador Sea is an ideal region to study the influence of environmental factors that shape the phytoplankton biogeography due to the Atlantic and Arctic waters that divides the region into distinct hydrographic zones. Hydrographic zones create distinct ecological niches, where phytoplankton species are largely structured by their functional traits. In this study, target phytoplankton species from the Labrador Sea during spring were identified and their functional traits that are potentially influencing phytoplankton species biogeography were investigated. A gradient in abundance of target phytoplankton species observed in Arctic and North Atlantic waters suggested that phytoplankton biogeography in the Labrador Sea is driven by examination of the phytoplankton community rather than a single species analysis. Species were not exclusively present in Arctic or North Atlantic waters because of 1) some degree of mixing and/or 2) some species present an ubiquitous distribution in the Labrador Sea region. In Arctic waters, colder temperatures (< 0°C) favoured psycrophilic phytoplankton species, and greater light availability resulted from haline-driven stratification that selected for larger sized cells, which increased self-shading, allowing them to cope with high irradiance. Higher silicate concentration favoured heavily silicified diatom species able to form resting spores. Morphological traits, such as chain formation (ribbon-, cylinder and/or star-shaped) may have conferred flexibility to ice breakage and/or positive buoyancy due to the mucous material that binds the cells together in highly stratified Arctic waters. In Atlantic-influenced waters larger surface area to volume ratio might be a trait selected to cope with a deeper mixed layer, whislt lower silicate to nitrate ratio may have selected for weakly silicified diatoms. Traits, such as possesing sharp cell projections, including setae, spines or long processes, as well as elongated shapes (needle-shaped) might be a response to grazing in warmer North Atlantic waters. This trait-based analysis gives an ecological explanation of phytoplankton biogeography in the Labrador Sea and increases the predictive power of phytoplankton biogeography and its functionality in the system as the climate continuously changes.

4.2 Introduction

Marine phytoplankton communities exhibit contrasting patterns of distribution across global marine systems (Cermeño et al., 2010; Follows et al., 2007). The biogeographical organisation of these communities occur in response of the individual's abilities to utilise the resources available (e.g. light, macronutrients and micronutrients), as well as the complex interplay of intra- and inter-specific relationships, such as predation, competition and mutualism that allow species exclusion or coexistence (Acevedo-Trejos et al., 2013). Although it is relatively simple to study the distributions of species using niche-based models, it is much more difficult to understand the mechanisms involved in structuring the community as a whole (McGill et al., 2006). One way to deal with this question is using trait-based approaches, which define species in terms of their ecological roles that captures key aspects of organismal functionality in the system (Glibert, 2016; Litchman et al., 2007; Litchman and Klausmeier, 2008). Thus, instead of using nomenclatural ecology to explain species distribution, biogeography, seasonality and/or long-term trends, functional traits analysis has the potential to give a realistic prediction of biological communities in response to changes in the environment (McGill et al., 2006).

Functional traits have been used extensively in terrestrial ecology to help understand the organisation of ecological communities across environmental gradients and potential reorganisation under climate change scenarios (Cornelissen et al., 2003; Lavorel et al., 2011; Westoby and Wright, 2006). Only recently, functional traits have been applied in phytoplankton studies to understand their distribution in freshwater (Edwards et al., 2013a; Jamil et al., 2014; Kruk et al., 2010; Schwaderer et al., 2011; Weithoff, 2003; Zwart et al., 2015) and, less frequently, in marine ecosystems (Barton et al., 2013a, 2013b; Edwards et al., 2013b). Examples of functional traits in the literature that explained phytoplankton seasonal or spatial patterns include: cell size (Acevedo-Trejos et al., 2015, 2013), nutrient affinity (Edwards et al., 2013a, 2013b), light tolerance (Edwards et al., 2016), mixotrophy (Barton et al., 2013a), morphology (Kruk et al., 2011), motility, N-fixation ability and Si requirements (Barton et al., 2013b; Weithoff, 2003).

The Labrador Sea is an ideal region to apply trait-based approaches on species biogeography due to the contrasting hydrographical zones that divides the region into distinct ecological provinces (Fragoso et al., 2016a, 2016b; Head et al., 2003; Li and Harrison, 2001; Platt et al., 2005; Sathyendranath et al., 2009, 1995). The hydrography of

the Labrador Sea comprises warmer and more saline waters of North Atlantic origin, occurring in the central deep basin, and cooler and fresher Arctic waters covering its shelves and shelf margins (Head et al., 2013). Moreover, the Labrador Shelf (near the coast of Canada) is a seasonal ice zone that unveils a rich and diverse ice-related plankton community as sea ice melts during spring (Fragoso et al., 2016b; Harrison et al., 2013; Wu et al., 2007). The contrasting hydrography of the Labrador Sea and its surrounding (e.g. Scotia Shelf) has been shown to influence phytoplankton composition (Fragoso et al., 2016a, 2016b; Luddington et al., 2016). While sea ice diatoms dominate the spring bloom in Labrador Shelf waters, the colony forming *Phaeocystis pouchetii* is the common phytoplankton in the areas of high chlorophyll in the central-eastern side (West Greenland shelf (Stuart et al., 2000) and dinoflagellates are common in North Atlantic waters after the spring bloom (Harrison et al., 2013). However, a trait-based analysis showing which functional traits shape plankton community biogeography in the Labrador Sea has never been carried out.

The Labrador Sea is also a region susceptible to climate change because it receives waters of Arctic origin, which could influence the structuring of biological communities. Accelerated sea ice melt has intensified Arctic freshwater inflow in the Labrador Sea and reduced deep convection (Yang et al., 2016), which can impact phytoplankton bloom phenology and community composition by decreasing nutrient input to surface waters (Drinkwater and Belgrano, 2003; Zhai et al., 2013). Further inflow of ice melt waters to the Labrador Sea, including from Greenland runoff, could strengthen eddy activity and haline-stratification in the north-eastern region of the Labrador Sea, which could potentially intensify *Phaeocystis pouchetii* blooms in this region (Frajka-Williams and Rhines, 2010). The intrusion of the Pacific diatom *Neodenticula seminae* in North Atlantic waters, including the Labrador Sea, via the Northwest Passage is another example that emphasises the consequence of intense Arctic sea ice melt during recent summers (Reid et al., 2007). Moreover, sea surface temperature has been reported to increase during the last decades in North Atlantic waters, including Labrador Sea (Yashayaev and Seidov, 2015). Warmer temperature have promoted biogeographical shifts in plankton in the North Atlantic due to the northward extension of thermal boundaries, favouring warmer-water species (Beaugrand et al., 2002). Likewise, future projections show displacement of phytoplankton niches due to changes in oceanic circulation in North Atlantic waters (Barton et al., 2016). Thus, it becomes really important to understand which functional traits are involved in

Arctic and North Atlantic phytoplankton biogeography to understand potential reorganization of phytoplankton communities as the warming scenario persists.

Here, a simple trait-based analysis was applied to understand the mechanisms involved in driving spring phytoplankton biogeography in the Labrador Sea. First, the potential phytoplankton indicator species of North Atlantic and Arctic waters during spring in the Labrador Sea were recognised and, then, possible traits that could be driving such biogeography was identified. A trait-based analysis would give an ecological explanation of why certain phytoplankton species thrive in Arctic or Atlantic waters, contributing to the biogeography typically observed in the Labrador Sea during spring (Fragoso et al., 2016a, 2016b). This analysis gives a better insight of the phytoplankton species performance that are flourishing in contrasting watermasses of the Labrador, which can increase the predictive power of phytoplankton biogeography and its functionality in the system. Finally, future implication in trait biogeography and species distribution under a global warming scenario are discussed.

4.3 Methods

4.3.1 Sampling and analysis

Data for this study were collected on two research cruises (HUD-2013-008, and JR302) to the Labrador Sea during May (2013) and June (2014), where stations were sampled within an east-west transect across the Labrador Sea. Water samples were collected from depths within the mixed layer for phytoplankton, nutrients and chlorophyll *a* (chl *a*) analyses. Phytoplankton identification and enumeration occurred primarily using a Leiss inverted light microscope (LM), where water samples (0.3 L) were preserved in acidic Lugol's solution at a final concentration of 2%. For taxa that could not be identified to species level using the LM (e.g. coccolithophores, *Thalassiosira* spp., *Fragilariopsis* spp. and other small diatoms), a further identification occurred using a Leo 1450VP scanning electron microscope (SEM). For SEM analysis, water samples were filtered (0.25- 0.5 mL) onto polycarbonate filters (0.8 µm pore size, Whatman), rinsed with trace ammonium solution

(pH ~ 10), oven dried and stored in Millipore PetriSlides. A subsection of the polycarbonate filters were fixed into aluminum stubs and sputter-coated using the Hummer VI-A gold coater (Daniels et al., 2012). Cells were counted under x3000 magnification using fields of view (FOV) as described in Daniels et al (2012). Nutrient concentrations and chl *a* analysis, as well as literature information used to identify phytoplankton species were described in Fragoso et al. (2016).

4.3.2 Trait-based analysis

An extensive literature research on life strategies and morphological traits of target phytoplankton species from the Labrador Sea was conducted to primarily identify the potential functional traits that determines species biogeography. It is challenging to classify species traits univocally to a single modality, since species often display multi-faceted behaviors and functions, depending on the conditions and resources available (Paganelli et al., 2012). It is also challenging to determine traits that are functional in the system at a given sampling time (Violle et al., 2007). Information on functional traits are very scarce, thus selection of functional traits also depends on the availability of data for a specific ecological function, collected either from observations in this study or literature information (Appendices D.1 and D.2). In this study, traits were selected based on their potential ecological role in the system and information accessibility, which could support meaningful responses of species to the environment and explain species biogeography. Some functional traits were considered quantitative, such as the measurements of cell dimensions. In this case, average values of these traits were extracted from extensive databases (Appendix D.1). Other traits were considered more complex to categorise, on the basis that species can display traits to different extents. For these traits, individual species were coded using a "fuzzy code" as described by Chevene et al. (1994), which allows species to exhibit a trait at a certain degree. These traits (herein termed *continuous traits*) were arbitrarily scaled to a value between 0 and 1 (e.g. lowest (=0) or highest (=1) probability of species having a certain trait). Finally, other traits were more straightforward, such as binary traits (presence or absence of a certain trait, e.g. yes=1 or no =0) (Appendix D.1).

Quantitative cell dimension traits used in this analysis were the average of estimated spherical diameter (ESD), maximum dimension (MLD) and surface area to volume ratio (S/V). Continuous traits, which mean characteristics that do not fit into defined groups, were referred to traits related to life history strategies, such as those used in survival strategies (e.g. low probability of producing spores=0, resting stages or seldom producing spores=0.5, spores produced frequently=1). Other functional traits were considered binary, such as 1) presence of sharp outer projections, 2) adhesion to substrates, 3) psychrophilic (ability to grow under low temperatures, e.g. 0°C) or 4) grazing deterrence behavior, 5) robustness (usually species noted for being heavily silicified or calcified) and 6) presence of chloroplasts in setae, as shown in Table 4.1. These traits were selected based on literature information of potential organism responses to changes in the environmental of the Labrador Sea (nutrients concentrations, temperature, irradiance levels and predator avoidance) (Appendix D.1).

Other phytoplankton traits, such as life form (solitary species or chain/colonial forms), as well as cellular or colonial shape were included in the analysis (see examples in Fig. 4.1) (Appendix D.2). These traits were selected because they may infer, though not directly, species nutrient acquisition, sinking and grazer susceptibility (Litchman and Klausmeier, 2008; Stanca et al., 2013). Coloniality, as well as cell or colonial shape and size are, however, plastic traits (Litchman and Klausmeier, 2008), which are particularly difficult to measure using non-automated techniques (e.g. microscopy), given that individual cell sizes can vary and colonies can be broken through sampling procedures (McFarland et al., 2015). Moreover, some species, which are well-known to form chains or colonies can also be observed in solitary forms (e.g. most *Thalassiosira* and *Chaetoceros* species). However, these traits were classified based on *eminent* information derived from classical literature, which provides valuable information of the ecological significance of species. Morphological traits were considered to be categorical traits, meaning that certain species can be found in two or more categories of a certain trait (e.g. *Phaeocystis* can be found in both life forms: single cells and colonies) (Appendix D.2).

Table 4.1 Quantitative, binary and continuous functional traits selected and examples used in this study.

	Selected functional trait	Examples:
QUANTITATIVE	Estimated spherical diameter (ESD)	
	Maximum dimension length (MDL)	
	Surface area to volume ratio (S/V)	
BINARY	Adhesive to substrate	Species attached to solid substrates using mucilaginous sheats[9] (e.g. *Thalassiosira gravida* colonies), basal attachment pads[1] (e.g. *Melosira arctica*) and/or exuded substances from the raphe lit[2] (e.g. *Navicula* spp.). Phytoplankton species that produces ice-binding compounds, such as *Attheya septentrionalis*[3] and *Pauliella taeniata*[4]. Phytoplankton species found often attached to other species, such as *Pseudo-nitzschia granii* in *Phaeocystis pouchetii* colonies or *Phaecystis* colonies growing attached to setae of diatoms frustules (*Chaetoceros* spp.)[5,6] were also considered to possess this trait.
	Psychrophylic	Cold-favouring species (< 0°C), including sea-ice or sea-ice related species (e.g. *Fragilariopsis cylindrus*[7], *Fossula artica*[8] species).
	Sharp projections	Siliceous setae[9] (e.g. *Chaetoceros* spp.), spines[9] (e.g. *Corethron* spp.), and pointed processes[9] (e.g. *Rhizosolenia hebetata* f. *semispina*) in diatoms, spines in chrysophytes[10] (e.g. *Merigosphaera mediterranea*), skeletons in silicoflagellates[10] (Dictyochales) and whorl appendages[11] in coccolithophores (e.g. *Calciopappus caudatus*).
	Chloroplasts in setae	*Chaetoceros* spp (subgenus Phaeoceros)[9]
	Robustness	Species notorious for being heavily calcified coccolithophores (e.g. *Coccolithus pelagicus*)[12,13] or silicified diatoms (e.g. *Neodenticula seminae*) as opposed to weakly silicified *Ephemera planamembranacea* (diatoms) [9] or *Calciopappus caudatus* (coccolithophores) [12,14]. Heavily silicified or calcified species dominate vertical fluxes and are often preserved in the sediments or fossils observed in palentological studies.
CONTINOUS	Survival strategy (dormancy or resting spores)	Species where resting stages or spores have not been reported or are unknown (coccolithophores)[9], domancy or resting stages are common (*Cylindrotheca closterium*)[15], resting spores are seldom (*Rhizosolenia* spp.)[9] or frequent (e.g. *Thalassiosira antarctica* var *borealis*[9] and *Chaetoceros*[9] spp (subgenus Hyalochaeta)).

[1]Mary, 1997, [2]Stanley and Callow, 2007, [3]Crawford et al. (2000), [4]Raymond and Kim, 2012, [5]Fragoso et al., 2016, [6]Rousseau et al., 1994, [7]Lundholm and Hasle, 2010, [8]Von Quillfeldt, 2001, [9]Hasle and Syvertsen, 1997,[10]Throndsen, 1997, [11]Heimdal, 1997, [12]Daniels et al., 2014, [13]Baumann et al., 2000, [14]Daniels et al., 2016, [15]McQuoid et al., 2002.

Table 4.2 Categorical morphological functional traits and examples used in this study.

	Selected trait	Categories	Examples:
CATEGORICAL	Coloniality	Solitary	Coccolithophores, some diatom species: *Corethron* spp., *Coscinodiscus* spp., *Cylindrotheca* spp.).
		Colonial	Most *Thalassiosira*, *Chaetoceros* spp.
		Both	*Phaeocystis pouchetii*; some *Thalassiosira* (*T. bulbosa* and *T. kushirensis*)
	General cell/colony shape	Ribbon-shaped chains	*Fragilariopsis* spp., *Fossula arctica*, *Neodenticula seminae*, *Navicula septentrionalis*, *N. granii*, *N. vanhoeffenii*, *Pauliella taeniata*
		Tube-shaped Chain	Cylinder-shaped, such *Bacterosira bathyomphala*, most *Thalassiosira* spp, *Porosira glacialis*, *Chaetoceros* spp.
		Star/zigzag -shapes chains	*Nitzschia frigida*, *Thalassionema nitzschizoides*
		Cloud-shaped Colonies	*Phaeocystis* colonies, *Chaetoceros socialis* colonies, *Rhizosolenia hebetata* mats and *Thalassiosira gravid*a colonial clumps
		Sphere/oval/cone/pill-shaped	*Dictyocha speculum* (sphere), *Calciopappus caudatus* (cone), *Corethron criophilum* (pill-shaped)
		Needle shape	*Pseudo-nitzschia* cells and chains spp., *Rhizosolenia* spp. cells and chains, *Thalassiothrix* spp.

4.3.3 Statistical analysis

Biogeographical patterns of phytoplankton species were analysed using the software Primer-E 7. The selection of target phytoplankton species included the 50 most significant species that were identified to species levels and/or were potential indicators of North Atlantic and Arctic waters. Abundance data was log-transformed to balance out the weight of dominant and rare species. Similarity within samples (Bray-Curtis similarity), as well as species index of association was calculated and clustered simultaneously on log-transformed data using the matrix "display wizard" tool in Primer-E 7. Simultaneous cluster analyses of samples (stations) and variables (species) were used to create a shade

plot of the species abundances within stations occurring in different water masses (Arctic- or North Atlantic-influenced).

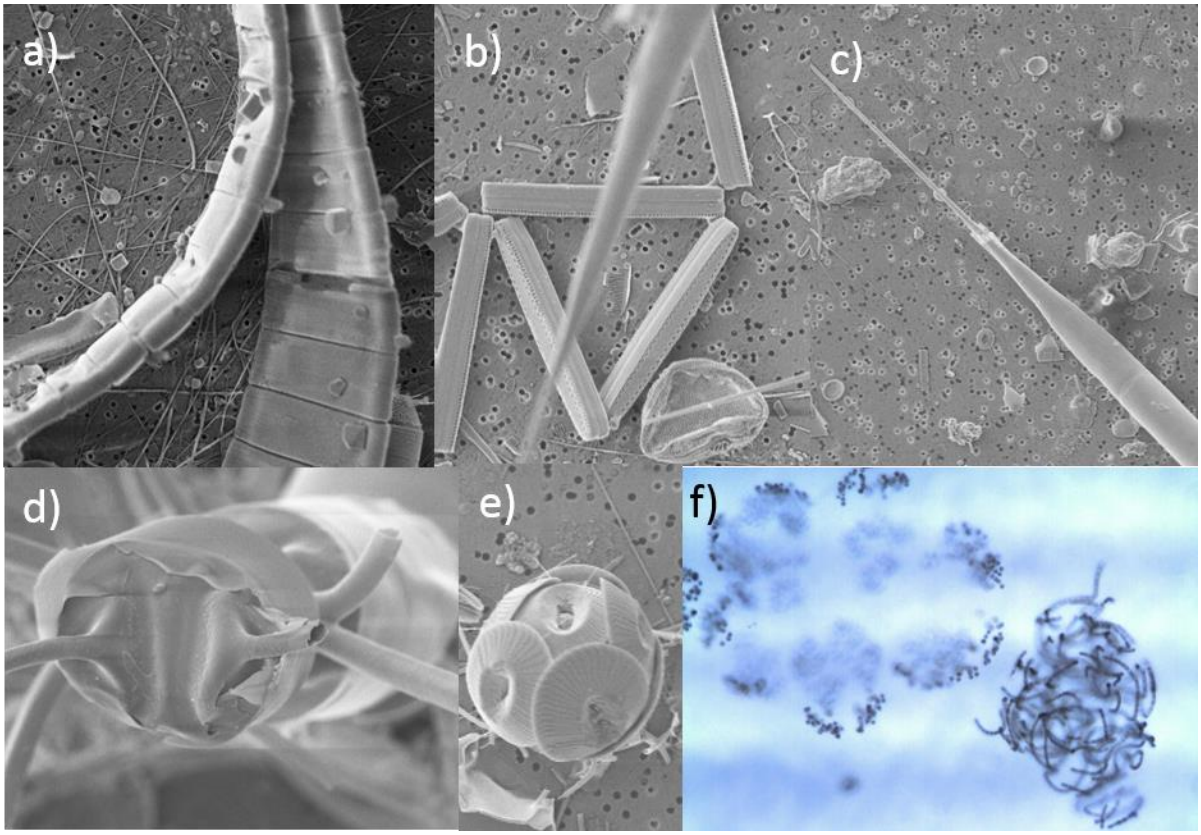

Figure 4.1 Examples of morphological traits derived from Table 4.2. a) Ribbon-shaped chains (potentially *Fossula arctica*), b) Star/Zig-Zag shape colonies (*Thalassionema nitzschoids*), c) needle shape cell or colonies (*Rhizosolenia hebetata* f. *semispina*), d) tube/cylinder shape (potentially *Chaetoceros borealis*), e) Sphere (*Coccolithus pelagicus*) and e) Cloud shape colonies (*Phaeocystis pouchetii* on the left and *Chaetoceros socialis* on the right). Credit of Figure 4.1f: Gunilla K. Eriksen.

Community-weighted trait mean (CWtM) values were calculated for each trait in each sample using a macro excel file "FunctDiv.xls" (Leps et al., 2006; available at http://botanika.bf.jcu.cz/suspa/FunctDiv.php). CWtM was calculated from two matrices: 1) a matrix that gives trait values for each species and 2) a matrix that has the relative abundance of species (after log-transformation) in each sample. CWtM calculates the single community trait value for each sample, according to the following equation:

$$\text{CWtM} = \sum_{i=1}^{S} p_i x_{i,}$$

where S is the number of species in the community, p_i is the species abundance proportion (after logarithm transformation) and x_i is the species-specific trait value.

To analyse the distribution of phytoplankton traits within Arctic- and North Atlantic-influenced waters, CWtM values for each sample were normalized and a scale from 0 to 1 (lowest=0 and highest=1 value for each CWtM) applied. Dendrogram and shade plots were generated by assessing the similarity of traits within samples (stations) (Bray-Curtis similarity) using the matrix display wizard tool in Primer-E 7.

4.4 Results

4.4.1 Environmental setting

Potential temperature and salinity data of upper waters (< 200 m) showed the partitioning and distribution of distinct water masses (Arctic- or North Atlantic-influenced waters) across shelves and the central basin of the Labrador Sea (Fig. 4.2). Arctic-influenced water masses had a strong pycnocline (upper waters σ_θ < 27 kg m^{-3}), where colder (temperature < 2°C) and fresher (salinity < 34) waters were found on and near shelves and slopes (Labrador in the west and Greenland in the east) (Fig. 4.2). Conversely, North Atlantic-related waters were warmer (temperature > 1°C), saltier (salinity > 33.5), had a weaker pycnocline (σ_θ > 27 kg.m^{-3}), and were found widely distributed in the central part of the Labrador Sea (Fig. 4.2).

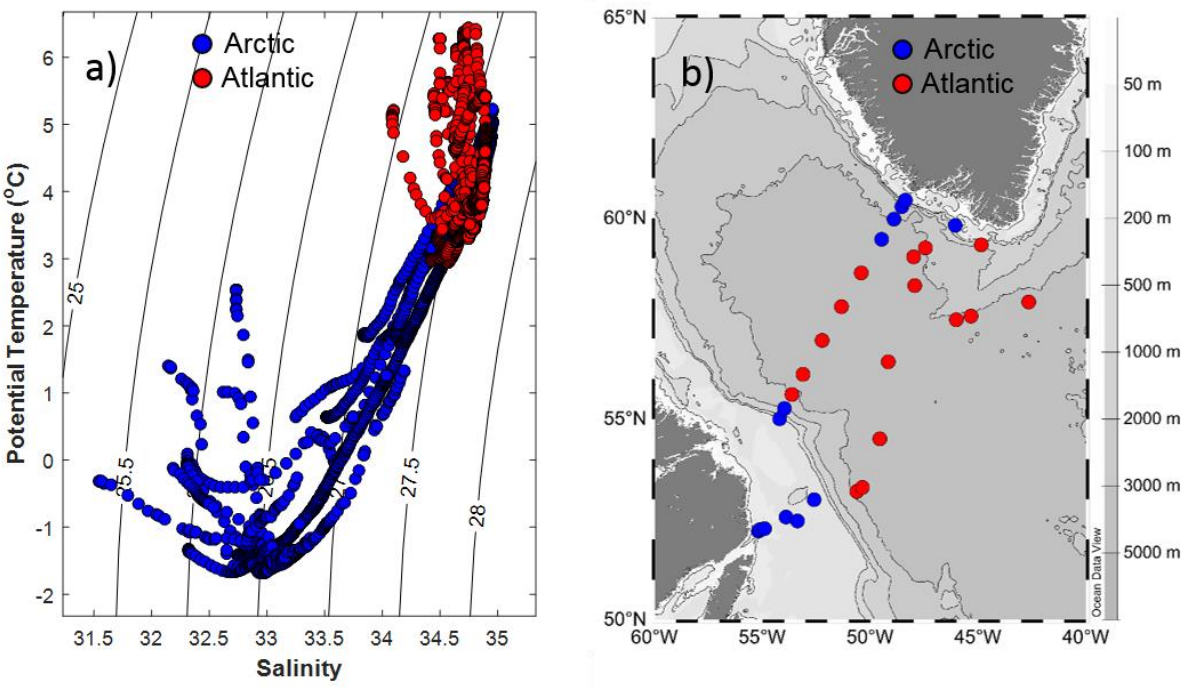

Figure 4.2 (a) Scatter plot of potential temperature and salinity (T-S) with isopycnals (σθ) of the upper waters (< 200m) from the Labrador Sea during May and June (2013/14). (b) Map showing the position of each station influenced by Arctic (on or near the shelves) or North Atlantic-influenced waters (central basin).

4.4.2 Phytoplankton species biogeography

Cluster analysis of phytoplankton species abundance of the Labrador Sea revealed two major groups of samples separated at similarity level of 36% (Fig. 4.3). These two groups were consistent with the geographic distributions of Arctic- and North Atlantic-related water masses, suggesting the influence of hydrography in determining species composition (Fig. 4.3) (see Appendix E for images of species from Arctic (Appendices E.1-E.4) and Atlantic waters (Appendix E.5). The contribution of the 50 most important species for each group (Arctic- and North Atlantic waters) is shown in the shade plot, where samples (stations) and variables (species) were arranged according to their similarity values (Fig. 4.3).

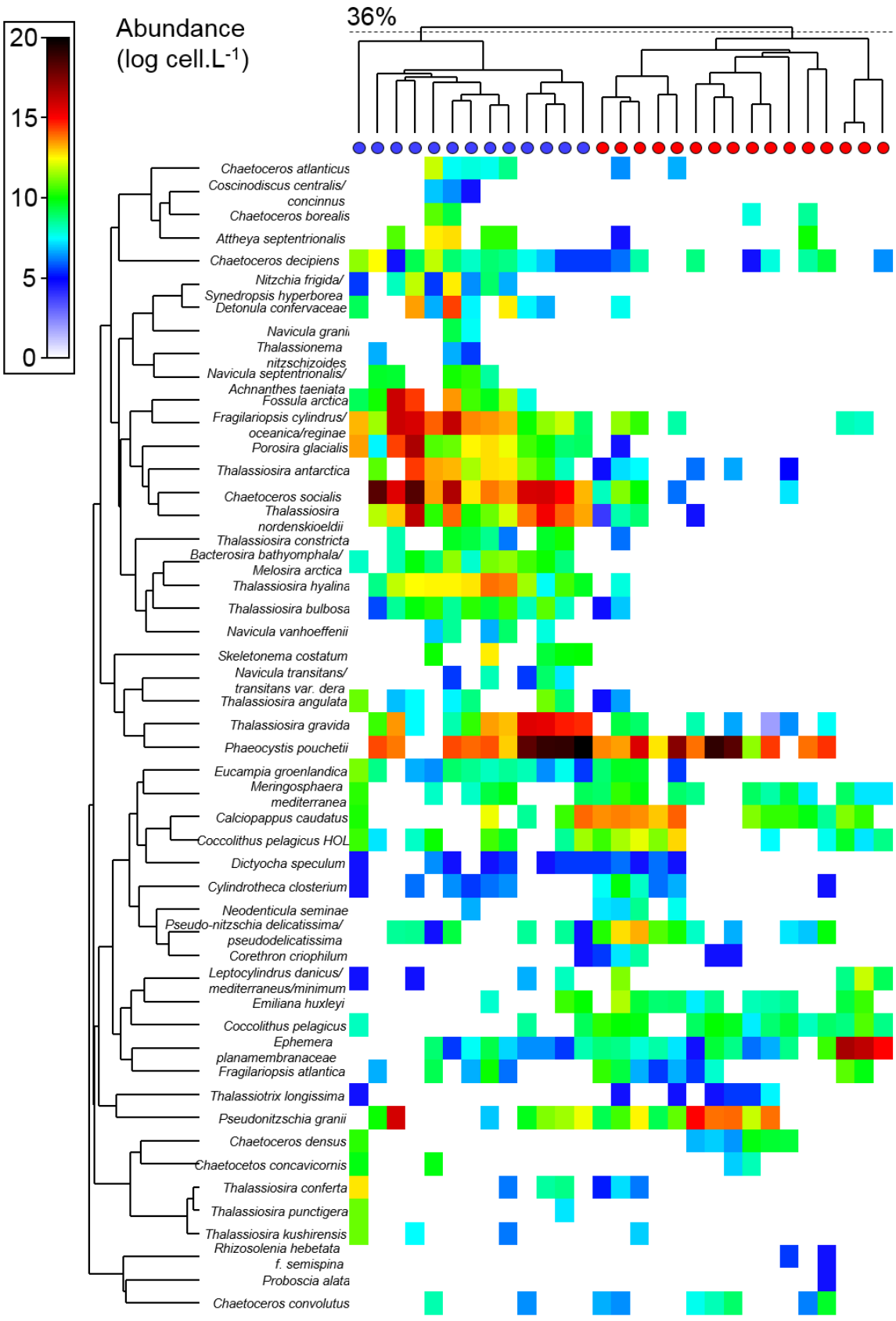

Figure 4.3 Shade plot showing the clustering of phytoplankton species (50 most important) abundance (after log-transformation) within different groups of samples (stations) at a 36% similarity level influenced by Arctic- (blue circles) or North Atlantic- (red circles) waters.

Cluster analysis revealed certain traits that occur together in phytoplankton communities from Arctic- and North Atlantic-related waters. In general, phytoplankton from Arctic waters were larger in biovolume (greater equivalent spherical diameter (ESD)), psychrophilic, robust (heavily silicified), able to form spores and colonies, with shapes resembling a ribbon, cylinder (or tube-shaped) or star (or zig-zag) (Fig. 4.4). Although not exclusively found in Arctic waters, traits including "adhesiveness" and morphological traits, such as "cloud-shaped colonies" were commonly found (Fig. 4.4). "Adhesiveness" was most often found in the group of diatoms that are typically encountered in sea ice, which use ice-binding molecules. While "cloud-shaped colonies" were represented by *Phaeocystis pouchetii*, *Chateoceros socialis* and *Rhizosolenia hebetata* f. *semispina* mats that were found in both Arctic and North Atlantic water masses (Fig. 4.4).

Traits that were commonly found in North Atlantic waters were those relating to shape, such as species resembling needles (represented by *Rhizosolenia hebetata* f. *semispina*, *Proboscia alata* and *Thalassiosthrix longissima*), which possibly reflected greater anti-grazing strategies and higher S/V and MDL (Fig. 4.4). Nonetheless, solitary phytoplankton that resembled sphere/oval/cone/pill shape, such as coccolithophores were also common in these waters. Phytoplankton from these waters typically had sharp projections and chlorophyll in the setae (probably because of the influence of *Phaeoceros*) (Fig. 4.4).

Pairwise correlation showed that that some traits presented positive or negative correlations (Fig. 4.5). For instance, individuals with larger biovolume (> ESD) positively correlated with colonial, robust and psychrophilic phytoplankton with morphological shapes that resembled stars (or zig-zag), tubes/cylinders or ribbons (Fig. 4.5). These same individuals were negatively correlated with phytoplankton that resembled a needle or spherical shape (cellular or colonial forms), possessed sharp projections (such as setae or skeletons), and were commonly found in solitary forms (Fig 4.5).

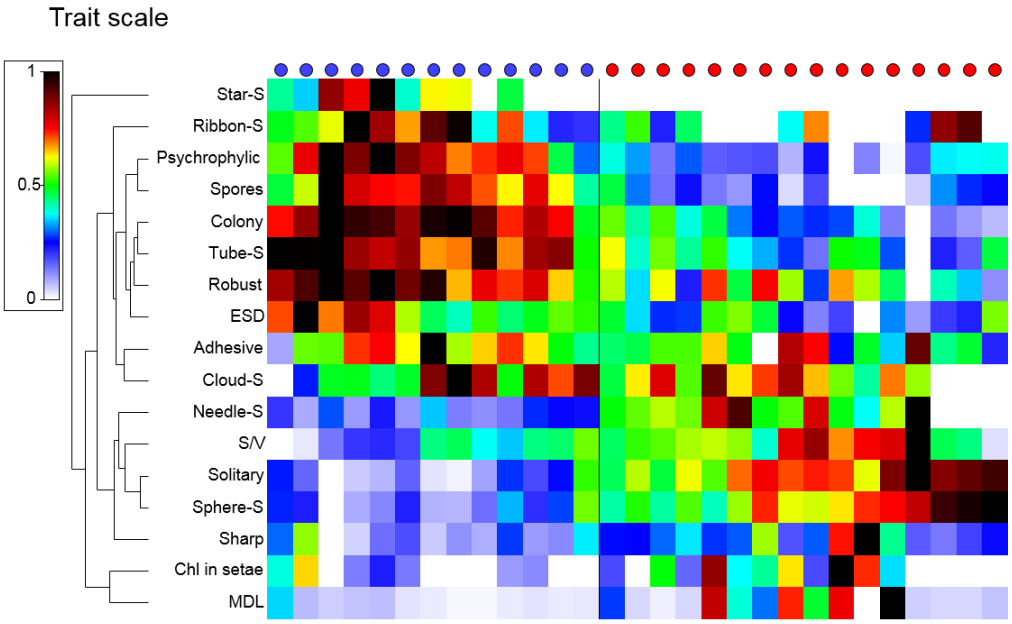

Figure 4.4 Shade plot showing the clustering of phytoplankton traits (after normalisation and scaling) distributed in Arctic- (blue circles) or North Atlantic-related (red circles) waters.

Pairwise correlation also showed that traits presented positive or negative correlations with environmental factors related to macronutrient concentrations (silicate, nitrate and phosphate and ratios) from spring (within the mixed layer) or winter values (from 200 m), stratification (Brunt-Vaisala, stratification index and mixed layer depth), temperature and salinity (Fig. 4.6). In general, phytoplankton traits, such as larger cell size (> ESD), coloniality, robustness, psychrophilia, as well as morphological colonial shapes that resembled stars (or zig zag), tubes/cylinders or ribbons (Fig. 4.6) correlated negatively with temperature, salinity, mixed layer depth, nitrate concentrations (from the mixed layer or pre-bloom values, such as those found at 200 m) and N/P (nitrate to phosphate ratios). These sample traits correlated positively with greater water column stratification (> stratification Index (SI) and Brunt-vaisala parameter) and higher winter values of silicate to nitrate ratios (Si/N from 200m depth).

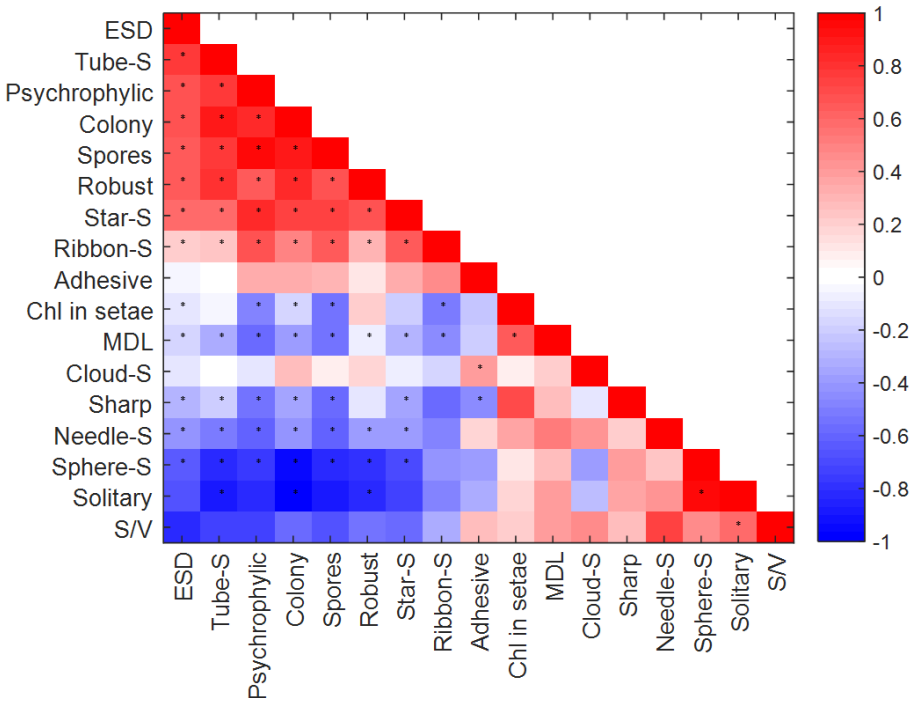

Figure 4.5 Pairwise Pearson correlation of functional traits, where blue indicate negative correlations and red indicate positive correlation. *Correlations that were statistically significant (p-value < 0.05). ESD = equivalent spherical diameter; Tube S = tube/cylinder-shaped form; psychrophilic = ability to grow under low temperature (< 0°C); Colony= colonial individuals; spores = ability to produce spores; Robust = heavily silicified/calcified organisms; Star-S = Star- or zigzag-shaped colony; Ribbon-S = Ribbon-shaped colony; Adhesive = high adhesion of individuals; Chl in setae = presence of chlorophyll a in setae; MDL = maximum dimension length; Cloud-S = cloud-shaped colony; needle-S = needle-shaped cell or colony; sphere-S = sphere-shaped cell; Solitary = solitary form; S/V = surface area to volume ratio.

Traits, including morphology (spherical or needle-shaped cells/colonies), S/V, solitary forms, and presence of sharp projection correlated positively with temperature, salinity, nitrate concentrations (within the upper mixed later and representative of winter values (from 200m)), nitrate to phosphate (N/P) ratios and mixed layer depth. These same traits correlated negatively with stratification (measured through Stratification Index (SI) and Brunt –Vaisala parameters) and silicate to nitrate (Si/N) ratio representative of pre-bloom waters (from 200 m).

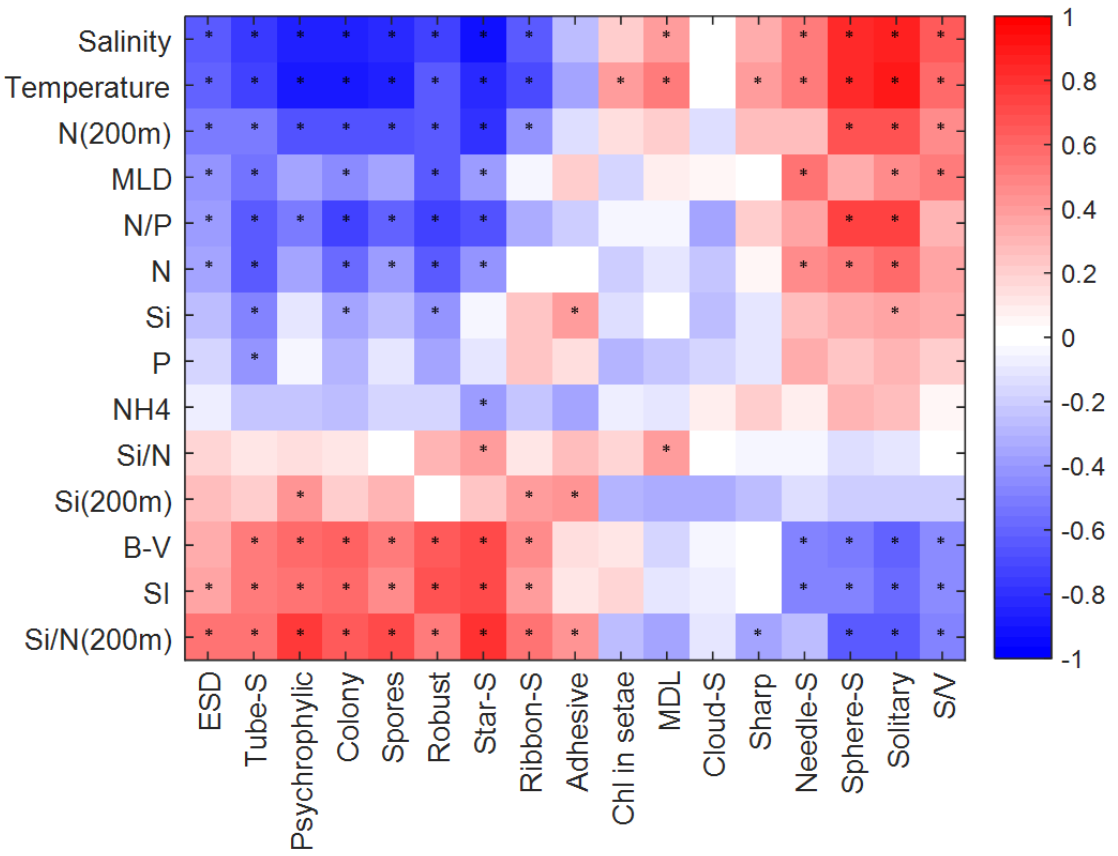

Figure 4.6 Pairwise Pearson correlation of functional traits and environmental variables, where blue indicate negative correlations and red indicate positive correlation. *Correlations that were statistically significant (p-value < 0.05).

4.5 Discussion

4.5.1 Phytoplankton species biogeography

The Labrador Sea receives North Atlantic and Arctic waters, where marked fronts shape the contrasting hydrography by maintaining the major currents of Arctic (Labrador Current in the west and West Greenland Current in the east) and Atlantic origin (Irminger Current in the center)) (Yashayaev, 2007). However, surface waters of the Labrador Sea undergo significant modification, where strong mesoscale physical processes, such as eddies, in addition to riverine and ice melt input (from sea ice, glaciers and icebergs) lead to mixing of these distinct waters masses, particularly during spring and summer (Straneo and

Saucier, 2008; Wu et al., 2007; Yebra et al., 2009). Consequently, species were not categorised as being indicators *exclusively* of Arctic and North Atlantic waters; instead, trends in abundance along these hydrographical zones were observed to determine the habitat preferences of selected species. In this study, Arctic and North Atlantic-related species did not present a clear-cut distribution between water masses; rather, a gradient of species was observed due to the 1) degree of mixing of neighbouring water masses and blending of phytoplankton communities and/or 2) ubiquitous distribution of certain species in both Arctic and sub-Arctic waters.

Although it is risky to delegate whether a species is exclusive or a bio-indicator of Arctic or North Atlantic waters, several authors have used species distributions as proxies to determine modern (Luddington et al., 2016; Riaux-Gobin et al., 2011) and ancient (Armand et al., 2005; Armand and Leventer, 2010; Leventer, 1998) water mass boundaries. In this study, the biogeography of some species agreed well with those that are typically found in Arctic or North Atlantic waters (see discussion below); however, interpretation of species as proxies of water masses was not always straightforward. For instance, some species, such as *Nitzschia frigida*, *Navicula granii*, *N. transitans*/ *N. transitans var. derasa*, *N. vanhoeffenii*, *N. septentrionalis*/*Pauliella taeniata*, *Fossula arctica*, *Thalassiosira hyalina*, *T. constricta*, *T. bulbosa*, *Bacterosira bathyomphala*/*Melosira arctica*, typically found in Arctic spring blooms and often associated with sea ice melting (Von Quillfeldt, 2001; von Quillfeldt et al., 2003), were also found in Arctic-related waters in this study (see Appendices E.1-E.4 for images of some of these species). Nonetheless, other species, such as *Thalassionema nitzschizoids*, *Skeletonema costatum*, *Coscinodiscus concinnus*/*centralis*, *Chaetoceros socialis*, are representative of neritic environments (Tomas, 1997), and were dominant because Arctic waters occur mostly in shelf regions of the Labrador Sea (Yashayaev, 2007). Other species that have been assigned as polar or sea ice-related species, such as *Fragilariopsis cylindrus* (Caissie et al., 2010) also occurred in North Atlantic waters in this study, although they were not as abundant as observed in Arctic-related waters (Appendices E.1-E.4).

Neodenticula seminae, a typically sub-Arctic Pacific diatom, extinct from the North Atlantic waters since the late Pleistocene until recent decades (1990's) (Miettinen et al., 2013), was also observed in North Atlantic waters during this study (Appendix E.5). This species could be perceived as a true indicator of subarctic waters due to its preference for slightly higher temperatures as compared to those of Arctic waters, including the sub-

Arctic North Atlantic, though its transition has been speculated to occur via the Arctic Ocean (Miettinen et al., 2013).

Coccolithophore species, such as *Emiliana huxleyi* and *Coccolithus pelagicus*, which are typically found in the sub-Arctic North Atlantic waters in blooming (Harlay et al., 2010; Holligan et al., 1993) or non-blooming conditions (Daniels et al., 2016; Poulton et al., 2010), were found in high abundance mostly in Atlantic-related waters in this study. The ubiquitous *E. huxleyi* species notoriously thrives in warm and saline Atlantic-derived waters, suggesting that these species prefer relatively warmer waters; although it has been rarely observed in Arctic-related waters (Balestra et al., 2004; Charalampopoulou et al., 2011; Dylmer et al., 2015), including under the sea-ice (Balch et al., 2014). *Coccolithus pelagicus* is a cold water species (optimum approximately at 8°C; (Baumann et al., 2000) and has been suggested as a sub-Arctic indicator species (Daniels et al., 2014), although the motile, haploid lifestage of *C. pelagicus* (herein called *C. pelagicus* HOL) has been observed in waters with Arctic influence, such as Greenland Sea (Daniels et al 2016) and Barents Sea (Giraudeau et al., 2016). Weakly calcified coccolithophores, such as *C. pelagicus* HOL and *Calciopappus caudatus* were found in both water masses, and co-occurrence has been reported in colder waters of North Atlantic and Arctic origin (Balestra et al., 2004; Baumann et al., 2000; Okada and Mclntyre, 1979). It is unclear why these distinguished weakly calcified coccolithophore species were present in Arctic-related waters, albeit in low numbers; however, temperature has been suggested to control coccolithophore biogeography in a large scale (Baumann et al., 2005).

Several studies have attributed Arctic and North Atlantic phytoplankton indicator species using molecular (Luddington et al., 2016) and morphological approaches (Barton et al., 2016; Degerlund and Eilertsen, 2010; Fragoso et al., 2016b). Although it has been suggested that the use of genetic approaches may be used to reliably identify Arctic and North Atlantic indicator species and their strains and variants (Luddington et al., 2016), appropriate hydrographical characterization is just as important to avoid misinterpretation of species indicators to certain water masses. A number of these studies underestimated the degree of surface water mixing (Lovejoy et al., 2002; von Quillfeldt, 2000), which could explain some controversial findings, such as the typical Arctic diatom *Thalassiosira hyalina* being reported in North Atlantic waters, where there is clearly influence of Arctic waters in the Scotian Shelf (salinity is < 34) (Luddington et al., 2016). Thus, better hydrographic characterization in combination with appropriate taxonomic methods are mandatory to properly assess species indicators of Arctic and Atlantic waters.

4.5.2 Trait biogeography

Although species presented a gradient distribution among water masses and were not necessarily considered exclusive to certain water masses, the structure of the phytoplankton community as a whole agreed well with the contrasting hydrography (Arctic- and North Atlantic- influenced) in this study. Thus, this suggests that analysis of phytoplankton communities, rather than single species, could lead to a more powerful understanding of their biogeographical distribution. This infer that certain traits, commonly found in different species that co-occur in communities, might be shaping the biogeographical distributions of these species.

Phytoplankton from Arctic and Atlantic-related waters typically presented distinct functional traits. Psychrophylia was one common trait found in species assemblages from Arctic waters, revealing that a number of phytoplankton found in Arctic waters in this study were incorporated from sea ice algae. Release of sea ice diatoms from melting ice, transfer of sympagic (ice-associated) algae to the pelagic community and accumulation in the water column has been assumed the primary cause for bloom development near ice melting regions (Ichinomiya et al., 2008; Leventer and Dunbar, 1996; Syvertsen, 1991), although most sympagic diatoms sink to the sea floor, given that they are unable to adapt to ice free waters (Riaux-Gobin et al., 2011). Positive buoyancy has been considered a trait that would favor the transfer of diatoms from a sympagic to a pelagic community and species released from the ice have been shown to exhibit different degrees of buoyancy control and sinking characteristics (Ichinomiya et al., 2008; Michel et al., 1993). Sea ice melt also provides a haline-stratified layer, where species associated with the transition from sea ice to meltwater and pelagic habitats are suddenly exposed to high-light levels (Smith and Nelson, 1985), as observed in this study. This implies that while sympagic diatoms are known to be adapted to low light, transitional (from ice to water column) species have a high plasticity to cope with rapid and relatively large changes in irradiance. *Fragilariopis cylindrus*, a diatom species found in high abundance in the sea ice as well as in the water column has been shown to display high degrees of phenotypic plasticity to environmental fluctuations (Kropuenske et al., 2010, 2009; Petrou et al., 2010; Sackett et al., 2013), which suggest that this might be a potential functional trait observed in this study.

Species assemblages from Arctic waters were often able to form resting spores. Resting spore formation does not imply psychrophilia, rather, it is is believed to be an hibernation strategy to overcome unfavorable environmental condition, including low (Zhang et al., 1998) or high light (Oku and Kamatani, 1999), low temperature (Durbin, 1978), nitrate (Kuwata and Takahashi, 1999; McQuoid and Hobson, 1996), phosphorus (Oku and Kamatani, 1995) and iron (Sugie and Kuma, 2008) limitation. Resting spores are heavily silicified when compared to vegetative cells (Sugie and Kuma, 2008), and formation occurs as a function of excess of silicate available in the water, as studies have shown that diatoms require additional levels of silicate (above basic requirement) to be able to form resting spores (Kuwata and Takahashi, 1990; Oku and Kamatani, 1995). The ability to produce spores correlated positively with winter silicate concentrations and Si/N ratios in this study, and, in general, Arctic waters are known to have a surplus of silicate compared to nitrate (Harrison et al., 2013). Thus, it is possible that higher silicate concentration in these waters could favour species that produces spores when light and nitrate becomes limiting. As the winter progresses, resting spores could be passively incorporated to the sea ice and reintroduced to the water column as sea ice melts in spring before bloom formation. Resting spores have been interpreted as a proxy for sea ice melting (Crosta et al., 2008) and an important life cycle strategy for ice-related species (Tsukazaki et al., 2013), suggesting that it is a common trait found in Arctic waters influenced by sea ice concentration.

A common feature of Arctic water assemblages, particularly diatoms, is that they were dominated by larger cells (> ESD), often found forming chains. Larger cell-size is a common feature of phytoplankton from ice-related waters (Arrigo et al., 2010b) and has been previously observed in the Arctic-influenced waters of the Labrador Current (Stuart et al., 2000). Size, as well as chain formation, has been suggested to be an important trait to reduce vertical percolation of cells in brine channels during flushing events of sea ice melt (Lizotte, 2003). Diatom chains were mostly ribbon- (e.g. *Fragilariopsis* spp., *Navicula septentrionalis*, *N. vanhofenni*, *N. granii*, *Fossula arctica*, *Pauliella taeniata*), cylinder- (*Melosira arctica*, *Bacterosira bathyomphala*, *Detonula confervace* and several *Thalassiosira* spp. and *Chaetoceros* spp.) or star-shaped (*Nitzschia frigida*/*Synedra hyperborea* and *Thalassionema nitzschoides*), although some solitary forms were also observed (*N. glaciei*/*N. transitans*). Such morphological traits have commonly been reported in ice-related phytoplankton blooms (Arrigo et al., 2014; Ichinomiya et al., 2008; Riaux-Gobin et al., 2011; Tsukazaki et al., 2013). More specifically, solitary pennate

diatoms have been found inside brine pockets in the ice (Fernández-Méndez et al., 2014) and chain-forming pennate diatoms have been suggested to grow strongly in the platelet ice layer (under sea ice) and released into the underlying water column (Ichinomiya et al., 2008; Palmisano and Sullivan, 1983). Filamentous strands of several meters of *Melosira arctica* grow attached to the underside of ice-flows (Arrigo et al., 2010b; Poulin et al., 2014) and neritic chains of centric, cylinder-shaped diatoms flourish in meltwaters (Arrigo et al., 2010b). It is intriguing why these species were so similar in shape and is possible that they shared similar metabolic functions that facilitated their success, given that some species evolved from the same family (e.g. *Thalassiosira*, *Bacterosira*, *Detonula* and *Porosira* are from Thalassiosiracea family (Tomas, 1997). Another possibility is that their morphology and the flexibility of these chain, including ribbon-shaped or thread-like colony-forming diatoms (e.g. *Thalassiosira*), represent an ecological function, such as resistance to breakage when subjected to shear (Nguyen and Fauci, 2014) from, for example, sea ice shredding. Moreover, such cells are united by mucous material that not only allow cells to be connected to each other but also to the sea ice. Extracellular polymeric substances (EPS) produced by sea ice diatoms to overcome extreme cold and salinity condition in the sea ice also may increase their buoyancy in the water column (Assmy et al., 2013; Fernández-Méndez et al., 2014).

Atlantic-related phytoplankton species presented distinct traits in this study, such as larger surface area to volume ratio, maximum dimension length (MDL), sharp projections, needle or sphere-shaped cells, presence of chloroplasts in the setae and were found in solitary forms. North Atlantic waters were less stratified and had deeper mixed layers, which might have selected for phytoplankton that are able to cope with a turbulent environment. Sharp projections, such as setae, spines, long processes, as well as elongated shapes (needle-shaped) have been suggested to improve the cell's ability to increase nutrient uptake efficiency under a turbulent environment because it can increase the spin of cells (Nguyen et al., 2011; Pahlow et al., 1997; Smetacek, 1985). These projections also increase shear rate, which could increase nutrient diffusion to the cell and retard sinking flux (Padisák et al., 2003), either increasing drag under strong mixing or keeping the cells within the mixing layer when waters are stratified. Traits, such as presence of chloroplasts in the setae (e.g. *Phaeoceros* subgenus) and elongated forms, greater MDL, and needle-shaped cell morphology may have increased the cells' capacity of assimilating light in the deeper mixing layer found in North Atlantic waters in this study. Cells with elongated, needle-shaped forms have their thylakoids linearly distributed in the cells, which reduces shelf

shading and increases absorption cross spectra. Streaming of chloroplasts has been observed in *Rhizosolenia* and other species where they tend to congregate at the center of the cell during high light intensities, and spread around the cell periphery in dimmer conditions (Round et al., 1990). This could explain the ability of needle-shaped phytoplankton, such as *Rhizosolenia* to migrate in the water column and grow under a wide range of irradiance (Richardson et al., 1996).

Diatoms found in Atlantic waters were also weakly silicified as compared to Arctic-related species, and this could be due to the lower silicate to nitrate ratio found in Atlantic related waters in this study and observed generally in North Atlantic waters (Harrison et al., 2013). Weakly silicified species included *Leptocylindrus mediterraneous*, and particularly *Ephemera planamembranacea*, which has been found blooming in North Atlantic waters (this study, Fragoso et al., 2016; Le Moigne et al., 2015). Sharp projections, such as setae, spines, long processes, as well as elongated shapes (needle-shaped) can also be used as an anti-grazing strategy, which correlated with relatively warmer temperature for North Atlantic waters, where zooplankton metabolism and grazing chance is higher (Ikeda et al., 2001).

4.5.3 Future implications

Changes in the high Arctic are evident, from rises in temperature to sea ice decline and increase in surface freshening as a result of higher precipitation, river flow and sea ice and glacier meltwater input (Anisimov et al., 2007). Several questions have arisen, including whether "Arctic will be the New Atlantic" if sea ice melt persist (Yool et al., 2015) and many studies have revealed changes occurring to phytoplankton community composition as a consequence of climate change, such as the intrusion of Atlantic species into high Arctic waters (Hegseth and Sundfjord, 2008).

In this study, several phytoplankton species appeared to be restricted to Arctic-influenced waters, whereas some other species, abundant in North Atlantic waters, were also found in Arctic waters but in lower concentration (e.g. *E. planamembranacea* and coccolithophores in general). This suggests that species abundant in Arctic-related waters have a less

generalised distribution, which could indicate greater dependence of certain species to the sea ice habitat or ice-influenced, well illuminated and stratified waters.

Sea ice is one of the largest and most extreme habitats in polar oceans, comprising up to 13% of Earth's surface at its maximum (Eicken, 1992; Mock and Junge, 2007). Predictions show that the Arctic will have a total ice free summer by mid-21st century (Wang and Overland 2009). Loss of sea ice coverage indicates losses of species habitat, diversity and reductions of phytoplankton blooms associated with sea ice melting (Yool et al., 2015). Traits that are linked to sea ice species, such as psychrophilia or ability to survive under extreme cold and harsh environments will also tend to decline, implying a great risk to seeding algae and bloom initiation. Phytoplankton that rely on sea-ice to hibernate as resting spores and germinate under stratified conditions will be affected as sea ice cover declines. Nutrient concentration reduction will also influence the size of phytoplankton, favouring smaller species that have lower nutrient requirements (Li et al., 2009), or mixotrophic phytoplankton that can supplement their nutrient demands by ingesting prey (Zubkov and Tarran, 2008).

4.6 Conclusions

Phytoplankton communities in the Labrador Sea differed between contrasting hydrography (Arctic- and North Atlantic- influenced) in this study. Most species were not *exclusively* found in Arctic or North Atlantic waters, instead, trends in abundance along these hydrographical zones were observed, suggesting the analysis of phytoplankton communities, rather than single species, can provide a more powerful understanding of their biogeographical distribution. Arctic and North Atlantic-related species did not present a definite distribution between water masses; however, a gradient of species abundance was observed because of the 1) degree of mixing of surface waters and blending of phytoplankton communities or/and 2) ubiquitous distribution of certain species between Arctic and sub-Arctic waters.

Phytoplankton traits have also differed among Arctic and sub-Arctic North Atlantic waters. Phytoplankton from Arctic-related waters were, in general, psychrophilic, chain-forming (ribbon-, cylinder and/or star-shaped), heavily silicified diatoms that form resting spores

with a larger biovolume (> ESD). Cold temperature, higher stratification, light availability and silicate concentration, in addition to presence of sea ice, which can store diatom resting spores during winter conditions, may have selected for phytoplankton species with such traits. Conversely, Atlantic-related phytoplankton species presented distinct cellular traits in this study, such as larger surface area to volume ratio, maximum dimension length (MDL), sharp projections, needle or sphere-shaped cells, weakly silicified cell walls and presence of chloroplasts in the setae, in addition to being found in solitary forms. North Atlantic waters were less stratified and had deeper mixed layers, which might have selected for phytoplankton that are able to cope with a turbulent environment. Lower silicate to nitrate ratio found in Atlantic related waters in this study and observed generally in North Atlantic waters (Harrison et al 2014) may have selected for weakly silicified diatoms. Traits, such as sharp projections, such as setae, spines, long processes, as well as elongated shapes (needle-shaped) might have acted as an anti-grazing strategy in warmer North Atlantic waters, where zooplankton metabolism and grazing rates are higher.

Chapter 5: Summary and Conclusions

5.1 Synthesis of research

The main aim of this research was to investigate the environmental controls involved in shaping the spring phytoplankton communities from contrasting hydrographical provinces of the Labrador Sea and their biochemical role in this high latitude region. The results presented in this thesis have answered many questions raised in the Introduction Chapter (Chapter 1). From this investigation the following conclusions can be drawn:

Chapter 2

- A thorough unprecedent quantitative microscopic analysis of phytoplankton composition in the Labrador Sea showed that phytoplankton communities had a remarkably similar spatial and temporal distribution across the four years of study (2011-2014), in spite of some temporal variability in sampling (six weeks) during spring and early summer.
- Phytoplankton communities from the Labrador Sea during spring and early summer of 2011 - 2014 varied **mostly** according to the major hydrographic features of distinct water masses of Atlantic (Irminger Current - IC), Arctic via Davis Strait (Labrador Current - LC) or Arctic via Denmark Strait (West Greenland Current - WGC) origin.
- The main composition of spring phytoplankton blooms from the Labrador Sea were: 1) Arctic/polar large (> 50 µm) diatoms dominating in the inshore branch of the LC, which were most influenced by Arctic and sea ice melt waters, 2) *P. pouchetii* co-dominated with diatoms (*Pseudo-nitzschia granii*, *Thalassiosira* spp.) at the interface of the Arctic (WGC) and Atlantic (IC) waters and 3) *Ephemera planamembranacea*, *Rhizosolenia hebetata* f. *semispina* and *Fragilariopsis atlantica* dominating the offshore waters of the central basin, which is strongly influenced by Atlantic waters (IC) (Fig 5.1).
- The environmental factors controlling for the phytoplankton community partitioning in Labrador Sea near surface waters were: 1) lower salinities and

temperatures associated with the Arctic/polar species found in the shelf waters with higher influence of the Arctic outflow, 2) higher pre-bloom Si* (Si* from deeper waters) on the Labrador Shelf and Slopes influenced the taxonomic segregation of polar diatoms dominating in the west, 3) ability of *P. pouchetii* to grow in deeper mixing layers, whereas Arctic/sea-ice diatom blooms were only found in shallower mixed layers (< 25 m) and 4) higher temperature and nutrient concentrations associated with Atlantic diatoms blooming in stratified waters.

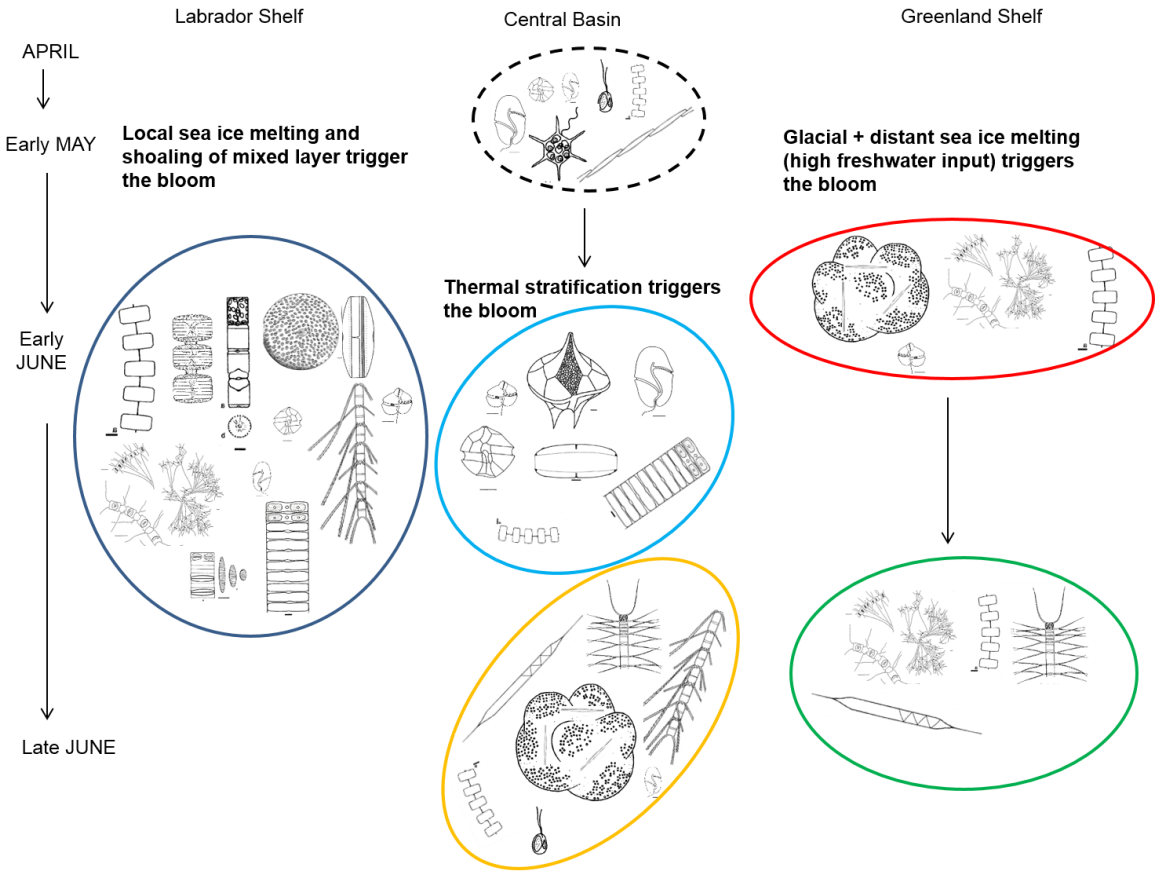

Figure 5.1 Schematic of the environmental controls and the temporal progression of distinct phytoplankton communities from contrasting hydrographical zones of the Labrador Sea as reported in Chapter 2. The colours in the circles refer to the same ones used in the Cluster analysis in Figure 2.5.

Chapter 3

- The results from Chapter 2 provided a foundation for the expanded analysis of phytoplankton community distribution and their photophysiological and biochemical signatures using ten-years (2005-2014) of pigment data as shown in Chapter 3. This chapter, however, included data from a wider variety of algal classes (e.g. flagellates) that were not identified from the microscopic analysis as reported in Chapter 2.
- Spring phytoplankton communities varied mainly spatially from southwest to northeast, whilst phytoplankton composition from the central region of the Labrador Sea varied temporally from May to June similarly as observed in results presented in Chapter 2.
- In terms of taxonomic groups, phytoplankton blooms (> 3 mg Chl*a* m^{-3}) were primarily observed in May in haline-stratified waters of the shelves, being co-dominated by diatoms and chlorophytes in the west and *Phaeocystis* and diatoms in the east. In the central Labrador Sea during May, a pre-bloom (low chlorophyll) condition was observed, where a diverse mixed flagellate assemblage occurred in deeper mixed waters, which later in the season (June) progressed to a bloom co-dominated by dinoflagellates and, again, diatoms in thermally-stratified waters (Fig 5.2).
- Phytoplankton communities presented contrasting ratios of accessory pigments to total chlorophyll *a*, as well as photophysiological strategies. Photosynthetic parameters varied primarily according to community composition, where *Phaeocystis* and diatom blooms in the east appeared to cope well with high light levels, given the minimal photo-inhibition observed in these communities. Conversely, phytoplankton communities from Atlantic waters (co-dominated by diatoms and dinoflagellates) were highly susceptible to photo-inhibition compared with other communities in the Labrador Sea. To cope with photo-damage, this phytoplankton community appeared to have increased the levels of photoprotective pigments, such as those used in the xanthophyll cycle (diadinoxanthin and diatoxanthin).
- Ratios of POC:PON were also influenced by phytoplankton community composition, where the western bloom (co-dominated by diatoms and chlorophytes) presented higher phytoplankton-derived organic carbon, whereas the

eastern bloom (*Phaeocystis* and diatoms) presented a higher contribution of detritus, possibly derived from the mucilaginous material of the colony-forming *Phaeocystis*. Nonetheless, freshwater input, likely from melting glacial and sea-ice and river outflows, possibly carried allochthonous carbon to shelf waters, which complicates the interpretation of POC:PON derived from phytoplankton communities. Similarly, overall POC:PON ratios and phytoplankton-derived organic carbon was low in waters of Atlantic origin in the central Labrador Sea. Higher contribution of bacterial biomass and/or higher nitrate concentrations in Atlantic waters may have influenced the low POC:PON ratios observed.

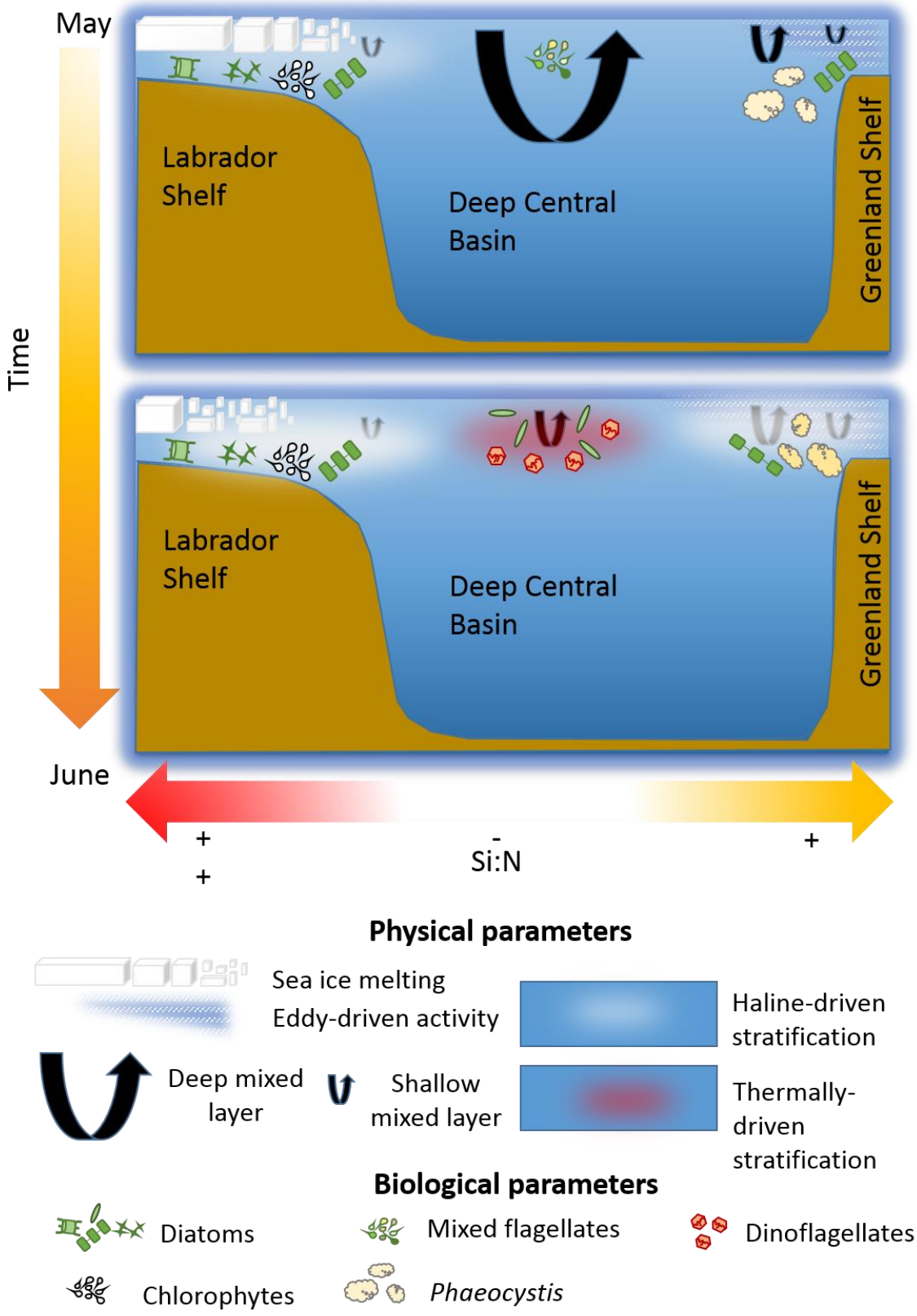

Figure 5.2 Schematic diagram summarising the environmental controls on spring (May to June) phytoplankton communities observed from ten-years (2005–2014) of pigment and hydrographical data.

Chapter 4

- Functional traits of phytoplankton species were investigated to assess their biogeographical pattern between Arctic- and North Atlantic- influenced waters. A gradient in abundance suggested that most species were not exclusively present in Arctic and North Atlantic waters, possibly because of some degree of mixing and/or some species having an ubiquitous distribution in the Labrador Sea region. However, the analysis of phytoplankton communities as a whole, rather than single species, gave a more powerful representation of phytoplankton biogeography from waters of Atlantic and Arctic origin in the Labrador Sea.

- The major traits of phytoplankton species from Arctic-related waters were psychrophilia (ability to grow at low temperatures), larger cell size, chain-formation (ribbon-, cylinder and/or star-shaped), heavy silicification and resting spore formation (in case of diatoms). Psychophilia was a selective trait of phytoplankton species in response to colder temperatures (< 0°C) found in these waters. Higher stratification in waters influenced by ice melt provides greater light availability, which might favour larger phytoplankton cells, given that these cells have high levels of shelf-shading, allowing them to cope with high irradiance. Higher silicate concentration might have favoured resting spore formation, as well as the presence of sea ice, which can retain diatom resting spores during winter conditions, favouring phytoplankton species with such traits. It is still unclear why morphological traits, such as chain formation (ribbon-, cylinder and/or star-shaped) in diatoms is an advantage in Arctic waters. It is possible that the the flexibility of these chains represented resistance to ice breakage and/or that the mucous material that binds the cells together may have confered positive buoyancy in highly stratified Arctic waters.

- Atlantic-related phytoplankton species were usually found in solitary form, had weakly silicified cell wall (in case of diatoms), as well as the following morphological characteristics: larger surface area to volume ratio, maximum dimension length (MDL), sharp projections and needle or sphere-shaped cells. Larger surface area to volume ratio might be a trait selected to cope with a turbulent environment, given that North Atlantic waters were less stratified and had a deeper mixed layer. Lower silicate to nitrate ratio found in Atlantic-related waters may have selected for weakly silicified diatoms. Traits, such as sharp projections,

including setae, spines, long processes, as well as elongated shapes (needle-shaped), might act as an anti-grazing strategy in warmer North Atlantic waters, where zooplankton metabolism and grazing rates are high.

5.2 Future work

- The results from this thesis provided a clear picture of the distribution and succession of spring phytoplankton communities from the Labrador Sea from May to June. However, the future of spring phytoplankton communities from the Labrador Sea under a climate change scenario is still unknown. Further work using species distribution modelling methods could address this question. The spatial distribution of target phytoplankton species from the Labrador Sea, such as those discussed in Chapter 4, can be obtained from large databases (Global Biodiversity Information Facility (GBIF) and Continuous Plankton Recorder (CPR), for example) and their niche distribution can be modelled. A cluster analyses of probability of occurrence of each species can be applied to identify the biogeographical distribution of major phytoplankton species from the Labrador Sea under present and future conditions.
- Samples from spring 2014 have also been collected for analysis in a CytoSense - a portable flow cytometer able to measure particules from > 1 µm up to 1.5 mm. In addition to measuring greater size range of particles, the CytoSense, as a flow cytometer, gathers fluorescence data and can collect images of particles. The light scattered from each particule analysed in the CytoSense can potentially provide real time information about the cell and colony size, as well as the amount of cells per chain and the morphological variation of phytoplankton species. In addition to scatter, the fluorescence emitted by photosynthetic pigments in algal cell can be detected using three different wavelengths: for phycoerythrin (orange), phycocyanin (yellow) and chlorophyll a (red), which can assist in classifying the algal class type. Information from all these phytoplankton traits could be used to construct a library, which would speed up the analysis of phytoplankton counts from the Labrador Sea in the future.

5.3 Concluding remark

This thesis has provided information about the spatial and temporal distributions of spring phytoplankton communities in the Labrador Sea using microscopic observations, as well as pigments and trait-based analysis. The results from this thesis have provided a new perspective on environmental processes that control phytoplankton community dynamics in the Labrador Sea. It has been demonstrated that phytoplankton composition in the Labrador Sea varied according to contrasting hydrographical zones of Arctic and Atlantic origin. The environmental controls in these communities were: temperature, stratification, nutrient concentrations and ratios (particularly silicate:nitrate). Distinct phytoplankton communities presented different biochemical (C:N ratios, phytoplankton-derived organic carbon concentrations) and photophysiological traits (pigments ratios and photosynthetic parameters). Phytoplankton functional traits, particularly those involved in morphology (cell size, surface area to volume ratio, presence of spines, etc.), in addition to life history (production of spores) and temperature-related traits (psychrophilia) largely contributed to the biogeography of species in Atlantic and Arctic waters of the Labrador Sea. Further analysis considering phytoplankton niche distribution will significantly improve scientific understanding of environmental controls on phytoplankton communities and their impact on pelagic ecosystem functioning and ocean carbon sinks under present and future scenarios.

Appendix A

A.1 : Chlorophyll *a* profiles (left) of hydrographical transects (right) across the Labrador Sea during late spring and early summer 2011-2014 (a-d). Arrows indicate stations where Lugol samples were collected for microscopic analysis. Colours of the arrows refer to clusters groups on Figure 2.5a.

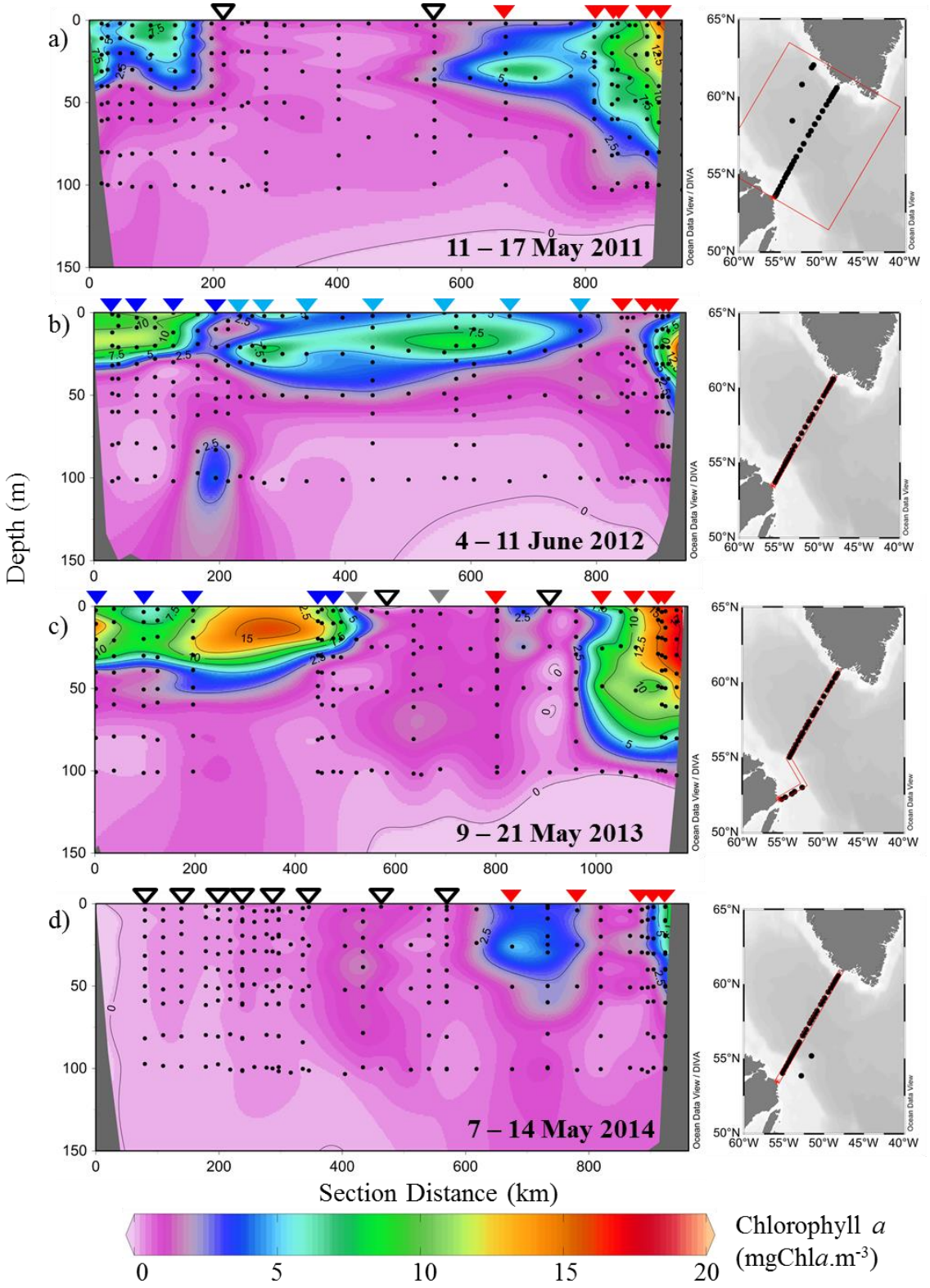

A.2 : Fluorescence profiles (left) of hydrographical transects (right) across the Labrador Sea during late spring and early summer 2011-2014 (a-d). Arrows indicate stations where Lugol samples were collected for microscopic analysis. Colours of the arrows refer to clusters groups on Figure 2.5a.

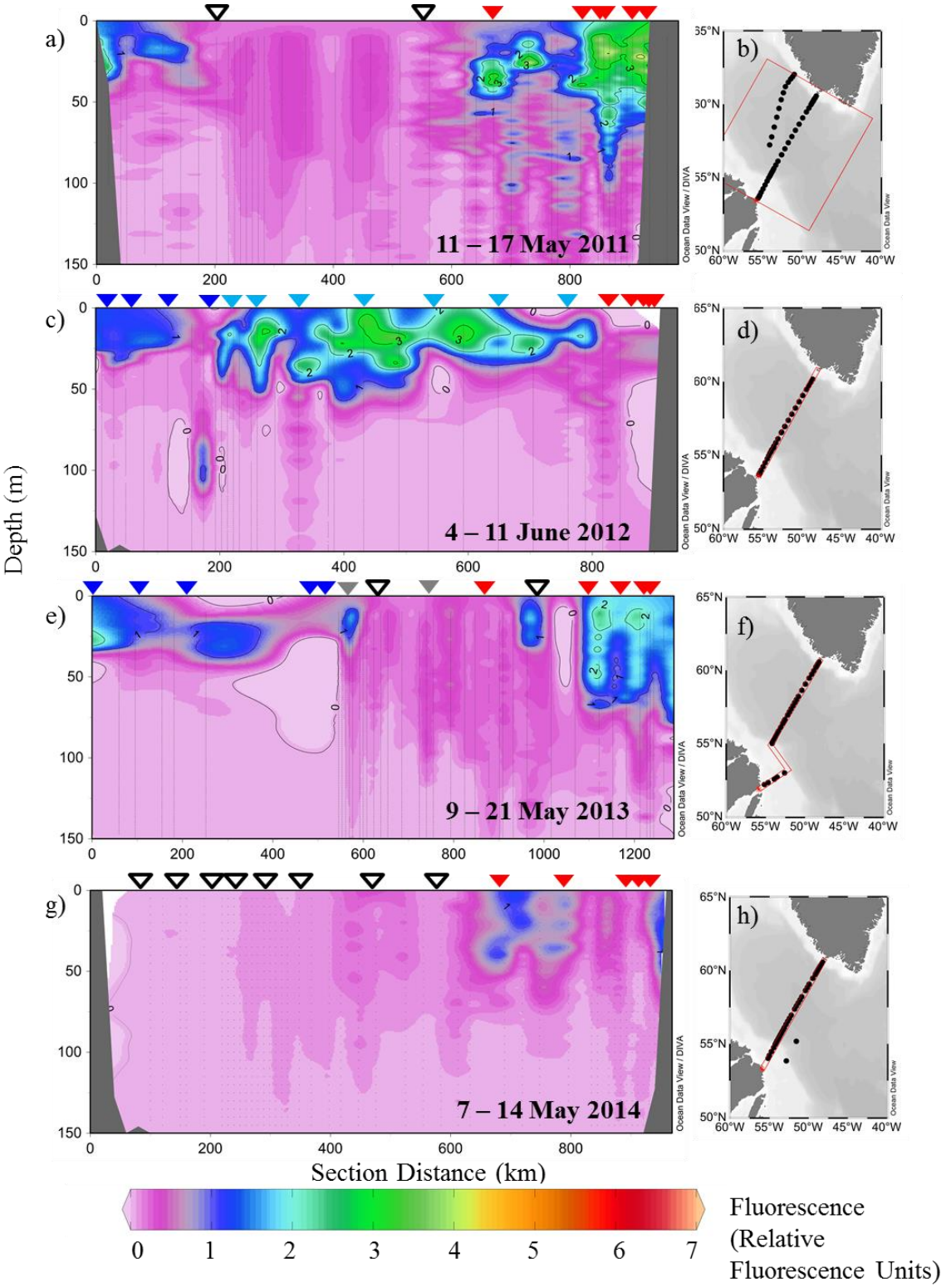

Appendix B

B.1 Photosynthesis-irradiance (P-E) data were fitted to the model of Platt et al (1980) using the equation:

$$P^B(E) = P_s^B (1- e^{-\alpha E/PsB}) . e^{-\beta E/PsB} \quad (1)$$

B.2 Additionally, the maximum photosynthetic rate attained was calculated using the formula:

$$Pm^B = P_s^B [\alpha/(\alpha + \beta)] . [\beta/(\alpha + \beta)]^{\beta/\alpha} \quad (2)$$

B.3 Photosynthesis-irradiance (P-E) curve and parameters.

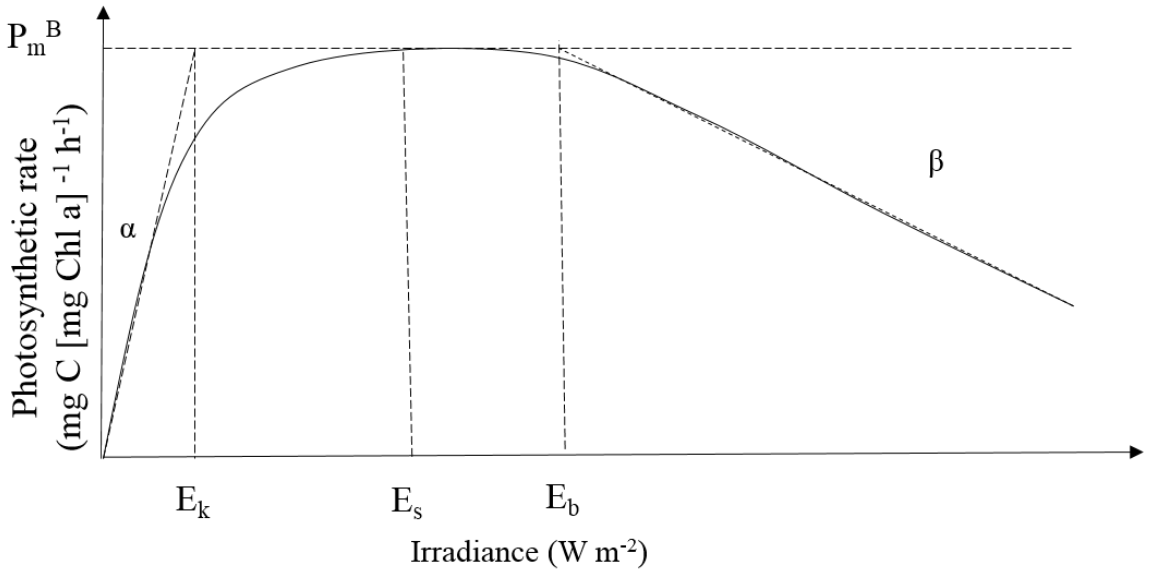

B.4 The table below shows the meaning and calculations for each P-E parameter calculated.

Parameters			
Symbol	Meaning		Unit
P_m^B	Maximum net photosynthetic rate	Equation (1,2)	(mg C [mg Chl *a*] $^{-1}$ h^{-1})
P_s^B	Maximum, *potential*, light saturated photosynthetic rate	Equation (1,2)	(mg C [mg Chl *a*] $^{-1}$ h^{-1})
α^B	Initial slope of the P-E curve	P_m^B/E_k	(mg C [mg Chl *a*] $^{-1}$ h^{-1} [W m^{-2}]$^{-1}$)
β	Photoinhibition parameter	P_m^B/E_b	(mg C [mg Chl *a*] $^{-1}$ h^{-1} [W m^{-2}]$^{-1}$)
E_k	Light intensity approximating the onset of saturation	P_m^B/α	W m^{-2}
E_s	Light intensity optimal for photosynthesis; saturation irradiance		W m^{-2}
E_b	Onset of photoinhibition	P_m^B/β	W m^{-2}

Appendix C

C.1 Scatterplot showing the correlations between the contributions of diatoms (a), *Phaeocystis* (b), dinoflagellates (c) and cryptophycea (d) biomasses estimated from CHEMTAX-derived chlorophyll *a* (y-axis) and microscopic counts carbon calculations (x-axis).

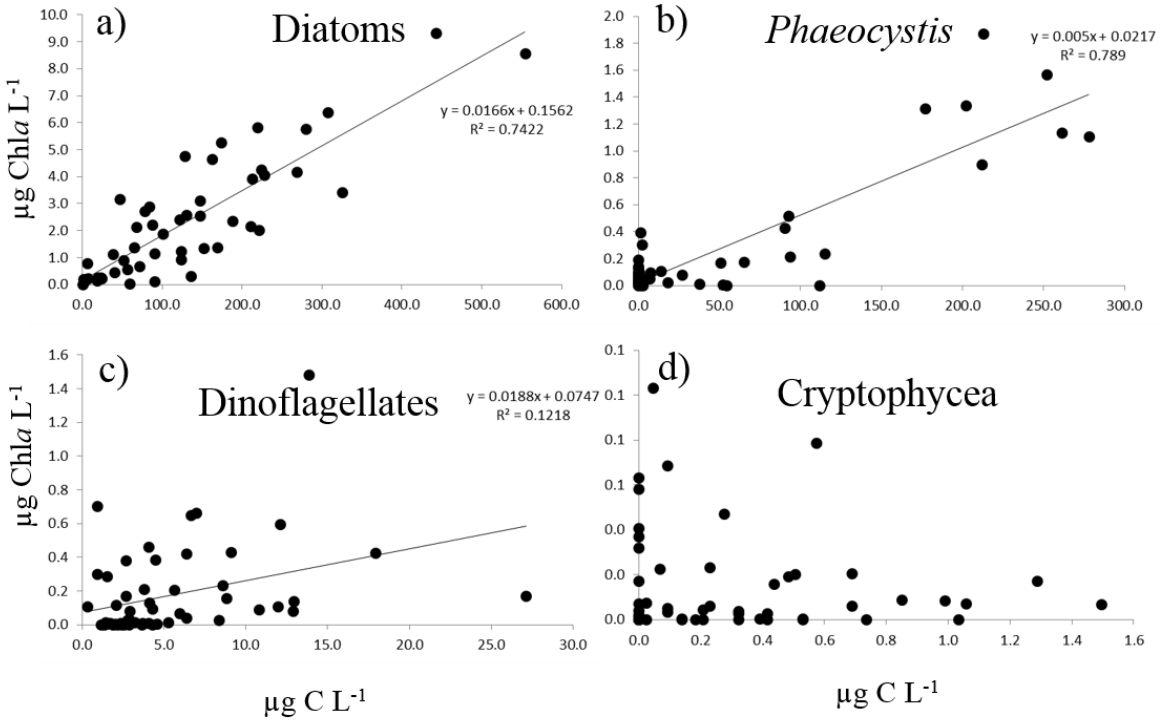

Appendix D

D.1 List of species and their quantitative, binary and continuous traits from Chapter 4.

	TRAITS	QUANTITATIVE			BINARY					CONTINOUS
Group	Taxa	ESD	MDL	S/V	Adhesive	Psychrophylic	Sharp	Chl in setae	Robust	Spores
PRYMN	*Phaeocystis pouchetii*	7	7	0.91	1[24]	0	0	0	0	0
DIAT	*Attheya septentrionalis*	6	8	0.57	1[21]	1[1,6,29]	1[6]	0	1[37]	0
DIAT	*Bacterosira bathyomphala*/*Melosira arctica*	24	25	0.29	1[10,22,23]	1[2,3]	0	0	1[36]	1[30]
DIAT	*Chaetoceros atlanticus*	29	35	0.13	0	0	1[6,25]	1[6]	1[26]	0
DIAT	*Chaetoceros borealis*	18	20	0.20	0	0	1[6,25]	1[6]	1[26]	0
DIAT	*Chaetoceros convolutus*	20	35	0.20	0	0	1[6,25]	1[6]	1[26]	0
DIAT	*Chaetoceros densus*	18	20	0.20	0	0	1[6,25]	1[6]	1[26]	0
DIAT	*Chaetocetos concavicornis*	23	10	0.16	0	0	1[6,25]	1[6]	1[26]	0
DIAT	*Chaetoceros socialis* (and others)	6	6	0.65	0	0	1[6,25]	0	0	1[29]
DIAT	*Chaetoceros decipiens* (and others)	20	25	0.19	0	0	1[6,25]	0	0	0
DIAT	*Corethron criophilum*	50	100	0.15	0	0	1[6,25]	0	0	0.5[7]
DIAT	*Coscinodiscus centralis*/*concinnus*	213	275	0.04	0	1[4,18]	0	0	1[27]	0
DIAT	*Cylindrotheca closterium*	7	35	0.83	1[6]	1[6,10,29]	0	0	0	0.5[8]
DIAT	*Detonula confervaceae*	17	28	0.44	0	1 [5]	0	0	1[28]	1[9]
SILICO	*Dictyocha speculum*	24	22	0.09	0	0	1[6]	0	0	0
DIAT	*Ephemera planamembranaceae*	16	53	0.32	1[6]	1 [10]	0	0	0	0
DIAT	*Eucampia groelandica*	14	25	0.28	0	1 [10]	0	0	0	0
DIAT	*Fossula arctica*	12	23	0.34	0	1 [13,29]	0	0	1 [12]	1[12,29]
DIAT	*Fragilariopsis atlantica*	10	26	0.46	1[6]	0	0	0	0	0
DIAT	*Fragilariopsis cylindrus*/*oceanica*/*reginae*	10	25	0.44	1[21]	1[14,19]	0	0	1[27]	1[6,29]
DIAT	*Leptocylindrus danicus*/*mediterraneus*/*minimum*	13	25	0.61	0	0	0	0	0	1[6]

TRAITS		QUANTITATIVE			BINARY					CONTINOUS
Group	Taxa	ESD	MDL	S/V	Adhesive	Psychrophylic	Sharp	Chl in setae	Robust	Spores
DIAT	*Navicula granii*	14	23	0.27	1[6]	1 [6]	0	0	0	0
DIAT	*Navicula transitans/ transitans var dera*	14	13	0.24	1[6]	1 [5,6,29]	0	0	0	0
DIAT	*Navicula septentrionalis/Achnanthes taeniata*	13	22	0.29	1[6]	1 [5,6,29]	0	0	0	1[6]
DIAT	*Navicula vanhoeffenii*	13	35	0.35	1[6]	1 [15]	0	0	1[37]	0
DIAT	*Neodenticula seminae*	14	23	0.28	1[6]	0	0	0	1[16]	0
DIAT	*Nitzchia frigida/Synedropsis hyperborea*	15	49	0.3	1[21]	1 [5,6,10,29]	0	0	1[27]	0
DIAT	*Porosira glacialis*	47	49	0.15	1[21]	1 [4]	0	0	1[36]	1[11,29]
DIAT	*Proboscia alata*	30	500	0.67	0	0	0	0	1[26]	0.5[6]
DIAT	*Pseudo-nitzschia delicatissima/pseudodelicatissima*	15	70	0.58	1[6]	0	0	0	0	0
DIAT	*Pseudonitzschia granii*	8	15	0.83	1[6]	0	0	0	0	0
DIAT	*Rhizosolenia hebetata* f. *semispina*	48	715	0.40	0	0	0	0	1[34,27]	0.5[6]
DIAT	*Skeletonema costatum*	9	9	0.762	0	0	1[6]	0	0	0
DIAT	*Thalassionema nitzschizoides*	10	45	0.93	0	0	0	0	1[36,27,32]	0
DIAT	*Thalassiosira angulata*	29	30	0.25	0	0	0	0	1[28]	0
DIAT	*Thalassiosira antarctica*	30	35	0.25	0	1 [11]	0	0	1[36,28]	1[11,29]
DIAT	*Thalassiosira bulbosa*	11	13	0.64	1[30]	1 [11]	0	0	0	1[6]
DIAT	*Thalassiosira conferta*	20	20	0.36	0	0	0	0	0	0
DIAT	*Thalassiosira constricta*	33	35	0.21	0	0	0	0	1[28]	1[11]
DIAT	*Thalassiosira gravida*	35	38	0.21	0	0	0	0	1[27,28]	0
DIAT	*Thalassiosira hyalina*	41	43	0.17	1[30]	0	0	0	1 [12,36,28]	1[29]
DIAT	*Thalassiosira kushirensis*	26	28	0.28	0	0	0	0	0	0
DIAT	*Thalassiosira nordenskioeldii*	23	25	0.32	0	1[20]	0	0	1[36,28]	1[17,29]
DIAT	*Thalassiosira punctigera*	32	35	0.23	0	0	0	0	1	0.5[6]
DIAT	*Thalassiotrix longissima*	40	2375	0.6	0	0	0	0	1[33, 34,36,32]	0
COCCO	*Coccolithus pelagicus*	25	25	0.24	0	0	0	0	1[35]	0

TRAITS		QUANTITATIVE			BINARY					CONTINOUS
Group	Taxa	ESD	MDL	S/V	Adhesive	Psychrophylic	Sharp	Chl in setae	Robust	Spores
COCCO	*Coccolithus pelagicus* HOL	38	38	0.16	0	0	0	0	0	0
COCCO	*Calciopappus caudatus*	9	30	0.80	0	0	1[6]	0	0	0
COCCO	*Emiliana huxleyi*	15	15	0.40	0	0	0	0	1[31]	0
CHRYSO	*Meringosphaera mediterranea*	13	13	0.48	0	0	1[6]	0	0	0

[1](Crawford et al., 2000), [2](Boetius et al., 2013), [3](Abelmann, 1992), [4](Melnikov et al., 2002), [5](Asami and Imada, 2001), [6](Tomas, 1997), [7](Crawford, 1995), [8](McQuoid et al., 2002), [9](Fryxell, 1983), [10](Mundy et al., 2011), [11](Herman, 2012), [12](Von Quillfeldt, 2001), [13](Onodera et al., 2015), [14](Lundholm and Hasle, 2010), [15](Smol and Stoermer, 2010), [16](Miettinen et al., 2013), [17](Sugie and Kuma, 2008), [18](Duerksen et al., 2014), [19](Mock and Junge, 2007), [20](von Quillfeldt et al., 2003), [21](Raymond and Kim, 2012), [22](Mary, 1997), [23](Krembs et al., 2011), [24](Rousseau et al., 1994), [25](Whyte et al., 1998), [26](Leventer et al., 2002), [27](De Sève, 1999), [28](Gil et al., 2015), [29](von Quillfeldt et al., 2003), [30](Jensen et al., 2004), [31](Colmenero-Hidalgo et al., 2002), [32](Assmy et al., 2013), [33](Tremblay et al., 2002), [34](Kemp et al., 2006), [35](Daniels et al., 2014), [36](Lapointe, 2000), [37](Gusev et al., 2014).

D.2 List of species and their categorical traits from Chapter 4.

TRAITS		CATEGORICAL			CATEGORICAL						
		COLONIALITY			INDIVIDUAL/COLONIAL GENERAL SHAPE						
Group	Taxa	Solitary	Colony	Sum	Ribbon-S	Tube-S	Star-S	Cloud-S	Sphere-S	Needle-S	Sum
PRYMN	*Phaeocystis pouchetii*	0.5	0.5	1.0				0.5	0.5		1.0
DIAT	*Attheya septentrionalis*	0.5	0.5	1.0					1.0		1.0
DIAT	*Bacterosira bathyomphala*/*Melosira arctica*		1.0	1.0		1.0					1.0
DIAT	*Chaetoceros atlanticus*		1.0	1.0		1.0					1.0
DIAT	*Chaetoceros borealis*		1.0	1.0		1.0					1.0
DIAT	*Chaetoceros convolutus*		1.0	1.0		1.0					1.0
DIAT	*Chaetoceros densus*		1.0	1.0		1.0					1.0
DIAT	*Chaetocetos concavicornis*		1.0	1.0		1.0					1.0
DIAT	*Chaetoceros socialis* (and others)		1.0	1.0				1.0			1.0
DIAT	*Chaetoceros decipiens* (and others)		1.0	1.0		1.0					1.0
DIAT	*Corethron criophilum*	1.0		1.0					1.0		1.0
DIAT	*Coscinodiscus centralis*/*concinnus*	1.0		1.0		1.0					1.0
DIAT	*Cylindrotheca closterium*	1.0		1.0						1.0	1.0
DIAT	*Detonula confervaceae*		1.0	1.0		1.0					1.0
SILICO	*Dictyocha speculum*	1.0		1.0					1.0		1.0
DIAT	*Ephemera planamembranaceae*	1.0		1.0					1.0		1.0
DIAT	*Eucampia groelandica*		1.0	1.0		1.0					1.0
DIAT	*Fossula arctica*		1.0	1.0	1.0						1.0
DIAT	*Fragilariopsis atlantica*		1.0	1.0	1.0						1.0
DIAT	*Fragilariopsis cylindrus*/*oceanica*/*reginae*		1.0	1.0	1.0						1.0
DIAT	*Leptocylindrus danicus*/*mediterraneus*/*minimum*		1.0	1.0		1.0					1.0
DIAT	*Navicula granii*		1.0	1.0	1.0						1.0
DIAT	*Navicula transitans*/ *transitans var dera*	1.0		1.0					1.0		1.0
DIAT	*Navicula septentrionalis*/*Achnanthes taeniata*		1.0	1.0	1.0						1.0
DIAT	*Navicula vanhoeffenii*		1.0	1.0	1.0						1.0

TRAITS		CATEGORICAL			CATEGORICAL						
		COLONIALITY			INDIVIDUAL/COLONIAL GENERAL SHAPE						
Group	Taxa	Solitary	Colony	Sum	Ribbon-S	Tube-S	Star-S	Cloud-S	Sphere-S	Needle-S	Sum
DIAT	*Neodenticula seminae*		1.0	1.0	1.0						1.0
DIAT	*Nitzchia frigida/Synedropsis hyperborea*		1.0	1.0			1.0				1.0
DIAT	*Porosira glacialis*		1.0	1.0		1.0					1.0
DIAT	*Proboscia alata*	0.5	0.5	1.0						1	1.0
DIAT	*Pseudo-nitzschia delicatissima/pseudodelicatissima*	0.5	0.5	1.0						1	1.0
DIAT	*Pseudonitzschia granii*	0.5	0.5	1.0				0.5		0.5	1.0
DIAT	*Rhizosolenia hebetata* f. *semispina*	0.5	0.5	1.0				0.5		0.5	1.0
DIAT	*Skeletonema costatum*		1.0	1.0		1.0					1.0
DIAT	*Thalassionema nitzschizoides*		1.0	1.0			1.0				1.0
DIAT	*Thalassiosira angulata*		1.0	1.0		1.0					1.0
DIAT	*Thalassiosira antarctica*		1.0	1.0		1.0					1.0
DIAT	*Thalassiosira bulbosa*	0.5	0.5	1.0		1.0					1.0
DIAT	*Thalassiosira conferta*		1.0	1.0		1.0					1.0
DIAT	*Thalassiosira constricta*		1.0	1.0		1.0					1.0
DIAT	*Thalassiosira gravida*		1.0	1.0		0.5		0.5			1.0
DIAT	*Thalassiosira hyalina*		1.0	1.0		1.0					1.0
DIAT	*Thalassiosira kushirensis*	0.5	0.5	1.0		1.0					1.0
DIAT	*Thalassiosira nordenskioeldii*		1.0	1.0		1.0					1.0
DIAT	*Thalassiosira punctigera*		1.0	1.0		1.0					1.0
DIAT	*Thalassiotrix longissima*	1.0		1.0						1.0	1.0
COCCO	*Coccolithus pelagicus*	1.0		1.0					1.0		1.0
COCCO	*Coccolithus pelagicus* HOL	1.0		1.0					1.0		1.0
COCCO	*Calciopappus caudatus*	1.0		1.0					1.0		1.0
COCCO	*Emiliana huxleyi*	1.0		1.0					1.0		1.0
CHRYSO	*Meringosphaera mediterranea*	1.0		1.0					1.0		1.0

Appendix E

E.1 Examples of phytoplankton species from Arctic waters (plate 1)

Fossula arctica

The outline of the valve varies somewhat between linear and lanceolate and the ends are usually capitate. There are two chloroplasts located toward the valve face, more or less displaced from each other. Each chloroplast is usually 1/2 or 1/3 of the length of the apical axis, and has rounded ends. It has no raphe but a sternum in the centre of valve. Sea-ice related.

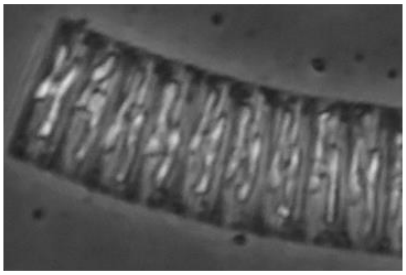
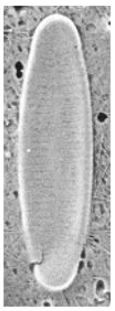
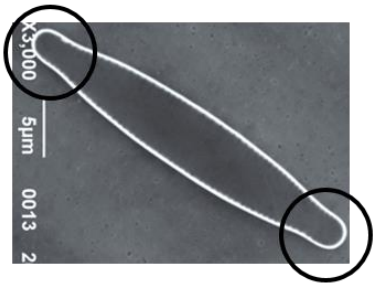

Porosira glacialis

Coastal cold water species (North & South). Central annulus , wavy aerolation, Numerous strutted processes all over the valve face . Labiate process at some distance of the margin,

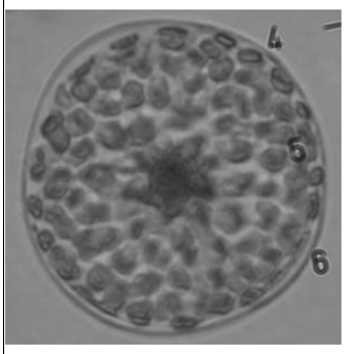
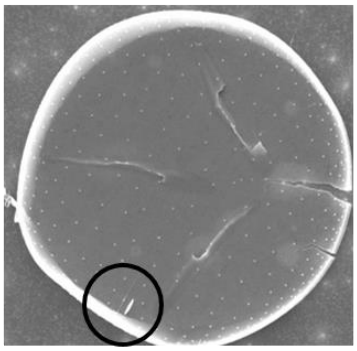
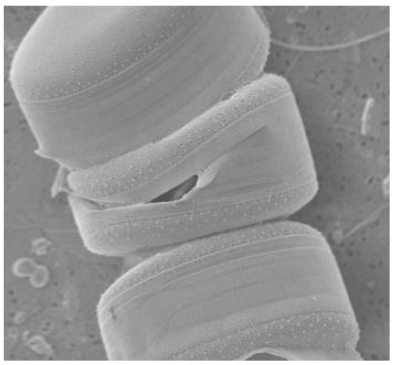

Fragilariopsis cylindrus

Cylinder-shaped. The fibulae are usually recognisable in the water mounts. It has two rectangular chloroplasts seen in girdle view, placed toward the girdle. Sea-ice related algae. Isopolar ends.

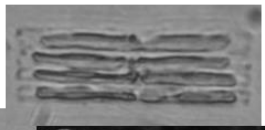
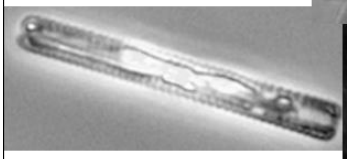
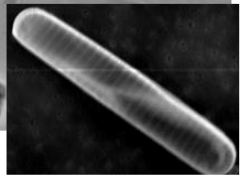

Fragilariopsis oceanica

Eliptical, lanceolate- shaped. Fibulae not easily recognisable. Two squarish/rectangular chloroplasts, with a distinct pyrenoid, placed toward the girdle. Sea-ice. Isopolar ends.

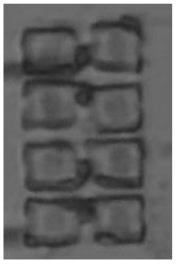
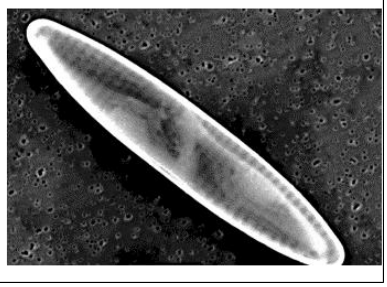

E.2 Examples of phytoplankton species from Arctic waters (plate 2)

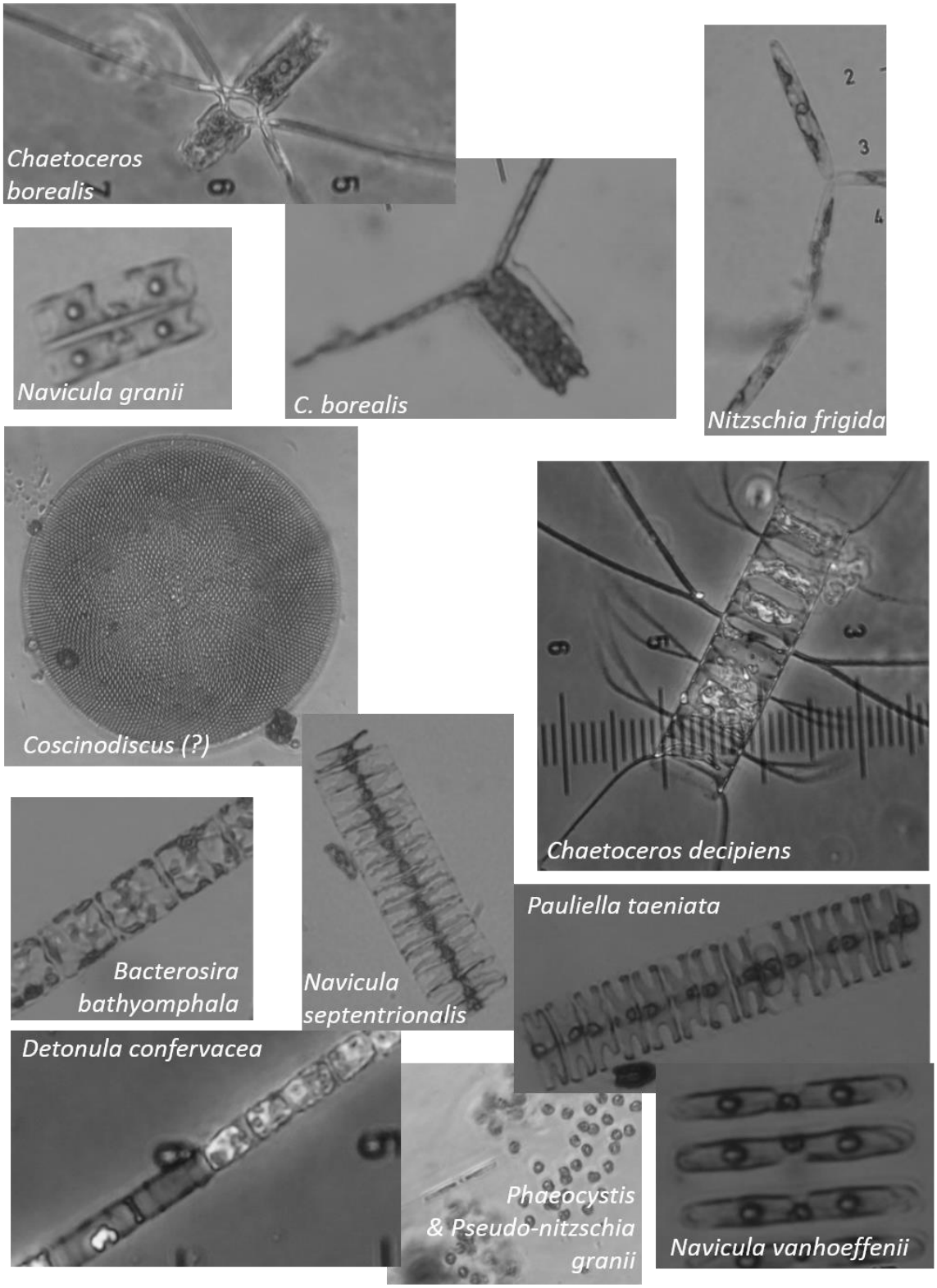

E.3 Examples of phytoplankton species from Arctic waters (plate 3)

Thalassiosira constricta – Cells about as high as wide. Flat valve face and slightly rounded corners. A central cluster of strutted processes (3-12), one ring of strutted processes, and one labiate process within this ring.

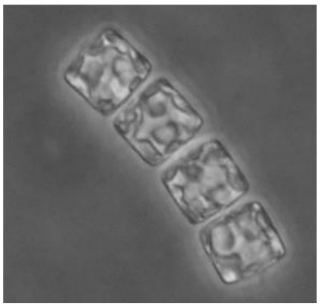
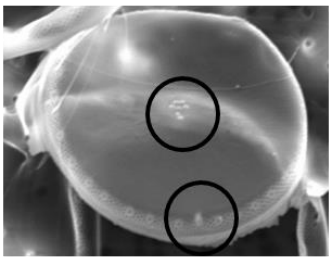
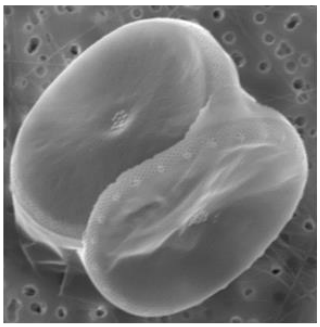

Thalassiosira nordenskioeldii– Cells octagonal. Strutted processes with long external tube. Areolae in radial rows. Labiate process replaces one strutted. One central process. Coastal.

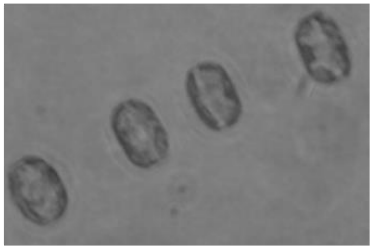
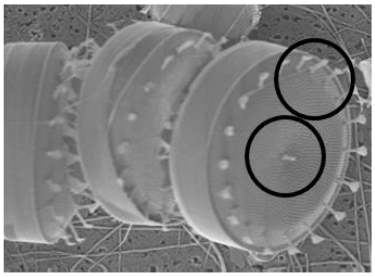
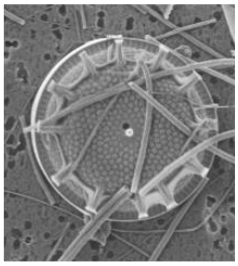

Thalassiosira gravida (or *antarctica var. borealis* or *rotula*?)– Thick connecting thread. Many strutted processes in valve centre and scattered in valve face. Large labiate process in the outer ring.

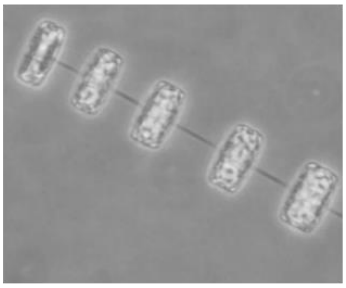
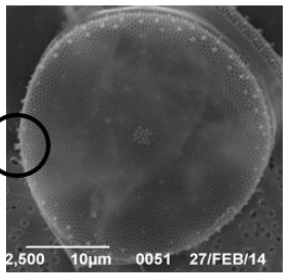

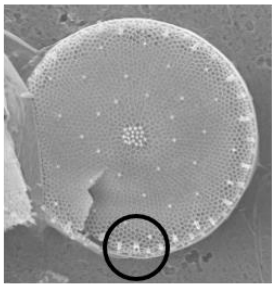

Thalassiosira antarctica var. borealis– Connected by a thin thread, usually as long or longer than pervalvar axis. Several central processes, two or three rings of marginal strutted processes . Resting spore with scattered processes as *T. gravida*.

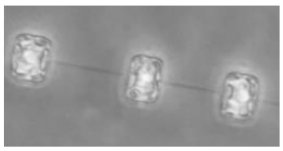
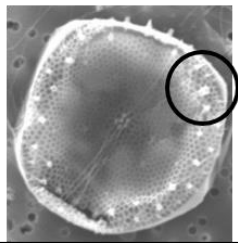
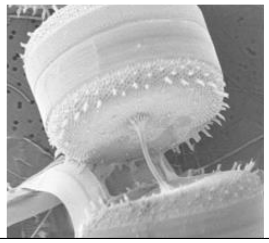
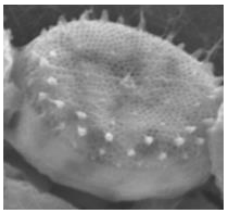

E.4 Examples of phytoplankton species from Arctic waters (plate 4)

Thalassiosira bulbosa – Small cell (~ 10 µm). Solitary or less frequently in short chains . Single central strutted process and one marginal ring of strutted processes. The later with low bulb shape outer parts. Close to ice border.

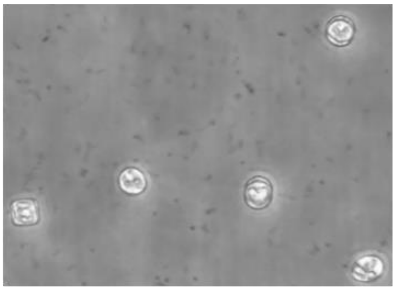

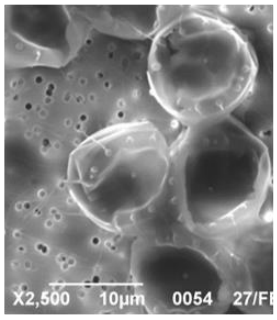

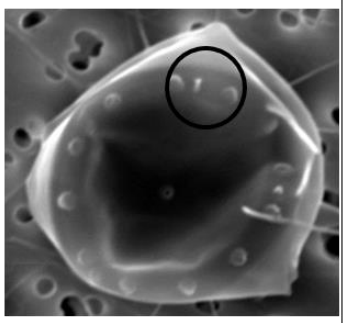

Thalassiosira hyalina – Cells disc-shaped. Two to 15 central strutted processes, one marginal ring of strutted processes with conspicuous external tubes. Labiate process taking the place of a marginal strutted process.

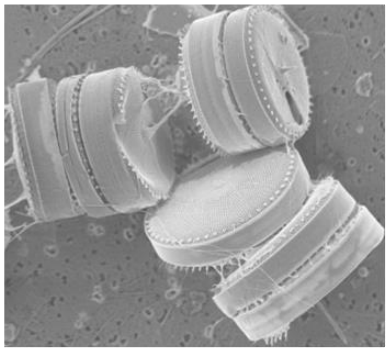

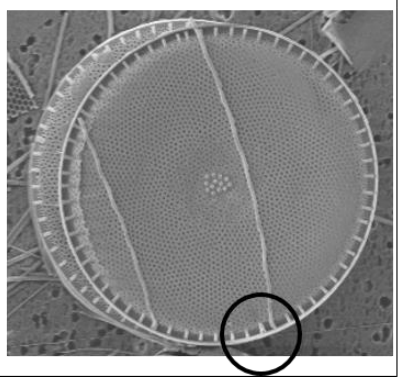

E.5 Examples of phytoplankton species from Atlantic waters (plate 5)

Ephemera planamembranaceae Paddock (1988: 86, pl. 31)

Usually solitary ,flattened transapically, usually seen in girdle view. Present in the North Atlantic but in Antarctic waters as well (temperate). Cell wall weakly silicified, four ribbon chloroplasts. Raphe located on a raised flat valve, dividing the valve into 2 unequal sides. Central nodule slightly depressed. Raphe fins small, located near valve ends. Helictoglossa large, rounded terminal pore.

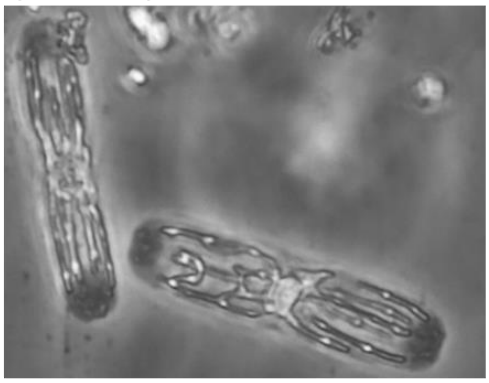

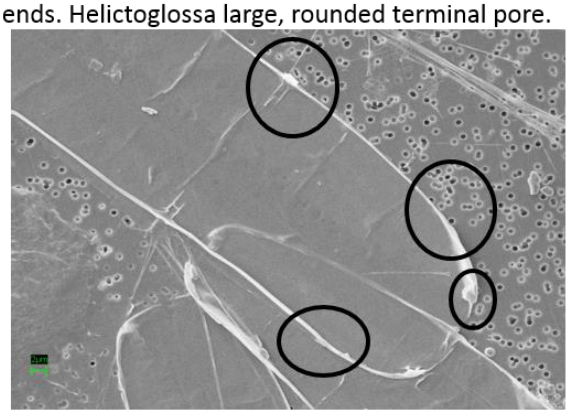

Fragilariopsis atlantica

Valve with sibling cells in ribbon, open ocean
Heteropolar apical axis
Presence of central node
Apices generally rounded

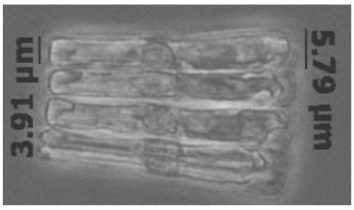

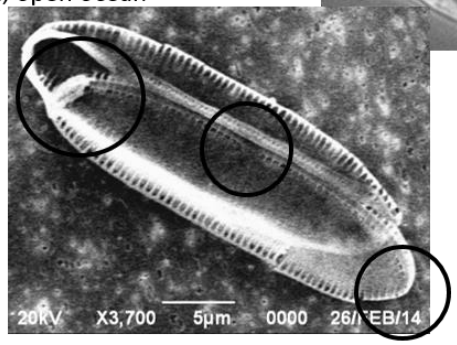

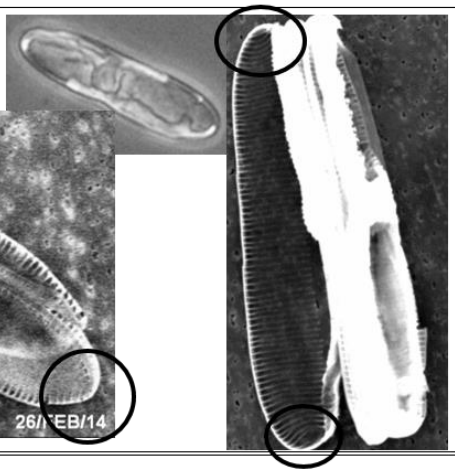

Neodenticula seminae (invasive species)

Strong pseudosepta (diaphagm-like ingrowth of valve penetrating into the cell interior)

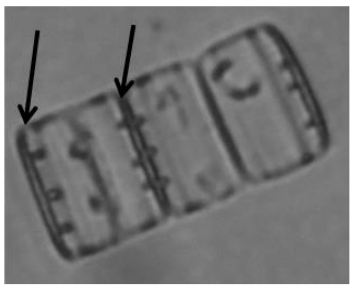

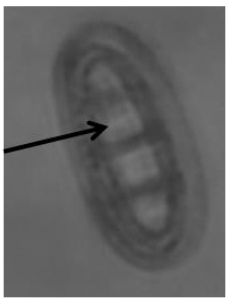

List of References

Aanesen, R.T., Eilertsen, H.C., Stabell, O.B., 1998. Light-induced toxic properties of the marine alga *Phaeocystis pouchetii* towards cod larvae. Aquat. Toxicol. 40, 109–121.

Abelmann, A., 1992. Diatom assemblages in Arctic sea ice-indicator for ice drift pathways. Deep Sea Res. Part A, Oceanogr. Res. Pap. 39, S525–S538. doi:10.1016/S0198-0149(06)80019-1

Acevedo-Trejos, E., Brandt, G., Bruggeman, J., Merico, A., 2015. Mechanisms shaping size structure and functional diversity of phytoplankton communities in the ocean. Sci. Rep. 5, 8918. doi:10.1038/srep08918

Acevedo-Trejos, E., Brandt, G., Merico, A., Smith, S.L., 2013. Biogeographical patterns of phytoplankton community size structure in the oceans. Glob. Ecol. Biogeogr. 22, 1060–1070. doi:10.1111/geb.12071

Aiken, J., Pradhan, Y., Barlow, R., Lavender, S., Poulton, A., Holligan, P., Hardman-Mountford, N., 2009. Phytoplankton pigments and functional types in the Atlantic Ocean: A decadal assessment, 1995–2005. Deep Sea Res. Part II Top. Stud. Oceanogr. 56, 899–917. doi:10.1016/j.dsr2.2008.09.017

Alderkamp, A.-C., Buma, A.G.J., van Rijssel, M., 2007. The carbohydrates of *Phaeocystis* and their degradation in the microbial food web. Biogeochemistry 83, 99–118. doi:10.1007/s10533-007-9078-2

Anisimov, O.A., Vaughan, D.G., Callaghan, T. V., Furgal, C., Marchant, H., Prowse, T.D., Vilhjálmsson, H., Walsh, J.E., Fitzharris, B., Zealand, N.E.W., Canada, T.P., Uk, D.G.V., 2007. Polar Regions (Arctic and Antarctic). Clim. Chang. 15, 653–685.

Antajan, E., Chrétiennot-Dinet, M.-J., Leblanc, C., Daro, M.-H., Lancelot, C., 2004. 19′-hexanoyloxyfucoxanthin may not be the appropriate pigment to trace occurrence and fate of *Phaeocystis*: the case of *P. globosa* in Belgian coastal waters. J. Sea Res. 52, 165–177. doi:10.1016/j.seares.2004.02.003

Ardyna, M., Babin, M., Gosselin, M., Devred, E., Rainville, L., Tremblay, J.-É., 2014. Recent Arctic Ocean sea-ice loss triggers novel fall phytoplankton blooms. Geophys. Res. Lett. 41, 6207–6212. doi:10.1002/2014GL061047

Armand, L.K., Crosta, X., Romero, O., Pichon, J.J., 2005. The biogeography of major

diatom taxa in Southern Ocean sediments: 1. Sea ice related species. Palaeogeogr. Palaeoclimatol. Palaeoecol. 223, 93–126. doi:10.1016/j.palaeo.2005.02.015

Armand, L.K., Leventer, A., 2010. Palaeo sea ice Distribution and Reconstruction Derived from the Geological Records, in: Thomas, D.N., Dieckmann, G. (Eds.), Sea Ice. Blackwell, Oxford, UK, pp. 469–530.

Arrigo, K.R., 2007. Carbon cycle: Marine manipulations. Nature 450, 491–492. doi:10.1038/450491a

Arrigo, K.R., 1999. Phytoplankton community structure and the drawdown of nutrients and CO_2 in the Southern Ocean. Science (80-.). 283, 365–367. doi:10.1126/science.283.5400.365

Arrigo, K.R., Brown, Z.W., Mills, M.M., 2014. Sea ice algal biomass and physiology in the Amundsen Sea, Antarctica. Elem. Sci. Anthr. 2, 28 p. doi:10.12952/journal.elementa.000028

Arrigo, K.R., Mills, M.M., Kropuenske, L.R., Van Dijken, G.L., Alderkamp, A.C., Robinson, D.H., 2010a. Photophysiology in two major southern ocean phytoplankton taxa: Photosynthesis and growth of *Phaeocystis antarctica* and *Fragilariopsis cylindrus* under different irradiance levels. Integr. Comp. Biol. 50, 950–966. doi:10.1093/icb/icq021

Arrigo, K.R., Mock, T., Lizotte, M.P., 2010b. Primary Producers and Sea Ice, in: Sea Ice. Wiley-Blackwell, Oxford, UK, pp. 283–325. doi:10.1002/9781444317145.ch8

Arrigo, K.R., Perovich, D.K., Pickart, R.S., Brown, Z.W., van Dijken, G.L., Lowry, K.E., Mills, M.M., Palmer, M.A., Balch, W.M., Bahr, F., Bates, N.R., Benitez-Nelson, C., Bowler, B., Brownlee, E., Ehn, J.K., Frey, K.E., Garley, R., Laney, S.R., Lubelczyk, L., Mathis, J., Matsuoka, A., Mitchell, B.G., Moore, G.W.K., Ortega-Retuerta, E., Pal, S., Polashenski, C.M., Reynolds, R.A., Schieber, B., Sosik, H.M., Stephens, M., Swift, J.H., 2012. Massive Phytoplankton Blooms Under Arctic Sea Ice. Science (80-.). 336, 1408–1408. doi:10.1126/science.1215065

Arrigo, K.R., van Dijken, G., Pabi, S., 2008. Impact of a shrinking Arctic ice cover on marine primary production. Geophys. Res. Lett. 35, L19603. doi:10.1029/2008GL035028

Asami, H., Imada, K., 2001. Ice algae and phytoplankton in the late ice-covered season in

Notoro KO lagoon, Hokkaido. Polar Biosci. 14, 24–32.

Assmy, P., Ehn, J.K., Fernández-Méndez, M., Hop, H., Katlein, C., Sundfjord, A., Bluhm, K., Daase, M., Engel, A., Fransson, A., Granskog, M.A., Hudson, S.R., Kristiansen, S., Nicolaus, M., Peeken, I., Renner, A.H.H., Spreen, G., Tatarek, A., Wiktor, J., 2013. Floating ice-algal aggregates below melting arctic sea ice. PLoS One 8, e76599. doi:10.1371/journal.pone.0076599

Azetsu-Scott, K., 2003. Time series study of CFC concentrations in the Labrador Sea during deep and shallow convection regimes (1991–2000). J. Geophys. Res. 108, 3354. doi:10.1029/2002JC001317

Balch, W.M., Bowler, B.C., Lubelczyk, L.C., Stevens, M.W., 2014. Aerial extent, composition, bio-optics and biogeochemistry of a massive under-ice algal bloom in the Arctic. Deep. Res. Part II Top. Stud. Oceanogr. 105, 42–58. doi:10.1016/j.dsr2.2014.04.001

Balestra, B., Ziveri, P., Monechi, S., Troelstra, S., 2004. Coccolithophorids from the Southeast Greenland Margin (Northern North Atlantic): production, ecology and the surface sediment record. Micropaleontology 50, 23–34. doi:10.2113/50.Suppl_1.23

Barnard, R., Batten, S.D., Beaugrand, G., Buckland, C., Conway, D.V.P., Edwards, M., Finlayson, J., Gregory, L.W., Halliday, N.C., John, A.W.G., Johns, D.G., Johnson, A.D., Jonas, T.D., Lindley, J.A., Nyman, J., Pritchard, P., Reid, P.C., Richardson, A.J., Saxby, R.E., Sidey, J., Smith, M.A., Stevens, D.P., Taylor, C.M., Tranter, P.R.G., Walne, A.W., Wootton, M., Wotton, C.O.M., Wright, J.C., 2004. Continuous plankton records: Plankton Atlas of the north Atlantic Ocean (1958-1999). II. Biogeographical charts. Mar. Ecol. Prog. Ser. doi:10.3554/mepscpr011

Barton, A.D., Finkel, Z. V, Ward, B.A., Johns, D.G., Follows, M.J., 2013a. On the roles of cell size and trophic strategy in North Atlantic diatom and dinoflagellate communities. Limnol. Oceanogr. 58, 254–266. doi:10.4319/lo.2013.58.1.0254

Barton, A.D., Irwin, A.J., Finkel, Z. V, Stock, C.A., 2016. Anthropogenic climate change drives shift and shuffle in North Atlantic phytoplankton communities. Proc. Natl. Acad. Sci. 113, 2964–2969. doi:10.1073/pnas.1519080113

Barton, A.D., Pershing, A.J., Litchman, E., Record, N.R., Edwards, K.F., Finkel, Z. V, Kiørboe, T., Ward, B.A., 2013b. The biogeography of marine plankton traits. Ecol.

Lett. 16, 522–34. doi:10.1111/ele.12063

Baumann, K.-H., Andruleit, H., Böckel, B., Geisen, M., Kinkel, H., 2005. The significance of extant coccolithophores as indicators of ocean water masses, surface water temperature, and paleoproductivity: a review. Paläontologische Zeitschrift 79, 93–112. doi:10.1007/bf03021756

Baumann, K.-H., Andruleit, H., Samtleben, C., 2000. Coccolithophores in the Nordic Seas: comparison of living communities with surface sediment assemblages. Deep Sea Res. Part II Top. Stud. Oceanogr. 47, 1743–1772. doi:10.1016/S0967-0645(00)00005-9

Beaugrand, G., 2005. Monitoring pelagic ecosystems using plankton indicators. ICES J. Mar. Sci. 62, 333–338. doi:10.1016/j.icesjms.2005.01.002

Beaugrand, G., Reid, P.C., Ibañez, F., Lindley, J.A., Edwards, M., 2002. Reorganization of North Atlantic marine copepod biodiversity and climate. Science (80-.). 296, 1692–1694. doi:10.1126/science.1071329

Berglund, J., Müren, U., Båmstedt, U., Andersson, A., Falkowski, P.G., 1994. Efficiency of a phytoplankton-based and a bacterial-based food web in a pelagic marine system. Photosynth. Res. 39, 235–258. doi:10.4319/lo.2007.52.1.0121

Bertilsson, S., Berglund, O., Karl, D.M., Chisholm, S.W., 2003. Elemental composition of marine *Prochlorococcus* and *Synechococcus*: Implications for the ecological stoichiometry of the sea. Limnol. Oceanogr. 48, 1721–1731. doi:10.4319/lo.2003.48.5.1721

Bhatia, M.P., Kujawinski, E.B., Das, S.B., Breier, C.F., Henderson, P.B., Charette, M.A., 2013. Greenland meltwater as a significant and potentially bioavailable source of iron to the ocean. Nat. Geosci. 6, 274–278. doi:10.1038/ngeo1746

Bibby, T.S., Zhang, Y., Chen, M., 2009. Biogeography of photosynthetic light-harvesting genes in marine phytoplankton. PLoS One 4, 19–21. doi:10.1371/journal.pone.0004601

Boetius, A., Albrecht, S., Bakker, K., Bienhold, C., Felden, J., Fernandez-Mendez, M., Hendricks, S., Katlein, C., Lalande, C., Krumpen, T., Nicolaus, M., Peeken, I., Rabe, B., Rogacheva, A., Rybakova, E., Somavilla, R., Wenzhofer, F., 2013. Export of algal biomass from the melting Arctic sea ice. Science (80-.). 339, 1430–1432. doi:10.1126/science.1231346

Bonachela, J.A., Klausmeier, C.A., Edwards, K.F., Litchman, E., Levin, S.A., 2015. The role of phytoplankton diversity in the emergent oceanic stoichiometry. J. Plankton Res. 0, fbv087. doi:10.1093/plankt/fbv087

Booth, B.C., Larouche, P., Bélanger, S., Klein, B., Amiel, D., Mei, Z.P., 2002. Dynamics of *Chaetoceros socialis* blooms in the North Water. Deep. Res. Part II Top. Stud. Oceanogr. 49, 5003–5025. doi:10.1016/S0967-0645(02)00175-3

Bouman, H., Platt, T., Sathyendranath, S., Li, W., Stuart, V., Fuentes-Yaco, C., Maass, H., Horne, E., Ulloa, O., Lutz, V., Kyewalyanga, M., 2003. Temperature as indicator of optical properties and community structure of marine phytoplankton: implications for remote sensing. Mar. Ecol. Prog. Ser. 258, 19–30. doi:10.3354/meps258019

Bouman, H., Platt, T., Sathyendranath, S., Stuart, V., 2005. Dependence of light-saturated photosynthesis on temperature and community structure. Deep Sea Res. Part I Oceanogr. Res. Pap. 52, 1284–1299. doi:10.1016/j.dsr.2005.01.008

Browning, T.J., Bouman, H.A., Moore, C.M., Schlosser, C., Tarran, G.A., Woodward, E.M.S., 2014. Nutrient regimes control phytoplankton ecophysiology in the South Atlantic 463–479. doi:10.5194/bg-11-463-2014

Brun, P., Vogt, M., Payne, M.R., Gruber, N., O'Brien, C.J., Buitenhuis, E.T., Le Quéré, C., Leblanc, K., Luo, Y.-W., 2015. Ecological niches of open ocean phytoplankton taxa. Limnol. Oceanogr. n/a-n/a. doi:10.1002/lno.10074

Burthe, S.J., Henrys, P.A., Mackay, E.B., Spears, B.M., Campbell, R., Carvalho, L., Dudley, B., Gunn, I.D.M., Johns, D.G., Maberly, S.C., May, L., Newell, M.A., Wanless, S., Winfield, I.J., Thackeray, S.J., Daunt, F., 2015. Do early warning indicators consistently predict nonlinear change in long-term ecological data? J. Appl. Ecol. 666–676. doi:10.1111/1365-2664.12519

Caissie, B.E., Brigham-Grette, J., Lawrence, K.T., Herbert, T.D., Cook, M.S., 2010. Last Glacial Maximum to Holocene sea surface conditions at Umnak Plateau, Bering Sea, as inferred from diatom, alkenone, and stable isotope records. Paleoceanography. doi:10.1029/2008PA001671

Calbet, A., 2001. Mesozooplankton grazing impact on primary production: A global comparative analysis in marine ecosystems. Limnol. Oceanogr. 46, 1824–1830. doi:10.4319/lo.2001.46.7.1824

Calijuri, M.C., Dos Santos, A.C.A., Jati, S., 2002. Temporal changes in the phytoplankton community structure in a tropical and eutrophic reservoir (Barra Bonita, S.P.--Brazil). J. Plankton Res. 24, 617–634. doi:10.1093/plankt/24.7.617

Caperon, J., 1968. Population growth response of *Isochrysis Galbana* to nitrate variation at limiting concentrations. Ecology 49, 866–872. doi:10.2307/1936538

Cermeño, P., de Vargas, C., Abrantes, F., Falkowski, P.G., 2010. Phytoplankton biogeography and community stability in the ocean. PLoS One 5, e10037. doi:10.1371/journal.pone.0010037

Chanut, J., Barnier, B., Large, W., Debreu, L., Penduff, T., Molines, J.M., Mathiot, P., 2008. Mesoscale eddies in the Labrador Sea and their contribution to convection and restratification. J. Phys. Oceanogr. 38, 1617–1643. doi:10.1175/2008JPO3485.1

Charalampopoulou, A., Poulton, A.J., Tyrrell, T., Lucas, M.I., 2011. Irradiance and pH affect coccolithophore community composition on a transect between the North Sea and the Arctic Ocean. Mar. Ecol. Prog. Ser. 431, 25–43. doi:10.3354/meps09140

Chevene, F., Doleadec, S., Chessel, D., 1994. A fuzzy coding approach for the analysis of long-term ecological data. Freshw. Biol. 31, 295–309. doi:10.1111/j.1365-2427.1994.tb01742.x

Clarke, K.R., 1993. Non-parametric multivariate analyses of changes in community structure. Austr. J. Ecol. 18, 117–143. doi:10.1111/j.1442-9993.1993.tb00438.x

Clarke, K.R., Warwick, R.M., 2001. Change in marine communities: an approach to statistical analysis and interpretation, 2nd Editio. ed. PRIMER-E, Plymouth.

Collos, Y., 2002. Determination of particulate carbon and nitrogen in coastal waters., in: Subba Rao DV (Ed.), Pelagic Ecology Methodology. A. A. Balkema Publishers, Tokyo, pp. 333–341.

Colmenero-Hidalgo, E., Flores, J.-A., Sierro, F.J., 2002. Biometry of *Emiliania huxleyi* and its biostratigraphic significance in the Eastern North Atlantic Ocean and Western Mediterranean Sea in the last 20 000 years. Mar. Micropaleontol. 46, 247–263. doi:10.1016/S0377-8398(02)00065-8

Comiso, J.C., Parkinson, C.L., Gersten, R., Stock, L., 2008. Accelerated decline in the Arctic sea ice cover. Geophys. Res. Lett. 35, L01703. doi:10.1029/2007GL031972

Cornelissen, J.H.C.A., Lavorel, S.B., Garnier, E.B., Díaz, S.C., Buchmann, N.D., Gurvich, D.E.C., Reich, P.B.E., Steege, H.F., Morgan, H.D.G., A, M.G.A.V.D.H., Pausas, J.G.H., Poorter, H.I., 2003. A handbook of protocols for standardised and easy measurement of plant functional traits worldwide 335–380.

Cota, G.F., 2003. Bio-optical properties of the Labrador Sea. J. Geophys. Res. doi:10.1029/2000JC000597

Coupel, P., Jin, H.Y., Joo, M., Horner, R., Bouvet, H.A., Sicre, M.A., Gascard, J.C., Chen, J.F., Garcon, V., Ruiz-Pino, D., 2012. Phytoplankton distribution in unusually low sea ice cover over the Pacific Arctic. Biogeosciences 9, 4835–4850. doi:10.5194/bg-9-4835-2012

Coupel, P., Matsuoka, A., Ruiz-Pino, D., Gosselin, M., Marie, D., Tremblay, J.E., Babin, M., 2015. Pigment signatures of phytoplankton communities in the Beaufort Sea. Biogeosciences 12, 991–1006. doi:10.5194/bg-12-991-2015

Crawford, D.W., Wyatt, S.N., Wrohan, I.A., Cefarelli, A.O., Giesbrecht, K.E., Kelly, B., Varela, D.E., 2015. Low particulate carbon to nitrogen ratios in marine surface waters of the Arctic. Global Biogeochem. Cycles 29, 2021–2033. doi:10.1002/2015GB005200.Received

Crawford, R.M., 1995. The role of sex in the sedimentation of a marine diatom bloom. Limnol. Oceanogr. 40, 200–204. doi:10.4319/lo.1995.40.1.0200

Crawford, R.M., Hinz, F., Koschinski, P., 2000. The combination of *Chaetoceros gaussii* (Bacillariophyta) with *Attheya*. Phycologia 39, 238–244. doi:10.2216/i0031-8884-39-3-238.1

Crosta, X., Denis, D., Ther, O., 2008. Sea ice seasonality during the Holocene, Adélie Land, East Antarctica. Mar. Micropaleontol. 66, 222–232. doi:10.1016/j.marmicro.2007.10.001

Curson, A.R.J., Todd, J.D., Sullivan, M.J., Johnston, A.W.B., 2011. Catabolism of dimethylsulphoniopropionate: microorganisms, enzymes and genes. Nat. Rev. Microbiol. 9, 849–859. doi:10.1038/nrmicro2653

Daly, K.L., Wallace, D.W.R., Smith, W.O., Skoog, A., Lara, R., Gosselin, M., Falck, E., Yager, P.L., 1999. Non-Redfield carbon and nitrogen cycling in the Arctic: Effects of ecosystem structure and dynamics. J. Geophys. Res. Ocean. 104, 3185–3199.

doi:10.1029/1998JC900071

Daniels, C., Poulton, A., Young, J., Esposito, M., Humphreys, M., Ribas-Ribas, M., Tynan, E., Tyrrell, T., 2016. Species-specific calcite production reveals *Coccolithus pelagicus* as the key calcifier in the Arctic Ocean. Mar. Ecol. Prog. Ser. 1–36. doi:10.3354/meps11820

Daniels, C.J., Sheward, R.M., Poulton, A.J., 2014. Biogeochemical implications of comparative growth rates of *Emiliania huxleyi* and *Coccolithus* species. Biogeosciences 11, 6915–6925. doi:10.5194/bg-11-6915-2014

Daniels, C.J., Tyrrell, T., Poulton, A.J., Pettit, L., 2012. The influence of lithogenic material on particulate inorganic carbon measurements of coccolithophores in the Bay of Biscay. Limnol. Oceanogr. 57, 145–153. doi:10.4319/lo.2012.57.1.0145

De Sève, M.A., 1999. Transfer function between surface sediment diatom assemblages and sea-surface temperature and salinity of the Labrador Sea. Mar. Micropaleontol. 36, 249–267. doi:10.1016/S0377-8398(99)00005-5

Degerlund, M., Eilertsen, H.C., 2010. Main species characteristics of phytoplankton spring blooms in NE Atlantic and Arctic waters (68-80º N). Estuaries and Coasts 33, 242–269. doi:10.1007/s12237-009-9167-7

DeGrandpre, M.D., Körtzinger, A., Send, U., Wallace, D.W.R., Bellerby, R.G.J., 2006. Uptake and sequestration of atmospheric CO_2 in the Labrador Sea deep convection region. Geophys. Res. Lett. 33, L21S03. doi:10.1029/2006GL026881

Devilla, R.A., Brown, M.T., Donkin, M., Readman, J.W., 2005. The effects of a PSII inhibitor on phytoplankton community structure as assessed by HPLC pigment analyses, microscopy and flow cytometry. Aquat. Toxicol. 71, 25–38. doi:10.1016/j.aquatox.2004.10.002

Dickson, B., Yashayaev, I., Meincke, J., Turrell, B., Dye, S., Holfort, J., 2002. Rapid freshening of the deep North Atlantic Ocean over the past four decades. Nature 416, 832–837. doi:10.1038/416832a

DiTullio, G.R., Garcia, N., Riseman, S.F., Sedwick, P.N., 2007. Effects of iron concentration on pigment composition in *Phaeocystis antarctica* grown at low irradiance, in: *Phaeocystis*, Major Link in the Biogeochemical Cycling of Climate-Relevant Elements. Springer Netherlands, Dordrecht, pp. 71–81. doi:10.1007/978-1-

4020-6214-8_7

Doney, S.C., 2006. Oceanography: Plankton in a warmer world. Nature 444, 695–696. doi:10.1038/444695a

Drinkwater, K., Belgrano, A., 2003. The response of marine ecosystems to climate variability associated with the North Atlantic Oscillation. North Atl. Oscil. Clim. Significance Environ. Impact. doi:0-87590-994-9

Droop, M.R., 1968. Vitamin B12 and marine ecology. IV. The kinetics of uptake, growth and inhibition in *Monochrysis lutheri*. J. Mar. Biol. Assoc. United Kingdom 48, 689. doi:10.1017/S0025315400019238

Duerksen, S.W., Thiemann, G.W., Budge, S.M., Poulin, M., Niemi, A., Michel, C., 2014. Large, omega-3 rich, pelagic diatoms under Arctic sea ice: sources and implications for food webs. PLoS One 9, e114070. doi:10.1371/journal.pone.0114070

Durbin, E.G., 1978. Aspects of the biology of resting spores of *Thalassiosira nordenskioeldii* and *Detonula confervacea*. Mar. Biol. 45, 31–37. doi:10.1007/BF00388975

Dutz, J., Klein Breteler, W.C.M., Kramer, G., 2005. Inhibition of copepod feeding by exudates and transparent exopolymer particles (TEP) derived from a *Phaeocystis globosa* dominated phytoplankton community. Harmful Algae 4, 929–940.

Dylmer, C. V., Giraudeau, J., Hanquiez, V., Husum, K., 2015. The coccolithophores *Emiliania huxleyi* and *Coccolithus pelagicus*: Extant populations from the Norwegian-Iceland Seas and Fram Strait. Deep. Res. Part I Oceanogr. Res. Pap. 98, 1–9. doi:10.1016/j.dsr.2014.11.012

Edwards, K.F., Litchman, E., Klausmeier, C.A., 2013a. Functional traits explain phytoplankton responses to environmental gradients across lakes of the United States. Ecology 94, 1626–1635. doi:10.1890/12-1459.1

Edwards, K.F., Litchman, E., Klausmeier, C.A., 2013b. Functional traits explain phytoplankton community structure and seasonal dynamics in a marine ecosystem. Ecol. Lett. 16, 56–63. doi:10.1111/ele.12012

Edwards, K.F., Thomas, M.K., Klausmeier, C.A., Litchman, E., 2016. Phytoplankton growth and the interaction of light and temperature: A synthesis at the species and

community level. doi:10.1002/lno.10282

Edwards, K.F., Thomas, M.K., Klausmeier, C.A., Litchman, E., 2012. Allometric scaling and taxonomic variation in nutrient utilization traits and maximum growth rate of phytoplankton. Limnol. Oceanogr. 57, 554–566. doi:10.4319/lo.2012.57.2.0554

Eggers, S.L., Lewandowska, A.M., Barcelos e Ramos, J., Blanco-Ameijeiras, S., Gallo, F., Matthiessen, B., 2014. Community composition has greater impact on the functioning of marine phytoplankton communities than ocean acidification. Glob. Chang. Biol. 20, 713–723. doi:10.1111/gcb.12421

Eicken, H., 1992. The role of sea ice in structuring Antarctic ecosystems, in: Weddell Sea Ecology. Springer Berlin Heidelberg, Berlin, Heidelberg, pp. 3–13. doi:10.1007/978-3-642-77595-6_1

Eker-develi, E., Berthon, J., Canuti, E., Slabakova, N., Moncheva, S., Shtereva, G., Dzhurova, B., 2012. Phytoplankton taxonomy based on CHEMTAX and microscopy in the northwestern Black Sea. J. Mar. Syst. 94, 18–32. doi:10.1016/j.jmarsys.2011.10.005

Eppley, R.W., 1972. Temperature and phytoplankton growth in the sea. Fish. Bull. 70, 1063–1085.

Falkowski, P., 2012. Ocean science: The power of plankton. Nature 483, S17–S20. doi:10.1038/483S17a

Falkowski, P.G., 2004. The evolution of modern eukaryotic phytoplankton. Science (80-.). 305, 354–360. doi:10.1126/science.1095964

Falkowski, P.G., 1998. Biogeochemical controls and feedbacks on ocean primary production. Science (80-.). 281, 200–206. doi:10.1126/science.281.5374.200

Falkowski, P.G., 1994. The role of phytoplankton photosyntesis in global biogeochemical cycles. Photosynth. Res. 39, 235–258.

Falkowski, P.G., Oliver, M.J., 2007. Mix and match: how climate selects phytoplankton. Nat. Rev. Microbiol. 5, 813–819. doi:10.1038/nrmicro1751

Falkowski, P.G., Raven, J.A., 1997. Aquatic photosynthesis. Blackwell, Oxford, UK.

Fernández-Méndez, M., Wenzhöfer, F., Peeken, I., Sørensen, H.L., Glud, R.N., Boetius,

A., 2014. Composition, buoyancy regulation and fate of ice algal aggregates in the central Arctic Ocean. PLoS One 9, e107452. doi:10.1371/journal.pone.0107452

Field, C.B., Behrenfeld, M., Randerson, J.T., Falkowski, P.G., 1998. Primary production of the biosphere: integrating terrestrial and oceanic components. Science (80-.). 281, 237–240. doi:10.1126/science.281.5374.237

Finkel, Z. V., Beardall, J., Flynn, K.J., Quigg, A., Rees, T.A. V., Raven, J.A., 2009. Phytoplankton in a changing world: cell size and elemental stoichiometry. J. Plankton Res. 32, 119–137. doi:10.1093/plankt/fbp098

Finkel, Z. V., Quigg, A., Raven, J.A., Reinfelder, J.R., Schofield, O.E., Falkowski, P.G., 2006. Irradiance and the elemental stoichiometry of marine phytoplankton. Limnol. Oceanogr. 51, 2690–2701. doi:10.4319/lo.2006.51.6.2690

Follows, M.J., Dutkiewicz, S., Grant, S., Chisholm, S.W., 2007. Emergent biogeography of microbial communities in a model ocean. Science (80-.). 315, 1843–1846. doi:10.1126/science.1138544

Fragoso, G.M., 2009. Hydrography and phytoplankton distribution in the Amundsen and Ross Seas. College of William and Mary.

Fragoso, G.M., Poulton, A.J., Yashayaev, I.M., Head, E.J.H., Purdie, D.A., 2016a. Spring phytoplankton communities of the Labrador Sea (2005 - 2014): pigment signatures, photophysiology and elemental ratios. Biogeosciences Discuss. 1–43. doi:10.5194/bg-2016-295

Fragoso, G.M., Poulton, A.J., Yashayaev, I.M., Head, E.J.H., Stinchcombe, M.C., Purdie, D.A., 2016b. Biogeographical patterns and environmental controls of phytoplankton communities from contrasting hydrographical zones of the Labrador Sea. Prog. Oceanogr. 141, 212–226. doi:10.1016/j.pocean.2015.12.007

Fragoso, G.M., Smith, W.O., 2012. Influence of hydrography on phytoplankton distribution in the Amundsen and Ross Seas, Antarctica. J. Mar. Syst. 89, 19–29. doi:10.1016/j.jmarsys.2011.07.008

Frajka-Williams, E., Rhines, P.B., 2010. Physical controls and interannual variability of the Labrador Sea spring phytoplankton bloom in distinct regions. Deep. Res. Part I Oceanogr. Res. Pap. 57, 541–552. doi:10.1016/j.dsr.2010.01.003

Frajka-Williams, E., Rhines, P.B., Eriksen, C.C., 2009. Physical controls and mesoscale variability in the Labrador Sea spring phytoplankton bloom observed by Seaglider. Deep. Res. Part I Oceanogr. Res. Pap. 56, 2144–2161. doi:10.1016/j.dsr.2009.07.008

Fryxell, G.A., 1983. Survival strategies of the algae. CUP Archive.

Fujiki, T., Matsumoto, K., Honda, M.C., Kawakami, H., Watanabe, S., 2009. Phytoplankton composition in the subarctic North Pacific during autumn 2005. J. Plankton Res. 31, 179–191. doi:10.1093/plankt/fbn108

Fujiki, T., Satotu, T., 2002. Variability in chlorophyll a specific absorption coefficient in marine phytoplankton as a function of cell size and irradiance. J. Plankton Res. 24, 859–874. doi:10.1093/plankt/24.9.859

Fujiwara, A., Hirawake, T., Suzuki, K., Imai, I., Saitoh, S.I., 2014. Timing of sea ice retreat can alter phytoplankton community structure in the western Arctic Ocean. Biogeosciences 11, 1705–1716. doi:10.5194/bg-11-1705-2014

Gil, I.M., Keigwin, L.D., Abrantes, F., 2015. The deglaciation over Laurentian Fan: History of diatoms, IRD, ice and fresh water. Quat. Sci. Rev. 129, 57–67. doi:10.1016/j.quascirev.2015.10.006

Giraudeau, J., Hulot, V., Hanquiez, V., Devaux, L., Howa, H., Garlan, T., 2016. A survey of the summer coccolithophore community in the western Barents Sea. J. Mar. Syst. 158, 93–105. doi:10.1016/j.jmarsys.2016.02.012

Glibert, P.M., 2016. Margalef revisited : A new phytoplankton mandala incorporating twelve dimensions , including nutritional physiology. Harmful Algae 55, 25–30. doi:10.1016/j.hal.2016.01.008

Goes, J.I., Gomes, H.D.R., Chekalyuk, A.M., Carpenter, E.J., Montoya, J.P., Coles, V.J., Yager, P.L., Berelson, W.M., Capone, D.G., Foster, R. a., Steinberg, D.K., Subramaniam, A., Hafez, M. a., 2014. Influence of the Amazon River discharge on the biogeography of phytoplankton communities in the western tropical north Atlantic. Prog. Oceanogr. 120, 29–40. doi:10.1016/j.pocean.2013.07.010

Goffart, A., Catalano, G., Hecq, J.H., 2000. Factors controlling the distribution of diatoms and *Phaeocystis* in the Ross Sea. J. Mar. Syst. 27, 161–175.

Goldman, J.C., McCarthy, J.J., Peavey, D.G., 1979. Growth rate influence on the chemical

composition of phytoplankton in oceanic waters. Nature 279, 210–215. doi:10.1038/279210a0

Gonçalves-Araujo, R., De Souza, M.S., Mendes, C.R.B., Tavano, V.M., Pollery, R.C., Garcia, C.A.E., 2012. Brazil-Malvinas confluence: Effects of environmental variability on phytoplankton community structure. J. Plankton Res. 34, 399–415. doi:10.1093/plankt/fbs013

Gradinger, 1996. Occurrence of an algal bloom under Arctic pack ice. Mar. Ecol. Prog. Ser. 131, 301–305.

Gregg, W.W., Casey, N.W., 2007. Modeling coccolithophores in the global oceans. Deep Sea Res. Part II Top. Stud. Oceanogr. 54, 447–477. doi:10.1016/j.dsr2.2006.12.007

Gregg, W.W., Ginoux, P., Schopf, P.S., Casey, N.W., 2003. Phytoplankton and iron: validation of a global three-dimensional ocean biogeochemical model. Deep Sea Res. Part II Top. Stud. Oceanogr. 50, 3143–3169. doi:10.1016/j.dsr2.2003.07.013

Guidi, L., Stemmann, L., Jackson, G. a., Ibanez, F., Claustre, H., Legendre, L., Picheral, M., Gorsky, G., 2009. Effects of phytoplankton community on production, size, and export of large aggregates: A world-ocean analysis. Limnol. Oceanogr. 54, 1951–1963. doi:10.4319/lo.2009.54.6.1951

Gusev, E.A., Anikina, N.Y., Derevyanko, L.G., Klyuvitkina, T.S., Polyak, L. V., Polyakova, E.I., Rekant, P. V., Stepanova, A.Y., 2014. Environmental evolution of the southern Chukchi Sea in the Holocene. Oceanology 54, 465–477. doi:10.1134/S0001437014030011

Haberman, K.L., Quetin, L.B., Ross, R.M., 2003. Diet of the Antarctic krill (*Euphausia superba* Dana). J. Exp. Mar. Bio. Ecol. 283, 79–95. doi:10.1016/S0022-0981(02)00466-5

Hall, M.M., Torres, D.J., Yashayaev, I., 2013. Absolute velocity along the AR7W section in the Labrador Sea. Deep. Res. Part I Oceanogr. Res. Pap. 72, 72–87. doi:10.1016/j.dsr.2012.11.005

Harlay, J., Borges, A. V., Van Der Zee, C., Delille, B., Godoi, R.H.M., Schiettecatte, L.S., Roevros, N., Aerts, K., Lapernat, P.E., Rebreanu, L., Groom, S., Daro, M.H., Van Grieken, R., Chou, L., 2010. Biogeochemical study of a coccolithophore bloom in the northern Bay of Biscay (NE Atlantic Ocean) in June 2004. Prog. Oceanogr. 86, 317–

336. doi:10.1016/j.pocean.2010.04.029

Harrison, G.W., Yngve Børsheim, K., Li, W.K.W., Maillet, G.L., Pepin, P., Sakshaug, E., Skogen, M.D., Yeats, P.A., 2013. Phytoplankton production and growth regulation in the Subarctic North Atlantic: A comparative study of the Labrador Sea-Labrador/Newfoundland shelves and Barents/Norwegian/Greenland seas and shelves. Prog. Oceanogr. 114, 26–45. doi:10.1016/j.pocean.2013.05.003

Harrison, W., Li, W., 2008. Phytoplankton growth and regulation in the Labrador Sea: light and nutrient limitation. J. Northwest Atl. Fish. Sci. doi:10.2960/J.v39.m592

Harrison, W.G., Platt, T., 1986. Photosynthesis-irradiance relationships in polar and temperate phytoplankton populations. Polar Biol. 5, 153–164.

Hasle, G.R., Heimdal, B.R., 1998. The net phytoplankton in Kongsfjorden, Svalbard, July 1988, with general remarks on species composition of Arctic phytoplankton. Polar Res. 17, 31–52. doi:10.1111/j.1751-8369.1998.tb00257.x

Hasle, G.R., Syvertsen, E.E., 1997. Marine diatoms, in: Tomas, C.R. (Ed.), Identifying Marine Phytoplankton. Academic Press, San Diego, pp. 5–385.

Hays, G., Richardson, A., Robinson, C., 2005. Climate change and marine plankton. Trends Ecol. Evol. 20, 337–344. doi:10.1016/j.tree.2005.03.004

Head, E.J.H., Harris, L.R., 1996. Chlorophyll destruction by *Calanus* spp. grazing on phytoplankton: Kinetics, effects of ingestion rate and feeding history, and a mechanistic interpretation. Mar. Ecol. Prog. Ser. 135, 223–235. doi:10.3354/meps135223

Head, E.J.H., Harris, L.R., Campbell, R.W., 2000. Investigations on the ecology of *Calanus* spp. in the Labrador Sea. I. Relationship between the phytoplankton bloom and reproduction and development of *Calanus finmarchicus* in spring. Mar. Ecol. Prog. Ser. 193, 53–73. doi:10.3354/meps193053

Head, E.J.H., Harris, L.R., Yashayaev, I., 2003. Distributions of *Calanus* spp. and other mesozooplankton in the Labrador Sea in relation to hydrography in spring and summer (1995-2000). Prog. Oceanogr. doi:10.1016/S0079-6611(03)00111-3

Head, E.J.H., Melle, W., Pepin, P., Bagøien, E., Broms, C., 2013. On the ecology of *Calanus finmarchicus* in the Subarctic North Atlantic: A comparison of population

dynamics and environmental conditions in areas of the Labrador Sea-Labrador/Newfoundland Shelf and Norwegian Sea Atlantic and Coastal Waters. Prog. Oceanogr. 114, 46–63. doi:10.1016/j.pocean.2013.05.004

Head, E.J.H., Pepin, P., 2010. Spatial and inter-decadal variability in plankton abundance and composition in the Northwest Atlantic (1958-2006). J. Plankton Res. 32, 1633–1648. doi:10.1093/plankt/fbq090

Hegseth, E.N., Sundfjord, A., 2008. Intrusion and blooming of Atlantic phytoplankton species in the high Arctic. J. Mar. Syst. 74, 108–119. doi:10.1016/j.jmarsys.2007.11.011

Heimdal, B., 1997. Modern coccolithophores, in: Tomas, C.R. (Ed.), Identifying Marine Phytoplankton. Academic Press, San Diego, pp. 731–831.

Henriksen, P., Riemann, B., Kaas, H., Sorensen, H.L.H.M., Sørensen, H.M.H.L., 2002. Effects of nutrient-limitation and irradiance on marine phytoplankton pigments. J. Plankton Res. 24, 835–858. doi:10.1093/plankt/24.9.835

Henson, S. a., Dunne, J.P., Sarmiento, J.L., 2009. Decadal variability in North Atlantic phytoplankton blooms. J. Geophys. Res. 114, C04013. doi:10.1029/2008JC005139

Henson, S., Lampitt, R., Johns, D., 2012. Variability in phytoplankton community structure in response to the North Atlantic Oscillation and implications for organic carbon flux. Limnol. Oceanogr. 57, 1591–1601. doi:10.4319/lo.2012.57.6.1591

Herman, Y., 2012. The Arctic Seas: climatology, oceanography, geology, and biology. Springer Science & Business Media.

Higgins, H.W., Wright, S.W., Schlüter, L., 2011. Quantitative interpretation of chemotaxonomic pigment data, in: Roy, S., Llewellyn, C., Egeland, E.S., Johnsen, G. (Eds.), Phytoplankton Pigments: Characterization, Chemotaxonomy and Applications in Oceanography. Cambridge University Press, Cambridge, pp. 257–313. doi:10.1017/CBO9780511732263.010

Hill, V., Cota, G., Stockwell, D., 2005. Spring and summer phytoplankton communities in the Chukchi and Eastern Beaufort Seas. Deep. Res. Part II Top. Stud. Oceanogr. 52, 3369–3385. doi:10.1016/j.dsr2.2005.10.010

Ho, T., Quigg, A., Zoe, V., Milligan, A.J., Wyman, K., Falkowski, P.G., Morel, F.M.M.,

2003. The elemental composition of some marine phytoplankton. J. Phycol. 1159, 1145–1159.

Holligan, P.M., Fernández, E., Aiken, J., Balch, W.M., Boyd, P., Burkill, P.H., Finch, M., Groom, S.B., Malin, G., Muller, K., Purdie, D.A., Robinson, C., Trees, C.C., Turner, S.M., van der Wal, P., 1993. A biogeochemical study of the coccolithophore, *Emiliania huxleyi*, in the North Atlantic. Global Biogeochem. Cycles 7, 879–900. doi:10.1029/93GB01731

Holm-Hansen, O., Lorenzen, C.J., Holmes, R.W., Strickland, J.D.H., 1965. Fluorometric determination of chlorophyll. ICES J. Mar. Sci. 30, 3–15. doi:10.1093/icesjms/30.1.3

Hood, E., Battin, T.J., Fellman, J., Neel, S.O., Spencer, R.G.M., 2015. Storage and release of organic carbon from glaciers and ice sheets. Nat. Publ. Gr. 8, 91–96. doi:10.1038/ngeo2331

Hoppenrath, M., Elbrächter, M., Drebes, G., 2009. Marine phytoplankton. E. Schweizerbart Science Publishers, Stuttgart, Germany.

Huot, Y., Babin, M., Bruyant, F., 2013. Photosynthetic parameters in the Beaufort Sea in relation to the phytoplankton community structure. Biogeosciences 10, 3445–3454. doi:10.5194/bg-10-3445-2013

Hutchinson, G.E., 1961. The paradox of the plankton. Am. Nat. 95, 137–145. doi:10.2307/2458386

Ichinomiya, M., Nakamachi, M., Fukuchi, M., Taniguchi, A., 2008. Resting cells of microorganisms in the 20–100μm fraction of marine sediments in an Antarctic coastal area. Polar Sci. 2, 27–32. doi:10.1016/j.polar.2007.12.001

Ikeda, T., Kanno, Y., Ozaki, K., Shinada, A., 2001. Metabolic rates of epipelagic marine copepods as a function of body mass and temperature. Mar. Biol. 139, 1020–1020. doi:10.1007/s002270100608

Irigoien, X., 2005. Phytoplankton blooms: a “loophole” in microzooplankton grazing impact? J. Plankton Res. 27, 313–321. doi:10.1093/plankt/fbi011

Irigoien, X., Huisman, J., Harris, R.P., 2004a. Global biodiversity patterns of marine phytoplankton and zooplankton. Nature 429, 863–867. doi:10.1038/nature02644.1.

Irigoien, X., Meyer, B., Harris, R., Harbour, D., 2004b. Using HPLC pigment analysis to

investigate phytoplankton taxonomy: The importance of knowing your species. Helgol. Mar. Res. 58, 77–82. doi:10.1007/s10152-004-0171-9

Jakobsen, H.H., Tang, K.W., 2002. Effects of protozoan grazing on colony formation in *Phaeocystis globosa* (Prymnesiophyceae) and the potential costs and benefits 27, 261–273.

Jamil, T., Kruk, C., ter Braak, C.J.F., 2014. A unimodal species response model relating traits to environment with application to phytoplankton communities. PLoS One 9, e97583. doi:10.1371/journal.pone.0097583

Jeffrey, S.W., Mantoura, R.F.C., Wright, S.W., 1997. Phytoplankton Pigments in Oceanography. SCOR and UNESCO, Paris.

Jensen, H.M., Pedersen, L., Burmeister, A., Winding Hansen, B., 1999. Pelagic primary production during summer along 65 to 72°N off West Greenland. Polar Biol. 21, 269–278. doi:10.1007/s003000050362

Jensen, K.G., Kuijpers, A., Koç, N., Heinemeier, J., 2004. Diatom evidence of hydrographic changes and ice conditions in Igaliku Fjord, South Greenland, during the past 1500 years. The Holocene 14, 152–164. doi:10.1191/0959683604hl698rp

Jiang, M., Borkman, D.G., Scott Libby, P., Townsend, D.W., Zhou, M., 2014. Nutrient input and the competition between *Phaeocystis pouchetii* and diatoms in Massachusetts Bay spring bloom. J. Mar. Syst. 134, 29–44. doi:10.1016/j.jmarsys.2014.02.011

Kahru, M., Brotas, V., Manzano-Sarabia, M., Mitchell, B.G., 2011. Are phytoplankton blooms occurring earlier in the Arctic? Glob. Chang. Biol. 17, 1733–1739. doi:10.1111/j.1365-2486.2010.02312.x

Karl, D.M., Björkman, K.M., Dore, J.E., Fujieki, L., Hebel, D. V., Houlihan, T., Letelier, R.M., Tupas, L.M., 2001. Ecological nitrogen-to-phosphorus stoichiometry at station ALOHA. Deep Sea Res. Part II Top. Stud. Oceanogr. 48, 1529–1566. doi:10.1016/S0967-0645(00)00152-1

Katz, M.E., Finkel, Z. V, Grzebyk, D., Knoll, A.H., Paul, G., Falkowski, P.G., 2004. Evolutionary trajectories and biogeochemical impacts of marine eukaryotic phytoplankton. Annu. Rev. Ecol. Evol. Syst. 35, 523–556. doi:10.2307/annurev.ecolsys.35.112202.30000020

Kemp, A.E.S., Pearce, R.B., Grigorov, I., Rance, J., Lange, C.B., Quilty, P., Salter, I., 2006. Production of giant marine diatoms and their export at oceanic frontal zones: Implications for Si and C flux from stratified oceans. Global Biogeochem. Cycles 20, n/a-n/a. doi:10.1029/2006GB002698

Kerouel, R., Aminot, a, 1997. Fluorometric determination of ammonia in sea and estuarine water by direct segmented flow analysis. Mar. Chem. 57, 265–275.

Key, T., McCarthy, A., Campbell, D.A., Six, C., Roy, S., Finkel, Z. V., 2010. Cell size trade-offs govern light exploitation strategies in marine phytoplankton. Environ. Microbiol. 12, 95–104. doi:10.1111/j.1462-2920.2009.02046.x

Khan, S.A., Wahr, J., Bevis, M., Velicogna, I., Kendrick, E., 2010. Spread of ice mass loss into northwest Greenland observed by GRACE and GPS. Geophys. Res. Lett. 37, n/a-n/a. doi:10.1029/2010GL042460

Kieke, D., Yashayaev, I., 2015. Studies of Labrador Sea Water formation and variability in the subpolar North Atlantic in the light of international partnership and collaboration. Prog. Oceanogr. 132, 220–232. doi:10.1016/j.pocean.2014.12.010

Kiørboe, T., 1993. Turbulence, Phytoplankton Cell Size, and the Structure of Pelagic Food Webs. pp. 1–72. doi:10.1016/S0065-2881(08)60129-7

Kirk, J.T.O., 1994. Characteristics of the light field in highly turbid waters: A Monte Carlo study. Limnol. Oceanogr. 39, 702–706. doi:10.4319/lo.1994.39.3.0702

Klausmeier, C.A., Litchman, E., Daufresne, T., Levin, S.A., 2008. Phytoplankton stoichiometry. Ecol. Res. 23, 479–485. doi:10.1007/s11284-008-0470-8

Krawczyk, D.W., Witkowski, A., Wroniecki, M., Waniek, J., Kurzydłowski, K.J., Płociński, T., 2012. Reinterpretation of two diatom species from the West Greenland margin — *Thalassiosira kushirensis* and *Thalassiosira antarctica* var. *borealis* — hydrological consequences. Mar. Micropaleontol. 88–89, 1–14. doi:10.1016/j.marmicro.2012.02.004

Krembs, C., Eicken, H., Deming, J.W., 2011. Exopolymer alteration of physical properties of sea ice and implications for ice habitability and biogeochemistry in a warmer Arctic. Proc. Natl. Acad. Sci. 108, 3653–3658. doi:10.1073/pnas.1100701108

Kropuenske, L.R., Mills, M.M., Van Dijken, G.L., Alderkamp, A.C., Mine Berg, G.,

Robinson, D.H., Welschmeyer, N.A., Arrigo, K.R., 2010. Strategies and rates of photoacclimation in two major southern ocean phytoplankton taxa: *Phaeocystis antarctica* (haptophyta) and *Fragilariopsis cylindrus* (bacillariophyceae). J. Phycol. 46, 1138–1151. doi:10.1111/j.1529-8817.2010.00922.x

Kropuenske, L.R., Mills, M.M., van Dijken, G.L., Bailey, S., Robinson, D.H., Welschmeyer, N.A., Arrigo, K.R., 2009. Photophysiology in two major Southern Ocean phytoplankton taxa: Photoprotection in *Phaeocystis antarctica* and *Fragilariopsis cylindrus* . Limnol. Oceanogr. 54, 1176–1196. doi:10.4319/lo.2009.54.4.1176

Kruk, C., Huszar, V.L.M., Peeters, E.T.H.M., Bonilla, S., Costa, L., Lurling, M., Reynolds, C.S., Scheffer, M., 2010. A morphological classification capturing functional variation in phytoplankton. Freshw. Biol. 55, 614–627. doi:10.1111/j.1365-2427.2009.02298.x

Kruk, C., Peeters, E.T.H.M., Van Nes, E.H., Huszar, V.L.M., Costa, L.S., Scheffer, M., 2011. Phytoplankton community composition can be predicted best in terms of morphological groups. Limnol. Oceanogr. 56, 110–118. doi:10.4319/lo.2011.56.1.0110

Kuwata, A., Takahashi, M., 1999. Survival and recovery of resting spores and resting cells of the marine planktonic diatom *Chaetoceros pseudocurvisetus* under fluctuating nitrate conditions. Mar. Biol. 134, 471–478. doi:10.1007/s002270050563

Kuwata, A., Takahashi, M., 1990. Life-form population responses of a marine planktonic diatom, *Chaetoceros pseudocurvisetus*, to oligotrophication in regionally upwelled water. Mar. Biol. 107, 503–512. doi:10.1007/BF01313435

Kwok, R., Cunningham, G.F., Wensnahan, M., Rigor, I., Zwally, H.J., Yi, D., 2009. Thinning and volume loss of the Arctic Ocean sea ice cover: 2003–2008. J. Geophys. Res. 114, C07005. doi:10.1029/2009JC005312

Lacour, L., Claustre, H., Prieur, L., Ortenzio, F.D., 2015. Phytoplankton biomass cycles in the North Atlantic subpolar gyre: A similar mechanism for two different blooms in the Labrador Sea 5403–5410. doi:10.1002/2015GL064540.Received

Landry, M.R., Calbet, A., 2004. Microzooplankton production in the oceans. ICES J. Mar. Sci. 61, 501–507. doi:10.1016/j.icesjms.2004.03.011

Lapointe, M., 2000. Late quaternary paleohydrology of the Gulf of St. Lawrence (Québec, Canada) based on diatom analysis. Palaeogeogr. Palaeoclimatol. Palaeoecol. 156, 261–276. doi:10.1016/S0031-0182(99)00144-3

Lavorel, S., Grigulis, K., Lamarque, P., Colace, M.-P., Garden, D., Girel, J., Pellet, G., Douzet, R., 2011. Using plant functional traits to understand the landscape distribution of multiple ecosystem services. J. Ecol. 99, 135–147. doi:10.1111/j.1365-2745.2010.01753.x

Le Moigne, F.A.C., Poulton, A.J., Henson, S.A., Daniels, C.J., Fragoso, G.M., Mitchell, E., Richier, S., Russell, B.C., Smith, H.E.K., Tarling, G.A., Young, J.R., Zubkov, M., 2015. Carbon export efficiency and phytoplankton community composition in the Atlantic sector of the Arctic Ocean. J. Geophys. Res. Ocean. 120, 3896–3912. doi:10.1002/2015JC010700.Received

Lee, S., Fuhrman, J.E.D.A., 1987. Relationships between biovolume and biomass of naturally derived marine bacterioplankton. Deep Sea Res. Part B. Oceanogr. Lit. Rev. 34, 1069. doi:10.1016/0198-0254(87)96080-8

Leps, J., De Bello, F., Lavorel, S., Berman, S., 2006. Quantifying and interpreting functional diversity of natural. Preslia 78, 481–501.

Lepš, J., Šmilauer, P., 2003. Multivariate analysis of ecological data using CANOCO. Cambridge university press.

Leterme, S.C., Edwards, M., Seuront, L., Attrill, M.J., Reid, P.C., John, A.W.G., 2005. Decadal basin-scale changes in diatoms, dinoflagellates, and phytoplankton color across the North Atlantic. Limnol. Oceanogr. 50, 1244–1253.

Leventer, A., 1998. The fate of Antarctic “sea ice diatoms” and their use as paleoenvironmental indicators. Antarct. sea ice Biol. Process. Interact. Var. Antarct. Res. Ser. 73, 121–137. doi:10.1029/AR073p0121

Leventer, A., Domack, E., Barkoukis, A., McAndrews, B., Murray, J., 2002. Laminations from the Palmer Deep: A diatom-based interpretation. Paleoceanography 17, PAL 3-1-PAL 3-15. doi:10.1029/2001PA000624

Leventer, A., Dunbar, R.B., 1996. Factors influencing the distribution of diatoms and other algae in the Ross Sea. J. Geophys. Res. Ocean. 101, 18489–18500. doi:10.1029/96JC00204

Li, W.K.W., Harrison, W.G., 2001. Chlorophyll, bacteria and picophytoplankton in ecological provinces of the North Atlantic. Deep. Res. Part II Top. Stud. Oceanogr. 48, 2271–2293. doi:10.1016/S0967-0645(00)00180-6

Li, W.K.W., Harrison, W.G., Head, E.J.H., 2006. Coherent assembly of phytoplankton communities in diverse temperate ocean ecosystems. Proc. Biol. Sci. 273, 1953–1960. doi:10.1098/rspb.2006.3529

Li, W.K.W., McLaughlin, F.A., Lovejoy, C., Carmack, E.C., 2009. Smallest algae thrive as the Arctic Ocean freshens. Science 326, 539. doi:10.1126/science.1179798

Litchman, E., de Tezanos Pinto, P., Klausmeier, C.A., Thomas, M.K., Yoshiyama, K., 2010. Linking traits to species diversity and community structure in phytoplankton. Hydrobiologia 653, 15–28. doi:10.1007/s10750-010-0341-5

Litchman, E., Edwards, K.F., Klausmeier, C.A., Thomas, M.K., 2012. Phytoplankton niches, traits and eco-evolutionary responses to global environmental change. Mar. Ecol. Prog. Ser. 470, 235–248. doi:10.3354/meps09912

Litchman, E., Klausmeier, C.A., 2008. Trait-based community ecology of phytoplankton. Annu. Rev. Ecol. Evol. Syst. 39, 615–639. doi:10.1146/annurev.ecolsys.39.110707.173549

Litchman, E., Klausmeier, C.A., Schofield, O.M., Falkowski, P.G., 2007. The role of functional traits and trade-offs in structuring phytoplankton communities: Scaling from cellular to ecosystem level. Ecol. Lett. 10, 1170–1181. doi:10.1111/j.1461-0248.2007.01117.x

Lizotte, M.P., 2003. The microbiology of sea ice, in: Thomas, D.N., Dieckmann, G. (Eds.), Sea Ice: An Introduction to Its Physics, Chemistry, Biology and Geology. Blackwell, Oxford, UK, pp. 184–210.

Lovejoy, C., Legendre, L., Martineau, M.-J., Bâcle, J., von Quillfeldt, C.H., 2002. Distribution of phytoplankton and other protists in the North Water. Deep Sea Res. Part II Top. Stud. Oceanogr. 49, 5027–5047. doi:10.1016/S0967-0645(02)00176-5

Lovejoy, C., Vincent, W.F., Bonilla, S., Roy, S., Martineau, M.-J., Terrado, R., Potvin, M., Massana, R., Pedrós-Alió, C., 2007. Distribution, phylogeny, and growth of cold-adapted picoprasinophytes in Arctic Seas. J. Phycol. 43, 78–89. doi:10.1111/j.1529-8817.2006.00310.x

Luddington, I.A.N.A., Lovejoy, C., Kaczmarska, I., 2016. Species-rich meta-communities of the diatom order Thalassiosirales in the Arctic and northern Atlantic Ocean 0, 1–17. doi:10.1093/plankt/fbw030

Lundholm, N., Hasle, G.R., 2010. *Fragilariopsis* (Bacillariophyceae) of the Northern Hemisphere – morphology, taxonomy, phylogeny and distribution, with a description of F. pacifica sp. nov. Phycologia. doi:10.2216/09-97.1

Lutz, V.A., Sathyendranath, S., Head, E.J.H., Li, W.K.W., 2003. Variability in pigment composition and optical characteristics of phytoplankton in the Labrador Sea and the Central North Atlantic. Mar. Ecol. Prog. Ser. 260, 1–18. doi:10.3354/meps260001

Mackey, M.D., Mackey, D.J., Higgins, H.W., Wright, S.W., 1996. CHEMTAX - a program for estimating class abundances from chemical markers: application to HPLC measurements of phytoplankton. Mar. Ecol. Prog. Ser. 144, 265–283.

Marañón, E., 2015. Cell size as a key determinant of phytoplankton metabolism and community structure. Ann. Rev. Mar. Sci. 7, 241–264. doi:10.1146/annurev-marine-010814-015955

Martiny, A.C., Pham, C.T.A., Primeau, F.W., Vrugt, J.A., Moore, J.K., Levin, S.A., Lomas, M.W., 2013a. Strong latitudinal patterns in the elemental ratios of marine plankton and organic matter. Nat. Geosci. 6, 279–283. doi:10.1038/ngeo1757

Martiny, A.C., Vrugt, J.A., Primeau, F.W., Lomas, M.W., 2013b. Regional variation in the particulate organic carbon to nitrogen ratio in the surface ocean. Global Biogeochem. Cycles 27, 723–731. doi:10.1002/gbc.20061

Martz, T.R., DeGrandpre, M.D., Strutton, P.G., McGillis, W.R., Drennan, W.M., 2009. Sea surface pCO_2 and carbon export during the Labrador Sea spring-summer bloom: An in situ mass balance approach. J. Geophys. Res. 114, C09008. doi:10.1029/2008JC005060

Mary, S.A., 1997. Marine microfouling algae: the diatoms. CRC Press.

Mathot, S., Smith, W.O., Carlson, C.A., Garrison, D.L., Gowing, M.M., Vickers, C.L., 2000. Carbon partitioning within *Phaeocystis antarctica* (prymnesiophyceae) colonies in the Ross sea, Antarctica. J. Phycol. 36, 1049–1056. doi:10.1046/j.1529-8817.2000.99078.x

McFarland, M.N., Rines, J., Sullivan, J., Donaghay, P., 2015. Impact of phytoplankton size and physiology on particulate optical properties determined with scanning flow cytometry. Mar. Ecol. Prog. Ser. 531, 43–61. doi:10.3354/meps11325

McGill, B., Enquist, B., Weiher, E., Westoby, M., 2006. Rebuilding community ecology from functional traits. Trends Ecol. Evol. 21, 178–185. doi:10.1016/j.tree.2006.02.002

McQuoid, M.R., Godhe, A., Nordberg, K., 2002. Viability of phytoplankton resting stages in the sediments of a coastal Swedish fjord. Eur. J. Phycol. 37, S0967026202003670. doi:10.1017/S0967026202003670

McQuoid, M.R., Hobson, L.A., 1996. Diatoms resting stages. J. Phycol. 32, 889–902. doi:10.1111/j.0022-3646.1996.00889.x

Medlin, L.K., Priddle, J., 1990. Polar marine diatoms. British Antarctic Survey, Cambridge.

Mei, Z.-P., Legendre, L., Tremblay, J.-E., Miller, L.A., Gratton, Y., Lovejoy, C., Yager, P.L., Gosselin, M., 2005. Carbon to nitrogen (C:N) stoichiometry of the spring – summer phytoplankton bloom in the North Water Polynya (NOW). Deep Sea Res. Part I Oceanogr. Res. Pap. 52, 2301–2314. doi:10.1016/j.dsr.2005.07.001

Melnikov, I. a, Kolosova, E.G., Welch, H.E., Zhitina, L.S., 2002. Sea ice biological communities and nutrient dynamics in the Canada Basin of the Arctic Ocean. Deep Sea Res. Part I Oceanogr. Res. Pap. 49, 1623–1649. doi:10.1016/S0967-0637(02)00042-0

Menden-Deuer, S., Lessard, E.J., 2000. Carbon to volume relationships for dinoflagellates, diatoms, and other protist plankton. Limnol. Oceanogr. 45, 569–579. doi:10.4319/lo.2000.45.3.0569

Michaels, A., Karl, D., Capone, D., 2001. Element stoichiometry, new production and nitrogen fixation. Oceanography 14, 68–77. doi:10.5670/oceanog.2001.08

Michel, C., Legendre, L., Therriault, J.-C., Demers, S., Vandevelde, T., 1993. Springtime coupling between ice algal and phytoplankton assemblages in southeastern Hudson Bay, Canadian Arctic. Polar Biol. 13, 441–449. doi:10.1007/BF00233135

Miettinen, A., Koç, N., Husum, K., 2013. Appearance of the Pacific diatom *Neodenticula seminae* in the northern Nordic Seas — An indication of changes in Arctic sea ice and

ocean circulation. Mar. Micropaleontol. 99, 2–7. doi:10.1016/j.marmicro.2012.06.002

Mills, M.M., Kropuenske, L.R., Van Dijken, G.L., Alderkamp, A.C., Berg, G.M., Robinson, D.H., Welschmeyer, N.A., Arrigo, K.R., 2010. Photophysiology in two southern ocean phytoplankton taxa: Photosynthesis of *Phaeocystis antarctica* (prymnesiophyceae) and *Fragilariopsis cylindrus* (bacillariophyceae) under simulated mixed-layer irradiance. J. Phycol. 46, 1114–1127. doi:10.1111/j.1529-8817.2010.00923.x

Mock, T., Junge, K., 2007. Psychrophilic diatoms: mechanism for survival in freeze-thaw cycles, in: Seckbach, J. (Ed.), Algae and Cyanobacteria in Extreme Environments. Springer, New York, pp. 345–364.

Moisan, T.A., Olaizola, M., Mitchell, B.G., 1998. Xanthophyll cycling in *Phaeocystis antarctica*: Changes in cellular fluorescence. Mar. Ecol. Prog. Ser. 169, 113–121. doi:10.3354/meps169113

Montagnes, D.J.S., Franklin, D.J., 2001. Effect of temperature on diatom volume, growth rate, and carbon and nitrogen content: Reconsidering some paradigms. Limnol. Oceanogr. 46, 2008–2018. doi:10.4319/lo.2001.46.8.2008

Montes-Hugo, M., Doney, S.C., Ducklow, H.W., Fraser, W., Martinson, D., Stammerjohn, S.E., Schofield, O., 2009. Recent changes in phytoplankton western Antarctic Peninsula. Science (80-.). 323, 1470–1473.

Moore, C.M., Mills, M.M., Arrigo, K.R., Berman-Frank, I., Bopp, L., Boyd, P.W., Galbraith, E.D., Geider, R.J., Guieu, C., Jaccard, S.L., Jickells, T.D., La Roche, J., Lenton, T.M., Mahowald, N.M., Marañón, E., Marinov, I., Moore, J.K., Nakatsuka, T., Oschlies, A., Saito, M.A., Thingstad, T.F., Tsuda, A., Ulloa, O., 2013. Processes and patterns of oceanic nutrient limitation. Nat. Geosci. 6, 701–710. doi:10.1038/ngeo1765

Moritz, R.E., Bitz, C.M., Steig, E.J., 2002. Dynamics of recent climate change in the Arctic. Science 297, 1497–502. doi:10.1126/science.1076522

Mundy, C.J., Gosselin, M., Ehn, J.K., Belzile, C., Poulin, M., Alou, E., Roy, S., Hop, H., Lessard, S., Papakyriakou, T.N., Barber, D.G., Stewart, J., 2011. Characteristics of two distinct high-light acclimated algal communities during advanced stages of sea ice melt. Polar Biol. 34, 1869–1886. doi:10.1007/s00300-011-0998-x

Muylaert, K., Gonzales, R., Franck, M., Lionard, M., Van der Zee, C., Cattrijsse, A., Sabbe, K., Chou, L., Vyverman, W., 2006. Spatial variation in phytoplankton dynamics in the Belgian coastal zone of the North Sea studied by microscopy, HPLC-CHEMTAX and underway fluorescence recordings. J. Sea Res. 55, 253–265. doi:10.1016/j.seares.2005.12.002

Nair, A., Sathyendranath, S., Platt, T., Morales, J., Stuart, V., Forget, M.H., Devred, E., Bouman, H., 2008. Remote sensing of phytoplankton functional types. Remote Sens. Environ. 112, 3366–3375. doi:10.1016/j.rse.2008.01.021

Nejstgaard, J.C., Tang, K.W., Steinke, M., Dutz, J., Koski, M., Antajan, E., Long, J.D., 2007. Zooplankton grazing on *Phaeocystis*: A quantitative review and future challenges. Biogeochemistry 83, 147–172. doi:10.1007/s10533-007-9098-y

Nguyen, H., Fauci, L., 2014. Hydrodynamics of diatom chains and semiflexible fibres. J. R. Soc. Interface 11, 20140314–20140314. doi:10.1098/rsif.2014.0314

Nguyen, H., Karp-Boss, L., Jumars, P.A., Fauci, L., 2011. Hydrodynamic effects of spines: A different spin. Limnol. Oceanogr. Fluids Environ. 1, 110–119. doi:10.1215/21573698-1303444

Not, F., Zapata, M., Pazos, Y., Campaña, E., Doval, M., Rodríguez, F., 2007. Size-fractionated phytoplankton diversity in the NW Iberian coast: a combination of microscopic, pigment and molecular analyses. Aquat. Microb. Ecol. 49, 255–265. doi:10.3354/ame01144

Okada, H., Mclntyre, A., 1979. Seasonal Distribution of Modern Coccolithophores in the Western North Atlantic Ocean. Mar. Biol. 54, 319–328. doi:10.1007/BF00395438

Oku, O., Kamatani, A., 1999. Resting spore formation and biochemical composition of the marine planktonic diatom *Chaetoceros pseudocurvisetus* in culture: ecological significance of decreased nucleotide content and activation of the xanthophyll cycle by resting spore formation. Mar Biol 135, 425–436. doi:10.1007/s002270050643

Oku, O., Kamatani, A., 1995. Resting spore formation and phosphorus composition of the marine diatom *Chaetoceros pseudocurvisetus* under various nutrient conditions. Mar. Biol. 393–399. doi:10.1007/BF00353630

Olenina, I., Hajdu, S., Edler, L., Andersson, A., Wasmund, N., Busch, S., Göbel, J., Gromisz, S., Huseby, S., Huttunen, M., Jaanus, A., Kokkonen, P., Ledaine, I.,

Niemkiewicz, E., 2006. Biovolumes and size-classes of phytoplankton in the Baltic Sea. HELCOM Balt.Sea Environ. Proc. No. 106.

Ondrusek, M.E., Bidigare, R.R., Sweet, S.T., Defreitas, D.A., Brooks, J.M., 1991. Distribution of phytoplankton pigments in the North Pacific Ocean in relation to physical and optical variability. Deep. Res. 38, 243–266.

Onodera, J., Watanabe, E., Harada, N., Honda, M.C., 2015. Diatom flux reflects water-mass conditions on the southern Northwind Abyssal Plain, Arctic Ocean. Biogeosciences 12, 1373–1385. doi:10.5194/bg-12-1373-2015

Pabi, S., van Dijken, G.L., Arrigo, K.R., 2008. Primary production in the Arctic Ocean, 1998–2006. J. Geophys. Res. 113, C08005. doi:10.1029/2007JC004578

Padisák, J., Borics, G., Fehér, G., Grigorszky, I., Oldal, I., Schmidt, A., Zámbóné-Doma, Z., 2003. Dominant species, functional assemblages and frequency of equilibrium phases in late summer phytoplankton assemblages in Hungarian small shallow lakes. Hydrobiologia 502, 157–168. doi:10.1023/B:HYDR.0000004278.10887.40

Paganelli, D., Marchini, A., Occhipinti-Ambrogi, A., 2012. Functional structure of marine benthic assemblages using Biological Traits Analysis (BTA): A study along the Emilia-Romagna coastline (Italy, North-West Adriatic Sea). Estuar. Coast. Shelf Sci. 96, 245–256. doi:10.1016/j.ecss.2011.11.014

Pahlow, M., Riebesell, U., Wolf-Gladrow, D. a., 1997. Impact of cell shape and chain formation on nutrient acquisition by marine diatoms. Limnol. Oceanogr. 42, 1660–1672. doi:10.4319/lo.1997.42.8.1660

Palmisano, A.C., Soohoo, J.B., Soohoo, S.L., Kottmeier, S.T., Craft, L.L., Sullivan, C.W., 1986. Photoadaptation in *Phaeocystis pouchetii* advected beneath annual sea ice in Mcmurdo Sound, Antarctica. J. Plankton Res. 8, 891–906.

Palmisano, A.C., Sullivan, C.W., 1983. Sea ice microbial communities (SIMCO). Polar Biol. 2, 171–177. doi:10.1007/BF00448967

Peloquin, J., Swan, C., Gruber, N., Vogt, M., Claustre, H., Ras, J., Uitz, J., Barlow, R., Behrenfeld, M., Bidigare, R., Dierssen, H., Ditullio, G., Fernandez, E., Gallienne, C., Gibb, S., Goericke, R., Harding, L., Head, E., Holligan, P., Hooker, S., Karl, D., Landry, M., Letelier, R., Llewellyn, C.A., Lomas, M., Lucas, M., Mannino, A., Marty, J.C., Mitchell, B.G., Muller-Karger, F., Nelson, N., O'Brien, C., Prezelin, B.,

Repeta, D., Smith, W.O., Smythe-Wright, D., Stumpf, R., Subramaniam, A., Suzuki, K., Trees, C., Vernet, M., Wasmund, N., Wright, S., 2013. The MAREDAT global database of high performance liquid chromatography marine pigment measurements. Earth Syst. Sci. Data 5, 109–123. doi:10.5194/essd-5-109-2013

Pepin, P., Head, E.J.H., 2009. Seasonal and depth-dependent variations in the size and lipid contents of stage 5 copepodites of *Calanus finmarchicus* in the waters of the Newfoundland Shelf and the Labrador Sea. Deep Sea Res. Part I Oceanogr. Res. Pap. 56, 989–1002. doi:10.1016/j.dsr.2009.01.005

Peterson, T.D., Toews, H.N.J., Robinson, C.L.K., Harrison, P.J., 2007. Nutrient and phytoplankton dynamics in the Queen Charlotte Islands (Canada) during the summer upwelling seasons of 2001-2002. J. Plankton Res. 29, 219–239. doi:10.1093/plankt/fbm010

Petrou, K., Hill, R., Brown, C.M., Campbell, D.A., Doblin, M.A., Ralph, P.J., 2010. Rapid photoprotection in sea-ice diatoms from the East Antarctic pack ice. Limnol. Oceanogr. 55, 1400–1407. doi:10.4319/lo.2010.55.3.1400

Pike, J., Crosta, X., Maddison, E.J., Stickley, C.E., Denis, D., Barbara, L., Renssen, H., 2009. Observations on the relationship between the Antarctic coastal diatoms *Thalassiosira antarctica* Comber and *Porosira glacialis* (Grunow) Jørgensen and sea ice concentrations during the late Quaternary. Mar. Micropaleontol. 73, 14–25. doi:10.1016/j.marmicro.2009.06.005

Piquet, A.M., Poll, W.H. Van De, Visser, R.J.W., Wiencke, C., Bolhuis, H., Buma, A.G.J., 2014. Springtime phytoplankton dynamics in Arctic Krossfjorden and Kongsfjorden (Spitsbergen) as a function of glacier proximity. Biogeochemistry 11, 2263–2279. doi:10.5194/bg-11-2263-2014

Platt, T., Bouman, H., Devred, E., Fuentes-Yaco, C., Sathyendranath, S., 2005. Physical forcing and phytoplankton distributions. Sci. Mar. 69, 55–73. doi:10.3989/scimar.2005.69s155

Platt, T., Gallegos, C.L., 1980. Modelling Primary Production, in: Falkowski, P.G. (Ed.), Primary Productivity in the Sea. Springer, US, pp. 339–362.

Platt, T., Harrison, G., Irwin, B., Horne, E.P., Gallegos, C.L., 1982. Photosynthesis and photoadaptation of marine phytoplankton in the Arctic. Deep. Res. 29, 1159–1170.

Poulin, M., Underwood, G.J.C., Michel, C., 2014. Sub-ice colonial *Melosira arctica* in Arctic first-year ice. Diatom Res. 29, 213–221. doi:10.1080/0269249X.2013.877085

Poulton, A.J., Charalampopoulou, A., Young, J.R., Tarran, G.A., Lucas, M.I., Quartly, G.D., 2010. Coccolithophore dynamics in non-bloom conditions during late summer in the central Iceland Basin (July-August 2007). Limnol. Oceanogr. 55, 1601–1613. doi:10.4319/lo.2010.55.4.1601

Poulton, A.J., Holligan, P.M., Hickman, A., Kim, Y.N., Adey, T.R., Stinchcombe, M.C., Holeton, C., Root, S., Woodward, E.M.S., 2006. Phytoplankton carbon fixation, chlorophyll-biomass and diagnostic pigments in the Atlantic Ocean. Deep. Res. Part II Top. Stud. Oceanogr. 53, 1593–1610. doi:10.1016/j.dsr2.2006.05.007

Quigg, A., Irwin, A.J., Finkel, Z. V, 2003. Evolutionary inheritance of elemental stoichiometry in phytoplankton. Proc. R. Soc. B Biol. Sci. 278, 526–534. doi:10.1098/rspb.2010.1356

Raymond, J.A., Kim, H.J., 2012. Possible role of horizontal gene transfer in the colonization of sea ice by algae. PLoS One 7, e35968. doi:10.1371/journal.pone.0035968

Read, B. a, Kegel, J., Klute, M.J., Kuo, A., Lefebvre, S.C., Maumus, F., Mayer, C., Miller, J., Monier, A., Salamov, A., Young, J., Aguilar, M., Claverie, J.-M., Frickenhaus, S., Gonzalez, K., Herman, E.K., Lin, Y.-C., Napier, J., Ogata, H., Sarno, A.F., Shmutz, J., Schroeder, D., de Vargas, C., Verret, F., von Dassow, P., Valentin, K., Van de Peer, Y., Wheeler, G., Dacks, J.B., Delwiche, C.F., Dyhrman, S.T., Glöckner, G., John, U., Richards, T., Worden, A.Z., Zhang, X., Grigoriev, I. V, 2013. Pan genome of the phytoplankton *Emiliania* underpins its global distribution. Nature 499, 209–13. doi:10.1038/nature12221

Redfield, A.C., 1958. The biological control of chemical factors in the environment. Am. Sci. 46, 205–221.

Reid, P.C., Johns, D.G., Edwards, M., Starr, M., Poulin, M., Snoeijs, P., 2007. A biological consequence of reducing Arctic ice cover: arrival of the Pacific diatom *Neodenticula seminae* in the North Atlantic for the first time in 800 000 years. Glob. Chang. Biol. 13, 1910–1921. doi:10.1111/j.1365-2486.2007.01413.x

Reigstad, M., Wassmann, P., Wexels Riser, C., Øygarden, S., Rey, F., 2002. Variations in

hydrography, nutrients and chlorophyll a in the marginal ice-zone and the central Barents Sea. J. Mar. Syst. 38, 9–29. doi:10.1016/S0924-7963(02)00167-7

Rey, F., 1991. Photosynthesis-irradiance relationships in natural phytoplankton populations of Barents Sea. Polar Res. 10, 105–116. doi:10.1111/j.1751-8369.1991.tb00638.x

Rhee, G.-Y., 1978. Effects of N:P atomic ratios and nitrate limitation on algal growth, cell composition, and nitrate uptake. Limnol. Oceanogr. 23, 10–25. doi:10.4319/lo.1978.23.1.0010

Rhein, M., Kieke, D., Hüttl-Kabus, S., Roessler, A., Mertens, C., Meissner, R., Klein, B., Böning, C.W., Yashayaev, I., 2011. Deep water formation, the subpolar gyre, and the meridional overturning circulation in the subpolar North Atlantic. Deep Sea Res. Part II Top. Stud. Oceanogr. 58, 1819–1832. doi:10.1016/j.dsr2.2010.10.061

Riaux-Gobin, C., Poulin, M., Dieckmann, G., Labrune, C., Vétion, G., 2011. Spring phytoplankton onset after the ice break-up and sea-ice signature (Adélie Land, East Antarctica). Polar Res. 30, 1–11. doi:10.3402/polar.v30i0.5910

Richardson, T.L., Ciotti, A.M., Cullen, J.J., Villareal, T.A., 1996. Physiological and optical properties of *Rhizosolenia formosa* (Bacillariophyceae) in the contex of open-ocean vertical migration. J. Phycol. 32, 741–757. doi:10.1111/j.0022-3646.1996.00741.x

Richardson, T.L., Jackson, G.A., 2007. Small phytoplankton and carbon export from the surface ocean. Science (80-.). 315, 838–840. doi:10.1126/science.1133471

Rost, B., Riesebell, U., 2004. Coccolithophores and the biological pump, in: Thierstein, H.R., Young, J.R. (Eds.), Coccolithophores: From Molecular Processes to Global Impact. Springer Berlin Heidelberg, Berlin, pp. 99–125.

Round, F.E., Crawford, R.M., Mann, D.G., 1990. Diatoms: Biology and Morphology of the Genera. Cambridge university press, Cambridge.

Rousseau, V., Mathot, S., Lancelot, C., 1990. Calculating carbon biomass of *Phaeocystis* sp. from microscopic observations. Mar. Biol. 107, 305–314. doi:10.1007/BF01319830

Rousseau, V., Vaulot, D., Casotti, R., Cariou, V., Lenz, J., Gunkel, J., Baumann, M., 1994. The life cycle of *Phaeocystis* (Prymnesiophycaea): evidence and hypotheses. J. Mar. Syst. 5, 23–39. doi:10.1016/0924-7963(94)90014-0

Sackett, O., Petrou, K., Reedy, B., De Grazia, A., Hill, R., Doblin, M., Beardall, J., Ralph, P., Heraud, P., 2013. Phenotypic plasticity of Southern Ocean diatoms: Key to success in the sea ice habitat? PLoS One 8, e81185. doi:10.1371/journal.pone.0081185

Sarthou, G., Timmermans, K.R., Blain, S., Tréguer, P., 2005. Growth physiology and fate of diatoms in the ocean: A review. J. sea 53, 25–42. doi:10.1016/j.seares.2004.01.007

Sathyendranath, S., Longhurst, A., Caverhill, C.M., Platt, T., 1995. Regionally and seasonally differentiated primary production in the North Atlantic. Deep. Res. 42, 1773–1802.

Sathyendranath, S., Stuart, V., Nair, A., Oka, K., Nakane, T., Bouman, H., Forget, M.H., Maass, H., Platt, T., 2009. Carbon-to-chlorophyll ratio and growth rate of phytoplankton in the sea. Mar. Ecol. Prog. Ser. 383, 73–84. doi:10.3354/meps07998

Sathyendranath, S., Watts, L., Devred, E., Platt, T., Caverhill, C., Maass, H., 2004. Discrimination of diatoms from other phytoplankton using ocean-colour data. Mar. Ecol. Prog. Ser. 272, 59–68. doi:10.3354/meps272059

Sazhin, A.F., Artigas, L.F., Nejstgaard, J.C., Frischer, M.E., 2007. The colonization of two *Phaeocystis* species (Prymnesiophyceae) by pennate diatoms and other protists: A significant contribution to colony biomass, in: *Phaeocystis* , Major Link in the Biogeochemical Cycling of Climate-Relevant Elements. pp. 137–145. doi:10.1007/978-1-4020-6214-8_11

Schofield, O., Ducklow, H.W., Martinson, D.G., Meredith, M.P., Moline, M.A., Fraser, W.R., 2010. How do polar marine ecosystems respond to rapid climate change? Science 328, 1520–3. doi:10.1126/science.1185779

Schwaderer, A.S., Yoshiyama, K., de Tezanos Pinto, P., Swenson, N.G., Klausmeier, C.A., Litchman, E., 2011. Eco-evolutionary differences in light utilization traits and distributions of freshwater phytoplankton. Limnol. Oceanogr. 56, 589–598. doi:10.4319/lo.2011.56.2.0589

Semina, H.J., 1997. An outline of the geographical distribution of oceanic phytoplankton., in: Blaxter, G.H.S., Southward, A.G., Gebruck, A.V., Southwards, E.C., Tyler, P.A. (Eds.), Advances in Marine Biology. Academic Press, London, pp. 527–563. doi:10.1016/S0065-2881(08)60020-6

Sergeeva, V.M., Sukhanova, I.N., Flint, M. V., Pautova, L.A., Grebmeier, J.M., Cooper,

L.W., 2010. Phytoplankton community in the Western Arctic in July–August 2003. Oceanology. doi:10.1134/S0001437010020049

Serreze, M.C., Barrett, A.P., Stroeve, J.C., Kindig, D.N., Holland, M.M., 2009. The Cryosphere The emergence of surface-based Arctic amplification 11–19.

Sigman, D.M., Boyle, E.A., 2000. Glacial/interglacial variations in atmospheric carbon dioxide. Nature 407, 859–869. doi:10.1038/35038000

Smetacek, V., Assmy, P., Henjes, J., 2004. The role of grazing in structuring Southern Ocean pelagic ecosystems and biogeochemical cycles. Antarct. Sci. 16, 541–558. doi:10.1017/S0954102004002317

Smetacek, V.S., 1985. Role of sinking in diatom life-hystory: ecological, evolutionary and geological significance. Mar. Biol. 84, 239–251. doi:10.1007/BF00392493

Smith, W.O., Asper, V.L., 2001. The influence of phytoplankton assemblage composition on biogeochemical characteristics and cycles in the southern Ross Sea, Antarctica. Deep. Res. Part I Oceanogr. Res. Pap. 48, 137–161. doi:10.1016/S0967-0637(00)00045-5

Smith, W.O., Comiso, J.C., 2008. Influence of sea ice on primary production in the Southern Ocean: A satellite perspective. J. Geophys. Res. 113, C05S93. doi:10.1029/2007JC004251

Smith, W.O., Jones, R.M., 2015. Vertical mixing, critical depths, and phytoplankton growth in the Ross Sea. ICES J. Mar. Sci. J. du Cons. 72, 1952–1960. doi:10.1093/icesjms/fsu234

Smith, W.O., Nelson, D.M., 1990. Phytoplankton growth and new production in the Weddell Sea marginal ice zone in the austral spring and autumn. Limnol. Oceanogr. 35, 809–821. doi:10.4319/lo.1990.35.4.0809

Smith, W.O., Nelson, D.M., 1985. Phytoplankton bloom produced by a receding ice edge in the Ross Sea: spatial coherence with the density field. Science (80-.). 227, 163–166. doi:10.1126/science.227.4683.163

Smol, J.P., Stoermer, E.F., 2010. The diatoms: applications for the environmental and earth sciences. Cambridge university press, Cambridge.

Snoeijs, P., Busse, S., Potapova, M., 2002. The importance of diatom cell size in

community analysis. J. Phycol. 38, 265–272. doi:10.1046/j.1529-8817.2002.01105.x

Snow, J.T., Schlosser, C., Woodward, E.M.S., Mills, M.M., Achterberg, E.P., Mahaffey, C., Bibby, T.S., Moore, C.M., 2015. Environmental controls on the biogeography of diazotrophy and *Trichodesmium* in the Atlantic Ocean. Global Biogeochem. Cycles 29, 865–884. doi:10.1002/2015GB005090

Solórzano, L., 1969. Determination of ammonia in natural waters by the phenol hypochlorite method. Limnol. Oceanogr. 14, 799–801. doi:10.4319/lo.1969.14.5.0799

Stanca, E., Cellamare, M., Basset, A., 2013. Geometric shape as a trait to study phytoplankton distributions in aquatic ecosystems. Hydrobiologia 701, 99–116. doi:10.1007/s10750-012-1262-2

Stanley, M.S., Callow, J.A., 2007. Whole cell adhesion strength of morphotypes and isolates of *Phaeodactylum tricornutum* (Bacillariophyceae). Eur. J. Phycol. 42, 191–197. doi:10.1080/09670260701240863

Steinfeldt, R., Rhein, M., Bullister, J.L., Tanhua, T., 2009. Inventory changes in anthropogenic carbon from 1997-2003 in the Atlantic Ocean between 20°S and 65°N. Global Biogeochem. Cycles 23, 1–11. doi:10.1029/2008GB003311

Stramska, M., Stramski, D., Kaczmarek, S.J., Allison, D.B., Schwarz, J., 2006. Seasonal and regional differentiation of bio-optical properties within the north polar Atlantic. J. Geophys. Res. 111, 1–16. doi:10.1029/2005JC003293

Straneo, F., Saucier, F., 2008. The outflow from Hudson Strait and its contribution to the Labrador Current. Deep Sea Res. Part I Oceanogr. Res. Pap. 55, 926–946. doi:10.1016/j.dsr.2008.03.012

Strutton, P.G., Martz, T.R., DeGrandpre, M.D., McGillis, W.R., Drennan, W.M., Boss, E., 2011. Bio-optical observations of the 2004 Labrador Sea phytoplankton bloom. J. Geophys. Res. 116, C11037. doi:10.1029/2010JC006872

Strzepek, R.F., Hunter, K. a., Frew, R.D., Harrison, P.J., Boyd, P.W., 2012. Iron-light interactions differ in Southern Ocean phytoplankton. Limnol. Oceanogr. 57, 1182–1200. doi:10.4319/lo.2012.57.4.1182

Strzepek, R.F., Maldonado, M.T., Hunter, K.A., Frew, R.D., Boyd, P.W., 2011. Adaptive strategies by Southern Ocean phytoplankton to lessen iron limitation: Uptake of

organically complexed iron and reduced cellular iron requirements. Limnol. Oceanogr. 56, 1983–2002. doi:10.4319/lo.2011.56.6.1983

Stuart, V., Head, E.J.H., 2005. The BIO method., in: ed. Hooker SB, et al. (Ed.), The Second SeaWiFS HPLC Analysis Round-Robin Experiment (SeaHARRE-2). p. 112.

Stuart, V., Sathyendranath, S., Head, E.J.H., Platt, T., Irwin, B., Maass, H., 2000. Bio-optical characteristics of diatom and prymnesiophyte populations in the Labrador Sea. Mar. Ecol. Prog. Ser. 201, 91–106. doi:10.3354/meps201091

Subba Rao, D. V, Platt, T., 1984. Primary production of Arctic waters. Polar Biol. 3, 191–201. doi:10.1007/BF00292623

Sugie, K., Kuma, K., 2008. Resting spore formation in the marine diatom *Thalassiosira nordenskioeldii* under iron- and nitrogen-limited conditions. J. Plankton Res. 30, 1245–1255. doi:10.1093/plankt/fbn080

Sun, J., Liu, D., 2003. Geometric models for calculating cell biovolume and surface area for phytoplankton. J. Plankton Res. 25, 1331–1346. doi:10.1093/plankt/fbg096

Sunda, W., Kieber, D.J., Kiene, R.P., Huntsman, S., 2002. An antioxidant function for DMSP and DMS in marine algae. Nature 418, 317–20. doi:10.1038/nature00851

Suttle, C.A., 2007. Marine viruses — major players in the global ecosystem. Nat. Rev. Microbiol. 5, 801–812. doi:10.1038/nrmicro1750

Suttle, C.A., Chan, A.M., Cottrell, M.T., 1990. Infection of phytoplankton by viruses and reduction of primary productivity. Nature 347, 467–469. doi:10.1038/347467a0

Sverdrup, H.U., 1953. On Conditions for the Vernal Blooming of Phytoplankton. ICES J. Mar. Sci. 18, 287–295. doi:10.1093/icesjms/18.3.287

Swan, C.M., Vogt, M., Gruber, N., Laufkoetter, C., 2015. A global seasonal surface ocean climatology of phytoplankton types based on CHEMTAX analysis of HPLC pigments. Deep. Res. Part I Oceanogr. Res. Pap. 109, 137–156. doi:10.1016/j.dsr.2015.12.002

Syvertsen, E.E., 1991. Ice algae in the Barents Sea: types of assemblages, origin, fate and role in the ice-edge phytoplankton bloom. Polar Res. 10, 277–288. doi:10.1111/j.1751-8369.1991.tb00653.x

Tamelander, T., Aubert, A.B., Riser, C.W., 2012. Export stoichiometry and contribution of copepod faecal pellets to vertical flux of particulate organic carbon, nitrogen and phosphorus. Mar. Ecol. Prog. Ser. 459, 17–28. doi:10.3354/meps09733

Tang, K.W., 2003. Grazing and colony size development in *Phaeocystis globosa* (Prymnesiophyceae): the role of a chemical signal. J. Plankton Res. 25, 831–842.

Tang, K.W., Jakobsen, H.H., Visser, A.W., 2001. *Phaeocystis globosa* (Prymnesiophyceae) and the planktonic food web: Feeding, growth, and trophic interactions among grazers. Limnol. Oceanogr. 46, 1860–1870. doi:10.4319/lo.2001.46.8.1860

Thomas, M.K., Kremer, C.T., Klausmeier, C. a, Litchman, E., 2012. A global pattern of thermal adaptation in marine phytoplankton. Science (80-.). 338, 1085–1088. doi:10.1126/science.1224836

Thompson, P.A., Bonham, P., Waite, A.M., Clementson, L.A., Cherukuru, N., Hassler, C., Doblin, M.A., 2011. Contrasting oceanographic conditions and phytoplankton communities on the east and west coasts of Australia. Deep Sea Res. Part II Top. Stud. Oceanogr. 58, 645–663. doi:10.1016/j.dsr2.2010.10.003

Throndsen, J., 1997. The planktonic marine flagellates, in: Tomas, C.R. (Ed.), Identifying Marine Phytoplankton. Academic Press, San Diego, pp. 591–729.

Throndsen, J., Hasle, G.R., Tangen, K., 2007. Phytoplankton of Norwegian coastal waters. Almater Forlag AS.

Tian, R.C., Deibel, D., Rivkin, R.B., Vézina, A.F., 2004. Biogenic carbon and nitrogen export in a deep-convection region: Simulations in the Labrador Sea. Deep. Res. Part I Oceanogr. Res. Pap. 51, 413–437. doi:10.1016/j.dsr.2003.10.015

Tomas, C.R., 1997. Identifying marine phytoplankton. Academic press.

Tortell, P.D., DiTullio, G.R., Sigman, D.M., Morel, F.M.M., 2002. CO_2 effects on taxonomic composition and nutrient utilization in an Equatorial Pacific phytoplankton assemblage. Mar. Ecol. Prog. Ser. 236, 37–43. doi:10.3354/meps236037

Trees, C.C., Clark, D.K., Bidigare, R.R., Ondrusek, M.E., Mueller, J.L., 2000. Accessory pigments versus chlorophyll a concentrations within the euphotic zone: A ubiquitous relationship. Limnol. Oceanogr. 45, 1130–1143.

Tremblay, J.-É., Simpson, K., Martin, J., Miller, L., Gratton, Y., Barber, D., Price, N.M., 2008. Vertical stability and the annual dynamics of nutrients and chlorophyll fluorescence in the coastal, southeast Beaufort Sea. J. Geophys. Res. 113, C07S90. doi:10.1029/2007JC004547

Tremblay, J.-éric, Gagnon, J., 2009. The effects of irradiance and nutrient supply on the productivity of Arctic waters: a perspective on climate change, in: Influence of Climate Change on the Changing Arctic and Sub-Arctic Conditions. Springer Netherlands, Dordrecht, pp. 73–93. doi:10.1007/978-1-4020-9460-6_7

Tremblay, J.E., Lucas, M.I., Kattner, G., Pollard, R., Strass, V.H., Bathmann, U., Bracher, A., 2002. Significance of the Polar Frontal Zone for large-sized diatoms and new production during summer in the Atlantic sector of the Southern Ocean. Deep Sea Res. Part II Top. Stud. Oceanogr. 49, 3793–3811. doi:10.1016/S0967-0645(02)00111-X

Troost, T.A., Kooi, B.W., Kooijman, S.A.L.M., 2005. Ecological specialization of mixotrophic plankton in a mixed water column. Am. Nat. 166, E45–E61. doi:10.1086/432038

Tsukazaki, C., Ishii, K.I., Saito, R., Matsuno, K., Yamaguchi, A., Imai, I., 2013. Distribution of viable diatom resting stage cells in bottom sediments of the eastern Bering Sea shelf. Deep. Res. Part II Top. Stud. Oceanogr. 94, 22–30. doi:10.1016/j.dsr2.2013.03.020

Tungaraza, C., Rousseau, V., Brion, N., Lancelot, C., Gichuki, J., Baeyens, W., Goeyens, L., 2003. Contrasting nitrogen uptake by diatom and *Phaeocystis*-dominated phytoplankton assemblages in the North Sea. J. Exp. Mar. Bio. Ecol. 292, 19–41. doi:10.1016/S0022-0981(03)00145-X

Tyrrell, T., 1999. The relative influences of nitrogen and phosphorus on oceanic primary production. Nature 400, 525–531. doi:10.1038/22941

Utermöhl, H., 1958. Improvement of the quantitative methods for phytoplankton. Mitt. Int. Ver. Limnol. 9, 1–38.

van den Meersche, K., Middelburg, J.J., Soetaert, K., van Rijswijk, P., Boschker, H.T.S., Heip, C.H.R., 2004. Carbon-nitrogen coupling and algal-bacterial interactions during an experimental bloom: Modeling a 13C tracer experiment. Limnol. Oceanogr. 49,

862–878. doi:10.4319/lo.2004.49.3.0862

van Leeuwe, M.A., Stefels, J., 2007. Photosynthetic responses in *Phaeocystis antarctica* towards varying light and iron conditions, in: Phaeocystis, Major Link in the Biogeochemical Cycling of Climate-Relevant Elements. Springer Netherlands, Dordrecht, pp. 61–70. doi:10.1007/978-1-4020-6214-8_6

van Leeuwe, M.A., Stefels, J., 1998. Effects of iron and light stress on the biogeochemical composition of Antarctic *Phaeocystis* sp. (Prymnesiophyceae). II. Pigment composition. J. Phycol. 34, 496–503.

Vidussi, F., Roy, S., Lovejoy, C., Gammelgaard, M., Thomsen, H.A., Booth, B., Tremblay, J.-E., Mostajir, B., 2004. Spatial and temporal variability of the phytoplankton community structure in the North Water Polynya, investigated using pigment biomarkers. Can. J. Fish. Aquat. Sci. 61, 2038–2052. doi:10.1139/f04-152

Violle, C., Navas, M.-L., Vile, D., Kazakou, E., Fortunel, C., Hummel, I., Garnier, E., 2007. Let the concept of trait be functional! Oikos 116, 882–892. doi:10.1111/j.2007.0030-1299.15559.x

Vogt, M., O'Brien, C., Peloquin, J., Schoemann, V., Breton, E., Estrada, M., Gibson, J., Karentz, D., Van Leeuwe, M.A., Stefels, J., Widdicombe, C., Peperzak, L., 2012. Global marine plankton functional type biomass distributions: *Phaeocystis* spp. Earth Syst. Sci. Data 4, 107–120. doi:10.5194/essd-4-107-2012

von Quillfeldt, C., 2000. Common diatom species in Arctic spring blooms: their distribution and abundance. Bot. Mar. 43, 499–516. doi:10.1515/BOT.2000.050

Von Quillfeldt, C., 2001. Identification of some easily confused common diatom species in Arctic spring blooms. Bot. Mar. 44, 375–389. doi:10.1515/BOT.2001.048

von Quillfeldt, C.H., Ambrose, W.G., Clough, L.M., 2003. High number of diatom species in first-year ice from the Chukchi Sea. Polar Biol. 26, 806–818. doi:10.1007/s00300-003-0549-1

Vrede, K., Heldal, M., Norland, S., Bratbak, G., 2002. Elemental composition (C, N, P) and cell volume of exponentially growing and nutrient-limited bacterioplankton. Appl. Environ. Microbiol. 68, 2965–2971. doi:10.1128/AEM.68.6.2965-2971.2002

Wang, X., Tang, K.W., 2010. Buoyancy regulation in *Phaeocystis globosa* Scherffel

colonies. Open Mar. Biol. J. 4, 115–121.

Waniek, J., Holliday, N., Davidson, R., Brown, L., Henson, S., 2005. Freshwater control of onset and species composition of Greenland shelf spring bloom. Mar. Ecol. Prog. Ser. 288, 45–57. doi:10.3354/meps288045

Wassmann, P., Vernet, M., Mitchell, B., Rey, F., 1990. Mass sedimentation of *Phaeocystis pouchetii* in the Barents Sea. Mar. Ecol. Prog. Ser. 66, 183–195. doi:10.3354/meps066183

Weber, T.S., Deutsch, C., 2010. Ocean nutrient ratios governed by plankton biogeography. Nature 467, 550–554. doi:10.1038/nature09403

Weithoff, G., 2003. The concepts of "plant functional types" and "functional diversity" in lake phytoplankton - a new understanding of phytoplankton ecology? Freshw. Biol. 48, 1669–1675. doi:10.1046/j.1365-2427.2003.01116.x

Weller, R.A., Plueddemann, A.J., 1996. Observations of the vertical structure of the oceanic boundary layer. J. Geophys. Res. doi:10.1029/96JC00206

Westoby, M., Wright, I.J., 2006. Land-plant ecology on the basis of functional traits. Trends Ecol. Evol. 21, 261–268. doi:10.1016/j.tree.2006.02.004

Whyte, J.N.C., Davis, J.C., Forbes, J.R., 1998. Harmful algae in Canadian waters and management strategies. Oceanogr. Lit. Rev. 7, 1234–1235.

Winder, M., Sommer, U., 2012. Phytoplankton response to a changing climate. Hydrobiologia 698, 5–16. doi:10.1007/s10750-012-1149-2

Witze, A., 2008. Climate change: Losing Greenland. Nature 452, 798–802. doi:10.1038/452798a

Wolfe, G. V, Levasseur, M., Cantin, G., Michaud, S., 2000. DMSP and DMS dynamics and microzooplankton grazing in the Labrador Sea: application of the dilution technique. Deep Sea Res. Part I Oceanogr. Res. Pap. 47, 2243–2264.

Wright, S.W., Thomas, D.P., Marchant, H.J., Higgins, H.W., Mackey, M.D., Mackey, D.J., 1996. Analysis of phytoplankton of the Australian sector of the Southern Ocean: Comparisons of microscopy and size frequency data with interpretations of pigment HPLC data using the "CHEMTAX" matrix factorisation program. Mar. Ecol. Prog. Ser. 144, 285–298. doi:10.3354/meps144285

Wright, S.W., Van den Enden, R.L., 2000. Phytoplankton community structure and stocks in the East Antarctic marginal ice zone (BROKE survey, January-March 1996) determined by CHEMTAX analysis of HPLC pigment signatures. Deep. Res. Part II Top. Stud. Oceanogr. 47, 2363–2400. doi:10.1016/S0967-0645(00)00029-1

Wu, Y., Peterson, I.K., Tang, C.C.L., Platt, T., Sathyendranath, S., Fuentes-Yaco, C., 2007. The impact of sea ice on the initiation of the spring bloom on the Newfoundland and Labrador Shelves. J. Plankton Res. 29, 509–514. doi:10.1093/plankt/fbm035

Wu, Y., Platt, T., Tang, C., Sathyendranath, S., 2008a. Regional differences in the timing of the spring bloom in the Labrador Sea. Mar. Ecol. Prog. Ser. 355, 9–20. doi:10.3354/meps07233

Wu, Y., Platt, T., Tang, C.C.L., Sathyendranath, S., Devred, E., Gu, S., 2008b. A summer phytoplankton bloom triggered by high wind events in the Labrador Sea, July 2006. Geophys. Res. Lett. 35, L10606.

Yallop, M.L., 2001. Distribution patterns and biomass estimates of diatoms and autotrophic dinoflagellates in the NE Atlantic during June and July 1996. Deep. Res. Part II Top. Stud. Oceanogr. 48, 825–844. doi:10.1016/S0967-0645(00)00099-0

Yang, Q., Dixon, T.H., Myers, P.G., Bonin, J., Chambers, D., van den Broeke, M.R., 2016. Recent increases in Arctic freshwater flux affects Labrador Sea convection and Atlantic overturning circulation. Nat. Commun. 7, 10525. doi:10.1038/ncomms10525

Yankovsky, A.E., Yashayaev, I., 2014. Surface buoyant plumes from melting icebergs in the Labrador Sea. Deep. Res. Part I Oceanogr. Res. Pap. 91, 1–9. doi:10.1016/j.dsr.2014.05.014

Yashayaev, I., 2007. Hydrographic changes in the Labrador Sea, 1960-2005. Prog. Oceanogr. 73, 242–276. doi:10.1016/j.pocean.2007.04.015

Yashayaev, I., Loder, J.W., 2009. Enhanced production of Labrador Sea Water in 2008. Geophys. Res. Lett. 36. doi:10.1029/2008GL036162

Yashayaev, I., Seidov, D., 2015. The role of the Atlantic Water in multidecadal ocean variability in the Nordic and Barents Seas. Prog. Oceanogr. 132, 68–127. doi:10.1016/j.pocean.2014.11.009

Yashayaev, I., Seidov, D., Demirov, E., 2015. A new collective view of oceanography of

the Arctic and North Atlantic basins. Prog. Oceanogr. doi:10.1016/j.pocean.2014.12.012

Yebra, L., Harris, R.P., Head, E.J.H., Yashayaev, I., Harris, L.R., Hirst, A.G., 2009. Mesoscale physical variability affects zooplankton production in the Labrador Sea. Deep Sea Res. Part I Oceanogr. Res. Pap. 56, 703–715. doi:10.1016/j.dsr.2008.11.008

Yool, A., Popova, E.E., Coward, A.C., 2015. Future change in ocean productivity: Is the Arctic the new Atlantic? J. Geophys. Res. Ocean. 120, 7771–7790. doi:10.1002/2015JC011167

Zapata, M., Jeffrey, S.W., Wright, S.W., Rodríguez, F., Garrido, J.L., Clementson, L., 2004. Photosynthetic pigments in 37 species (65 strains) of Haptophyta: Implications for oceanography and chemotaxonomy. Mar. Ecol. Prog. Ser. 270, 83–102. doi:10.3354/meps270083

Zhai, L., Platt, T., Tang, C., Sathyendranath, S., Walne, A., 2013. The response of phytoplankton to climate variability associated with the North Atlantic Oscillation. Deep Sea Res. Part II Top. Stud. Oceanogr. 93, 159–168. doi:10.1016/j.dsr2.2013.04.009

Zhang, F., He, J., Lin, L., Jin, H., 2015. Dominance of picophytoplankton in the newly open surface water of the central Arctic Ocean. Polar Biol. 1081–1089. doi:10.1007/s00300-015-1662-7

Zhang, Q., Gradinger, R., Spindler, M., 1998. Dark survival of marine microalgae in the High Arctic (Greenland Sea). Polarforschung 65, 111–116.

Zhang, X., Walsh, J.E., Zhang, J., Bhatt, U.S., Ikeda, M., 2004. Climatology and interannual variability of Arctic cyclone activity: 1948–2002. J. Clim. 17, 2300–2317. doi:10.1175/1520-0442(2004)017<2300:CAIVOA>2.0.CO;2

Zubkov, M. V, Tarran, G.A., 2008. High bacterivory by the smallest phytoplankton in the North Atlantic Ocean. Nature 455, 224–226. doi:10.1038/nature07236

Zwart, J.A., Solomon, C.T., Jones, S.E., 2015. Phytoplankton traits predict ecosystem function in a global set of lakes. Ecology 96, 2257–2264. doi:10.1890/14-2102.1